

ATMOSPHERIC PARTICLES AND ELECTRICAL CONDUCTIVITY DURING DIFFERENT WEATHER CONDITIONS

A THESIS

*Submitted in fulfilment of the
requirements for the award of the degree*

of

DOCTOR OF PHILOSOPHY

in

EARTH SCIENCES

By

ARVIND KUMAR SINGH



DEPARTMENT OF EARTH SCIENCES
UNIVERSITY OF ROORKEE
ROORKEE-247 667 (INDIA)

JANUARY, 2000

CANDIDATE'S DECLARATION


I hereby certify that the work, which is being presented in the thesis entitled "ATMOSPHERIC PARTICLES AND ELECTRICAL CONDUCTIVITY DURING DIFFERENT WEATHER CONDITIONS" in fulfillment of the requirement for the award of the degree of Doctor of Philosophy, submitted in the Department of Earth Sciences, University of Roorkee, is an authentic record of my own work carried out during period from September 1995 to January 2000 under the supervision of **Prof. Sri Niwas** and **Prof. Jagdish Rai**.


The matter presented in this thesis has not been submitted by me for the award of any other degree of this or any other university.

Dated: 11-09-2000



(ARVIND KUMAR SINGH)

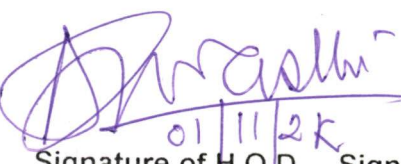
This is to certify that the above statement made by the candidate is correct to the best of our knowledge.

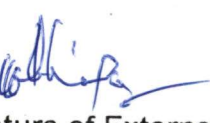

(Dr. Jagdish Rai)
Professor
Department of Physics,
University of Roorkee,
Roorkee - 247 667, India


(Dr. Sri Niwas)
Professor
Department of Earth Sciences,
University of Roorkee,
Roorkee - 247 667, India

The Ph.D. viva-voce examination of Mr. Arvind Kumar Singh, Research Scholar, has been held on...1-11-2K...at...10-00 A.M....


Signature of Supervisor(s)


Signature of H.O.D.


Signature of External Examiner

RESUME

Atmospheric aerosols or suspended particulates are the dispersed solid or liquid or mixture of both kind of particles in air which are most complex and least understood atmospheric constituents. These particles are present in the atmosphere with varied chemical composition and wide range of size from $0.001\ \mu\text{m}$ to $100\ \mu\text{m}$ in radius. Study of such atmospheric particles is important to understanding their influence directly or indirectly on climate and human health. The atmospheric electrical parameters, viz. atmospheric electrical conductivity, air-earth current density, electric field etc. are affected by various environmental and meteorological factors. The atmospheric particles and electrical parameters can not be in a steady state at all the times at a particular place. Therefore a clear knowledge of the nature of atmospheric particle concentration and their distribution and atmospheric electrical conductivity at a given location during different weather conditions (disturbed and fair-weather) is very important to characterize the aerosols and particulate system over the location and also to get information on the meteorological condition in lower atmosphere. The region lying between 65-70 km to about 1000 km altitude above the earth surface containing free electrons and ions is known as ionosphere and is primarily responsible for introducing errors in transionospheric radio signals. The equatorial ionosphere is formed primarily by the ionization of neutral gas atoms/molecules present in the upper atmosphere by exposure to solar radiation. The free thermal electrons, having energies of a few tens of electron volts and produced by high energy photoelectron collision

with neutrals, form more than 90% of the flux in the ionosphere. The weather disturbances like thunderstorms may alter the ion-electron production rate and hence change the ionospheric electrical parameters. The characteristics of these ion-electrons are studied in order to characterize the ionosphere.

The present thesis presents some experimental studies on atmospheric particle concentration, their size distribution and atmospheric electrical conductivity in the light of some meteorological parameters (like temperature, humidity, rain, wind speed etc.). It also includes a study on the low latitude ionosphere and the behavior of electrons and ion density and temperature anomaly in the low latitude region. The data for this purpose has been obtained from Retarding Potential Analyzer (RPA) payload of SROSS-C2 mission, operative since May 1994. This is a combined effort of Indian Space Research Organization (ISRO), National Physical Laboratory (NPL) and the University of Roorkee (UOR).

A brief survey on the present-state-of-art regarding aerosols and particulate generation and distribution has been presented in **Chapter-I**. The different mechanisms involved in aerosol formation and their distribution in the atmosphere in different weather conditions has been described in this chapter and has the potential to advance knowledge in this area. It also includes various studies on atmospheric electrical parameters with respect to the environmental effects including the particulate pollution. It also includes the existing knowledge about the ionospheric phenomenon. Since the characteristics of the ionosphere show a large spatial and temporal variation, its long term study helps in improving the existing reference ionospheric models

being used to apply ionospheric corrections. In brief, this chapter gives introductory remarks to the existing knowledge and the glimpse of the work carried out for the present study in subsequent chapters.

Chapter-II deals with the instrumentation part of the thesis. It gives brief description of the instruments fabricated for present studies. The atmospheric particle concentration and their size distribution are measured by using a specially designed laser scatterometer. It works on the principal of Mie Scattering with an assumption that the atmospheric particles follow the normal Gaussian distribution in the atmosphere. This scetterometer involves 5mW He-Ne laser, photo-diode and two strip chart recorders. For measuring the atmospheric electrical conductivity a Gerdian Condenser was fabricated. It uses a sensitive electrometer amplifier, high voltage power supply, multichannel chart recorder and blower having a sucking capacity of 1500 liter/minute. Gerdian condenser is a cylindrical capacitor consisting of a central electrode (conducting rod) and an outer electrode (cylindrical tube). The function of various parts, working principle and theoretical concepts of Gerdian Condenser have been described in detail.

The tropospheric aerosols and electrical environment are closely related to the solar activity. Atmospheric ions play an important role in governing the aerosols and electrical conductivity at ground surface. Solar Cosmic Rays (SCR) and Galactic Cosmic Rays (GCR) are the chief sources of ionization in the atmosphere. During solar eclipse the moon stops GCR and SCR particles and the effect is felt to the ground surface. Therefore an experimental study on aerosol concentration and size distribution as well as atmospheric electrical

conductivity has been performed during the total solar eclipse of October 24, 1995, and is reported in **Chapter-III**. The variance of these factors in view of some meteorological parameters has also been presented. The result shows that both aerosol concentration and electrical conductivity increases during the solar eclipse; which is contrary to the normal atmospheric conditions. It has been argued that the causes are not local. The stoppage of solar wind flux by moon increases the GCR at lower altitudes thereby causing the increased ionization. The increased ionization during the solar eclipse is responsible for the increase of atmospheric electrical conductivity. Also the atmospheric ions increase the cloud condensation nuclei which plays an important role in aerosol formation and hence the increase in aerosol concentration.

Various meteorological changes may have influence on the atmospheric aerosols and the surface electrical conductivity. Therefore it may be very helpful to study the nature of aerosols and electrical conductivity during different weather conditions. For this purpose we have chosen the monsoon period and winter season as disturbed and fair-weather atmospheric conditions respectively. The experimental studies on tropospheric aerosols and electrical conductivity have been done for the monsoon period (June-September, 1996) and the fair-weather region (November, 1996-February, 1997) at Roorkee, India. The results of these studies have been presented in **Chapter-IV**. The atmospheric electrical conductivity has been found to decrease with increasing relative humidity and temperature. Wind was an important factor, which modified the behavior of conductivity in short-term range. The atmospheric aerosol concentration and size were found to decrease with increase in rainfall.

Also, the relative humidity plays an important role and changes the aerosol density distribution. However, relative humidity less than 95% do not affect effectively the aerosol concentration.

The ionospheric weather has become the most important topic of the day. It is affected by the solar geomagnetic disturbances and the tropospheric fluctuations. As a result of extensive research work, it is now well known that the ionospheric system varies markedly with altitude, longitude, universal time, season, solar cycle, geomagnetic activity and solar flares. The ionospheric parameters can vary appreciably from hour to hour or from day to day and it can display a considerable amount of structure. The ion and electron density fluctuations are associated with the ionospheric structure, where thermalized electrons play very important role. Even the small fluctuations in ion-electron density can cause signal fluctuations, which affect HF communication. Therefore **Chapter-V** is dedicated to the studies of ion-electron structure, with an objective to study the behavior of electron and ion number densities and temperature anomaly in the low latitude region. The data for this purpose has been obtained from RPA payload aboard SROSS-C2 satellite launched by ISRO. This chapter also includes the RPA payload and spacecraft configuration for measuring ion-electron densities and temperature along with the RPA data reduction and analysis.

The present study reveals the fact that the behavior of atmospheric aerosols distribution and electrical conductivity are very much affected by some processes like solar eclipse and disturbed and fair weather conditions. The major meteorological factors like wind speed, temperature, rain fall and relative

humidity plays an important role in characterization of the tropospheric aerosols and atmospheric electrical conductivity. Studies during the solar eclipse show that SCR and GCR also play an important role in the atmospheric processes. The investigations regarding ionospheric ion and electron densities and their temperature anomalies reveal the fact that these parameters are highly affected by different weather conditions in the troposphere. The summary and conclusions regarding the present work and suggestions for future studies have been given in **Chapter-VI**.

ACKNOWLEDGEMENTS

It is my great pleasure and privilege to express my deep sense of gratitude and profound indebtedness towards **Prof. Sri Niwas**, Department of Earth Sciences and **Prof. Jagdish Rai**, Department of Physics, University of Roorkee, Roorkee, for their incessant invaluable guidance, inspiring encouragement and kind cooperation during the progress of the work. I am very thankful to them for suggesting the problem and for having had the opportunity to work with them. The work could not have been completed without their helpful counsel and constant cooperation. The long hours of fruitful discussions and pertinent suggestions not only strengthened my skills in research methodology but also helped me a more confident personality. Right from the very beginning I have admired them for their wonderful homely behavior.

During this research, the department has had two heads Prof. S. K. Upadhyay and Prof. A. K. Awasthi and most fortunately both of them encouraged me by extending every sort of help as and when sought for. I wish to express my gratefulness to Prof. S. Auluck, the Head of Physics Department and Prof. A. N. Tripathi, former head of Physics Department for supporting my efforts in various ways and for providing necessary lab facilities for my present work.

I would like to make a special note of thank to Prof. V. N. Singh, Prof. H. Sinhval, Prof. A. K. Jain and other faculty members of the Department of Earth Sciences for their co-operation whenever need came for them. I shall equally remain indebted to Dr. Vir Singh, Associate Professor, Department of Physics for his constant encouragement and keen interest shown by him at every stage of my research studies. Thanks are also due to Dr. Pratap Singh, Scientist, National Institute of Hydrology for providing the meteorological data to complete the experimental work.

I extend my heartfelt thanks to my friends Neerja, Manoj, Savinder, Piyush, Kshamata, Adarsh, Amita, Amit Rai, Yogendra and Dinesh for their

enthusiastic and ever-entertainmental support during the tenure of my research work. Thanks are also due to the employees of both departments, Earth Sciences and Physics, for their excellent cooperation and helpful behavior extended to me.

The financial support from Indian Space Research Organization (ISRO), Bangalore through a research grant to the Department of Physics, University of Roorkee, Roorkee is gratefully acknowledged.

Finally my vocabulary fails to express my love and gratitude for my parents whose blessings have always been with me as a source of inspiration and encouragement to fulfil my ambition of higher studies. This thesis is more of a fulfilment of their dreams than mine. The ever-enthusiastic help of my family members specially my uncle Sri H. P. Singh, which has been a tool for me to work peacefully during the study period. I am in dearth of proper words to express my abounding feelings and affection for my younger brother Ashok. It is complementary contributions of the Supreme Being, which made it possible to bring all the research work in the present form within the scheduled time.



(ARVIND KUMAR SINGH)

LIST OF PUBLICATIONS

A. In Journals

1. "Effect of orographic features on atmospheric electrical parameters of different cities of India", *Indian J. Radio Space Phys.*, **27**, 215, 1998.
2. "Variation in atmospheric aerosols and electrical conductivity at Roorkee during total solar eclipse of Oct. 95", *Indian J. Radio Space Phys.*, **28**, 1, 1999.
3. "Measurement of atmospheric electrical conductivity during monsoon period", Proc. 11th Int. Conf. on Atmospheric Electricity, MSFC, Alabama, 591-594, 1999.
4. "Variation of aerosols in relation to some meteorological parameters during different weather conditions", *Atmosfera*, Mexico in press.
5. "Measurements of aerosols during monsoon at Roorkee", Submitted revised script to the *Earth & Planetary Science*, India for publication.

B. In Conferences/Seminars/Symposiums (International)

1. "Solar effects on atmospheric electrical parameters", presented in first International Workshop on Long Term Changes and Trends in the Atmosphere, at Indian Institute of Tropical Meteorology, Pune from February 16-19, 1999.
2. "Measurement of atmospheric electrical conductivity during monsoon period", presented in International Workshop on Atmospheric Electricity organized by ICAE, held at Guntersville, Alabama, U.S.A. during June 7-11, 1999.

C. In Conferences/Seminars/Symposiums (National)

1. "Effect of solar eclipse on some atmospheric parameters" paper presented at National Meeting on total Solar Eclipse Oct. 24 at IIA, Bangalore on Feb. 26, 1996.

2. "Ground water investigations using atmospheric" paper presented in conference on "Application of mathematics in Engineering and Industries" at Dept. of Mathematics, University of Roorkee, Roorkee, from Dec. 14-16, 1996.
3. "A Laser scatterometer for air pollution monitoring", presented in NLS'97 at Centre for Advanced Technology (CAT), Indore, from Feb. 6-8, 1997.
4. "Measurement of aerosols during monsoon at Roorkee", presented in TROPMET'97 at Indian Institute of Science, Bangalore from Feb. 10-14, 1997.
5. "Study of air-conductivity during monsoon period at Roorkee", presented in TROPMET'97 at Indian Institute of Science, Bangalore from Feb. 10-14, 1997.
6. "Effect of cosmic rays on global electric circuit (GEC) parameters over some cities of India", presented in 10th National Space Science Symposium, at PRL, Ahmedabad from Nov. 25-28, 1997.
7. "Variation of aerosols during winter season at Roorkee", presented in seminar on Stratosphere-Troposphere Interactions at Cochin University of Science & Technology, Cochin from Nov. 24-26, 1998.
8. "Study of atmospheric conductivity during monsoon period at Roorkee", presented in seminar on Stratosphere-Troposphere Interactions at Cochin University of Science & Technology, Cochin from Nov. 24-26, 1998.
9. "A comparative study of aerosol distribution for two years : Influence of meteorological parameters", accepted for presentation in TROPMET-2000 at Cochin University of Science and Technology, Cochin.

CONTENTS

	Page No.
RESUME	i
ACKNOWLEDGEMENT	vii
LIST OF PUBLICATIONS	ix
Chapter 1: INTRODUCTION	1
1.1 ATMOSPHERIC PARTICLES	2
1.1.1 Size and Types of Aerosols	2
1.1.2 Formation of Aerosols	4
1.1.3 Aerosol Residence Time and Coagulation	6
1.1.4 Aerosol Sources	7
1.1.5 Aerosol Removal from the Atmosphere	9
1.1.6 Condensation of Aerosol Particles	10
1.1.7 Aerosols in the Troposphere and Stratosphere	11
1.1.8 Aerosol Size Distribution	12
1.1.9 Properties of Aerosols	15
1.1.10 Interaction of the Atmospheric Particles with Light	18
1.1.11 Implications of Aerosols	23
1.2 ATMOSPHERIC ELECTRICITY: A BRIEF HISTORY	27
1.2.1 Ion Production in the Atmosphere	28
1.2.2 Atmospheric Electrical Parameters	30
1.2.2.1 Variation of Atmospheric Electrical Parameters	31
1.2.3 Electrical Conductivity of the Atmosphere	32
1.2.3.1 Variation of Conductivity and Electric Field	33
1.2.4 Effects of Aerosols on Electrical Parameters	34
1.3 THE IONOSPHERE	35
1.3.1 Production of Ions in the Ionosphere	37
1.3.1.1 Primary Photochemical Processes	37
1.3.1.2 Thermal Structure of the Ionosphere	38
1.3.2 Studies on the Ionosphere	39
1.4 PRESENT WORK	41
TABLES	43

Chapter 2: INSTRUMENTATION	45
2.1 ATMOSPHERIC ELECTRICAL CONDUCTIVITY	47
2.1.1 Measurement of Electrical Conductivity	48
2.1.2 Experimental Setup	50
2.2 ATMOSPHERIC PARTICLES OR AEROSOLS	53
2.2.1 Measurement of Atmospheric Aerosols	53
2.2.2 Experimental Setup	56
Chapter 3: SOLAR ECLIPSE OF OCTOBER 24, 1995: ATMOSPHERIC AEROSOLS AND ELECTRICAL CONDUCTIVITY	59
3.1 A BRIEF SURVEY OF EARLIER STUDIES	59
3.2 THE SOLAR ECLIPSE OF OCTOBER 24, 1995 IN INDIA	62
3.3 SITE AND PERIOD OF OBSERVATION	63
3.4 MEASUREMENT OF AEROSOLS AND CONDUCTIVITY	63
3.5 RESULTS AND DISCUSSION	65
TABLES	71
Chapter 4: ATMOSPHERIC AEROSOLS AND ELECTRICAL CONDUCTIVITY DURING MONSOON AND WINTER SEASONS	72
4.1 MEASUREMENTS OF AEROSOLS AND CONDUCTIVITY	74
4.2 RESULTS AND DISCUSSION	75
TABLES	80
Chapter 5: STUDY OF IONOSPHERIC PARTICLES AT LOW LATITUDE F₂-REGION USING SROSS-C2 DATA	81
5.1 STUDIES ON D, E AND F REGION	82
5.2 THE SROSS MISSION AND RPA PAYLOAD	83
5.2.1 Objective	86
5.2.2 Principal of Operation	87
5.2.3 Data Collection and Dissemination	87
5.2.4 Data Reduction and Analysis	89
5.2.4.1 Determination of Total Ion Density from Ion RPA Data	90
5.2.4.2 Determination of Ion Density, Composition and Temperature	90
5.2.4.3 Determination of Electron Temperature	93

5.3 RESULTS AND DISCUSSION	95
5.3.1 Variation of Ion densities	97
5.3.2 Variation of Ion and Electron Temperature	99
5.3.3 Discussion	102
TABLES	105
Chapter 6: CONCLUSIONS AND RECOMMENDATIONS	111
6.1 CONCLUSIONS	111
6.2 RECOMMENDATIONS FOR FUTURE STUDIES	115
REFERENCES	117

Chapter 1

Introduction

Various processes occurring in our atmosphere are the subjects of great concern to the scientific community. The extensive efforts made by the researchers provide us a platform to understand it up to some extent but still it needs more attention. It is a well known fact that our atmosphere is changing rapidly because of variety of influences from natural and as well as human origin. These changes have implications for a multitude problem and in particular demonstrate the connection among the atmospheric particles, electrical parameters and meteorological variables. Atmospheric particles or aerosols and atmospheric electrical parameters play very important role in many atmospheric processes and some of which may in turn an impact on weather and climate. Our ability to assess the role of atmospheric aerosols and electrical parameters in atmospheric processes is mainly due to the availability of limited information on their properties. Study of atmospheric particles/aerosols and electrical parameters is important for the understanding of their influence directly or indirectly on climate and possibly on health. Moreover, they affect the satellite remote sensing, communication, aviation, power supplies etc. in a great manner. The objective of this chapter is to present a broad view on atmospheric aerosols, atmospheric electrical parameters (conductivity) and ionospheric particles (ion and electrons) with existing knowledge without detailed mechanism.

1.1 ATMOSPHERIC PARTICLES

The basic constituents of atmospheric particles are aerosols or suspended particulates, which are defined as dispersed solid or liquid or mixture of both particles in air. These are one of the most complex and least understood atmospheric constituents. The inputs to atmospheric aerosols come from the natural and man-made sources. The possible adverse effects of natural and man-made aerosols on atmospheric processes and climate guide the recent thrusts to aerosol studies. However, a realistic assessment of this can not be made due to our incomplete knowledge about the characteristics of natural and anthropogenic aerosols and their role in various atmospheric processes.

It is being increasingly realized that aerosols in the troposphere and stratosphere have major role in climate change process, particularly as a counter-balance to the effects of warming due to the greenhouse gases [63]. These aerosols also affect the air and water quality in the troposphere [230]. Knowledge of the physical and chemical properties of atmospheric aerosols is essential to assess these possible impacts. Ideally, knowledge of these aerosol properties should be known regionally and as a function of meteorological parameters viz. Solar flux, temperature, relative humidity, wind speed and direction, atmospheric pressure, rainfall and altitude.

1.1.1 Size and Types of Aerosols

Aerosols present in the atmosphere with varied chemical composition and possess a wide dynamic range in size from 0.001 μm to about 100 μm in radius. The size range can again be subdivided into three ranges based on

atmospheric effects. The smallest particle size, less than $0.1 \mu\text{m}$ are called Aitken particles and are important in atmospheric electricity [140]. Particles in the size range $0.1 \mu\text{m}$ to $1.0 \mu\text{m}$ are referred to as large particles and are effective in atmospheric optics and in radiation budget [108]. These are also effective as condensation nuclei [6]. Particles of size greater than $1.0 \mu\text{m}$ play an important role in cloud physics and are effective as condensation nuclei [201]. The large particles (0.1 to $1.0 \mu\text{m}$) are sometimes called haze particles [135].

Basically, aerosols are of two types, defined on the basis of composition or source characteristics and distribution characteristics respectively. The first type includes both manmade or anthropogenic and natural aerosols. The anthropogenic aerosols mainly originate from emissions such as soot, Al_2O_3 , SO_2 from rocket and aircraft, industrial emissions, traffic and road dust etc. The natural aerosols are produced in the atmosphere by (i) the chemical reactions of a variety of trace gases (gas-to-particle conversion), these are also called secondary particles, (ii) sea spray (maritime) aerosols, (iii) mineral dust from wind-erosion of soils, (iv) volcanic effluvia including both direct particle emissions and products derived from the subsequent reactions of emitted gases, (v) smoke from the burning land biota, (vi) organic aerosols emitted by plants and trees and biological aerosols such as pollens or spores and (vii) meteoric debris.

The second type of aerosols includes (i) tropospheric background aerosols and continuous production from large-area sources such as ocean and (ii) stratospheric aerosols from volcanic effluvia. The natural atmospheric

aerosols can also be characterized according to the international global aerosol program (IGAP, 1991) as desert aerosols, remote continental aerosols, marine aerosols, polar aerosols, mid tropospheric and upper tropospheric aerosols (also termed as background aerosols), biogenic aerosols, cloud and stratospheric aerosols.

1.1.2 Formation of Aerosols

Aerosol particles are either directly produced or formed by various gas-to-particle conversion processes. In either case, the original aerosol particle undergo a variety of chemical processes and physical modifications resulting in continually changing chemical composition and particle size distribution and hence physical properties. Particles from different sources are mixed by Brownian diffusion and coagulation process on a micro scale and by atmospheric turbulence and circulation on a macro scale. The principal sources of aerosols are listed in Table 1.1 with approximate estimate of their input levels.

Some of the characteristics of the size distribution of aerosols depend upon various formation and transformation processes of aerosols. Particles in the size range $1.0 \mu\text{m}$ or greater are produced directly by mechanical processes such as wind blown dust and sea salt spray. Particles of lower size range have relatively short residence time because of chemical reactivity and greater physical mobility. These particles are eventually incorporated in the $0.1 \mu\text{m}$ to $1.0 \mu\text{m}$ (Aitken nuclei range), which is generally referred to as the accumulation mode.

It is seen from Table 1.1 that gas-to-particle conversion process is a major contribution to the aerosol particle production. It contributes more than half of the total particle production due to natural as well as man-made sources. Gases can interact in the atmosphere with particles. Similarly, atmospheric gases interact and react with particles and form new particles or modify the existing particles by different processes as

- (1) Homogenous homomolecular interaction
- (2) Homogeneous heteromolecular interaction
- (3) Heterogeneous heteromolecular interaction

Process (1) involves the formation of new liquid and solid ultra-fine particles from a gas phase consisting of a single gas species only. The process (2) consists of formation of new particles from a gas phase consisting of two or more gas species. In this process the most common species is the water vapour. In the process (3) i.e. heterogenous heteromolecular nucleation, growth of pre-existing particles takes place due to condensation of gaseous species.

The particles formed by these mechanisms are in the fine particle size range ($<0.05 \mu\text{m}$). Gas-to-particle conversion can also take place through direct reaction of gases with particles on the surface or in the interior in case of liquid particles. Gas-to-particle conversion processes also play an important role in the formation of stratospheric aerosols and are primarily responsible for the well-known Junge layer in the stratosphere. Ever since it's discovered by Junge [89] the stratospheric aerosol layer has been the subject of great interest [215].

One of the factors of producing stratospheric aerosols is meteoric debris. The meteoric influx to the earth amounts is about 1.6×10^7 kg/year. The meteor input, to the total stratospheric particulate mass input constitutes only a few percent. Hunten *et al.* [75] and Turco *et al.* [215] made detailed theoretical calculations on the effects of meteoric debris on stratospheric aerosols. Turco *et al.* [215] concluded from their model calculations that meteoric debris is an important natural aerosol constituent for particles larger than 1.0 μm radius throughout the stratosphere and may be dominant for particles smaller than 0.1 μm radius above 20 km. For other sizes, the meteoric debris generally constitutes less than 10 percent of the total aerosol mass.

1.1.3 Aerosol Residence Time and Coagulation

The residence time of aerosol depends on their size and location in the atmosphere. The particulates at the lower end of the size spectrum (Aitken nuclei range) have a relatively short residence time in the atmosphere because of the chemical reactivity and physical mobility of these particles. For particles in the size range of 0.1 to 10 μm radius, the residence time in the troposphere is about one week whereas in the stratosphere it varies months to years.

Once formed, the aerosol may undergo different changes caused by chemical reaction and other processes such as diffusion, coagulation, sedimentation, evaporation and nucleation. The coagulation process, in the aerosol transformation is basically controlled by the diffusion coefficient, which is particle size dependent and normally involves smaller particles. Thus coagulation process controls the smaller particle end of the aerosol size

(c) Surface winds: The surface winds of more than a few km per hour are effective in lifting and transporting the soil dust of all lands during dry seasons. In modern times the winds continue to create and transport large quantities of surface dust. Even a moderate breeze across a dry, tilled field produces a cloud of dust.

(d) Bursting of bubbles at the sea surface: Due to bursting of number of bubbles formed by cresting waves at all ocean surfaces, small droplets of sea water are injected into the atmosphere [14, 133]. On the average each bubble produces a few large droplets and 100 or more small droplets. The largest are of such a size that the salt residue, which has an effective diameter of 2.0 to 3.0 μm when the water is evaporated. The small droplets tend to give residue less than 0.3 μm in diameter. Most of the droplets are caught up by the wind and transported over great distances. Thus entrained in atmospheric motion, each bit of sea salt is a condensation nuclei, alternating between the crystalline and aqueous states as the relative humidity decreases and increases.

(e) Miscellaneous human activities: Besides above mentioned natural sources, the particulate matters are also introduced into the atmosphere by many man-made activities. Many industrial operations, agricultural activities and construction activities are prolific sources of aerosols. Iron and steel mills, ore smelters and cement plants without which our technologically based society will not be able to exist, inject many forms of mineral dusts into the atmosphere. The particles are mostly non-hygroscopic and exist over a wide range of sizes. The larger ones settle down within minutes of their origin and

distribution. During this process smaller particles get attached to the larger ones and result in rapid decrease in the smaller particle concentration and displacement of maximum concentration towards large particles.

1.1.4 Aerosol Sources

The aerosols are introduced into the atmosphere by various sources. However, in general, the classification can be done on the basis of mode of introduction, i.e. the particles are introduced directly in solid and liquid form or they are as a result of condensation products of gaseous pollutants introduced in the atmosphere by man as well as nature. The two modes lead to difference in size of the particles also. The first generally introduces coarse or bigger particles while the second produces smaller particles. The various natural sources in this category are

(a) Interplanetary dust: Large amounts interplanetary of dust are continually placed in the atmosphere of earth as it moves through 3×10^{16} m³ of space each year [135]. Pettersen [172] estimated that approximately 10^7 tons of the aerosols can be collected in a single year.

(b) Volcanic eruptions: The volcanic eruptions inject huge amount of fine ash into the atmosphere. Over the globe, hundreds of volcanoes erupt in a single year. Among these some are extremely violent in nature and remembered over decades for their effects, like the famous eruptions of Krakatau in 1883, Gunnung Agung in 1963, Mount St. Helens in 1980 and El-Chichon in 1982. The violent eruptions inject particulate matter directly into the stratosphere. There they stay for years and produce spectacular lighting effects and influence the climate as well.

cover the ground surface for miles around. However the smaller ones, about $1.0\ \mu\text{m}$ in size, move with wind and remain suspended for days together.

The condensation of gaseous products is one of the most important natural processes, which introduces aerosols in their solid or liquid form into the atmosphere. This gas-to-particle conversion may result from homogenous gas phase processes, or it may be controlled by process in the particulate phase. The various mechanisms involved in homogenous as well as heterogeneous condensation, given by Friedlander [48] can be classified as I. Homogenous nucleation, II. Heterogeneous condensation.

As the industrialization is increasing, the gas phase chemical reactions become a major source of particles in the atmosphere. The various gaseous pollutants produced by the burning of fossil fuels for energy requirements in automobiles, industries etc. react in the presence of solar radiation and yield the products which condense into particulate phase.

1.1.5 Aerosol Removal from the Atmosphere

There are two processes for direct removal of particles from the atmosphere. These are dry deposition i.e. gravitational sedimentation and wet removal. Wet removal is of two types, namely rain out and washout. In rain out, the particles are incorporated in precipitate nuclei during process occurring within the clouds. Washout involves incorporation of a material into precipitation as a consequence of processes occurring below the cloud. The wet removal processes are important mainly in the lower troposphere where cloud formation exists. These removal processes are highly size-dependent. In the next few paragraphs, their removal has been explained considering the size. Figure 1.1

shows various size ranges of aerosols and their removal processes in the atmosphere. Also Figure 1.2 shows the production and removal of the particulate matter in the atmosphere.

It is generally believed that, particles larger than 5.0-10 μm is efficiently removed from the atmosphere by sedimentation process. The particles have significant settling velocities and deposit on horizontal surfaces quickly. The performance of their removal is affected by the nature of the surface and of the particles and by meteorological and other factors. Falling rain drops also remove the large particles with appreciable efficiencies.

At the smaller end of the size spectrum the particles below 0.1 μm are removed predominantly by coagulation which results due to the collision of these particles with larger particles in the size range from 0.1-2.0 μm and also with each other. Moreover their Brownian motion is sufficiently great that if they approach close to a solid surface a certain fraction diffuses to it and gets removed. Thus these particles are also limited in life-time and are rarely found in significantly mass concentrations away from their sources of origin.

1.1.6 Condensation of Aerosol Particles

The concentrations of aerosol particles depend upon the sources and the meteorological conditions at the sampling site. The instruments, which measure particles over the wide spectrum of size generally give number density in thousands and tens of thousands particles per unit volume of air. At remote places isolated from industrial and other human activities like polar-regions, the number density is quite low, of the order of 100 cm^{-3} [167]. While in cities and industrialized locations, the values as high as 10^6 cm^{-3} have been

reported [186]. Khemani *et al.* [101] studied the Aitken nuclei concentration at different location in India and found that sampling site is highly responsible for concentration (Figure 1.3). Devara *et al.* [39] studied the long term variation in total aerosol concentration at an urban location (Pune, India) and found that the concentration is highly dependent on meteorological conditions (Figure 1.4).

1.1.7 Aerosols in the Troposphere and Stratosphere

As the density of the permanent gases and water vapour of the atmosphere steadily decreases with height, so do the concentration of aerosols. This decrease primarily is an exponential one. However, deviations have been observed at different places for the particles lying in different size ranges. The lower troposphere is usually well stirred by winds and convection currents, so that the mixing of particles to air tends to remain constant in a given weather condition. This mixing region extends from the ground to an altitude of several kilometers. Blifford and Ringer [15] found a fairly constant mixing ratio to about 5 km for particles in the size range 0.5 to 2.0 μm . The mixing ratio may be expressed either as total mass of particles to unit mass of air or as particles concentration to molecular number density. Air density, however, decreases exponentially as a given parcel of air rises and expands so that from this reason alone the particle concentration decreases with altitude. Additional factors responsible for the above are the particle removal processes and the fact that many of the particle sources are at or near the earth's surface.

The aerosols in the stratosphere have been studied extensively by Rosen [181], and Junge [87, 88]. The concentration of particles smaller than 0.1 μm radii decreases rapidly with altitude sometimes become zero near 20

km. The highest concentration at about 20 km is achieved by particles having radii in the range 0.1 to 1.0 μm forming a layer known as Junge layer. At Junge layer most of the particles are sulphates and sulphuric acid droplets.

The layers of particulate above the sulfate layer have often been observed in the stratosphere. For example Meinel and Meinel [138] and Cunnold *et al.* [31] have observed the particulate layer to be at about 50 km. However such higher layers are transient in nature.

1.1.8 Aerosol Size Distribution

The size distribution of aerosols is very important information in the study of the effect of aerosols on atmospheric processes. The size distribution is considered the most prominent physical property of the aerosols, which first attracted the attention of scientists. The aerosol particles are not of the same size as they come into existence due to different processes. These are of different size and follow some distribution function, which are influenced by the meteorological conditions and the sources of aerosols as well. Aerosols generally consist of several modes. Each mode is characterized by one or more dominant constituents (and hence differing refractive indices) and their particles size ranges. It is not possible to define a particular mathematical function, which could be used universally to define the distribution of aerosols. However, the three functions, which have been observed by various workers at different places, are given below.

(a) Exponential size distribution function: A function much used for model aerosols in studies of scattering, one proposed by Deirmendjian [34] is given by

$$n(r) = ar^\alpha \exp(-br^\gamma) \quad (1.01)$$

Where, a , b , α and γ are positive constants. The function vanishes at $r=0$ and ∞ and is known as Deirmendjian modified gamma distribution function when $\gamma = 1$. The aerosol concentration is obtained by integrating equation (1.01) between the limits zero and infinity, and is given by

$$N = a\gamma^{-1}b^{-\left(\frac{\alpha+1}{\gamma}\right)}\Gamma\left(\frac{\alpha+1}{\gamma}\right) \quad (1.02)$$

Where, Γ represents the gamma function.

The mode radius is found by setting the derivative of equation (1.01) equals to zero, which yields

$$r_c^\gamma = \alpha / b\gamma \quad (1.03)$$

When this is substituted in equation (1.01) the distribution becomes

$$n(r_c) = \alpha r_c^\alpha \exp\left(-\frac{\alpha}{\gamma}\right) \quad (1.04)$$

Where $n(r_c)$ is the number of particles per unit radius interval at the value r_c per unit volume.

(b) Power law size distribution function: This function developed by Junge [86, 88] and also described by Manson [129], is given mathematically as

$$n(r) = \frac{dN}{d \log r} = cr^{-\nu} \quad (1.05)$$

Here, $n(r)$ represents the number of particles per unit volume per unit increment of logarithm of radii, N gives the total number of particles per unit volume, c is a constant and depends on the particles concentration and the exponent ν determines the slope of the distribution curve. Figure 1.5 shows distribution

curve for a typical continental and more maritime aerosols. In non-logarithmic form equation (1.05) can be written as

$$n(r) = \frac{dN}{dr} = 0.434cr^{-(v+1)} \quad (1.06)$$

The power law is used very often and is best followed by the particles in the range, $0.1 < r < 2.0 \mu\text{m}$. The generally observed values of v for the continental atmosphere lie in the range, $3 < v < 4$ [135]. The number density, N , can be calculated using the expression,

$$N = 0.434c \int_{r_1}^{r_2} r^{-(v+1)} dr \quad (1.07)$$

Here, r_1 and r_2 being the lower and upper limits of the distribution.

(c) Log-Normal distribution function: A normal (Gaussian) curve is symmetric about its mean. As far aerosols are concerned, their distribution does not follow the normal curve in which the radius is argument. Instead it has been observed that resemblance in the observed nature of curve is better to the normal curve which has been plotted taking $\log r$ as argument. This amounts to using $\log r$ as the measure of size and a log normal distribution is simply a normal curve in which the argument is $x = \log r$ [216]

$$n(x) = \frac{N_0}{\delta\sqrt{2\pi}} \exp\left[\frac{-(x - x_m)^2}{2\delta^2}\right] \quad (1.08)$$

$$\text{or } n(\log r) = \frac{N_0}{\delta\sqrt{2\pi}} r \exp\left[\frac{-(\log r - \log r_m)^2}{2\delta^2}\right] \quad (1.09)$$

Here, N_0 being the total number per unit volume under the curve, δ the standard deviation, x_m is model size parameter and r being the model radius.

Generally the natural aerosol distribution does not exhibit the symmetry found in log-normal distribution. However, for the artificially produced aerosols, the approximation is much close. For natural aerosols, the combination of more than one log-normal distributions are used.

The three distribution functions, described above are well observed distributions. Generally the distribution function fits over a portion of the whole size spectrum of particles. To represents the whole range, people have used combinations of two or more than two log-normal functions. For the present study we have used normal Gaussian distribution function.

1.1.9 Properties of Aerosols

Since the particles in the atmosphere include every mineral exposed on the surface of the earth, every conceivable combustion product, dissolved salts in the sea, meteoritic particles, the products of variety of atmospheric reactions and others, therefore it is not possible to determine properties of the aerosols as a whole. Also the properties tend to vary with particle size and composition. However, a few general physical and chemical properties are listed below.

(a) Surface properties: These properties include absorption, nucleation and adhesion. The behavior is actually due to the collision of individual molecules on the particle surface. This may be elastic as well as inelastic. If this impact is perfectly elastic, there is transfer of some momentum to the particle only. If it is not, there will be a local accumulation of the gas on or near the particle surface, which is adsorption. Adsorption caused by chemical interaction between the surface and the gas is known as chemisorption. If the gas molecules actually

dissolve in the substance of the particle, then absorption is involved. It happens when the particles are in liquid state and chemically similar to the gas [119].

The second major surface property is condensation. The natural formation of clouds and fogs in the atmosphere is an example condensation. Another property of interest is adhesion. It is well established that solid particles with diameter less than about $2.0\ \mu\text{m}$ and liquid particles regardless of size (with the exception of very large raindrops) always adhere, when they collide with each other or with a large particle. Adhesion is important in the growth of fine particles in the atmosphere.

(b) Motion of particles in the atmosphere: The second major property common to all particles regardless of the size and composition, is their motion. The particles on collision, with gas molecules get some kinetic energy. Those with sizes less than $0.1\ \mu\text{m}$ have small mass and due to the momentum transferred by collision, undergo large random (Brownian) motion. Above about $2.0\ \mu\text{m}$, gravitational forces and settling velocities become dominant and momentum is high enough to deviate the particles from the motion of the surrounding medium so the particles are removed from the air by precipitation, sedimentation or a sudden direction change in the surrounding air. In the intermediate size range 0.1 to $2.0\ \mu\text{m}$, sedimentation is decreased as having less inertia compared to the larger particles. So the particles tend to remain suspended for long periods of time. As a result, the particles in this intermediate size range have a relatively long life in the atmosphere.

(c) Chemical composition: Looking at the various sources of aerosol particles, it is not possible to discuss the chemistry of airborne particulate

matter. However, there are some generalizations that are valid for different classes of the particles.

Barring a few exceptions, particles in the coarse size range (diameter > 2.0 μm) are predominantly dust particles raised by natural winds and road traffic. Measurements at number of sites, well separated from specific local sources have shown that the particles in the large size range are the mean composition of the earth's crust i.e. sand, granite, lava etc. exposed on the earth's surface [119]. As a result, the total mass of the particles in this size range can be relatively accurately correlated with the major ingredients like iron, aluminum or silicon [47].

The particle mode between 0.1 and 2.0 μm also contains traces of many elements, which vary with location and time. But this range of particle size is simpler in its major ingredients than are the larger particles. Predominantly this mode is composed of sulphates, nitrates, ammonium, lead, bromine, carbon and organic material. These are the species that are formed by reactions and condensation processes in the atmosphere. The relative amounts of these ingredients vary from one location to another, but their sum is very close to the total mass of particles in the size range 0.1 to 2.0 μm .

There is not much information available on the chemistry of the particles smaller than 0.1 μm in diameter. In all probability they are similar in composition to the accumulation mode particles, which are formed by coagulation. These nuclei mode particles represent too little mass and are very short lived in the atmosphere.

1.1.10 Interaction of the Atmospheric Particles with Light

The interaction of electromagnetic radiation with the constituents of the atmosphere, which is of importance, can be classified as given below

(1) Elastic scattering

(i) Rayleigh scattering, and (ii) Mie scattering

(2) Inelastic scattering

(i) Resonance scattering, and (ii) Raman scattering.

In the elastic scattering the wavelength of the scattered light is same as that of the incident wave. It shows that there is no interchange of energy between the interacting radiation and the scatterer, only redistribution of the incident light occurs. Rayleigh theory explains the scattering of light by very small particles like gas molecules, while Mie scattering deals with the interaction of radiation with the particles comparable to or larger than the wavelength of radiation.

The inelastic scattering involves the exchange of energy between the two, scatterer and the incident photon. A photon incident on the scatterer, gets absorbed and the scatterer is elevated to higher energy state. This energy state is for very short time ($\sim 10^{-8}$ sec.). If during this time it undergoes collision with some other atom or molecule the energy is transferred to the colliding particle. In other words the energy is utilized in heating up the system. This is also termed as true absorption.

The second possibility being that the scatterer return to its original or ground state after the excitation period is over, thus emitting the radiation back. In case of resonance scattering the wavelength of the emitting photon is similar

to two wavelengths of the absorbed quanta. When the frequency of the scattered radiation is shifted with respect to excitation frequency, the amount of shift being characteristic of the scattering molecule is known as Raman scattering. The scattering in which the scattered radiation is shifted to the lower frequency side of the excitation frequency is called the Stokes scattering and one in which shifts towards the higher frequency side is called the Anti-Stokes scattering. But the probability of occurrence of Anti-Stokes scattering is far less than the Stokes scattering at normal temperatures.

(a) Rayleigh theory: The colorful displays in sky have always attracted the scientists. However, it was Lord Rayleigh, who provided an explanation of such optical phenomenon on the basis of scattering of light by the molecules of the atmospheric gases. He assumed the particles or scatterer to be isotropic, spherical, far smaller than the wavelength of light and very dense with respect to the surrounding medium. On the basis of these simple assumptions, employing the elastic-solid ether theory he has given certain postulates. According to these, the scattering varies directly as the square of the particle volume and inversely as the fourth power of the wavelength [135].

The energy distribution in case of scattering of electromagnetic radiation by a molecule (Rayleigh scatterer) is given in terms of angular scattering cross-section. It is defined as the cross-section of an incident wave, acted on by the molecule, having an area such that the power flowing across it is equal to the power scattered by the molecule per steradian of a particular angle θ . Mathematically it can be written as

$$\sigma_M(\theta)I_o = I(\theta) \quad (1.10)$$

Where, I_0 is the irradiance of the incident wave, $\sigma_M(\theta)$ is the angular scattering cross-section and $I(\theta)$ is the intensity of scattered light.

As in practice, we deal with the scattered light by the scatterers in a particular volume, as scattering cross-section of a single molecule is very small and the atmospheric density of gas molecules is very high. The parameter, which represents the angular scattering characteristic of a unit volume is volume angular scattering coefficient and is found directly from the angular scattering cross-section of a molecule.

The volume angular coefficient represents for angular characteristics of unit volume of scatterers and is given by

$$\beta_M(\theta) = N\sigma_M(\theta) \quad (1.11)$$

Here $\beta_M(\theta)$ represents the volume angular coefficient and N is the number of molecules per unit volume.

The most general relation for the volume angular scattering coefficient for the incident unpolarized light is given by

$$\beta_M(\theta) = \frac{\pi^2(m^2 - 1)^2}{2N\lambda^4} (1 + \cos^2 \theta) \quad (1.12)$$

Here m is the refractive index of the scatterer, λ the wavelength of the incident radiation and θ the angle of scattering.

The expression for the scattered light intensity $I_M(\theta)$, can simply be given as

$$I_M(\theta) = \frac{3\pi^2(m^2 - 1)^2}{8N\lambda^4} \left(\frac{6 + 3\rho}{6 - 7\rho} \right) (1 + \cos^2 \theta) I_0 \quad (1.13)$$

I_0 , being the irradiance of the incident unpolarized light, p is the polarization factor and $(6+3p)/(6-7p)$ is the correction factor for molecular anisotropy.

(b) Mie theory: The theory of scattering of electromagnetic waves by the particles quite small in comparison with the wavelength of radiation is able to explain many optical phenomenon in nature. However, certain other phenomenon like gray hue appearance at the horizon, very faded color of rising and setting sun etc. led to the development of a theory which could explain the scattering of electromagnetic radiation by particles comparable to or even larger in size than the wavelength of interacting radiation. The present theory known as Mie theory is the most general one and it is applicable even for the smaller particles. It has been developed by many workers principally from the basic research by Mie [141] on scattering by colloidal metal particles. Hodgkinson [69], Logan [120] and others contributed in the development of the Mie theory of scattering.

The basic principles involved in Mie theory are the same as in Rayleigh theory. However, since a particle consists of many molecules, the treatment here is quite complex. Here, the interaction of electromagnetic radiation with the electric charges, that constitute matter, is considered. An aerosol particle consists of many closely packed complex molecules and may be considered an array of multipoles. These are excited by the primary and incident waves, thus creating oscillating multipoles. The multipoles give rise to secondary electromagnetic waves, which combine in the far field to produce the scattered wave. These secondary waves are called partial waves. The partial waves are represented in theory by successive amplitude terms in a slowly converging

series whose squared summation gives the scattered intensity at a particular observation angle. Because the size of the particles is comparable to the wavelength, the phase of the primary wave is not uniform over the particle, resulting the spatial and temporal phase differences between the various partial waves [135].

Where the partial waves combine to form the secondary or scattered wave, as the detector would sense, interference caused by the phase differences occur between the partial waves. The interference depends on the wavelength of the incident light, the size and refractive index of the particle and the angular location of the detector. Thus sharp variations in scattered intensity are found when the detector is moved around the particle to various observation angles. The complexities in the angular distribution pattern increases as the particle size increases.

The scattered light intensity in a direction θ when the particle is incident upon by unpolarized electromagnetic radiation is given as

$$I(\theta) = I_0 \frac{\lambda^2}{4\pi^2} \left(\frac{\rho_1 + \rho_2}{2} \right) \quad (1.14)$$

Here, I_0 is the irradiance of incident radiation, λ is the wavelength and ρ_1 and ρ_2 are the intensity distribution functions corresponding to the perpendicular and parallel polarized components respectively. These functions depend on the size, refractive index of the scatterer and wavelength of the radiation as well as angle of scattering. They can be defined as

$$\rho_1 = \int I_1(\theta, \lambda, m, r) n(r) dr \quad (1.15)$$

$$\rho_2 = \int I_2(\theta, \lambda, m, r) n(r) dr \quad (1.16)$$

Here, $I_1(\theta, \lambda, m, r)$ and $I_2(\theta, \lambda, m, r)$ are intensity distribution function for a single particle at a scattering angle θ , wavelength λ , refractive index m and radius r .

Mathematically these are given as [74]

$$I_1(\theta, \lambda, m, r) = \left| \sum_{j=1}^{\infty} \frac{2j+1}{j(j+1)} (a_j \pi_j + b_j \tau_j) \right|^2 \quad (1.17)$$

$$I_2(\theta, \lambda, m, r) = \left| \sum_{j=1}^{\infty} \frac{2j+1}{j(j+1)} (a_j \tau_j + b_j \pi_j) \right|^2 \quad (1.18)$$

Where, j is a positive integer. Each intensity function is found as the sum of an infinite series. Each series converges slowly, when the size parameter ($x = 2\pi r/\lambda$) becomes greater than unity. The number of terms required for satisfactory convergence is somewhat greater than the value of x . The values of a_j and b_j (Mie coefficients) are found from Ricatti-Bessel functions, whose arguments are formed from the particle characteristics i.e. size parameter(x) and refractive index(m) but are independent of the scattering angle(θ). The functions π_j and τ_j in the above expression depend only on the angle θ and involve the first and second derivatives of Legendre polynomials having order j and argument $\cos \theta$. For the practical purposes measurements are carried out for the scatterers in the particular volume.

1.1.11 Implications of Aerosols

(a) **Effects on radiation budget in the middle atmosphere:** As the topic of radiation budget in middle atmosphere is extensively huge and is also beyond the scope of this presentation however, a very little attention is drawn here. For

the sake of completeness a few of the important aspects of this are being presented here.

The radiation field should be defined at each point in space and for each wavelength of interaction of radiation with the atmosphere and resulting aeronomic thermal effects. The analysis of the radiation field can be done from the equation of radiative transfer [24, 106]. The radiative transfer equation expresses the energy balance in each unit volume of the atmosphere including absorption, scattering and emission. The equation can be solved by analytical methods only for the simple cases. To obtain quantitative solutions numerical methods are generally used [118]. However, a detailed discussion on the role of aerosols in radiation budget of the middle atmosphere has been given by Krishana Murthy [108]. The most important elements contributing to the middle atmosphere radiation budget in terms of cooling and heating rates are O_3 , O_2 , NO_2 , H_2O and CO_2 . The mean heating due to O_3 is balanced by the corresponding cooling due to infrared radiation from CO_2 , O_3 and water vapour.

(b) Role of aerosols in atmosphere heating: Aerosols absorb energy from the solar and planetary radiation fields and exchanges energy by collisions with the ambient gas and emits thermal radiation. In cases of possible phase change, they acquire or lose latent heat. The collisional heat exchange with the ambient gas depends upon the temperature and density of the ambient gas and also upon the temperature of the particles.

During volcanic eruptions when stratospheric aerosols loading increases enormously the aerosol heating rates become significant. For example, the results of Cadle *et al.* [19] indicates that the fine ash particles from the

Mt. Agung (1963) eruption were located during the winter of 1964/65 in a broad latitude range over the equatorial region. There is a clear indication of a large temperature increase at the two altitudes of 16.5 and 19.5 km (stratosphere) associated with the Mt. Agung (1963) eruption. There is no significant effect noticeable at 9.5 km. An increase in stratospheric temperature is reported due to the El Chichon volcanic eruption in 1982 and Mt. Pinatubo in June 1991.

(c) Effects on climate: Any change in the radiative balance of the earth, including anthropogenic increase in green house gases or in aerosols will tend to alter atmospheric temperature and the associated circulation and weather patterns. During the past two decades a number of numerical modeling studies have been undertaken to assess the effect of increasing greenhouse gases on the earth's climate [30, 125, 137, 154, 214]. The numerical experiments performed with the coupled ocean-atmosphere general circulation models (GCMs) estimated that the increase in greenhouse gases in the atmosphere increases the global temperature of about 0.6-1.3⁰C [78]. In reality, the global mean temperature have risen by about 0.45±0.15⁰C. In 1994 Climate Change Report of the IPCC (Intergovernmental Panel on Climate Change)[79] has identified sulphate aerosols as a secondary but potentially important component that can affect the climate system by changing the radiative balance of the atmosphere. Sulphate aerosols interact mainly with solar radiation and enhance the earth's albedo thereby cooling the surface temperature [26]. Lal *et al.* [109] suggested that the mean surface temperature over the mean subcontinent could rise by $\geq 2^{\circ}\text{C}$ in the next 100 years due to increasing of anthropogenic greenhouse gases.

(d) Effects on precipitation: Over the last 20 years many authors have shown that urban and industrial emissions have altered downwind precipitation patterns and amounts. Landsberg [110] has reported 5-15% increases in precipitation downwind of large urban areas. Changnon [25] has reported an increases of 31% at La Porte, 30 miles east of Chicago. Hobbs *et al.* [68] have reported increases of 10-30% precipitation, downwind of sources such as wood pulp processing plants and metal refining operations. Huff and In all the studies, authors compared recent precipitation levels for sites in the area with either earlier records for the same sites or with precipitation at nearby sites not under the influence of urban or industrial sources.

In Indian context, an increase in monsoon rain about 2mm day^{-1} has been predicted when green house gases were taken into account [13, 20]. Also a decrease of about 0.5 mm day^{-1} in summer monsoon rain fall for the decade 2040s has been predicted when greenhouse gases and aerosol forcing taken into account.

(e) Effects on materials: The effects of particulate matter on materials include corrosion of metals when the air is humid, erosion and soiling of buildings, sculpture, painted surfaces and clothes. Another problem caused by particulate matter is corrosion and damage of electronic equipments, especially through chemical or mechanical action on electrical contacts.

(f) Toxic effects of aerosols: The toxic effects of particulate matter on animals and human being can be classified as intrinsic toxicity due to chemical or physical properties, interference with clearance mechanisms in the respiratory tract, and toxicity due to adsorbed toxic substances.

Many toxic particles have been discovered in polluted urban atmospheres, including metal dusts, asbestos and aromatic hydrocarbons such as the carcinogen 3, 4-benzpyrene. Their concentrations are generally extremely small but they may play a role in the higher cancer rates that occur in urban areas as compared to rural areas even after taking into consideration the greater amount of smoking that occurs in urban areas [119].

1.2 ATMOSPHERIC ELECTRICITY: A BRIEF HISTORY

The existence of electricity in the earth's atmosphere was first discovered by d'Alibard [4]. Being unknown of Alibard's discovery, at the same time Benjamin Franklin proved the existence of electrical charges in thunderclouds. Larsen [112] established the multi stroke structure of lightning flash by photographic experiments. Wilson [227] was first scientist who made an extensive effort to study the electric fields produced by lightning. Boys [16] invented a camera, which proved to be very useful for lightning research. Appleton *et al.* [9] and Schonland and Craib [187] measured the field changes and concluded that thundercloud is an electric dipole with a net positive charge in the upper and net negative charge in their lower part. The reason of being atmosphere electrically conducting is the existence of ions in the atmosphere due to radioactivity and cosmic rays [45].

Wilson [229] suggested that all thunderclouds over the earth are electrical generators of atmospheric electrical phenomenon, which by their violent discharges continuously supply electrical charge to the earth-ionosphere system. This hypothesis has been supported by the observations of electric

field at the oceanic stations, where the diurnal variation of electric field is parallel to the diurnal variation of thundercloud activity [81].

Experimental and theoretical studies on thundercloud electrification and critical assessment of various charge generation have been provided in literature [56, 76, 113, 114, 134, 158, 160, 185, 207, 222]. The studies on atmospheric electricity not only include the study of thunder cloud activity and measurement of atmospheric electrical parameters but it is also affected by the many other parameters viz. the earth's orography, aerosols and pollutants, solar activity etc. Markson [132] and Herman and Goldberg [66] have suggested some physical mechanisms for solar terrestrial relationship. The aerosols ejected from volcanoes also affect the atmospheric electric circuit at stratospheric heights [139].

Hays and Roble [65] presented a comprehensive analytical model for the global electric circuit (GEC) using spherical harmonic functions. Makino and Ogawa [123, 124] and Sapkota and Varshneya [184] also presented numerical models for the global electric circuit.

1.2.1 Ion Production in the Atmosphere

The presence of ions in the air is mainly responsible for the existence of electrical phenomenon in the atmosphere. In the earth's atmosphere ions are produced by different agencies. Above about 65 km altitudes the main sources of ionization is the electromagnetic radiation from sun. Below about 65 km, galactic cosmic rays (GCR) and solar cosmic rays (SCR) are the main sources of ionization. But below about 3 km altitude, the dominant source of ionization

is the radioactive emanation from the earth crust and airborne radioactive substances.

(a) Cosmic rays as sources of ion production: The cosmic rays are the charged particles from the space either of galactic (GCR) or solar (SCR) origin. In the region, where the ionization is due to SCR, the rate of ionization shows large variations with time because of the variation in the incident cosmic ray due to variant solar activity.

The intensity of galactic cosmic rays is modulated over a solar cycle [182] and are almost isotropically distributed in the vicinity of earth [66]. The earth's geomagnetic field further alters the incident flux before entering in the earth's atmosphere. GCRs are having high range of energy from tens of MeV to hundreds of GeV, which allows them to penetrate deep into the earth's atmosphere and produce secondary radiations. Neher [157] found from his balloon measurements that the ionization rate is modulated over a solar cycle and is a function of altitude and geomagnetic latitude. The galactic cosmic ray activity varies by about a factor of 2 in the lower atmosphere between the equator and pole [65, 81]. The maximum ion production takes place at altitudes from about 12 km to 20 km depending upon the season, phase of solar cycle and latitude.

(b) Other sources responsible for ionization: The radioactive elements, present in the earth's atmosphere also contribute to the ionization of air. The natural radioactivity of air is borne by the radioactive inert gases released from rocks, soils and plants transpiration etc. Rocks and soils contain radioactive elements like uranium and thorium. Nuclear radiations emitted from these

elements ionize the air in a thin layer close to the ground surface. The decay products of these elements are radioactive gases like radon, thoron and actinon, which are carried upward in the air and produce ionization there. Since the occurrence of radioactive minerals varies from place to place, the ionization also depends upon the place.

There are some other sources in the atmosphere whose contribution to the total ionization is small but may be important at specific locations. The lightning discharges and point discharges are important among them. Lightning is produced mainly as a part of thundercloud activity. Similar discharges have been observed during volcanic eruptions and dust storms [90]. There are some common processes also, which can generate ions i.e., water splashing at the bottom of the water fall [173], ocean waves [14, 151], human activities like industrial plants, automobile exhaust [21, 149] etc. and structures like high voltage power transmission lines, communication towers, chimneys etc. [92].

1.2.2 Atmospheric Electrical Parameters

There are three basic atmospheric electrical parameters, namely, electric field (E), conductivity (σ) and current density (J). They are related by simple Ohm's law, $J = \sigma E$.

In the classical picture of global atmospheric electric circuit, the ionosphere is assumed to be maintained at a constant potential. The current density can be obtained dividing ionosphere potential by columnar resistance (the resistance of a vertical column of unit cross-section). In this picture the electrical conductivity is an independent parameter while the electric field and

current density are dependent parameters. The local conductivity shows diurnal variation and can dominate the behavior of the electric field.

1.2.2.1 Variation of atmospheric electrical parameters

The atmospheric electrical phenomenon can be studied in two different areas, the fair weather region and the disturbed weather region. The diurnal and seasonal variations of the electrical parameters usually refer to the variations during fair weather.

The atmospheric electrical parameters do not remain in the constant steady state at all the times as they are affected by various environmental factors. There are two types of variations in electrical parameters: one is global in nature and the second is of local origin.

(a) Diurnal variations: It has been observed that the atmospheric electric field under fair weather conditions displays a typical universal time (UT) dependent diurnal variation. Wilson [228] pointed out a global maximum at a time when thundercloud activity was at a maximum.

The ionospheric voltage depends upon the thundercloud activity, which results due to the flow of upward charging current. A high thundercloud activity results in a higher ionospheric voltage. This in turn reflects in a well defined diurnal variation pattern of the vertical electrical field observed over the oceans and on remote areas of the Antarctica.

Takagi and Kanada [212] observed that the electric field variations on the same day at a two or three globally representative stations often show a good likeness between their patterns. Takagi and Iwata [211] also observed an UT-dependent diurnal variation in the electric field measured over pacific

ocean. Figure 1.6 [147] shows diurnal variations of electric field (E) and conductivity (σ) and current density (J) for fair-weather conditions over pacific ocean.

Some investigators have also reported a double oscillation type variation of electrical parameters at the stations situated at the populated areas with heavy pollution [81, 179]. Such variations are shown in Figure 1.7. Also the variation of electrical conductivity as a function of altitude is shown in Figure 1.8.

(b) Seasonal variations: The mean diurnal variation of electric field and conductivity in summer and winter at Hongo (Tokyo) has been shown in Figure 1.9. In winter the conductivity in general is low and the electric field is high, but in summer the conductivity increases while the electric field decreases. Similar trends was also obtained by Uchikawa [217] and Manes [126] that the maximum potential gradient occurs in winter and minimum in summer. Takagi and Iwata [211] also observed that the electric field shows a characteristic diurnal variation, which regularly altered its phase according to season. In summer, the electric field variation is mainly due to the diurnal variation in conductivity but in the winter when there is a little or no diurnal variation in conductivity, the electric field is similar to the world wide universal pattern.

1.2.3 Electrical Conductivity of the Atmosphere

The conductivity of the air is produced by ions of both signs i.e. positive and negative in the atmosphere. These ions move in the electric field E, under the force of field. The atmosphere obeys the Ohm's law. If J is the current density (current across unit area) and E is the electric field then $J/E=\sigma$, where σ

is called the specific conductivity or simple conductivity. It is measured in $\text{ohm}^{-1}\text{meter}^{-1}$ or mho/meter or Sm^{-1} . In atmospheric electricity it is convenient to measure conductivity rather than resistance because different ion species simultaneously contribute towards the conduction of current in parallel in the vertical across the equipotential surfaces in atmosphere. So the total conductivity can be obtained by adding contributed by different ions species.

1.2.3.1 Variation of conductivity and electric field

The measurements of conductivity over land and oceans have shown that over the oceans it is higher than over the lands. An average land value is about $1.8 \times 10^{-14} \text{ mho m}^{-1}$ while over the oceans it is about $2.8 \times 10^{-14} \text{ mho m}^{-1}$ [22]. Most of the studies have shown that fine weather conductivity lies maximum in the early morning hours with a fall in it following the time of sunrise. This fall of conductivity is accounted because of two reasons. At such a time the formation of mist or fog particles causes lose of small ions due to high humidity [46, 204]. Secondly, during the sunrise, the increase in nuclei, close to ground causes an increase in large ions. Thus in both circumstances the reduction in conductivity is a normal phenomenon. During winter, the minimum in annual conductivity is attributed to relative increase in nuclei concentration. To support the information furnished above, Figure 1.6 show diurnal variation of electrical conductivity, field and current density over pacific oceans [147]. Figure 1.10 shows conductivity variation at Kew, a land station, during winter and summer [22].

The fair weather electric field varies considerably from one part of the world to another. The range of surface level fair weather mean value of electric field depends on the local conditions decided by AN concentrations and levels of pollution there. It is observed that this mean value may lie in the range $50\text{-}300 \text{ Vm}^{-1}$ [22, 84, 178, 194, 206, 221]. Such a significant variation of electric

field is attributed to the variation of the conductivity of the lowest layers of the atmosphere.

Over the oceans and a few remote locations free from the sources of pollution, there is a single period with a simultaneous world wide maxima (Figure 1.6). At most land stations the times of maxima and minima depend on local time and local influences. In many cases, double oscillations occur with minima from 0400 to 0600 hrs (local times) and from mid day up to 1600 hours while the maxima occur during 0700 to 1000 hrs and 1900-2100 hrs.

1.2.4 Effects of Aerosols on Electrical Parameters

It has been found from balloon measurements that the electric conductivity is caused mainly by cosmic rays and it increases almost exponentially with altitude from its average ocean surface value of about 2.8×10^{-14} mho m^{-1} [51]. Table 1.2 contains summary of measurements of electrical conductivity by various investigators at different places. It is generally believed that the measurements of atmospheric electrical parameters over ocean leads to a better understanding of the physical processes involved rather than the measurements over land. This is because of the global increase of man-made aerosols due to various human activities, which reduces the electrical conductivity. The atmospheric particles consists small ions with high mobility, which are the main carrier of electrical conductivity and large ions with low mobility, which ~~do not~~ contribute in atmospheric electrical conductivity. As aerosols increases the small ions decreases due to attachment with the aerosols which causes decrease in the electrical conductivity. So the measurements of electrical parameter over oceans are justified to provide natural results. In the middle of ocean also the conductivity gradually decreases due to the global pollution of the atmosphere

[209]. The average conductivity drops by about 50% from 1.6×10^{-14} mho-m⁻¹ in 1966 to about 0.8×10^{-14} mho m⁻¹ in 1974 [126]. This decreasing trend in conductivity is attributed to a significant rise in aerosol concentration. Retalis and Retalis [179] measured the diurnal, seasonal and yearly variation of electrical parameters at Athens, Greece (a highly polluted and heavy industrialized area). The mean values of electric field were found 314.4 Vm⁻¹ and 335.2 Vm⁻¹ for all weather and for fair-weather, respectively. Kandalgaonkar and Manohar [96] also measured the electric field at Athens and obtained the same order of electric field as obtained by Retalis and Retalis [179].

The product of local conductivity and the local vertical electric field with an atmospheric column gives an air-earth current flowing downward. Markson [132] observed that the air-earth density is particularly sensitive to the local variation in columnar resistance and convection of space charge. The columnar resistance is also a parameter, which is proportional to the aerosol concentration. The columnar resistance of the air in all fair-weather regions of the atmosphere is of the order of 10^{17} ohm m² [52]. It varies with time and space. The maximum columnar resistance lies in the exchange layer which is again attributed to the aerosol concentration and is strongly dependent on weather conditions [150]. This is the reason that the average current density is lower in the areas of columnar resistance varying in magnitude.

1.3 THE IONOSPHERE

Perhaps the most important effect of solar ultraviolet radiation on the upper atmosphere is the ionization of its constituent gases. The ionization

commences from a height of about 60 km and extends up to the highest limit of the atmosphere. The density of ionization is not uniform throughout this region. There are "regions" or "layers" of high ionization. These ionized regions known collectively as ionosphere (a name given by Watson Watt) play a fundamental role in the propagation of radio waves around the curved surface of the earth, long distance radio communication, maintenance of atmospheric electricity and others.

There are four regions mainly in which ionosphere has been divided.

These are

- (i) D region (between 60 to 90 km),
- (ii) E region (between 90 to 170 km),
- (iii) F_1 region (between 170 to 250 km) and
- (iv) F_2 region (above 250 km).

Figure 1.11 shows some physical features and the phenomena occurring in the upper atmosphere. This illustration is particularly applicable to the density distribution above 100 km, which is subject to uncertainty due to uncertainty of temperature distribution.

During daytime another region of ionization E_2 is sometimes formed immediately above E. Region D is mainly an absorbing region particularly for medium frequencies. This region is produced during daytime only. At night this region disappears. Out of these F_2 and E are more persistent layers. The intermediate region F_1 is also observable during daytime only. It coalesces with F_2 at night forming a single region F (Figure 1.12). The E and F_2 regions are also known as Kennelly-Heaviside and Appleton layers respectively.

1.3.1 Production of Ions in the Ionosphere

The ionosphere is formed primarily by the ionization of neutral gas atoms/molecules present in the upper atmosphere by exposure to solar radiation. When the high energy photoelectrons/photons collide with neutrals, they produce positive ions and free electrons having energies about tens of electron volts (eV). These electrons can travel long distances in the ionosphere and produce more ion-electron pairs by collision with other neutrals. This process continues until the electrons thermalize and attain the energy of few eV. These are called thermal electrons and form more than 90% of the flux in the ionosphere.

1.3.1.1 Primary photochemical processes

As mentioned above the ionospheric structure is dominated by the photochemistry. The results of primary photo-chemical changes are mostly decided by the relative rates of different chemical reactions occurring in the ionosphere.

When a neutral molecule absorbs an energetic photon, the process leading to electronic excitation can be written symbolically as



Figure 1.13 represents the various processes that the molecule AB^* can go through. Here those processes have been presented those encountered frequently in the terrestrial atmosphere. Process (i) and (ii) end up with some kind of fragmentation. Route (iii) gives rise to re-emission of radiation as luminescence and if it is an allowed transition, it is called fluorescence and if it

is a forbidden transition, it is called phosphorescence. Process (iv) represents intra-molecular energy transfer generating a new electronic state of the same molecule by a radiationless transition. Process (v) represents inter-molecular transfer of energy quietly to a different molecule. Quenching (vi) is a special case of inter-molecular energy transfer where electronic excitation is degraded to vibrational, rotational and translational modes. Process (vii) includes all processes where chemical reaction becomes possible because the reaction rates may be enhanced due to the excited nature of reactants.

The free electrons and ions produced by these processes are primarily responsible for introducing errors in radio signals. These errors introduced in phase, amplitude and frequency of radio wave propagation and are very important in satellite communication, geodesy, navigation and many other fields. Since the characteristics of the ionosphere show large spatial and temporal variations therefore to characterize it, the study of its basic constituents are necessary.

1.3.1.2 Thermal structure of the ionosphere

In the ionosphere, the temperature of neutrals, ions and electrons are usually different and sometimes this difference can be amazing. This difference can be appreciated if we look into the heating mechanism of the ionosphere. The dominant sources are solar EUV and X-rays with some additional and significant sources which participates in Joule Heating and particle precipitation at high latitudes. In the process of photo-ionization photoelectrons with high energy are produced. These high energy electrons collide with neutral particles increasing their internal energy (i.e. electronic excitation) which radiate in

longer wave lengths and hence do not contribute to local heating. Until seventies, it was believed that the heating efficiency of photons in the ionosphere was about 30% of total heating by all of its constituents [23]. Later estimations brought down the efficiency to as low as 5%, with most of the energy going into space through air-glow emissions from atomic and molecular states excited through the inelastic collision process.

In the lower thermosphere, a good part of the potential energy of the ions is lost to lower altitudes during the dissociation of molecular oxygen. When the photoelectrons cool down to a few eV, they collide with ambient electrons (elastic collisions) and also with ions (coulomb collisions). Collisions with neutrals are more important below 200 km. Subsequently, the ambient electrons pass on the heat to the neutrals via the ions. This is why generally electrons have a larger temperature than ions and neutrals and the ions more than neutrals ($T_e > T_i > T_n$) (Figure 1.17).

1.3.2 Studies on the Ionosphere

Over the last several years so many theoretical models have been developed in order to determine the extent to which chemical and transport processes affect the ion composition and electron density as well as their thermal behavior in the ionosphere [10, 17, 103, 104, 121, 188, 189, 191, 202, 205, 220, 226]. These studies show that the ionosphere is highly influenced by solar EUV radiation, energetic particle precipitation, diffusion, thermospheric winds, electrodynamic drift, energy-dependent chemical reactions and magnetic storm.

Schunk and Raitt [190] presented an improved model, which gives the

ion composition changes with solar activity, season and geomagnetic activity. This model takes account of diffusion, electrodynamic drifts, thermospheric winds and ion production due to solar EUV radiation and energetic particle precipitation. This study was limited to the daytime study and performed for geographic latitude 80° N. This model gives the information of ions like N^+ , NO^+ , O_2^+ , N_2^+ , O^+ . They found that the change in the atmospheric composition due to solar cycle, seasonal and geomagnetic activity variations has pronounced effect on the high-latitude ion densities and composition. Solar zenith angle also plays very important role. Some results of this study has been presented in Figure 1.14. It shows the ion densities (N^+ , He^+ , NO^+ , O_2^+ , N_2^+ , O^+) profile with altitude for summer and winter season and for solar maximum and high geomagnetic activity. From this Figure it is clear that the maximum contribution is by O^+ ion which is more dominant in summer season.

Again in 1982, Schunk and Sojka [192] improved there model including thermal conduction and diffusion-thermal heat flow terms. This study was performed for geographic latitude 73° N. By this model, they studied the ion temperature variations and density at middle and low latitudes. Figure 1.15 shows ion density (O^+) profile with altitude for solar maximum and solar minimum, for summer and winter and for high and low geomagnetic activity. Figure 1.16 presents some results of ion (O^+) temperature variations for the same conditions as discussed above. In general it was found that the ion temperature is higher in summer than winter and in the solar maximum condition. At high altitudes the ion temperature profile becomes isothermal because of ion thermal conduction. The electron and neutral temperature

profiles with altitude have been presented in Figure 1.17 for solar maximum and solar minimum conditions for summer and low geomagnetic activity. At all altitudes ion temperature is considerably below the electron temperature, which reaches 3000 K at the upper boundary.

1.4 PRESENT WORK

The present thesis presents some experimental studies on atmospheric particle concentration, their size distribution and surface atmospheric electrical conductivity during different weather conditions, like monsoon, winter season and solar eclipse period. The variations in particles concentration, their size distribution and electrical conductivity have been studied in relation to some meteorological parameters like wind speed, temperature, humidity and rainfall. These studies have been carried out at the University of Roorkee, Roorkee, India, during above mentioned periods. This presentation also includes a study of ion electron density and temperature anomalies of the ionosphere. The data for this purpose has been obtained from Retarding Potential Analyzer (RPA) payload of SROSS-C2 satellite mission of ISRO, India, operative since May 1994. This work is a joint effort of the University of Roorkee, Roorkee, National Physical Laboratory (NPL), New Delhi, and Indian Space Research Organization (ISRO), Bangalore, India. The behavior of ion-electron temperature and density has been studied in relation to altitude, longitude and latitude.

The instrumentation part of the thesis has been given in chapter II. It gives the detailed description of the instruments used for aerosol and electrical conductivity measurement. The theory used for this purpose has also been

given in brief. The tropospheric aerosols and electrical environment are closely related to the solar activity. Atmospheric ions play an important role in governing the aerosol and electrical conductivity at the ground surface. The solar eclipse is an important event to modulate the galactic cosmic rays and solar cosmic rays and hence the ionization at the ground surface. So an experimental study of aerosol concentration and atmospheric electrical conductivity has been given in chapter III. Variance of these factors in view of some meteorological parameters has also been presented. Various meteorological changes (i.e. different weather conditions) may have influence on the atmospheric aerosols and the surface electrical conductivity. Therefore some experimental studies on tropospheric aerosols and conductivity have been done for the monsoon period and fair-weather region (winter) at Roorkee, India and have been presented in chapter IV. The ionospheric weather has become the most important phenomena these days. Thanks to extensive research, which has provided the knowledge that ionospheric system varies markedly with altitude, latitude, longitude, universal time, season, solar cycle and solar flares. The ion and electron temperature and density fluctuations are associated with the ionospheric structure. Chapter V is dedicated to the studies of ion-electron temperature and density anomalies with respect to altitude, longitude and latitude in the ionosphere and tropospheric weather. In last a brief conclusion of the thesis and the scope for further research in the relevant related areas has been given in chapter VI.

Table 1.1- Estimate of Particle Production (10^6 tons/year)

Source		After Peterson and Junge [171]	After Hidy and Brook [67]
Man Made	1. Direct Particle Production		
	Transportation	1.8	
	Stationary fuel sources	9.6	
	Industrial Processes	12.4	
	Solid waste disposal	0.4	
	Miscellaneous	5.4	
	Sub-total	29.6	37-110
	2. Particles formed from gases		
	Converted Sulphates	200	110
	Converted Nitrates	35	23
	Converted Hydrocarbons	15	27
	Sub-total	250	160
	Total Man made	280	197-270
	Natural	1. Direct Particle Production	
Sea salt		500	1095
Wind blown dust		250	60-360
Volcanic emissions		25	4
Meteoritic debris		0	0.02-0.2
Forest fires		5	146
Sub-total		780	1610
2. Particles formed from gases			
Converted Sulphates		335	37-365
Converted Nitrates		60	600-620
Converted Hydrocarbons		75	182-1095
Sub-total		470	2080
Total Natural Sources		1250	3690
Grand Total		1530	3960

Table 1.2- A Summary of Measurements of Electrical Conductivity (σ) by Various Investigators

Investigators	σ 10^{-14} Sm^{-1}	Place	Remarks
Gish [52]	2.80	Ocean	
Chalmers [21]	2.80	Ocean	Average values over ocean surfaces
Ruhnke [[183]	3.30	Greenland	Positive polar conductivity
	1.70	Greenland	Negative polar conductivity
Cobb and Wells [29]	1.97	North Atlantic	
Mani <i>et al.</i> [127]	1.50	Indian Coastal Regions	
Misaki <i>et al.</i> [143]	2.54	North Pacific Ocean	
Mortia and Ishikawa [148]	2.30	North Pacific Ocean	Measured in 1968
	2.10	North Pacific Ocean	Measured in 1970
	2.06	Bonin Island	
Sapkota and Varshneya [184]	1.50	North Pacific Ocean	Less effect of pollution over high mountains plains having high pollution
	2.00	South Pacific Ocean	
	>10.00	High Mountains	
	0.50	Plains	

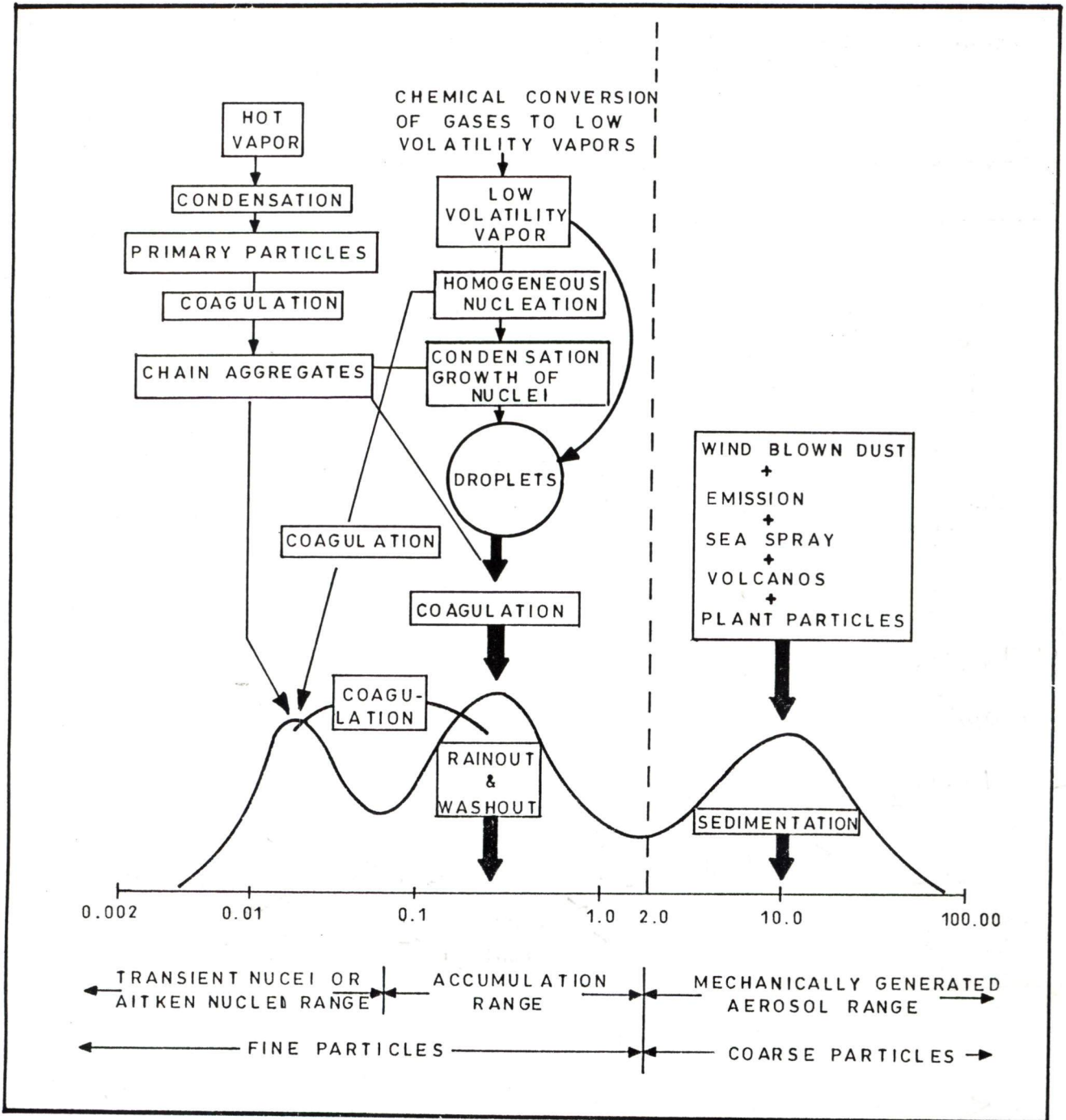


Figure 1.1 - Surface area distribution of atmospheric aerosols and principal removal mechanisms [174]

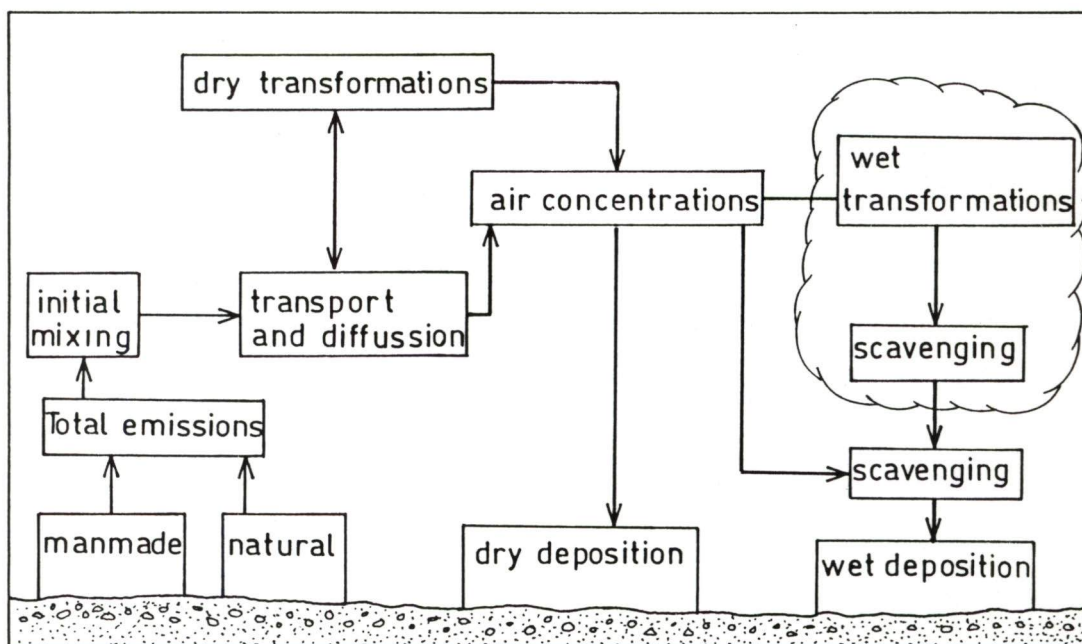


Figure 1.2 - Typical atmospheric cycle of particulate matters [62]

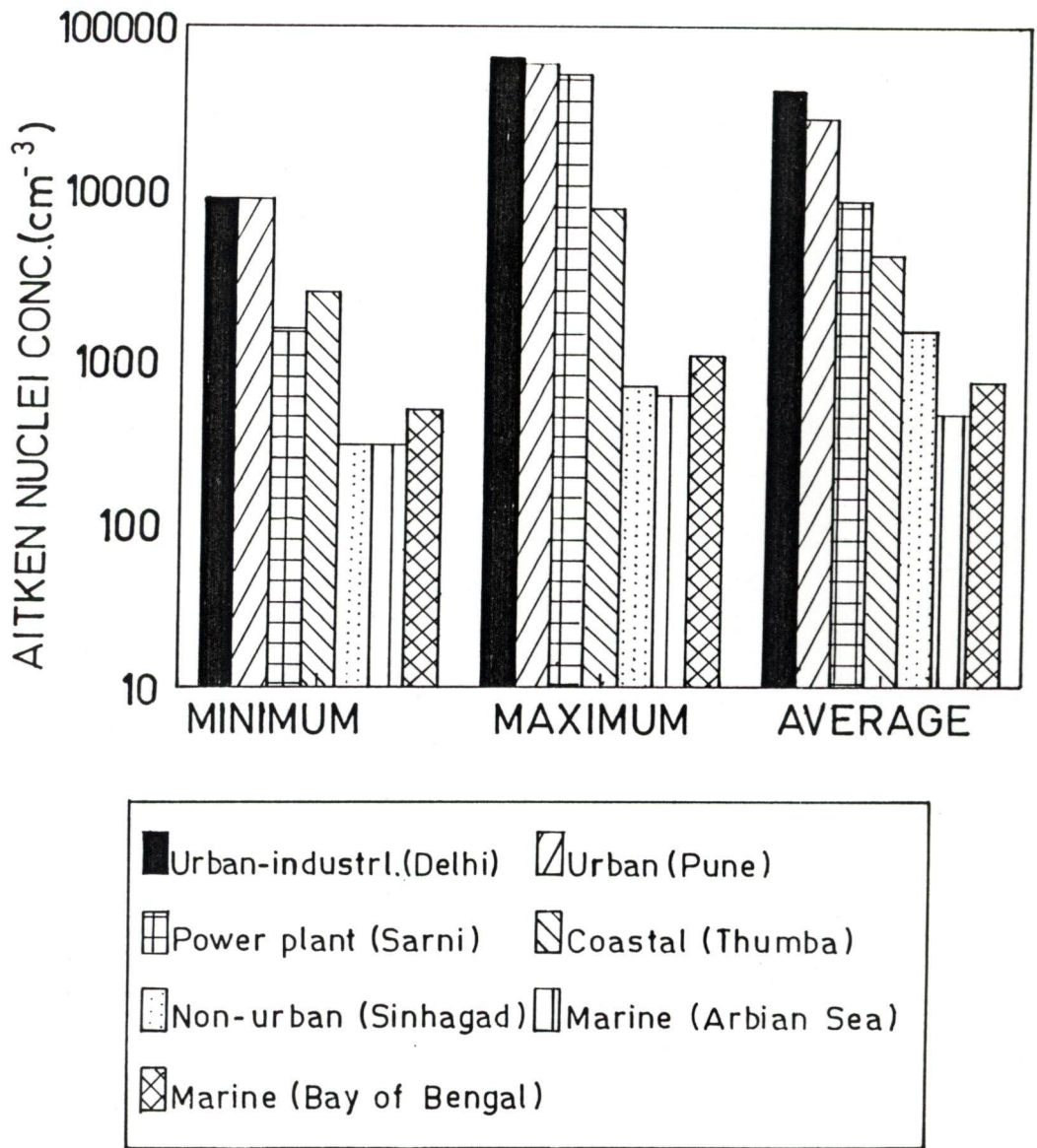


Figure 1.3 - Aitken nuclei concentration in different environment in India

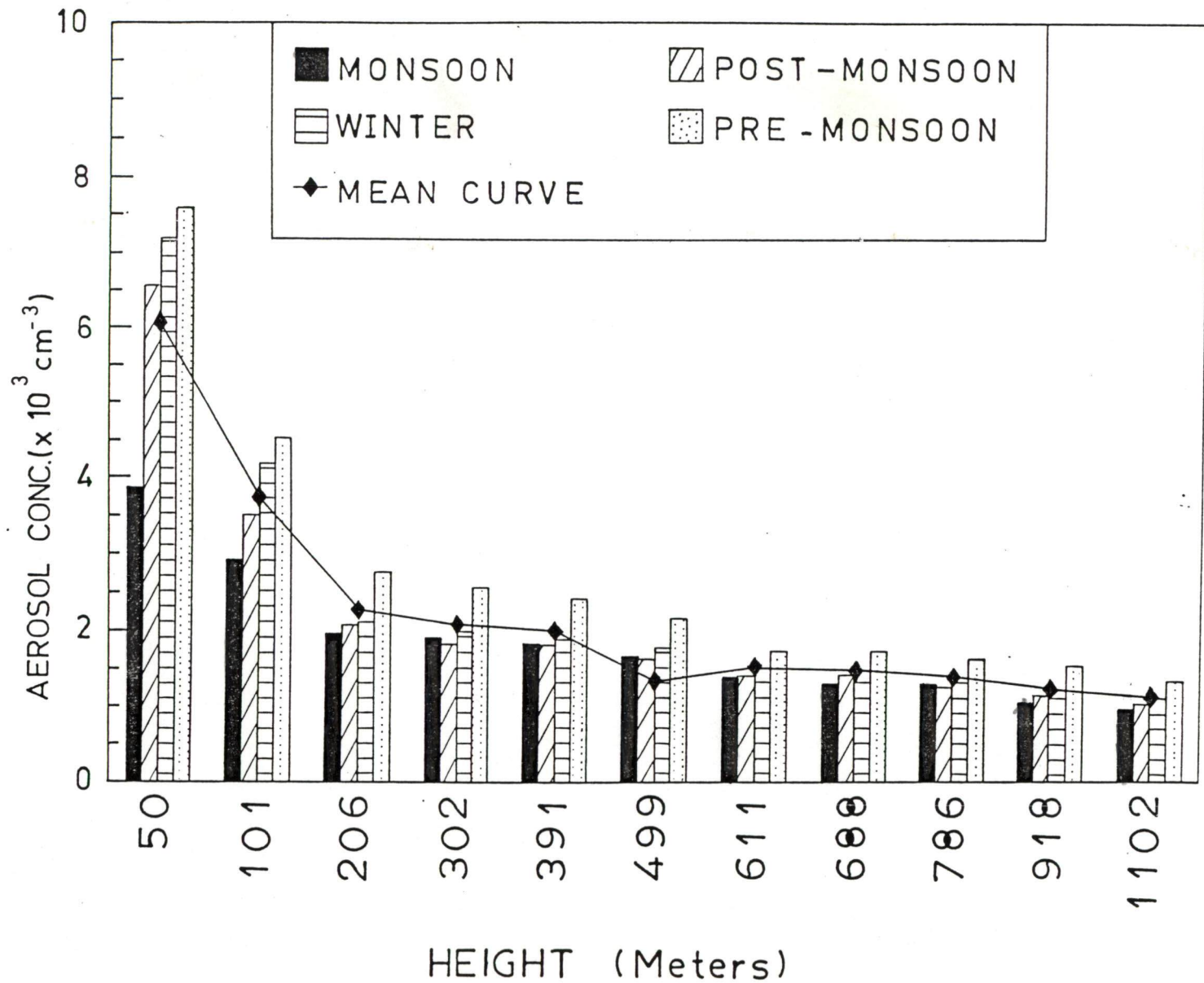


Figure 1.4 - Altitude-seasonal variation of aerosol concentration at Pune, India during October 1986-September 1993

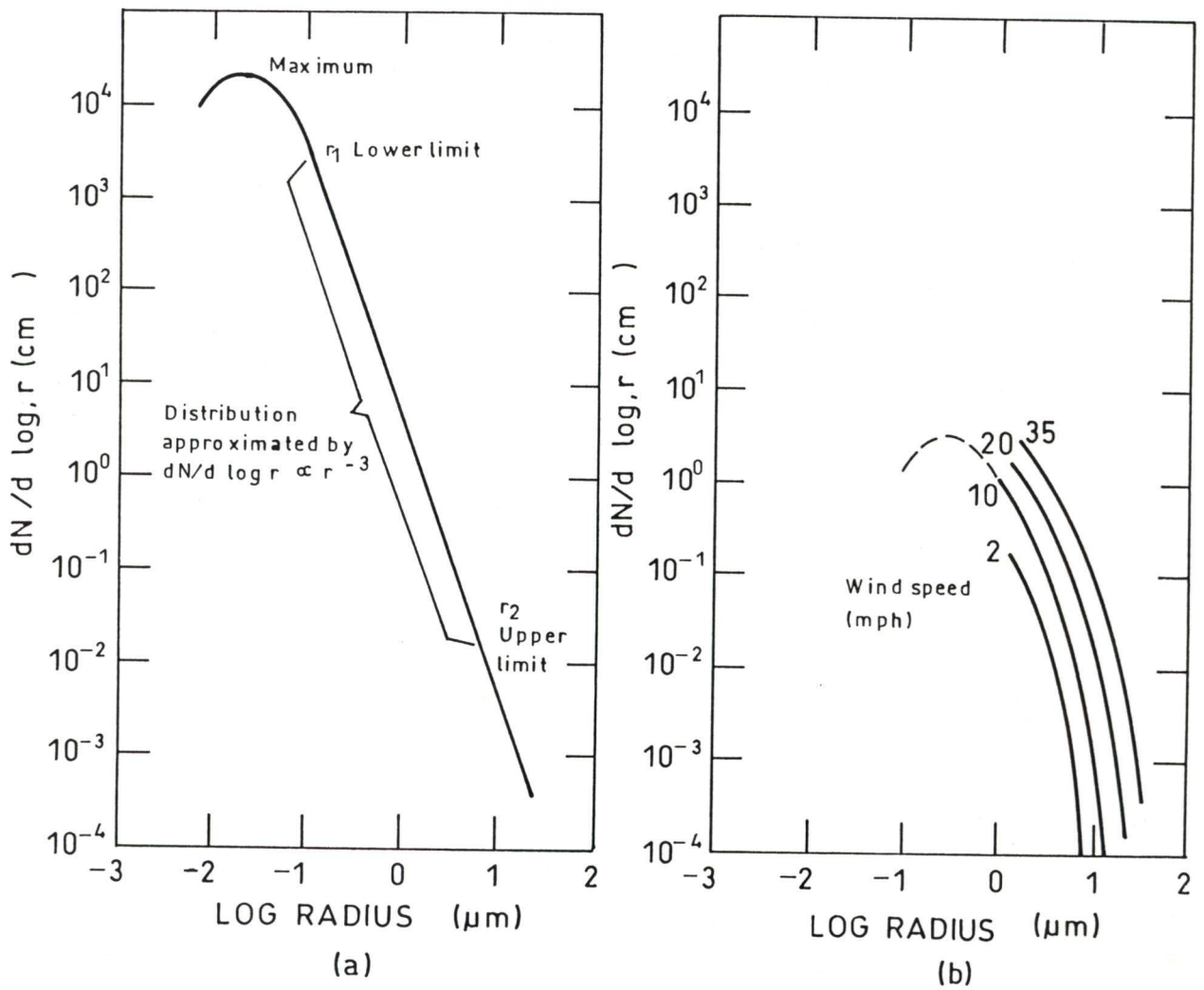


Figure 1.5 - Power-law size distributions of particles in continental and maritime (Eq. 1.05). (a) Continental type (b) Maritime type [86]

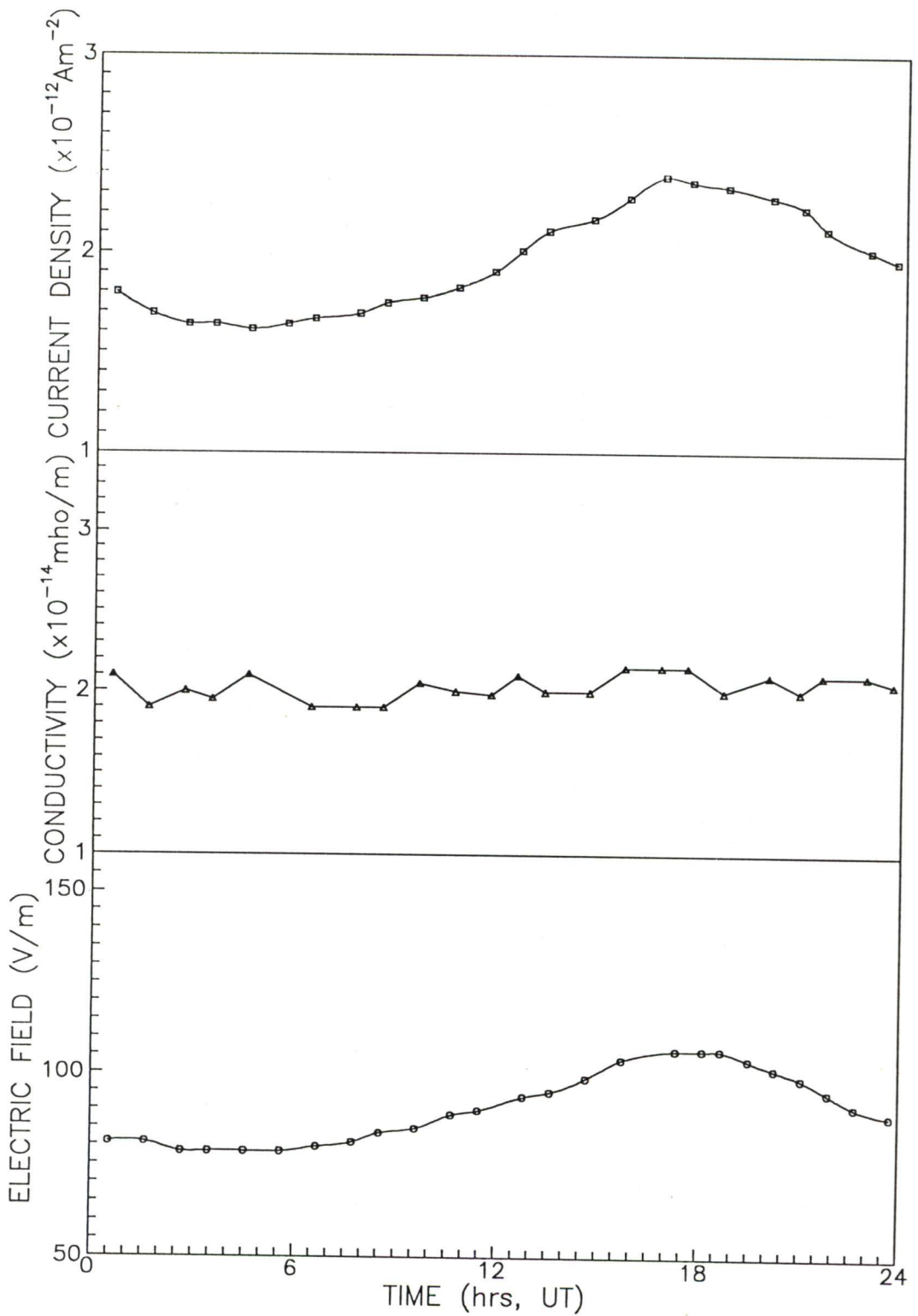


Figure 1.6 - Diurnal variation of electric field (E), conductivity (σ) and current density (J) at a distance of 1000 km in Pacific Ocean [147]

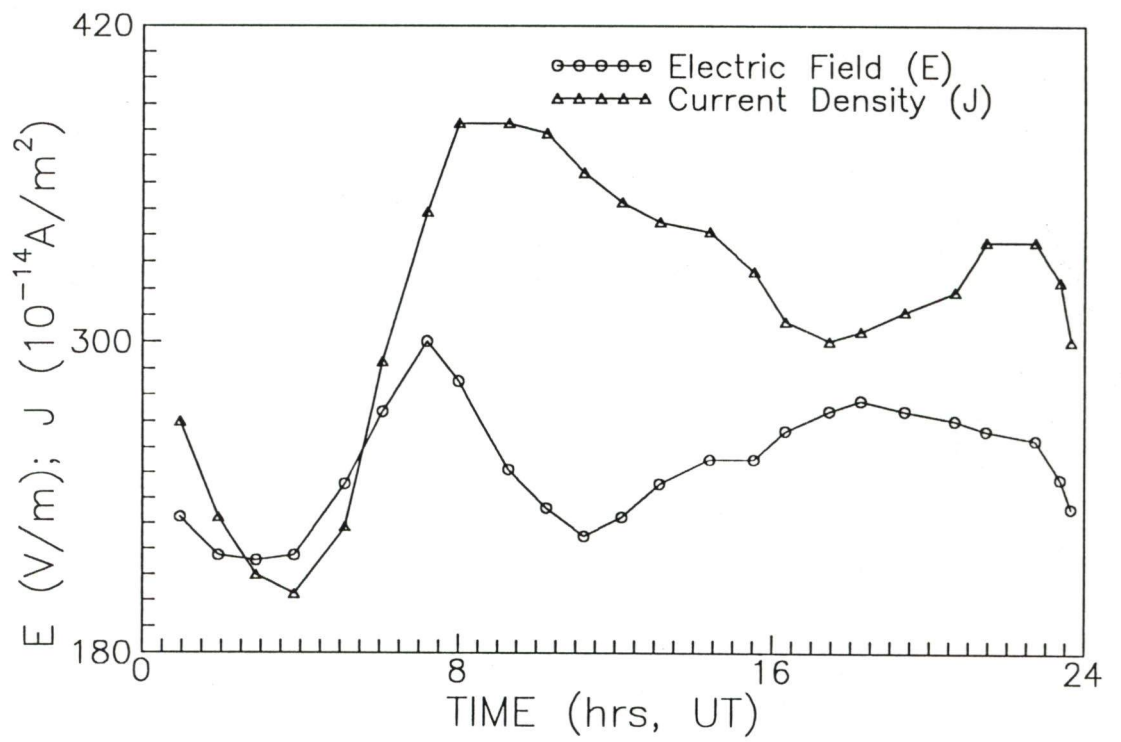


Figure 1.7- Mean diurnal variation of electric field (E) and current density (J) [179]

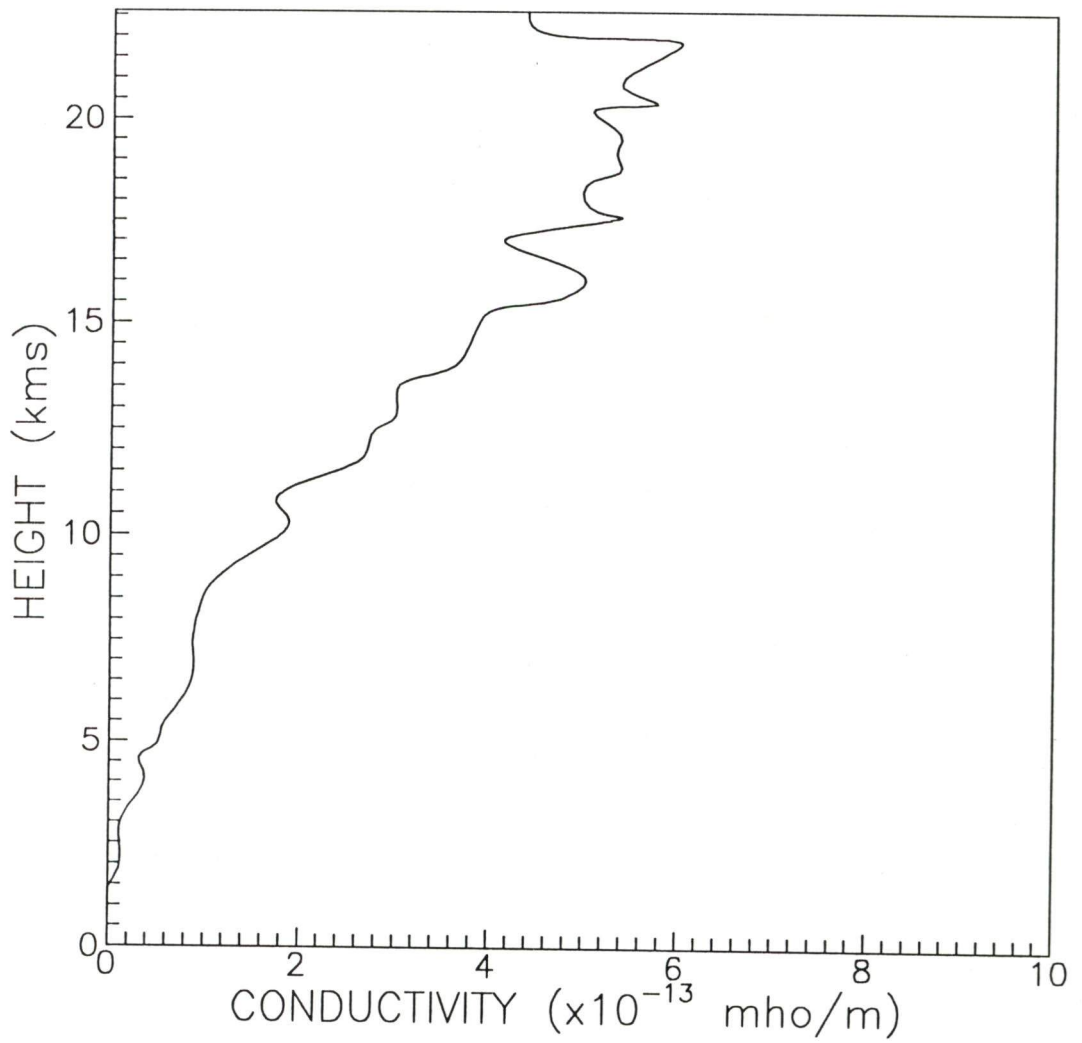


Figure 1.8 - Altitude variation of atmospheric electrical conductivity (σ) [223]

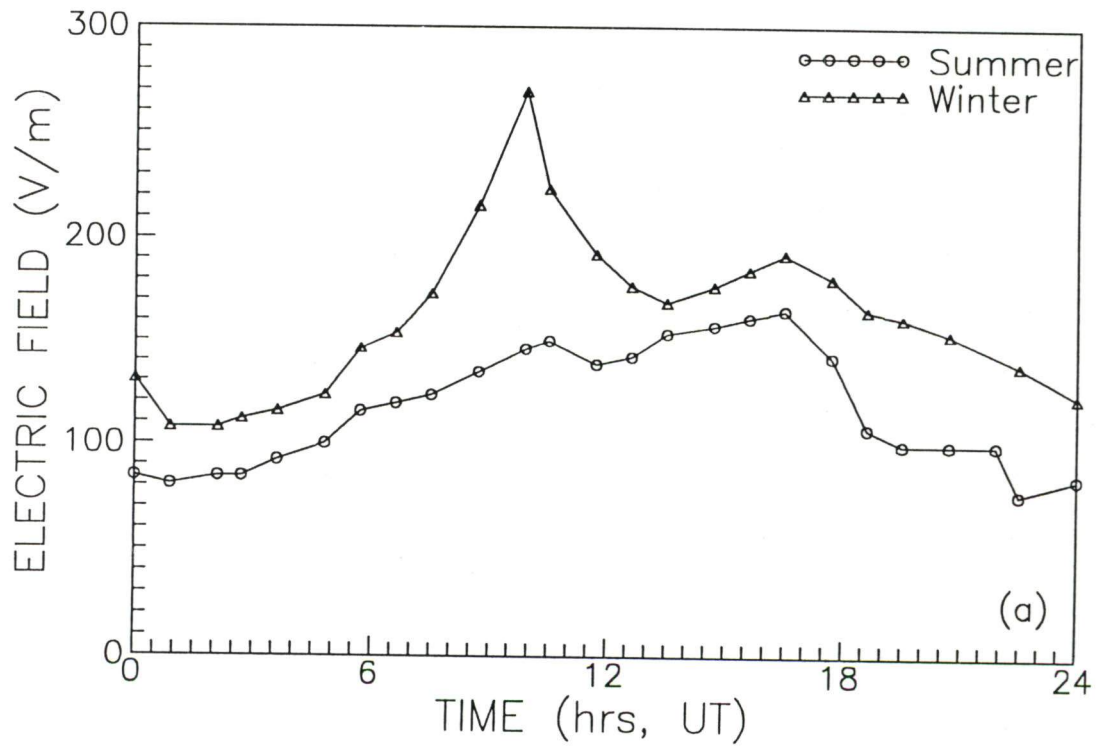
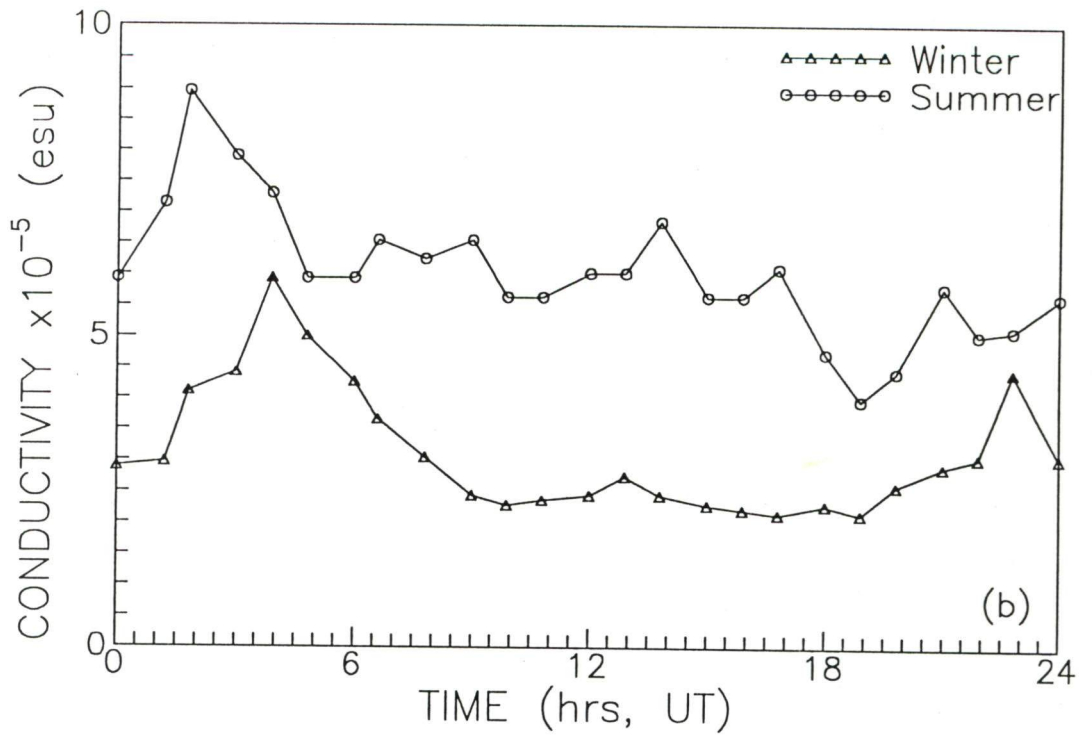


Figure 1.9 - Diurnal variation of (a) electric field (b) conductivity at Hongo, Japan [99]

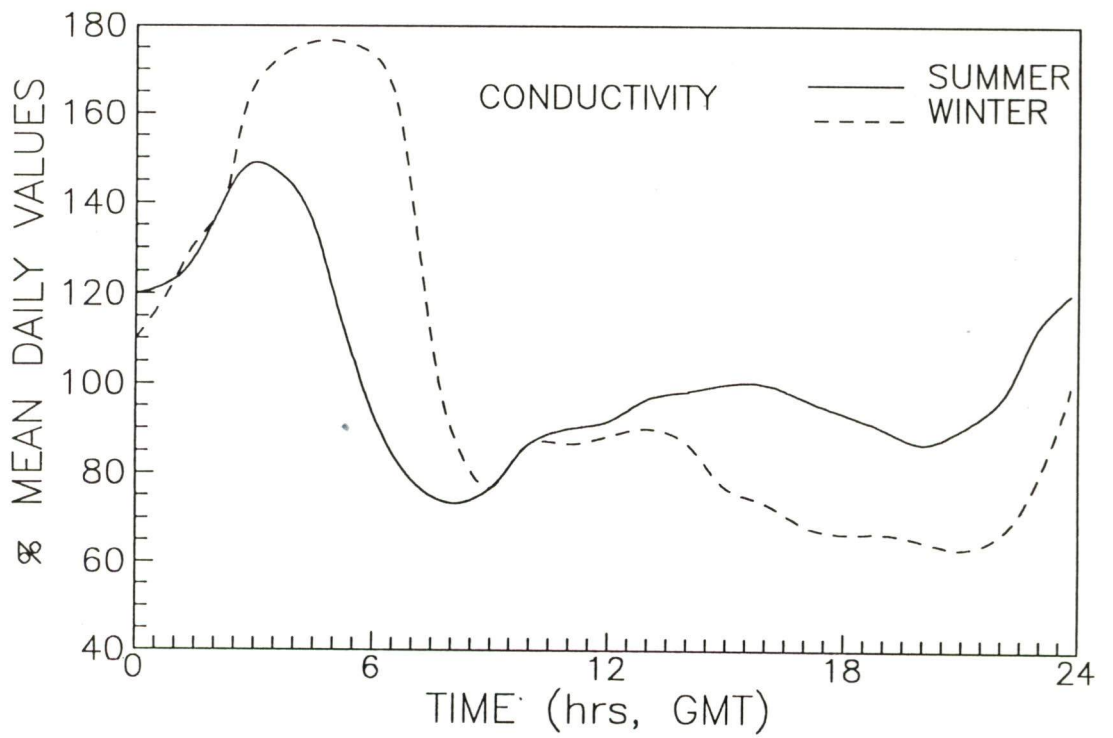


Figure 1.10 - Diurnal variation of electric conductivity at Kew for summer and winter season [22]

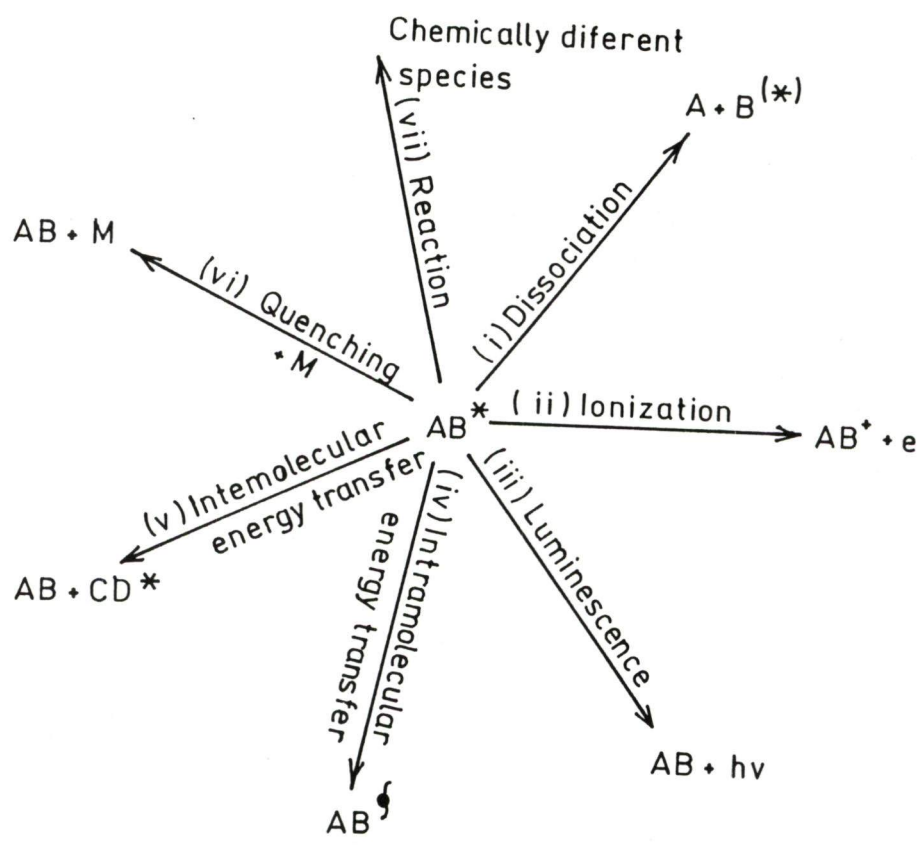


Figure 1.13 - Routes for decay of electronic excitation that are important in upper atmospheric chemistry

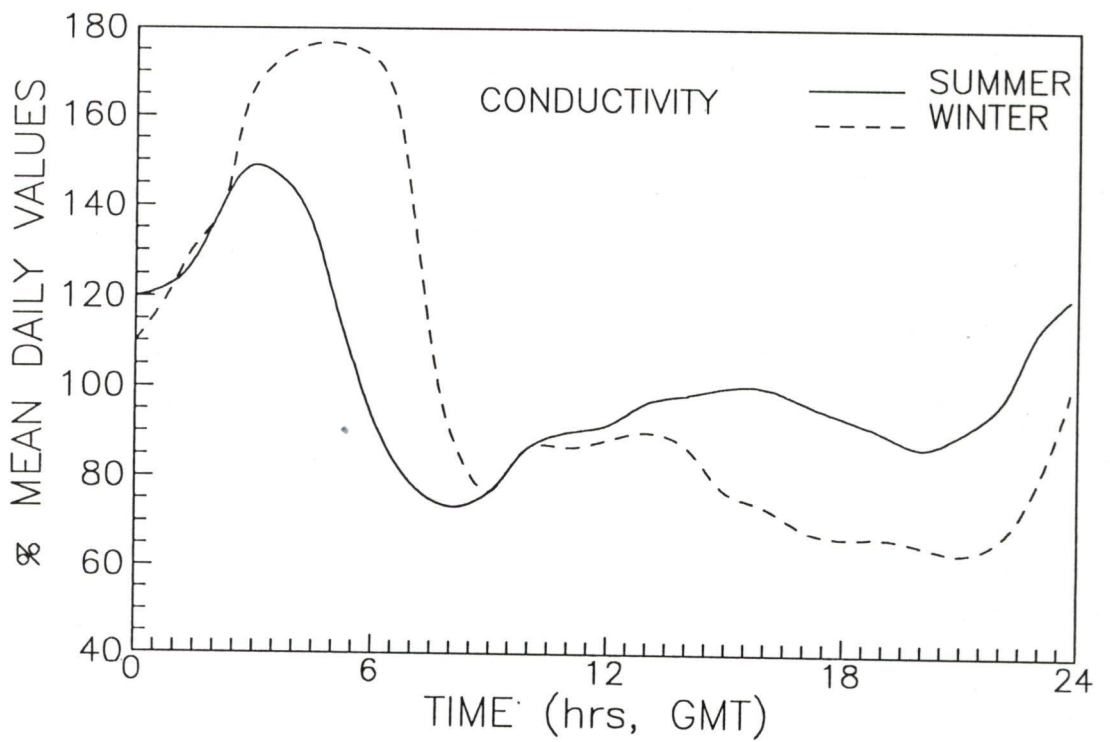


Figure 1.10 - Diurnal variation of electric conductivity at Kew for summer and winter season [22]

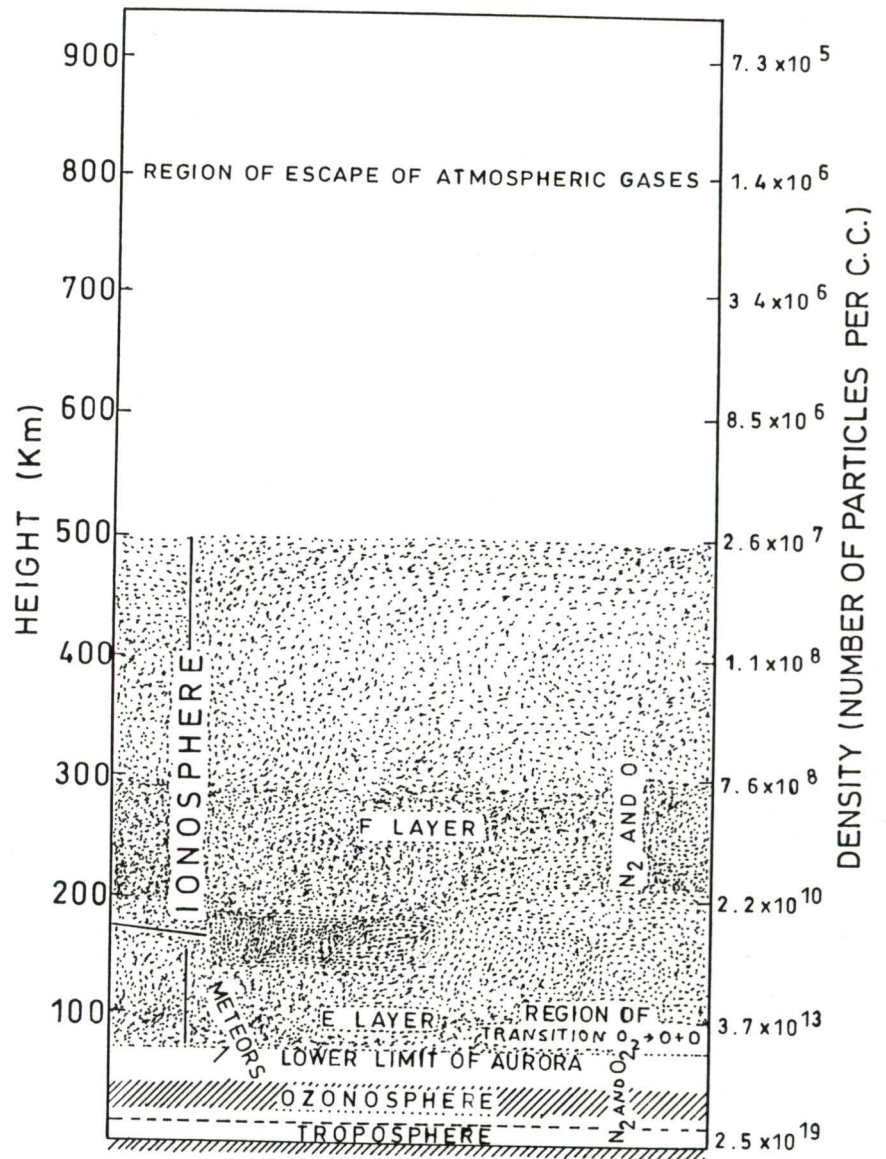


Figure 1.11 - Some physical features of the terrestrial atmosphere
 Ionospheric regions are indicated by shading [145]

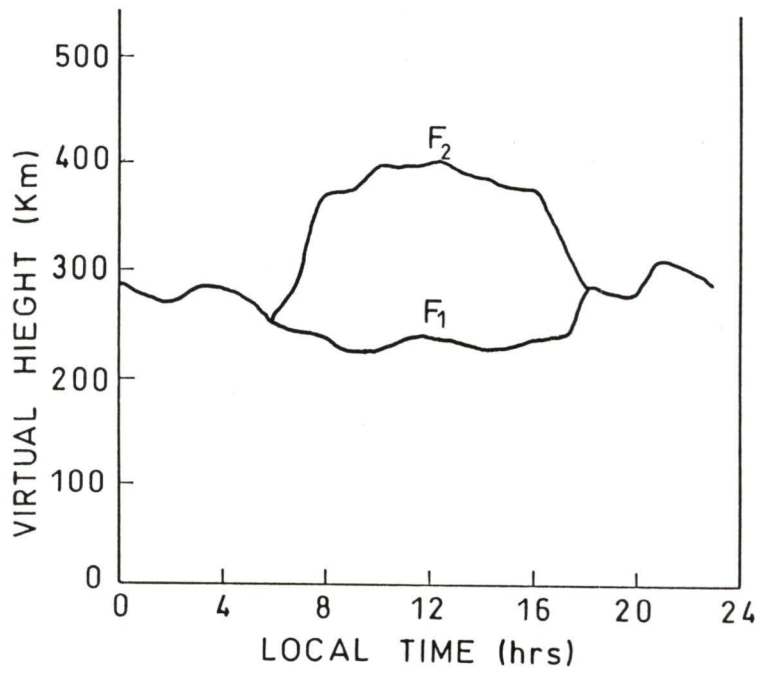


Figure 1.12 - The day time splitting of region F into regions F₁ and F₂ at Canberra [145]

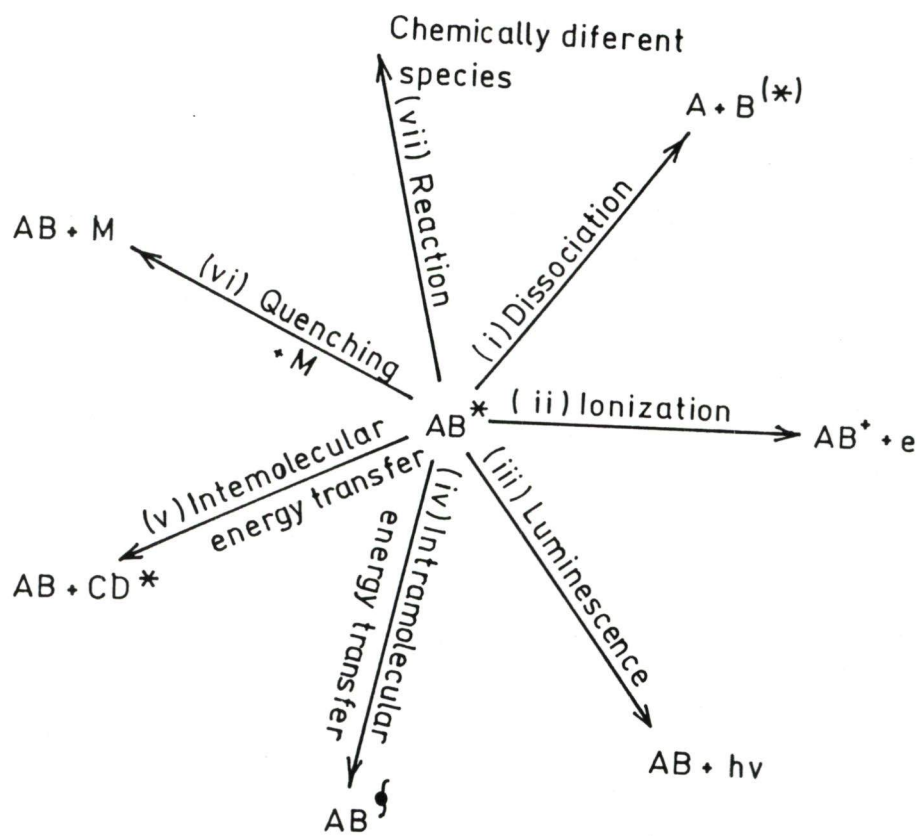


Figure 1.13 - Routes for decay of electronic excitation that are important in upper atmospheric chemistry

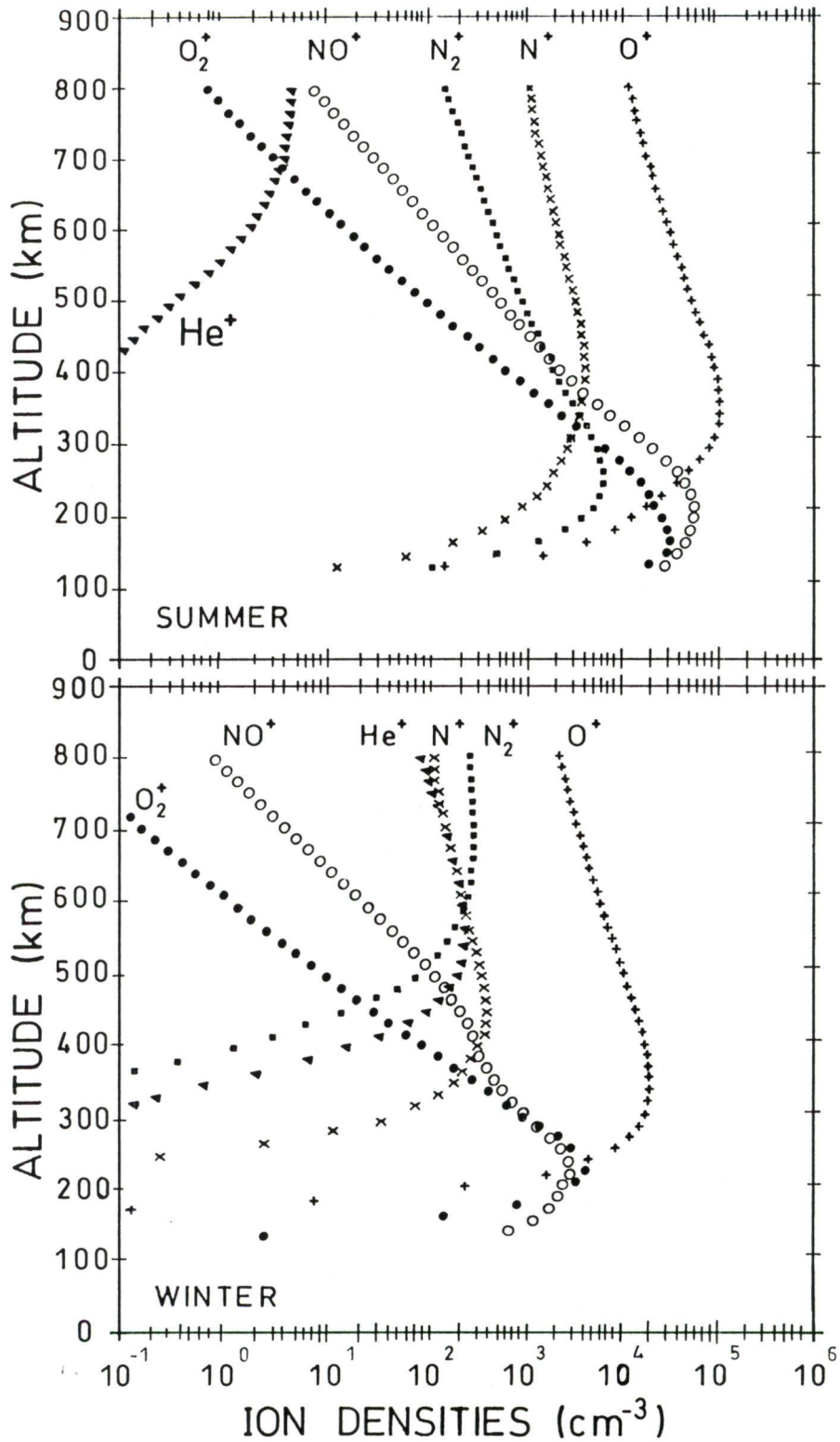


Figure 1.14 - Ion densities versus altitude for summer and winter season and for solar maximum and high geomagnetic activity [190]

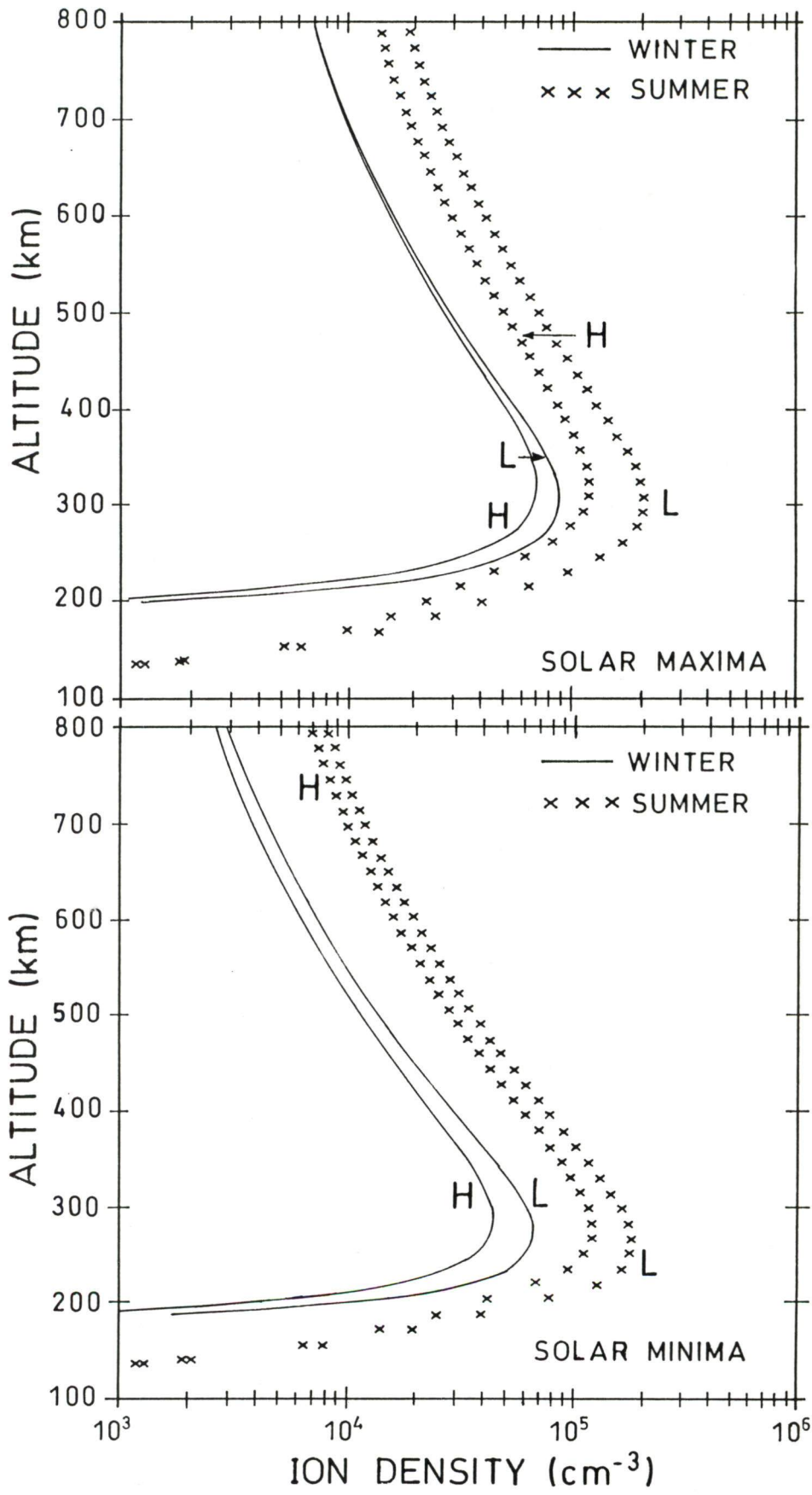


Figure 1.15 - O^+ density profiles for solar maximum and solar minimum for summer and winter and for high (H) and low (L) geomagnetic activity [192]

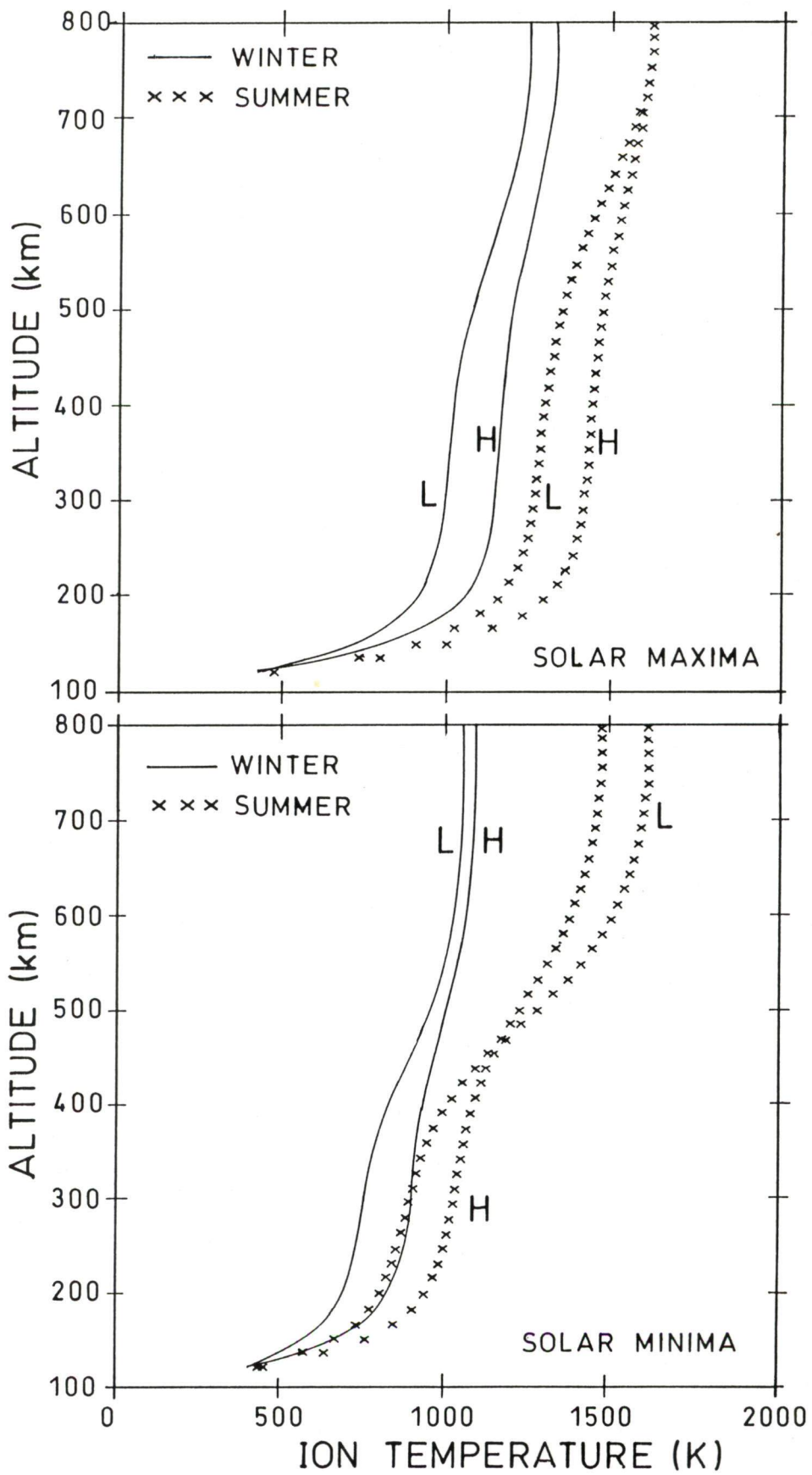


Figure 1.16 - O^+ temperature profiles for solar maximum and solar minimum for summer and winter and for high (H) and low (L) geomagnetic activity [192]

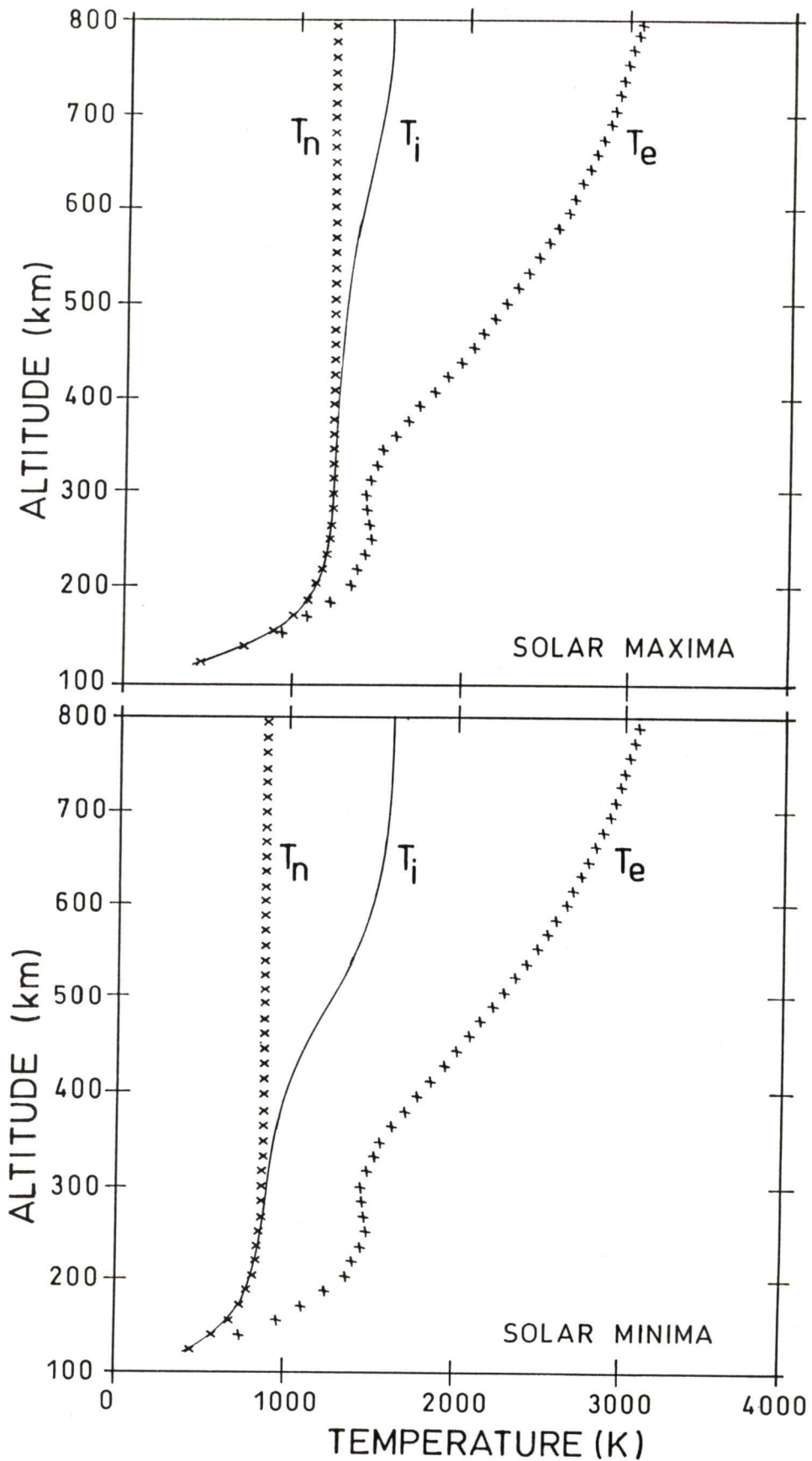


Figure 1.17 - Ion (O^+), electron and neutral temperature profiles for solar maximum and solar minimum for summer and low geomagnetic activity [192]

Chapter 2

Instrumentation

Monitoring and controlling of air pollution is the most important task of the day. The study of atmospheric particles in relation to air pollution and atmospheric electricity is increasingly gaining importance because of the atmospheric electrical elements like electrical conductivity, air-earth current, atmospheric electric field and potential are known to be strongly influenced by various parameters of the environment. Dolezalek [43] suggested that the atmospheric conductivity is preferable than other atmospheric electrical parameters for correlative studies with reference to air pollution because it is largely controlled by aerosol concentration in the air.

Today everybody is strongly concerned with the environmental issues, such as destruction of ozone layer, acid rain and global warming. Therefore local pollution issues have become significant in relation to the global environmental problems. Various types of instruments are used to measure the composition and concentration of air pollutants. By monitoring some parameters scientists can understand the various phenomena such as aerosol behavior in different weather conditions and atmospheric electricity. Paolette and Spagnolo [163] studied experimentally the variation of small ion concentration of both polarities and the conductivity of the lower atmosphere simultaneously with the presence of small traces of pollutants under different meteorological conditions. Jonsson and Vonnegut [85] designed and fabricated

an apparatus for real time measurement of the electrical conductivity of rainwater. Kamra and Deshpande [93] found that the age of air mass over sea is a better determining factor for conductivity measurement than the distance from the coastline. They investigated the problem of land-to-ocean extension of air pollution from the conductivity measurements made in monsoon season. John and Garg [83] have studied the vertical profile of atmospheric electrical conductivity using a Langmuir Probe fitted in a balloon over Hyderabad, India.

Study of aerosol size distribution and concentration can be done using various techniques available. Pahwa *et al.* [161] and Goyal [53] have used Cascade Impactor for aerosol studies. Lidar was used to study the vertical profile of aerosols by Devara and Raj [40], Parameswaran *et al.* [165] and McCormick *et al.* [136]. Parameswaran and Vijayakumar [164] have used Low Pressure Impactor to study the aerosol distribution in relation to relative humidity of the atmosphere. Some of the instruments are listed below with their capacity of measuring size range. These instruments are used specially for marine aerosols.

Reference	Instrument	Measuring Range
Haaf and Jaenicke [59]	Electric Mobility Analyzer	$0.003 < r < 0.4 \mu\text{m}$
Grass and Ayers [55]	Diffusion Battery with Pollak CNC	$0.002 < r < 0.1 \mu\text{m}$
de Leeuw [116]	Rotorod Inertial Impactor	$5.5 < r < 42.5 \mu\text{m}$
Hoppel <i>et al.</i> [70]	Replicator Impactor	$0.5 < r < 15 \mu\text{m}$
Bansal and Verma [11]	Optical Particle Counter	$0.3 < r < 5.0 \mu\text{m}$

In this chapter the instruments used for simultaneous measurement of atmospheric electrical conductivity and atmospheric particles (aerosols), have been described in detail. Measuring principles and techniques involved in different parts of an experimental unit have also been described in detail.

2.1 ATMOSPHERIC ELECTRICAL CONDUCTIVITY

The presence of small ions in the atmosphere contribute maximum to make air conducting. Various sources such as cosmic rays and radioactive elements produce ions in the atmosphere. These ions play very important role in the determination of atmospheric electrical conductivity. Cosmic rays of galactic origin are the main source of ionization in the lower atmosphere. Along with the cosmic rays there are radioactive emanations due to radon decay near the earth surface which cause measurable amount of ionization. However, this ionization decreases very fast with altitudes. The ionization due to solar cosmic rays and galactic cosmic rays extend well within the lower atmosphere of our interest [2].

The ionization rate, recombination rate, attachment of ions to aerosols (attachment rate) and various meteorological factors are the main sources of alteration in atmospheric conductivity. Also, natural radioactivity and aerosol concentration control the air conductivity in the boundary layer [43]. They also control the other electrical parameters like electric field, columnar resistance, current density etc. The conductivity is markedly reduced by the presence of particulate matter in air produced by natural and anthropogenic sources [58]. This reduction in electrical conductivity due to aerosol concentration depends on the values of ion-aerosol attachment coefficient and recombination rate.

2.1.1 Measurement of Electrical Conductivity

For the measurement of atmospheric conductivity, Gerdian Cylinder was used. The block diagram of the instrument is shown in Figure 2.1. The measuring principle of Gerdian's chamber was discussed by Mukku [153] in detail. This instrument has been used widely for the measurement of electrical conductivity, ion mobility and density. It has also been used for balloon borne experiments as well as ground based measurements.

Gerdian Cylinder is like cylindrical capacitor consisting of central electrode (conducting rod) and an outer electrode (cylindrical tube). When the air consisting of ions is sucked by the help of air blower passing through the cylindrical tube, the ions of opposite polarity are attracted by the charged electrode and the ions of other sign will be repelled and hence collected by the central electrode. The charge collected by the central electrode is fed to the ground through a high resistance. The voltage drop across the resistor is measured. In the V-I characteristics of Gerdian's chamber, the current increases linearly with increasing voltage and reaches saturation at central point. The rising portion gives electrical conductivity and the constant portion gives ionic concentration.

A positive potential at the outer electrode makes electrons and negative ions move to the central electrode, thereby constituting a current. This gives the negative conductivity. The negative potential on the outer electrode similarly provides the positive conductivity. The total conductivity σ , in terms of positive (σ_p) and negative (σ_n) conductivities, is given by

$$\sigma = \sigma_p + \sigma_n \quad (2.01)$$

From the measurement of output current of Electrometer Amplifier (Figure 2.1), the positive and negative conductivities can be obtained as [153]

$$i_p = Men_p \frac{\omega_p}{\omega_c} = \frac{M\sigma_p}{\omega_c} \quad (2.02)$$

Where,

ω_p = Mobility of positive ions

ω_c = Critical mobility of ions

M = Aspiration rate = $\pi R_o^2 v$

R_o = Radius of outer electrode = 4.25 cms

v = Velocity of air being aspirated

e = Electronic charge

n_p = Number of positive ions

σ_p = Conductivity of positive ions = $n_p e \omega_p$

Also,

$$\omega_c = \frac{M \ln(R_o / R_i)}{2\pi L V} \quad (2.03)$$

where,

R_i = Radius of inner electrode = 0.5 cm

V = Voltage applied across the electrodes of the capacitor = $\pm 30V$

L = Length of the central capacitor = 25.4 cm

The meaning of critical mobility is that the ions having mobility greater than the critical mobility of chamber will only be captured by central electrode. The ions having less mobility than the critical mobility will be removed by the aspiration before being collected by the central electrode. A fraction of ion with

mobility less than ω_c will also be collected. This was calculated to be ω_p/ω_c and ω_n/ω_c for positive and negative ions respectively. Therefore, if ω_p/ω_c or ω_n/ω_c is the fraction of ions with mobility less than the critical mobility that are being captured, then the rising section of V-I characteristics can be represented by

$$\sigma_p = \frac{i_p \omega_c}{M} = \frac{i_p \ln(R_o / R_i)}{2\pi L V} \quad (2.04)$$

Similarly, one may write

$$i_n = \frac{Me(n_n \omega_n + n_e \omega_e)}{\omega_c} = \frac{M \sigma_n}{\omega_c} \quad (2.05)$$

or
$$\sigma_n = \frac{i_n \ln(R_o / R_i)}{2\pi L V} \quad (2.06)$$

where, i_n is the current due to negative ions and electrons, n_n the number of negative ions and n_e that of electrons, ω_n and ω_e are, respectively, the mobility of negative ions and electrons. Therefore using equations 2.04 and 2.05, the atmospheric electrical conductivity for positive and negative polarities, respectively, can be calculated easily.

In the present case, since the applied voltage was the same in each case ($\pm 30V$), the critical mobility is given by

$$\omega_c = 2.6624 \times 10^{-4} \text{ m}^2 \text{ V}^{-1} \text{ s}^{-1} \quad (2.07)$$

2.1.2 Experimental Setup

The Gerdian Condenser named after Prof. Gerdian was used for the present study. The block diagram of the instrument is shown in Figure 2.1. The detailed description of experimental unit given in the following paragraphs.

G10, 2021



Gerdian cylinder or chamber is made of Aluminum. Diameter of cylinder is 9.5 cm. This cylinder works as outer electrode. This electrode is used to suck the air containing ions and electrons and directed them towards the central electrode depending upon the potential provided (± 30 volts). This outer electrode has two layers sealed with Teflon to avoid the interference of charged air, which is always in contact with the outer layer of the electrode. The outer layer is grounded as the charge collected will pass to the ground so inner layer will be free from any disturbance.

The sample air consists of ions of both (positive and negative) polarities and electrons. The ions of opposite polarity depending upon the potential applied to the outer electrode move towards the central electrode. This central electrode is made of steel rod having length 25.4 cm and diameter 1 cm. Now the charge collected by this electrode is fed to ground through a high resistance.

An electrometer amplifier (type EA815) supplied by Electronics Corporation of India Limited, Hyderabad, India is used to measure the voltage drop across the high resistance. This instrument is highly efficient in measuring the small direct current, low DC potential from high impedance sources, small charges and high resistance. It has wide range of voltage measurement which varies from 10^{-2} volts to 10 volts of both polarities, with input sensitivity 10^{-4} V per division. The current measurement ranges from 10^{-5} A to 10^{-14} A of both polarities with sensitivity 10^{-16} A per division. The input resistances are 10^6 , 10^8 , 10^{10} , 10^{12} and 10^{14} ohms. Electrometer Amplifier requires the input power of 210-250 V AC.

The sample air is sucked by help of the air blower, which provides continuous supply of air to the Gerdian capacitors. The rest of the air particles, which are not collected by the central electrode are removed out side by the air blower. It is connected to the cylindrical tube through a 20 cm long rubber tubing. The blower used for present work is manufactured by WOLF Electric Tools Limited, London (U.K.). This blower requires a current of 1.6 A and input voltage varying from 220-230 volts. The blower can be operated continuously over a period of 24 hours with a capacity of 1500 liters of air per minute.

A potential of 30 volts (positive and negative) is applied to the outer electrode in order to attract the ions of opposite sign. This potential is obtained by Transistor Power Supply-613 supplied by Systronics Lektrolab equipment company

To measure the output signal a single pen Ten-Inch Chart Elektronik-194 Lab Recorder, made by Honeywell Automation Fort, Washington (U.S.A) is used. It was attached to the output terminal of electrometer amplifier in order to record the flow of ions to central electrode in the form of voltage. The recorder has two main parts, (i) measuring system, and (ii) recording system. The measuring system includes an electronics circuit, constant voltage unit, DC balancing motor and servo amplifier. The measuring circuit compares the developed feedback voltage with the input voltage. The difference between these voltages is applied to servo amplifier, which amplifies the generated signal. The recording system includes the pen, ink and the multiple speed charts drive system. The chart speed is selected 1.2 inches per hour for continuous use for 24 hours.

2.2 ATMOSPHERIC PARTICLES OR AEROSOLS

There are several ways in which natural as well as man made activities can affect the short or long term global climatic pattern. Suspended particulates or aerosols are the main constituent of air pollution at a particular location or in global scenario. The sources of these particles are vehicular traffic, industrialization, dust storms, volcanic eruptions, sea sprays etc. These aerosols are found in the wide range of sizes. These particles play an important role in atmospheric processes like condensation of vapour, ice-nucleation, scattering, photochemical reactions etc [224].

2.2.1 Measurement of Atmospheric Aerosols

There are several ways to measure the aerosols but most effective and easy way is to use the scattering property of particles. When, the particles having size of the order of the wavelength of visible light are illuminated by a beam of light, the amount of light scattered by the particles varies with the projected area of that particle. The amount of light (scattered intensity) and its angular distribution depends upon the size, shape, and refractive index of the particle. The particle size distribution and concentration can be calculated by using Mie theory of scattering [100,120,135]. A number of instruments based on Mie scattering have been manufactured for the determination of particle size and concentration [142].

Study of size distribution and number density of atmospheric aerosols include variety of techniques such as, multi-wavelength radar [107], cascade impactor [53, 161], lidar [37, 38, 40, 165], atmospheric turbidity measurements [152] and low pressure impactor [164].

In the present study, the measurements of aerosol concentration and size distribution were carried out using a specially designed and fabricated Laser Beam Scatterometer [200]. Figure 2.2 shows the simplified block diagram of the instrument showing various parts. The specifications of various parts have also been given in the diagram. This instrument measures the intensity of scattered laser beam by particles of a specified volume at angles 45° and 135° . By using the intensities of scattered light the concentration of aerosols and size distribution were computed.

When the particles are illuminated by the laser light (He-Ne laser, 6328 \AA), as written earlier, the intensity of scattered light varies with size, shape, concentration and refractive indices of the particles. Assuming the normal Gaussian distribution of scatterers, the number of particles $n(x)dx$ per unit volume in the size parameter range between x and $x+dx$ is given by

$$n(x)dx = \frac{N_0}{\delta\sqrt{2\pi}} \exp\left[-\frac{(x - x_m)^2}{2\delta^2}\right] dx \quad (2.08)$$

where,

N_0 = Total number of particles

δ = Standard deviation of size distribution curve

$x = 2\pi r/\lambda$ (r = radius of scatterer),

x_m = Model size parameter = $2\pi r_m/\lambda$, r_m being the mode radius

λ = Wavelength of incident radiation (6328 \AA)

The resultant scattered light intensity $I(\theta)$ in a given direction θ due to scattering per unit volume is given by

$$I(\theta) = I_0 \frac{\lambda^2}{4\pi^2} \left(\frac{\rho_1 + \rho_2}{2} \right) \quad (2.09)$$

Here,

I_0 = Irradiance of incident radiation

ρ_1 = Intensity distribution functions corresponding to the perpendicular polarized component

ρ_2 = Intensity distribution functions corresponding to the parallel polarized component

These functions depend on the size, refractive index of the scatterer and wavelength of the radiation as well as angle of scattering. These can be defined as

$$\rho_1 = \int I_1(\theta, \lambda, m, r) n(r) dr \quad (2.10)$$

$$\rho_2 = \int I_2(\theta, \lambda, m, r) n(r) dr \quad (2.11)$$

Here, $I_1(\theta, \lambda, m, r)$ and $I_2(\theta, \lambda, m, r)$ are intensity distribution functions for a single particle at a scattering angle θ , wavelength λ , refractive index m and radius r and $n(r)$ is the number of particles in the radius range r and $r+dr$ and thus $n(r)dr$ represents the size distribution function.

The intensity distribution functions $I_1(\theta, \lambda, m, r)$ and $I_2(\theta, \lambda, m, r)$ have been computed by other workers for different refractive indices and size parameter [35, 57, 162, 199]. For the present calculation we have taken the values of $I_1(\theta, \lambda, m, r)$ and $I_2(\theta, \lambda, m, r)$ in model size parameter range 0.1-30 for refractive indices 1.30 and 1.33 from Denmann *et al.* [35].

The ratio of scattered intensities (theoretical values) in the direction θ_1 and θ_2 can be found using equation 2.09. The experimental ratio can be found

by measured scattered intensities at angles 45° and 135° . The experimentally obtained ratio is matched with the theoretical values and model size parameter x_m is selected for which the experimental ratio tallies best with the theoretical one. For computation of size distribution by Mie Theory a sharp peak distribution of aerosol size with standard deviation $\delta=0.69$ has been selected. Once the size parameter is known, particle size can be obtained easily. The whole process, i.e. matching the experimental ratio with the theoretical one, extracting the model size parameter and finding the size and concentration of particles in six different size ranges ($0.01-0.05 \mu\text{m}$, $0.05-0.10 \mu\text{m}$, $0.10-0.30 \mu\text{m}$, $0.30-0.50 \mu\text{m}$, $0.50-1.0 \mu\text{m}$, $1.0-3.0 \mu\text{m}$) have been calculated using a computer programme developed in C/C++ language in UNIX environment. The programme is also compatible for the DOS platform with some minor changes. This programme is used to run on Tata Elxsi Power Series 3220 computer provided in New Computation Facility at University of Roorkee, Roorkee.

2.2.2 Experimental Setup

The block diagram of the Laser Beam Scatterometer has been shown in Figure 2.2. A detailed description of setup has been presented here.

The sampling cylinder is made of plastic having the length 53 cm and inner diameter 12 cm. The thickness of the plastic sheet is 0.04 cm. This cylinder is made narrow at one end, which is attached with the inlet of an air blower. In this cylinder, four windows have been provided in the same horizontal plane at right angles to the axis of the cylindrical chamber. Iron bars support the whole assembly including cylinder and air blower. The lower base

is made of iron bars which provides easy and necessary handling of equipment to any experimental site for field observation. Two optical sensors (phototransistors with common emitter configuration) are fitted at 45° and 135° with respect to the direction of incident monochromatic light source (He-Ne laser). This cylinder is supplied a cap to avoid the ambient light to interfere in scattering process by laser light. Also, this cylinder is made black inside to avoid the multiple scattering. An air blower is used to suck the sample air having suspended particles to make the possible scattering of particles with the incident beam of light. The specifications of air blower are described already in section 2.1.2 in this chapter. This blower is attached with the sampling cylinder permanently with the help of an iron pipe fitted with the nuts and bolts. It can continuously operated for 24 hours at any experimental site.

The light source used for scattering purpose is a 5 mW He-Ne laser source (model L-200) emitting a monochromatic light of wavelength 6328 Å. The laser tube has rectangular shape and supported at a iron stand attached with the sampling cylinder with output point facing a window made in cylinder. The axis of window makes angles 45° and 135° with the axis of those windows having optical sensors at their end.

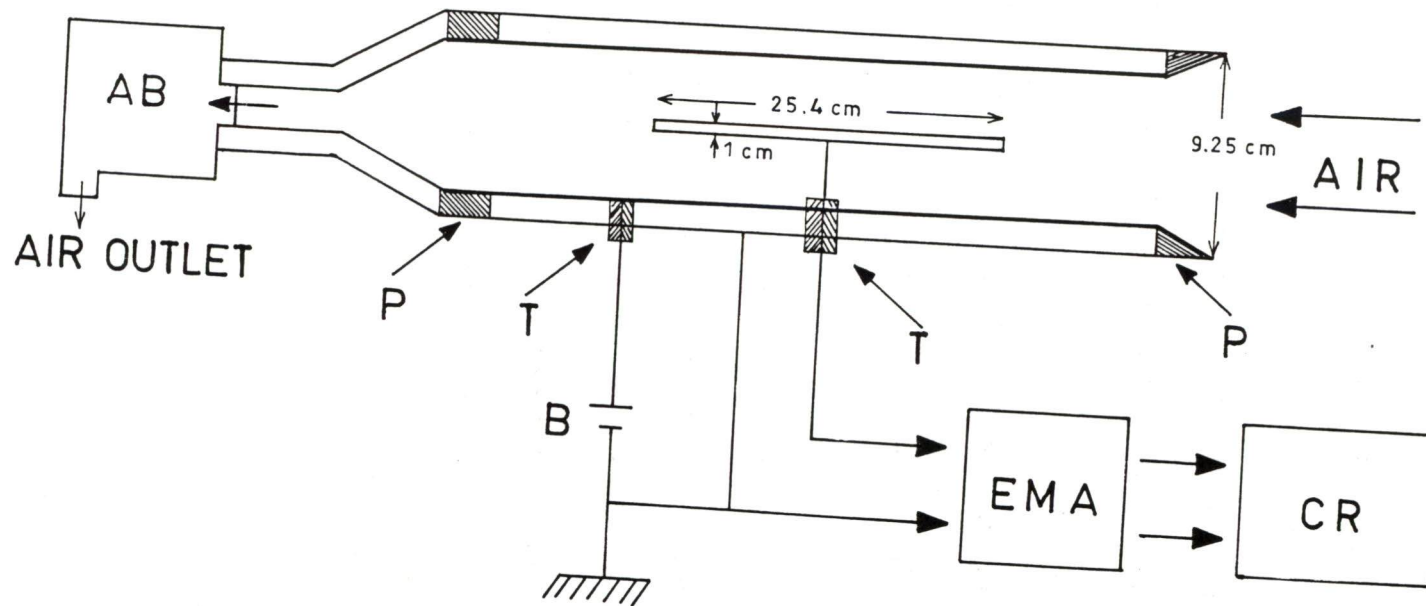
A photodetector is used to measure the scattered radiation by atmospheric particles present in the sample air. This device consists, a phototransistor with a collector resistance of 100 k Ω . A 5 volts supply is used at the collector terminal. The output of the collector is measured by a chart recorder. This detector is fitted with in an aluminum tube having blackened surface inside. This aluminum tube is tightly fixed on the windows of the

cylinder through a transparent plane glass. This tube allows a very small solid angle through which the scattered radiation reaches the detector.

A continuous variable power supply (AH 1-27/15, maximum load 15 ampere), manufactured by Automatic Electric Private Limited, Mumbai, India is used in this experiment. It requires 240 V input voltage at 50-60 Hz and can provide output ranging from 0 to 240 V. The power supply is easy to use and can be carried to any place conveniently.

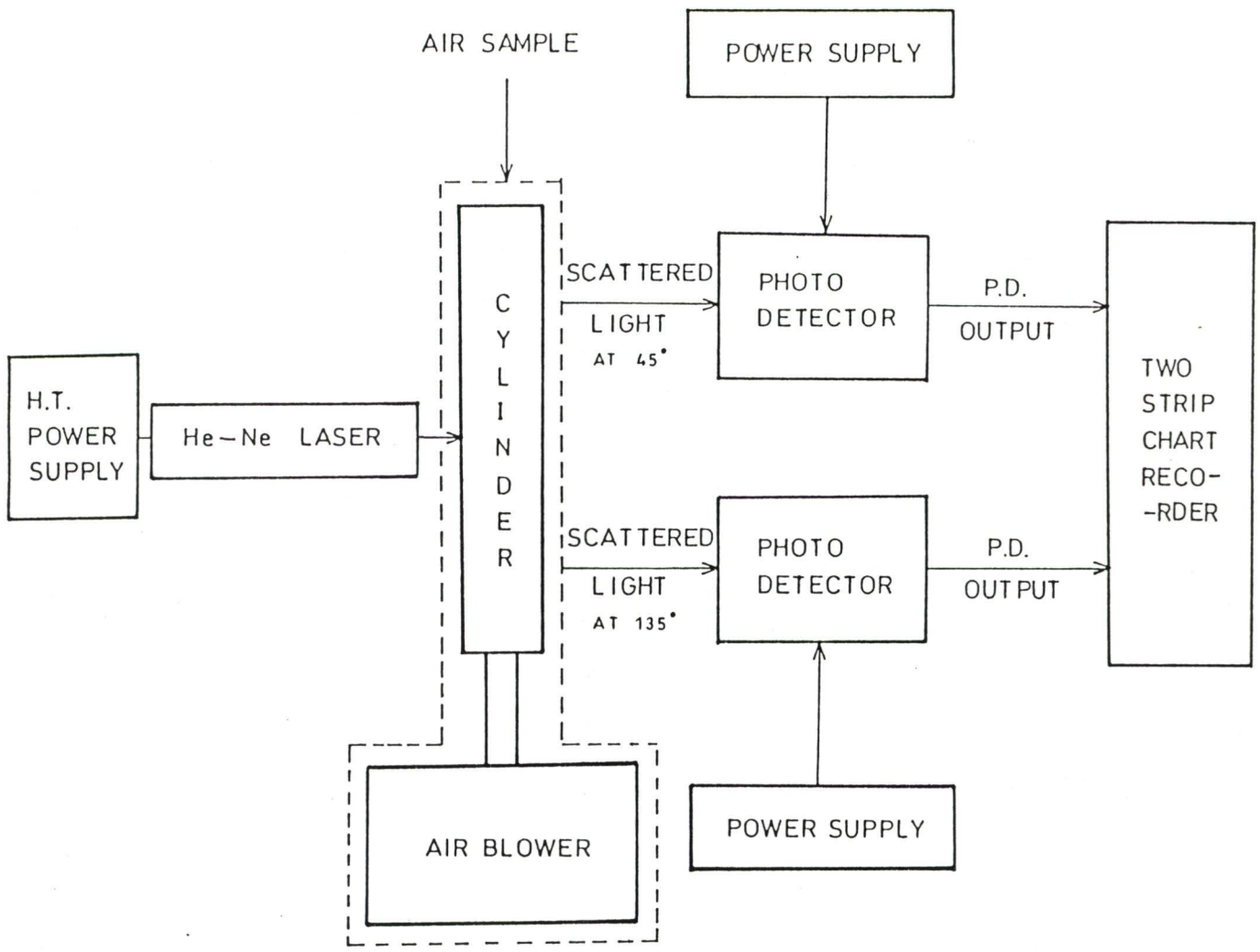
An Omniscribe Chart Recorder (model 5212-14) is used for recording the voltages available from the output terminals of the photo detectors. It is a two channels strip recorder with voltage sensitivity range between 0.001 volts/25 cm to 10 volts/25 cm in different steps. The speed of the chart is also adjustable by selector switch with a variation from 2.5 cm to 20 cm per minute in steps.

These instruments were used to study the variation in atmospheric electrical conductivity and aerosol concentration during different weather conditions i.e. solar eclipse (1995), monsoon (1996) and winter (1996-97). The study on these parameters during solar eclipse has been presented in next chapter, while chapter four contains the study during monsoon and winter season.



- B = Battery
- EMA = Electrometer Amplifier
- CR = Chart Recorder
- P = Percepax
- T = Teflon
- AB = Air Blower

Figure 2.1 - Experimental set-up for atmospheric electrical conductivity measurement



CYLINDER

Length 53 cm.
Inner Diameter 12 cm.

MOTOR

Power 1.8 Bhp.
Current Required 1.6 amp.
Operating Voltage 220-230 V

PHOTOTRANSISTORS (DETECTOR)

Common Emitter Configuration
Angles 45° and 135°
Supply 5-12 Volts
Collector resistance (R_C) 100k Ω

He-Ne LASER

Wavelength 6328 Å
Power 5 mW

CHART RECORDER

Omniscribe Model 5212-14
Sensitivity range 0.001V/25cm - 10V/25cm

Figure 2.2 - Experimental set-up for atmospheric aerosol measurements

Chapter 3

*Solar Eclipse Of
October 24, 1995:
Atmospheric Aerosols
And
Electrical Conductivity*

Sun and weather have close relationship as minor changes in the solar radiation can cause significant effects on weather and climate. The solar eclipse is a peculiar phenomenon that takes place over the known region on the surface of the earth at known times but lasts for a brief period of time. The interest of mankind to understand the event of eclipse itself and its effect in many disciplines of science has been continued for long years. An eclipse constitutes a rapid, profound and widespread perturbation of the solar radiation received by the earth's surface and its atmosphere. Therefore the effects of the eclipse on atmospheric conditions provide a tool to investigate the dependence of weather conditions on solar radiation. The atmospheric parameters like aerosols, electrical conductivity, air-earth current density, electric field, potential gradient, space charge, temperature and relative humidity are also affected by these radiations. Many workers have done extensive amount of work to study the effect of solar eclipse on these parameters [7, 8, 42, 50, 52, 82, 99, 101, 111, 128, 130, 146, 159].

3.1 A BRIEF SURVEY OF EARLIER STUDIES

During the period of solar eclipse, particularly the total solar eclipse, favoured by fine weather conditions, some changes of great significance in the surface meteorological parameters do take place.

With the commencement of the obscuration of the sun's disc the oncoming solar radiation is cutoff and as a result the earth's surface temperature falls rapidly relative to the upper levels. This observation has been documented by many workers [33, 44,130, 170, 206]. Das *et al.* [33] reported fall in the temperature as much as 20 °C during the maximum obscuration phase of the 16 February 1980 eclipse at Raichur, India. Such a feature results in setting up the inversion conditions. During such conditions, Brown [18] reported that the concentration centers of aerosols moves downwards (sedimentation as a result of reduced eddy diffusion).

Manohar *et al.* [128] have observed a cooling of about 3 °C of the entire surface air layer and a considerable drop in wind speed over the stretch of totality occupied land region during the eclipse of 16 February 1980. Also, he observed 5 to 8 times increase in potential gradient during the 3-4 hours of post eclipse period. Jain *et al.* [82] measured various atmospheric parameters like water vapour, temperature, humidity and ozone at National Physical Laboratory, New Delhi, India during total solar eclipse of October 24, 1995. They observed a decrease of 1.5 °C in temperature before the completion of eclipse. Around totality it was 6 to 8 °C decrement in temperature while humidity was increases by 8 to 10%. They also reported the decrease of water vapour during the eclipse period. Ghosh *et al.* [50] observed an increase in larger aerosols and decrease in water vapour due to phase change of water from vapour to liquid state. The suppressed level of atmospheric turbulence and coagulation of liquid water with aerosols were given as possible cause of increase in aerosols.

Another effect, that has been noticed in majority of eclipses was fall in the surface layer wind speed around the time of totality [117, 130, 156, 196]. Reports on the effect of solar eclipse on atmospheric electrical parameters have generally indicated that the measurements were generally confined to electric field in association with a few meteorological parameters like surface temperature and wind. Israël [80] summarized such reports up to 1954. His study indicated that in a majority of events the electric field diminished after sometime from the start of eclipse, while in some cases the electric field increased. Koenigsfeld [105] and Markson and Kamra [130] made observations of electric field by balloon radiosonde and by using aircraft facility respectively. Koenigsfeld's observations of electric field decreased to near zero between 5-15 km height. During the same eclipse, however, ground observations of Koenigsfeld [105] showed the electric field passed through zero and reversed. Kamra and Varshneya [94] at Roorkee, India reported similar field reversal.

In spite of a large number of reports on the effects of a solar eclipse on atmospheric electrical parameters [22, 42, 44, 194, 206], the nature of the effect is not conclusively established. Dolezalek [44] explains his observations at Waldorf in terms of boundary layer processes since the total solar eclipse produces a brisk "sunset-sunrise" event, which is different from the normal sunset and sunrise.

In the Indian region an excellent opportunity to study the effects of solar eclipse came during the Total Solar Eclipse of October 24, 1995. A well-organized programme was carefully made to utilize this phenomenon of the nature. With an objective of determining the local atmospheric response to

a sudden removal of solar radiation, the continuous observations of some meteorological and electrical parameters and aerosols were made during the near total solar eclipse at Roorkee. The positive and negative conductivities of atmosphere and aerosols of different sizes along with the wind speed, temperature and relative humidity were recorded.

3.2 THE SOLAR ECLIPSE OF OCTOBER 24, 1995 IN INDIA

The solar eclipse of 24 October 1995 began at 0722 hrs IST and ended at 1243 hrs IST. The partial phases of the eclipse covered the region bounded approximately by longitude 36° E and 173° W and latitude 70° N and 30° S encompassing the extreme North East Africa, Central South and Eastern Asia, the Indian Ocean, the northern half of Australia and the Western Pacific Ocean [77]. It was noted that the sun was totally obscured by the moon's disc from a narrow path over which the umbral cone of the moon's shadow swept across the earth. At approximately 0823 hrs IST on 24 October 1995 the centre of the umbra touched the earth at sunrise at a point south of Teheran ($51^{\circ}6'$ E, $34^{\circ}50'$ N) having a path of totality 19 km wide and 25 seconds in duration at this point. The central line after crossing Iran, Afghanistan and Pakistan reached the northwestern end of India roughly around 0830 hrs. The total phase in India, as shown in Figure 3.1 [77], extends over the north Indian plain passing north of Rajasthan, over Uttar Pradesh and Diamond Harbour in West Bengal.

The duration of totality along the central line in India varied from 48 seconds in the west (Rajasthan) to about 82 seconds in east (West Bengal). The maximum duration of totality was 134 seconds at 1010 hrs IST close to

Bornao in South China Sea, where the width was 81 km. The central eclipse ended at 1142 hrs IST, when the umbral cone left earth over the Pacific Ocean ($171^{\circ}48'$ E, $5^{\circ}39'$ N). At Roorkee the maximum obscuration of eclipse was 90-92% as this place is about 250-300 km away from the path of totality (Figure 3.1). The progress of solar eclipse has been shown in Figure 3.2 with time (IST).

3.3 SITE AND PERIOD OF OBSERVATION

The instruments for the measurement of aerosols and electrical conductivity were installed on the top of the Physics Department building of Roorkee University, at a height of 12 meters from the ground far from any type of interference. At this site, only the aerosols and conductivity were measured while, all other meteorological parameters (temperature, humidity and wind speed) were measured at National Institute of Hydrology (NIH), Roorkee, situated very close to the Physics Department within the university campus.

Roorkee ($29^{\circ}52'$ N, $77^{\circ}53'52''$ E) lies at a height of 275 meters from the sea level. The measurements were made continuously from 22 to 27 October 1995 for 24 hours daily. Only the observation made one day before and after the eclipse day were analyzed and compared. During the eclipse and even on the control days the weather conditions were very much favourable. An attempt has been made to give a theoretical explanation of the experimental findings.

3.4 MEASUREMENT OF AEROSOLS AND CONDUCTIVITY

The detailed description of instruments and measuring techniques of aerosols and electrical conductivity has been given in Chapter 2. The positive and negative conductivities were measured using the equations 2.04 and 2.06

therefore total conductivity was calculated by equation 2.01, while concentration of aerosols and size were calculated by equations 2.08 and $r = \lambda x / 2\pi$, where x is size parameter of aerosol and λ is the wavelength of incident radiation. Mode radius was calculated using $r_m = \lambda x_m / 2\pi$, where x_m is the model size parameter of the aerosols.

Equation 2.08 represents the normal Gaussian distribution function for the atmospheric aerosols. For natural aerosols d'Almeida [5] have taken log-normal distribution, while others [169, 225] have used normal Gaussian distribution for their measurements on atmospheric particles which may consist of condensed particles and particulates along with the natural aerosols. The presence of anthropogenic aerosols can not be eliminated at the site of observation as the night before eclipse was Diwali, an Indian festival in which a huge amount of firework are set off. So the aerosol particles at the site of observation were mixture of natural particles, particulates and condensed droplets. Therefore for the present study we have used the normal Gaussian distribution.

As mentioned in section 2.2.1, the values of $I_1(\theta, \lambda, m, r)$ and $I_2(\theta, \lambda, m, r)$ in the model size parameter range 0.1 to 30 have been taken from [35] for the refractive indices 1.30 and 1.33. Gumprecht and Sliepcevich [57] have taken the refractive indices 1.20 to 1.60 in their studies on atmospheric aerosols. Pendorf [170] has also taken the refractive indices ranging from 1.33 to 1.50 for the size parameter range 0.1 to 30. Houghton and Chalkar [72] also considered the same value of 1.33 for the size parameter range from 7 to 24. In the present case due to sudden decrease of temperature and increase of humidity

water content of the air increases and condensation had already started and therefore, we have taken representative refractive indices 1.30 and 1.33.

3.5 RESULTS AND DISCUSSION

The observations of temperature, relative humidity and wind speed on the day of solar eclipse (24 October 1995) are shown in Figure 3.3. The temperature decreases with the onset of the eclipse and reaches a minimum at the time of maximum obscuration. The relative humidity increases due to the decrease of temperature. However, there is a difference of about 40 min between the times of minimum temperature and maximum humidity. This difference can be attributed to the atmospheric relaxation time, which falls in the range 30 min to 1 h. Wind speed, remained relatively constant and was lower than that on 23 or 25 October 1995. The wind on the day of eclipse was about one third of that of the previous day. On the day after the eclipse, the wind doubled.

The aerosol concentration on 24 October 1995 was more than twice that of the 23 October. The concentration on 25 October was the same as that for 23 October. Khemani *et al.* [101] has reported that hygroscopic atmospheric particles, in the size range 0.1-1.0 μm , increased by 43% during total solar eclipse of 16 February 1980 at Pune. This enhancement was attributed to the increased condensation and high relative humidity during the eclipse. In the present case, the measured total aerosol concentration in the size range of 0.05-3.0 μm was increased by about two times as compared to a non-eclipse day (Figure 3.4). The maximum increase was observed in the 0.5-3.0 μm size

range (Figure 3.5). The behavior of the variation of humidity was the same as for the aerosol concentration. This trend shows that the increase in aerosol concentration was influenced by the increase in humidity. However, Parameswaran and Vijayakumar [164] found that the humidity did not affect aerosol number density appreciably up to a relative humidity of 94%. Further, Parameswaran *et al.* [165] has shown that the increase of wind speed increases the aerosol number density, because more surface particles become air borne. The wind speed in the present observation decreased on the day of eclipse (Figure 3.3) and, therefore, the increase in aerosol concentration cannot be attributed to the wind speed. The increase in aerosol concentration in this study is attributed to the formation of aerosols due to increased condensation by atmospheric ions as discussed later in this section.

For the present calculations, the shape of the size distribution has been assumed to be Gaussian in all size ranges. Therefore, one may question the calculation of size distribution in different size bins. However, it is important to know the size range in which the maximum increase has taken place during the solar eclipse. This has been shown in Figure 3.5, which reveals that on the eclipse day the maximum increase above the average values of 23 and 25 October 1995 in the aerosol concentration took place in the size ranges 0.5-1.0 μm and 1.0-3.0 μm . The minimum increase in concentration was in the size range 0.05-0.1 μm . McCartney [135] has mentioned that the cloud condensation nuclei lie in the size range 0.1-1.0 μm (large) and greater than 1.0 μm (giant). Patel [169] studied the effect of ions on condensation using a diffusion chamber and found that the droplet size ranged from 0.75 μm to

1.01 μm . McCartney [135] citing different references has shown that the concentration of the cloud particles in the lower atmosphere peaked around 2.5 μm . Thus, the maximum increase of aerosol concentration in the present study, during the solar eclipse, lies in the range of the droplets. The decreased temperature, increased humidity and enhanced concentration of atmospheric ions [1, 200, 201] during the solar eclipse make the concentration of aerosols to increase to a maximum in the size range 0.5-3.0 μm due to the condensation process. Wark and Warner [225] describe that the particles below 0.1 μm (known as Aitken particles) behave in a way similar to the molecules undergoing random motion and collision. Any condensed particle in this range is likely to be evaporated soon.

One may also examine the variation of mode radius of aerosol particles during the total solar eclipse. The mode radius in the size range of the present observation, i.e., 0.05-3.0 μm for 23, 24 and 25 October 1995 has been shown in Figure 3.6. It can be seen from Figure 3.6 that the mode radius ranges from 0.5 μm to above 2 μm . The slope of best fit regression line for 24 October 1995 increases with time, while on other days, it decreases slowly. This can be attributed to the fall of temperature on eclipse day, while on other days, the

temperature monotonically rises with time. The mode radius decreases with the rise in temperature on all the days. Similarly, the mode radius increases with relative humidity, increase being faster on the eclipse day.

The observed variation in electrical conductivity of the atmosphere is shown in Figure 3.7. At the time of eclipse, on the average conductivity increases by 25-30%. The duration of peak of the conductivity on 24 October 1995 is also larger than for any other day. Anderson and Dolezalek [8, 42, 111, 159] measured the conductivity at Waldorf Annex of Naval Research Laboratory, USA (eclipse, 7 March 1970), Malignant Cove, USA (eclipse, 10 July 1972), Nagarampalam, India (eclipse, 16 February 1980) and Pune, India (eclipse, 18 March 1988) respectively. The observed variations in conductivity are in good agreement with the present results. A comparison of Figures 3.5 and 3.7 shows that during the solar eclipse both aerosol concentration and electrical conductivity increase. This is contrary to normal atmospheric conditions in which the increase of aerosol concentration normally occurs with the decrease in atmospheric electrical conductivity.

In the next chapter the atmospheric electrical conductivity and aerosol concentration has been studied in weather conditions like disturbed (monsoon) and fair weather (winter). The various effects of meteorological variables on these parameters have been discussed in detail.

Table 3.1- A summary of measurements of electrical conductivity by various investigators

Investigator(s)	Solar eclipse period	Place	Remarks
Anderson and Dolezalek [8]	7 March 1970	Waldorf Annex of the Naval Research Laboratory, Washington D.C. (USA)	Clear decrease in negative conductivity.
Lane-Smith and Markson [111]	10 July 1972	Malignant Cove Nova Scotia (USA)	The negative conductivity began to rise up to high values about 5 min after the totality.
Nizamuddin <i>et al.</i> [159]	16 February 1980	Nagarampalam, Visakhapatnam (India)	Both types of polar conductivities increase but increase in positive conductivity is more pronounced than negative conductivity.
Dhanorkar <i>et al.</i> , [42]	18 March 1988	Pune (India)	Remarkable changes in atmospheric conductivity during the period of eclipse.
Present work	24 October 1995	Roorkee (India)	Increase total conductivity.

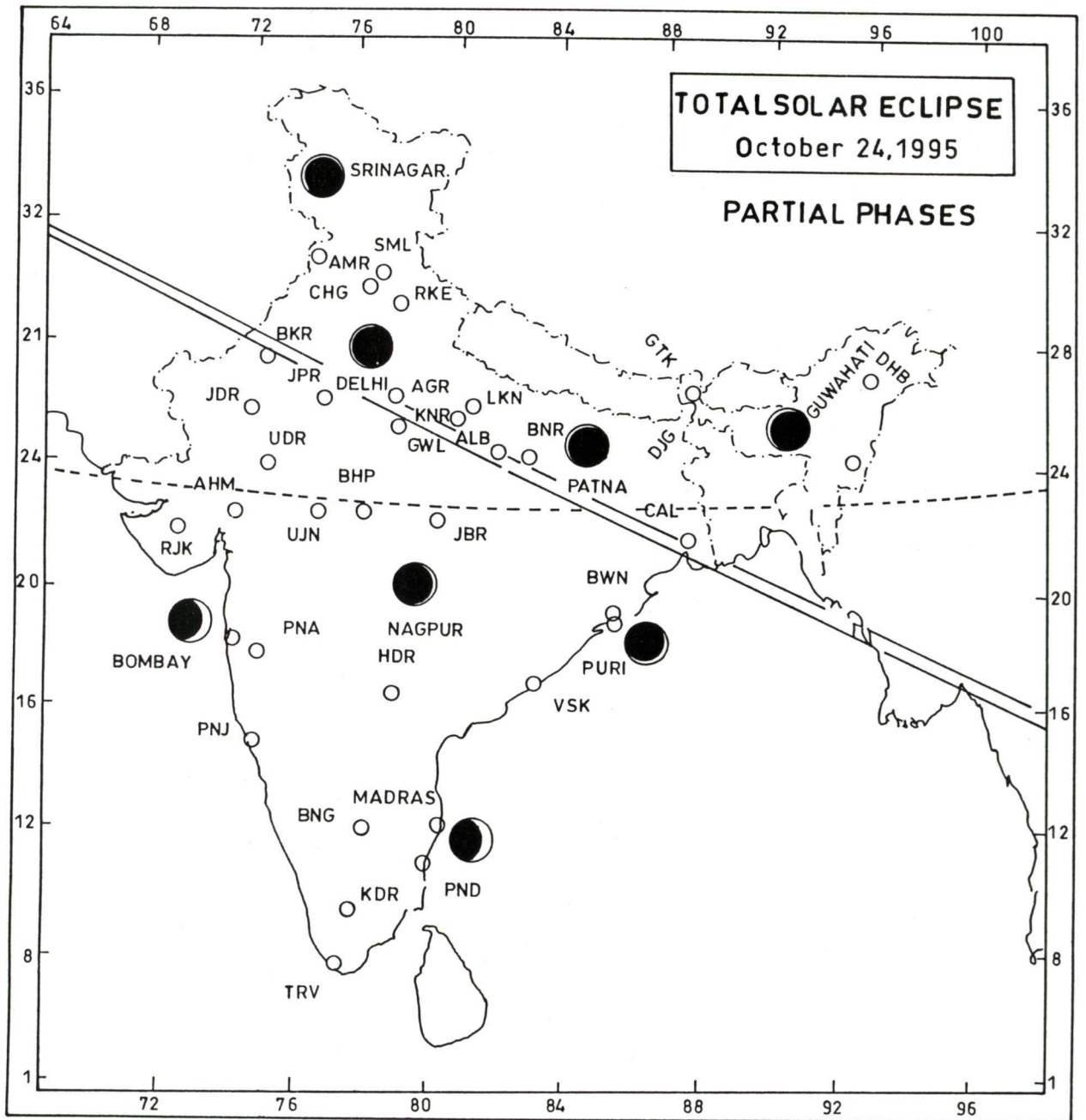


Figure 3.1 - Path of the total and partial solar eclipse on 24 October 1995 over India [77]

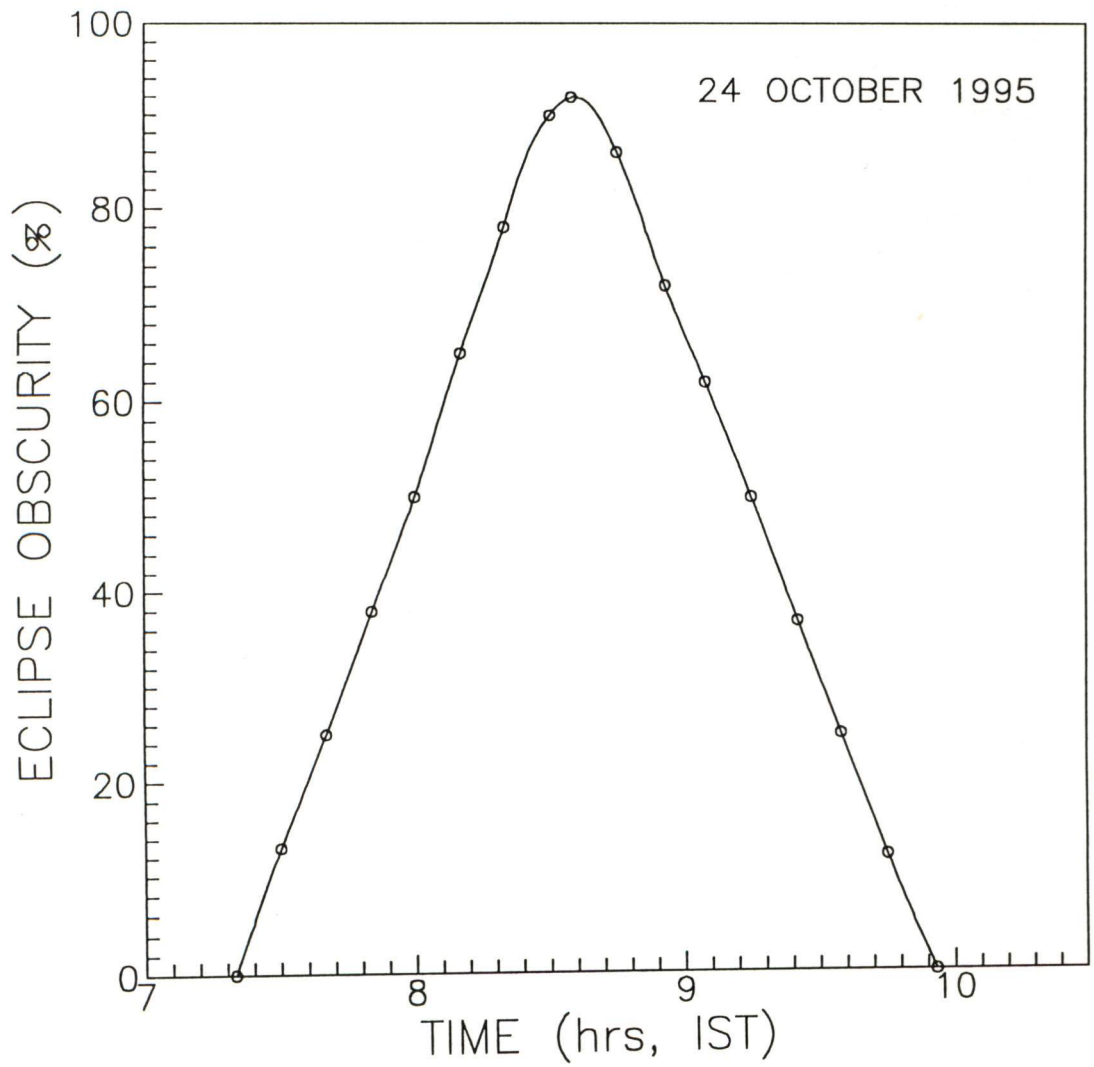


Figure 3.2 - Progress of solar eclipse at Roorkee, India

process. Hanel and Lehmann [61] and Shaw [198] have tried to study the size distribution of atmospheric aerosols in different meteorological conditions.

The man's activity in a world of rapidly growing population may lead to inadvertent change of the climate on a local basis and even on a global scale. Since the governing conditions of the human life style and the increasing air pollution are on an average related together and may have influence on the atmospheric electrical parameters. Therefore, it is considered that parallel with the problem of pollution by industrial sources, vehicular traffic etc, the surface electrical parameters may also be altered [1, 95]. The atmospheric electrical parameters viz. atmospheric electrical conductivity, air-earth current density, electric field etc are affected by various environmental and meteorological factors and hence they do not remain in steady state at all the times. So, the atmospheric electrical phenomena can be studied in two different areas, the fair-weather region and the disturbed weather region with two types of variations in electrical parameters, i.e. one is global in nature and the other is of local type. The local variations in the atmospheric electrical parameters are considered to give information on the meteorological conditions in the lower layers of the atmosphere.

The study on the relation of atmospheric electrical parameters with meteorological conditions is important because both of them are associated with each other. Therefore, the characteristics of the environment such as the aerosol, moisture content, surface wind, temperature, atmospheric pressure, relative humidity, dew point etc, which influence the variation of these electrical parameters, need to be studied in greater detail. Some investigators [91, 97

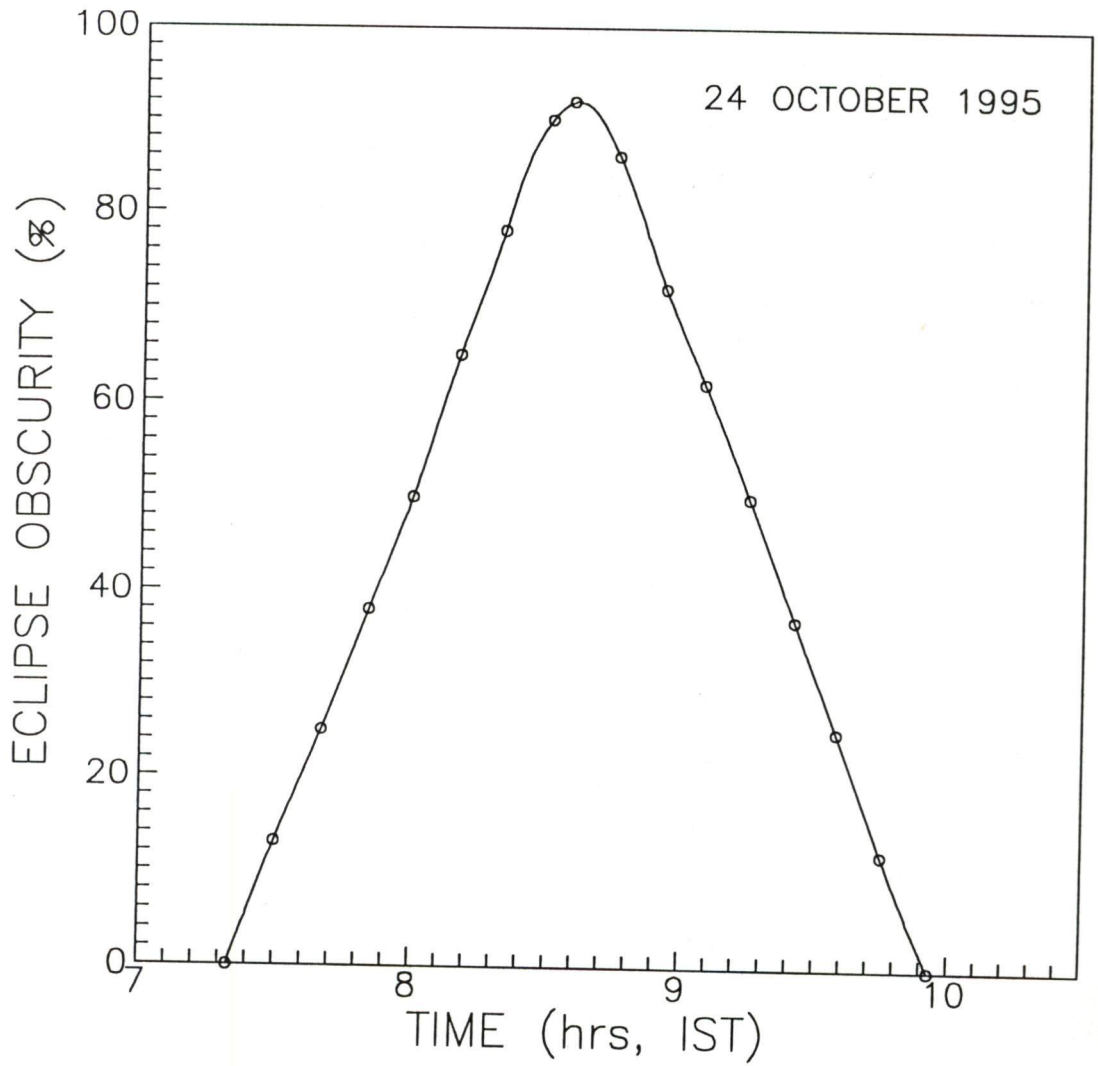


Figure 3.2 - Progress of solar eclipse at Roorkee, India

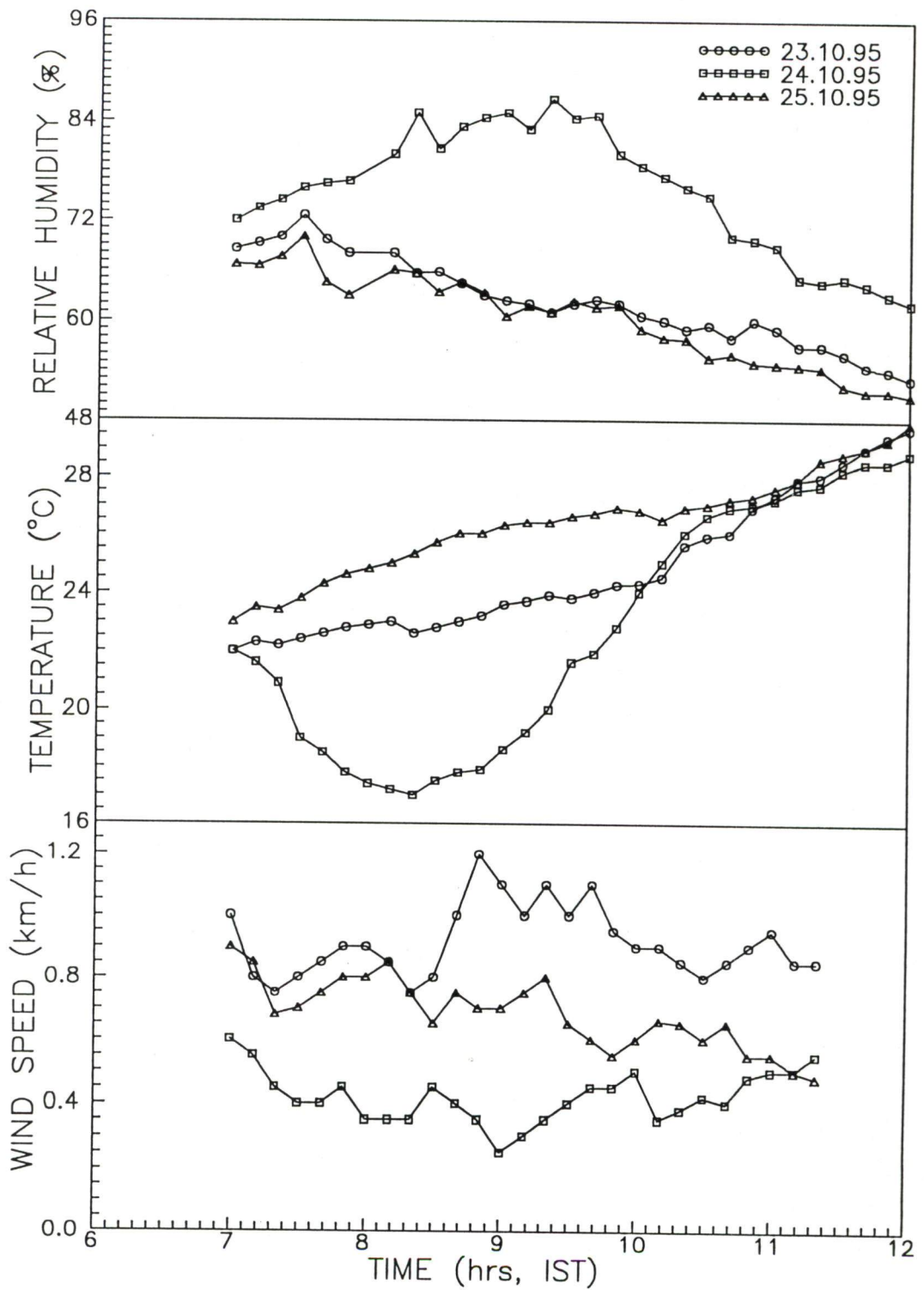


Figure 3.3 - Time variation of wind speed, temperature and relative humidity

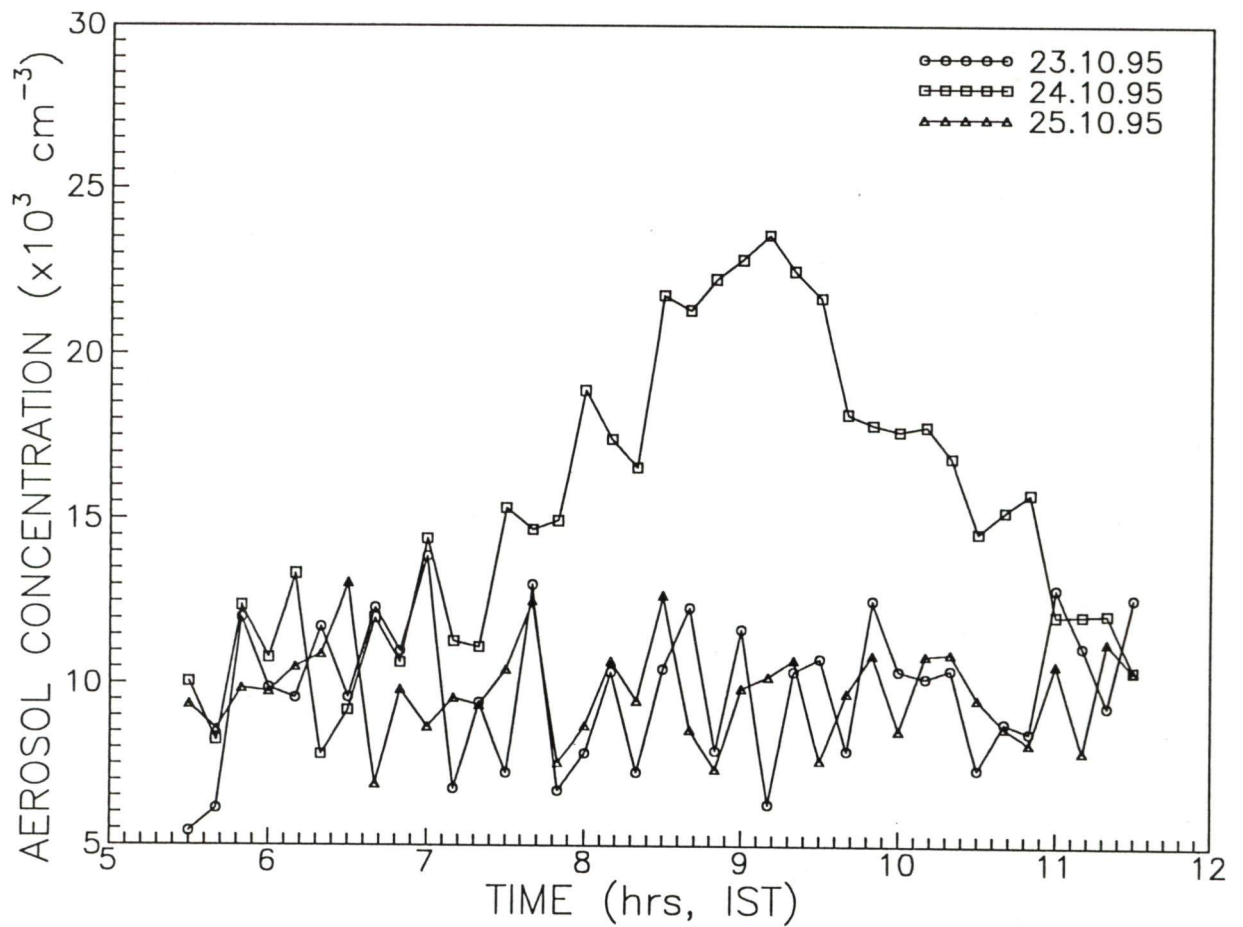


Figure 3.4 - Time variation of total aerosol concentration (0.05-3.0 μm)

- - - 23.10.95
 — 24.10.95
 - - - 25.10.95

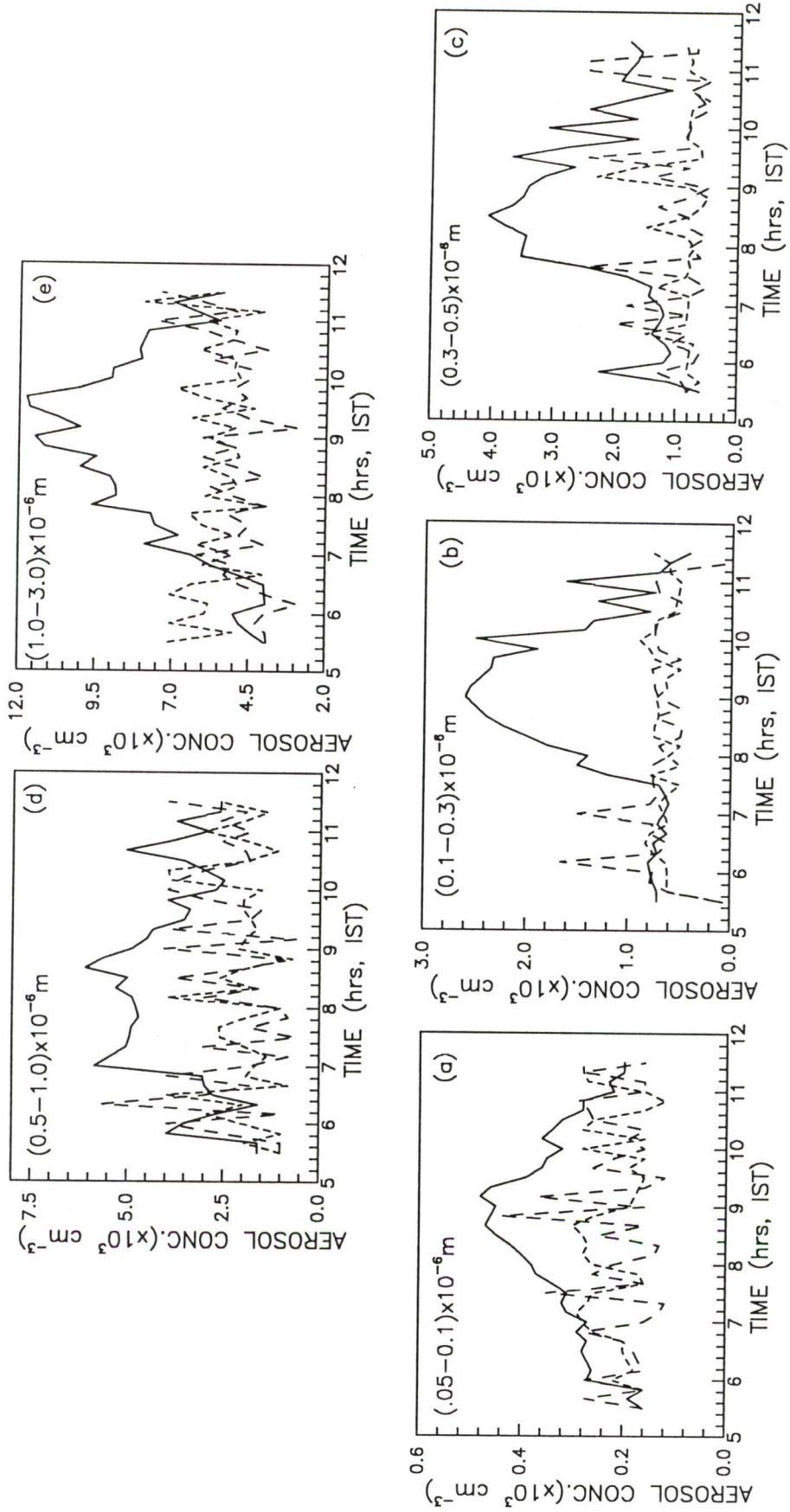


Figure 3.5 - Time variation of aerosol concentration in different size ranges [(a) for 0.05-0.1 μm , (b) for 0.1-0.3 μm , (c) for 0.3-0.5 μm , (d) for 0.5-1.0 μm , and (e) for 1.0-3.0 μm].

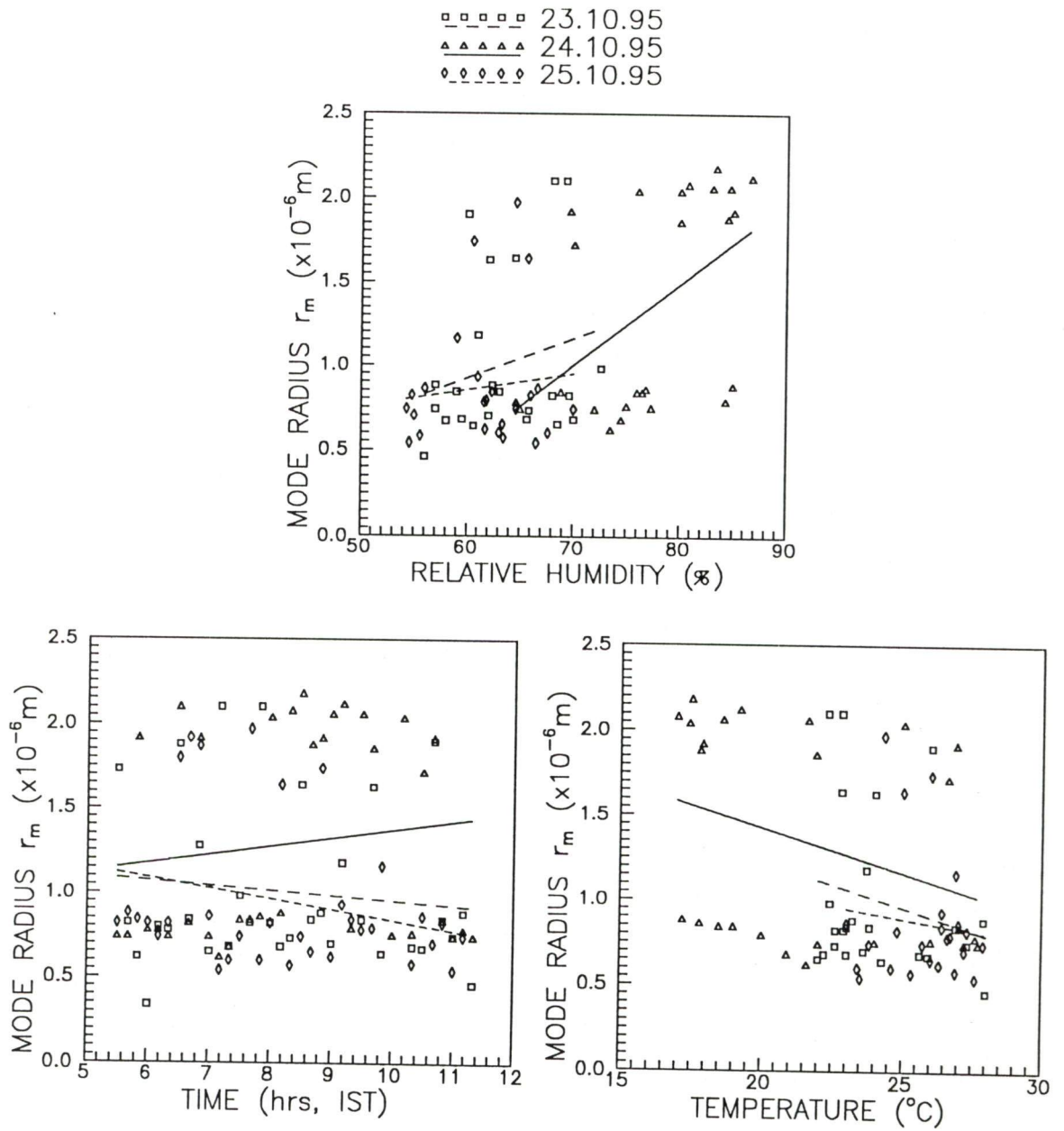


Figure 3.6 - Variation of mode radius with respect to time, temperature and relative humidity

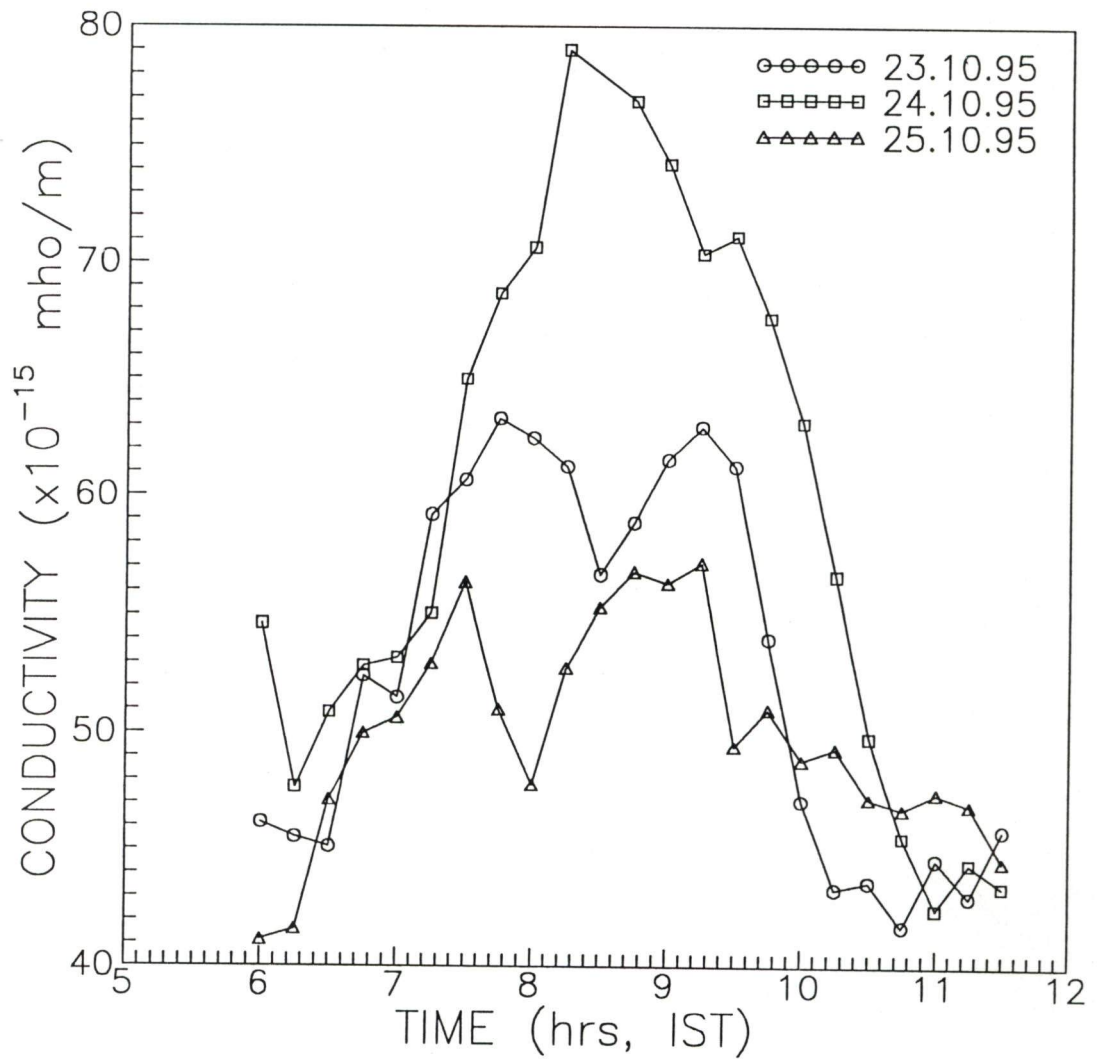


Figure 3.7 - Time variation of atmospheric electrical conductivity

Chapter 4

*Atmospheric Aerosols
And
Electrical Conductivity
During Monsoon And
Winter Seasons*

The atmospheric aerosols are produced by variety of processes and are very much important to characterize various lower tropospheric phenomena. A study on the variation of atmospheric aerosol concentration in relation to their dependence on some meteorological parameters, close to the earth surface, can greatly help to understand the role of meteorology in the aerosol distribution and vice versa. A clear knowledge of the nature of size distribution of aerosols at any location is very important not only to characterize the aerosol system but also to study the cloud process [231], radiative properties [108] and atmospheric heating due to green house gases [63] at that location. While such studies have been carried out [70, 166] at high latitudes, the studies at low latitudes are few [203].

The atmospheric aerosols are generally hygroscopic, so relative humidity plays very important role to alter the radiative property of aerosols [164]. Hanel [60] studied the changes in aerosol properties as a function of relative humidity. Devara and Raj [40] have tried to find out some relationship between meteorological parameters and columnar aerosol distribution. Parameswaran *et al.*, [165] studied the variation of aerosol optical depth covering the period of June 1989 to December 1990 in relation to various meteorological factors like wind speed, rain fall, relative humidity at a coastal station, where sea plays very important role to govern the meteorological

process. Hanel and Lehmann [61] and Shaw [198] have tried to study the size distribution of atmospheric aerosols in different meteorological conditions.

The man's activity in a world of rapidly growing population may lead to inadvertent change of the climate on a local basis and even on a global scale. Since the governing conditions of the human life style and the increasing air pollution are on an average related together and may have influence on the atmospheric electrical parameters. Therefore, it is considered that parallel with the problem of pollution by industrial sources, vehicular traffic etc, the surface electrical parameters may also be altered [1, 95]. The atmospheric electrical parameters viz. atmospheric electrical conductivity, air-earth current density, electric field etc are affected by various environmental and meteorological factors and hence they do not remain in steady state at all the times. So, the atmospheric electrical phenomena can be studied in two different areas, the fair-weather region and the disturbed weather region with two types of variations in electrical parameters, i.e. one is global in nature and the other is of local type. The local variations in the atmospheric electrical parameters are considered to give information on the meteorological conditions in the lower layers of the atmosphere.

The study on the relation of atmospheric electrical parameters with meteorological conditions is important because both of them are associated with each other. Therefore, the characteristics of the environment such as the aerosol, moisture content, surface wind, temperature, atmospheric pressure, relative humidity, dew point etc, which influence the variation of these electrical parameters, need to be studied in greater detail. Some investigators [91, 97,

124, 184] made an attempt in this direction.

In the study of the relationship of atmospheric electrical conductivity with meteorology, it is important to know which meteorological parameters exhibit the maximum correlation. Therefore, simultaneous measurements of unipolar conductivity and useful meteorological variables, viz atmospheric pressure, temperature, relative humidity, wind speed and precipitation should be made and also taken into account the time dependent nature of these elements. In this context the survey of recent literatures indicated that the aspects of diurnal, seasonal, annual, long-term and incidental variations of some surface atmospheric electrical parameters were examined more frequently by different workers at different places but the short-term variations of electrical conductivity with due consideration to these meteorological parameters have been reported much less [36, 195].

4.1 MEASUREMENTS OF AEROSOLS AND CONDUCTIVITY

The purpose of the present work is to study the experimental results of direct measurements of positive conductivity and aerosols and correlate them with some meteorological parameters viz. temperature, relative humidity, rain fall and wind speed. Therefore measurements of positive conductivity and aerosols have been made daily for twenty four hours at the top floor (about 12 m from ground) of the Physics Department, University of Roorkee, Roorkee (29° 52' N, 77° 53' 52" E, 275 m above sea level) during disturbed (SE monsoon, 1996) and fair weather (winter, 1996-97) conditions. However the result of conductivity measurements have been presented here only during the period of June 1996 to August 1996. Roorkee has natural as well as anthropogenic sources for atmospheric

particles. Since place is not an industrial one the man made particles are produced only by vehicular traffic and household activities.

For the measurement of atmospheric electrical conductivity and aerosols, the detailed description of instruments and methodology have been given in sections 2.1.1 and 2.2.1 respectively.

4.2 RESULTS AND DISCUSSION

The observations on meteorological parameters like temperature, wind speed, relative humidity and rainfall and aerosol concentration have been shown in Figures 4.1 and 4.4 for the monsoon and winter seasons respectively. The variation of aerosol concentration with wind speed (WS), average temperature, relative humidity (RH) and rainfall (RF) are shown in Figure 4.2 and 4.5. Also the behavior of mode radius with these parameters has been shown in Figure 4.3 and 4.6 respectively for both seasons. A close scrutiny of these data shows that the aerosol concentration decreases continuously during monsoon season while RH was minimum in June and maximum in September 1996. In the month of June and July, 1996 the average aerosol concentration was maximum while RH was minimum in these months (Figure 4.1). Also, concentration varies in phase with temperature and wind speed (Figure 4.2). Hanel and Lehmann [61] and Shaw [198] suggest that the size distribution of atmospheric aerosols varies significantly with change in temperature and relative humidity. Parameswaran and Vijayakumar [164] found that the RH does not affect significantly the aerosol concentration and size distribution up to a limit of 95%. Here at Roorkee in the month of August and September 1996 average RH was almost close to this limit. Devara and Raj [40] have observed

that the higher relative humidity, lower temperature during SW monsoon (1988) at Pune, India caused the growth of cloud droplets which results higher rainfall. The same physical process appears to have happened in 1996 at Roorkee during the SE monsoon. The decrease in aerosol concentration varies in phase with the increasing activity of monsoon. This is attributed to the RF, which was the powerful factor to lower the aerosol concentration involving rain out process.

The mode radius of aerosols decreases continuously during monsoon season. Wind does not play significant role in governing the mode radius while it varies in phase with average temperature and out of phase with RF and RH. Parameswaran and Vijayakumar [164] have found that the aerosol size distribution remains unaffected by the relative humidity up to a limit of 95%. After this value the mode radius increases with RH. However our findings are contrary to the work of Parameswaran and Vijayakumar [164]. During monsoon period the aerosols are removed from the atmosphere by scavenging which explains our observations that the mode radius inversely correlated with relative humidity. For other seasons it is not true situation.

The winter season (November, 1996-February, 1997) at Roorkee was quite different from SE monsoon. The rain does not occur significantly during this period. Wind also does not play any effective role during first half (November-December, 1996) but varies in phase with the concentration during second half (January-February, 1997)(Figure 4.4). The high humidity and low temperature was observed during this season (Figure 4.4). The aerosol concentration increases with increase in RH and WS and decrease with

temperature (Figure 4.5). The same is true for mode radius also (Figure 4.6). Wind speed plays important role in governing the mode radius as large number of particles become air-borne and takes part in condensation due to low temperature and high relative humidity. The average value of RH was found to be above 90% during the second half of winter and about 80% during the first half. The average temperature touches a minimum of 10 °C during January 1997. The increased mode radius and aerosol concentration is attributed to the growth of particles due to high RH and low temperature during the whole season.

The results indicate a strong correlation between the aerosol number density and size distribution and meteorological parameters in different weather conditions. Although the observations were taken at Roorkee, the findings are expected to be valid for all subtropical regions.

Figures (4.7, 4.8 & 4.9) show the variation of atmospheric electrical conductivity for the months of June, July and August 1996 respectively. The electrical conductivity for the three consecutive months were in the ranges of (16.86-37.11), (11.30-64.93) and (16.91-59.11) $\times 10^{-16}$ mho/m respectively while the relative humidity was found to be within limits of (65-96), (67-94) and (86-95) for June, July and August 1996. The atmospheric electrical conductivity in the month of June is positively correlated with relative humidity while in the months of July and August 1996 it is negatively correlated. Table 4.1 shows daily rainfall data for the months of June, July and August 1996 respectively. As seen from Table 4.1, in Roorkee, it rarely rained in the months of June 1996 except for last four days. The increased relative humidity is due to the

increased moisture content of the atmosphere. Uman [218, 219] has mentioned that the electrical conductivity of the moist air is greater than that of the dry air.

However, July and August 1996 are the months of rain. Condensation of water molecules starts on aerosol particles. The atmospheric ions attached to the droplets and aerosols decrease the mobility of these ions. Even when the droplets grow to become a drop and rain, it brings the atmospheric charge carriers to the ground. Thus the increasing relative humidity decreases the atmospheric electrical conductivity either by decreasing the mobility of charge carriers or by bringing the charge carriers to the ground through precipitation. Bhartendu [12] also reported that the changes in relative humidity are inversely correlated to atmospheric electrical parameters.

The variation of temperature for the above months has been shown in Figures 4.7, 4.8 and 4.9. The Figures show that during all the three months of monsoon period the conductivity has a negative correlation with temperature. Nizamuddin *et al.* [159] found that with the onset of solar eclipse of March 7, 1980 an increment in both types of conductivity was reported. It is well known that the solar eclipse event is followed by a decrease in temperature. This has been attributed to the increased relative humidity in the atmosphere and hence the increase in atmospheric conductivity. However, the conditions during monsoon period are quite different. During this period the water droplets are formed in the atmosphere thereby increasing the total aerosol concentration. A rise in temperature vaporizes the existing droplets and a decreasing temperature creates more droplets due to increased condensation.

Our results for unipolar (positive) conductivity and wind speed (Figures 4.7, 4.8 and 4.9) show somewhat positive correlation for the three months of

June, July and August 1996 respectively and slight enhancement were noted for increased wind speed. However to establish any correlation a cross-correlation study may become quite helpful. Mukku [153] also found that the wind speed influences conductivity mostly in the short-term range.

The present work deals with experimentally unipolar conductivity, density of aerosols and meteorological parameters such as relative humidity, temperature, wind speed and rain fall during the June, July and August 1996. The conductivity has been found to decrease with increasing relative humidity and temperature. Wind is an important factor, which modifies the behavior of conductivity in short-term range. It also brings out the fact that the number density of aerosols is very much affected by the meteorological parameters. The aerosol concentration was minimum in the August, September and November 1996 and remained around maximum in June-July 1996 and January-February 1997. The variation of aerosols is in phase with relative humidity during winter season while it is out of phase with temperature. Its variation with relative humidity has been explained in terms of condensation taking place in the atmosphere. During monsoon period the rain plays very important role in characterizing the aerosol density. The aerosol concentration and size were found to be decreased during September 1996 although the humidity was very high. The credit goes to scavenging of aerosol particles.

Table 4.1- Daily rain fall data for the months of June, July and August 1996

Date (June'96)	Rainfall (mm)	Date (July'96)	Rainfall (mm)	Date (August'96)	Rainfall (mm)
11	0.2	1	0.3	1	7.8
12	-	2	-	2	18.6
13	-	3	-	3	11.4
14	-	4	-	4	31.0
15	-	5	32.1	5	-
16	-	6	-	6	-
17	-	7	-	7	-
18	-	8	-	8	3.2
19	-	9	-	9	11.6
20	-	10	15.2	10	1.4
21	0.3	11	21.4	11	1.6
22	-	12	4.2	12	0.2
23	-	13	4.0	13	76
24	-	14	-	14	23.5
25	3.1	15	7.4		
26	-	16	-		
27	20.4	17	5.0		
28	3.2	18	-		
29	0.5	19	32.2		
30	14.2	20	11.2		

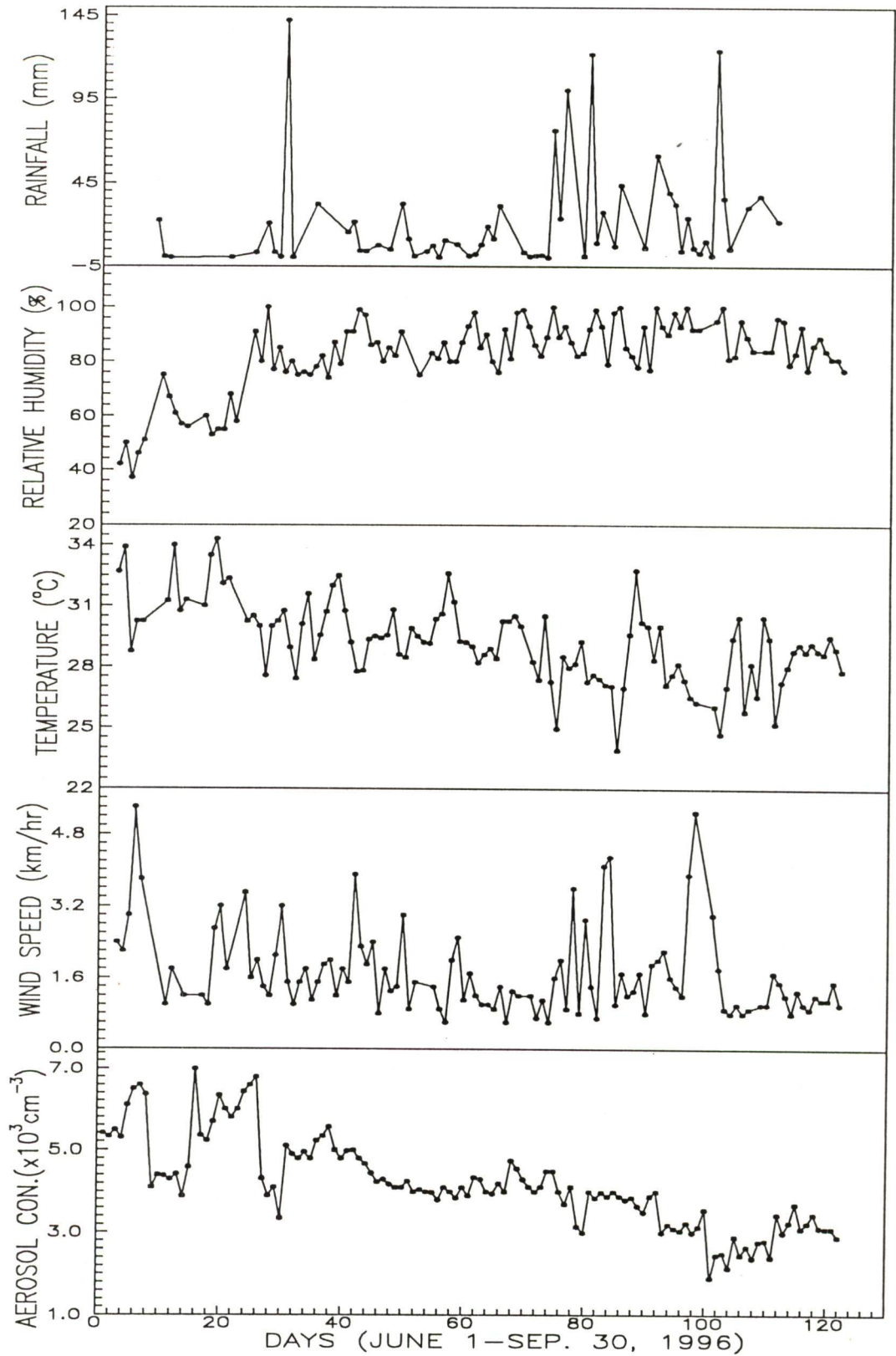


Figure 4.1 - Variation of aerosol concentration, wind speed, temperature, relative humidity and rainfall during June-September, 1996

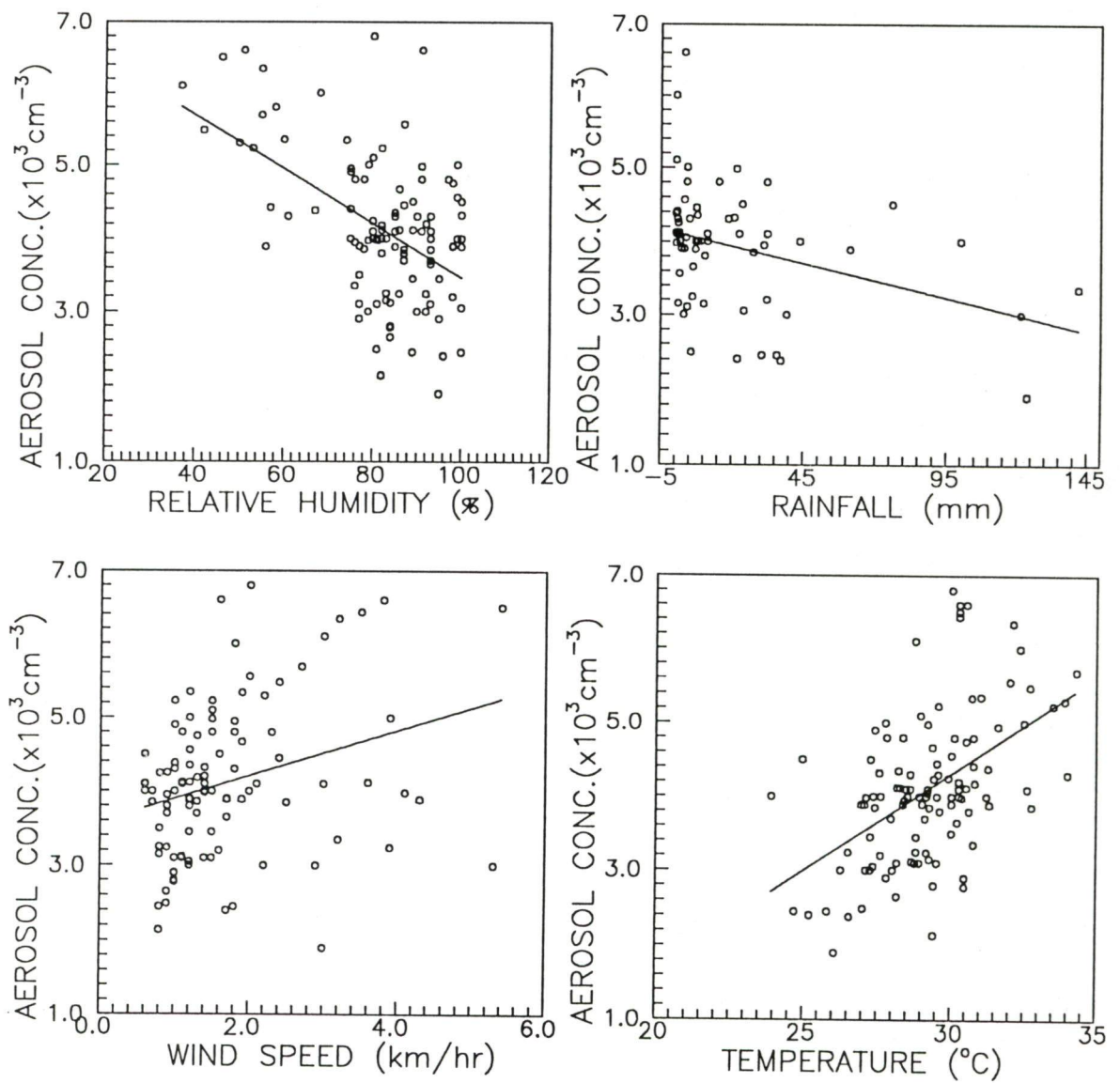


Figure 4.2 - Variation of aerosol concentration in relation to wind speed, temperature, relative humidity and rainfall during June-September, 1996.

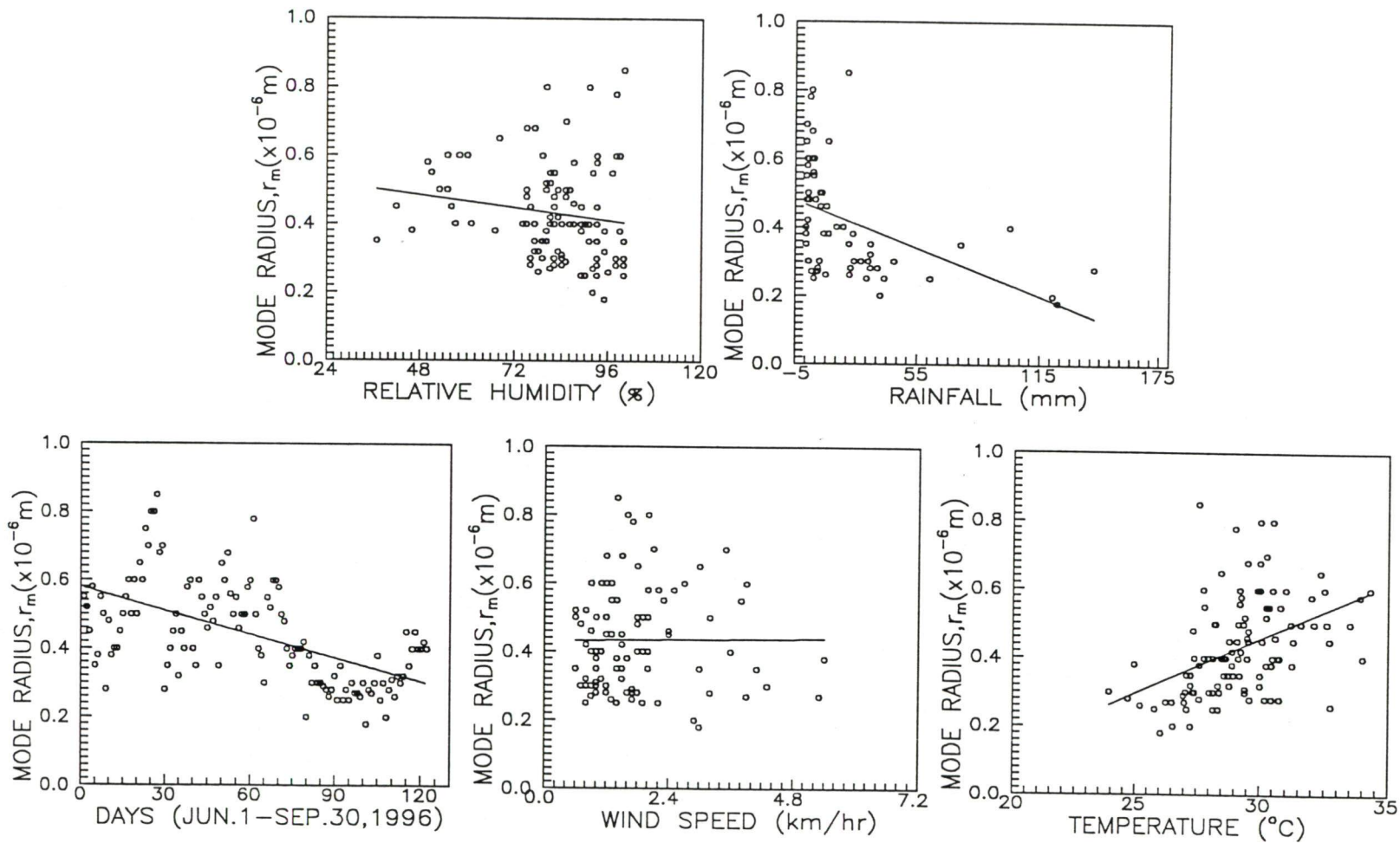


Figure 4.3 - Variation of mode radius in relation to wind speed, temperature, relative humidity and rainfall during June-September, 1996

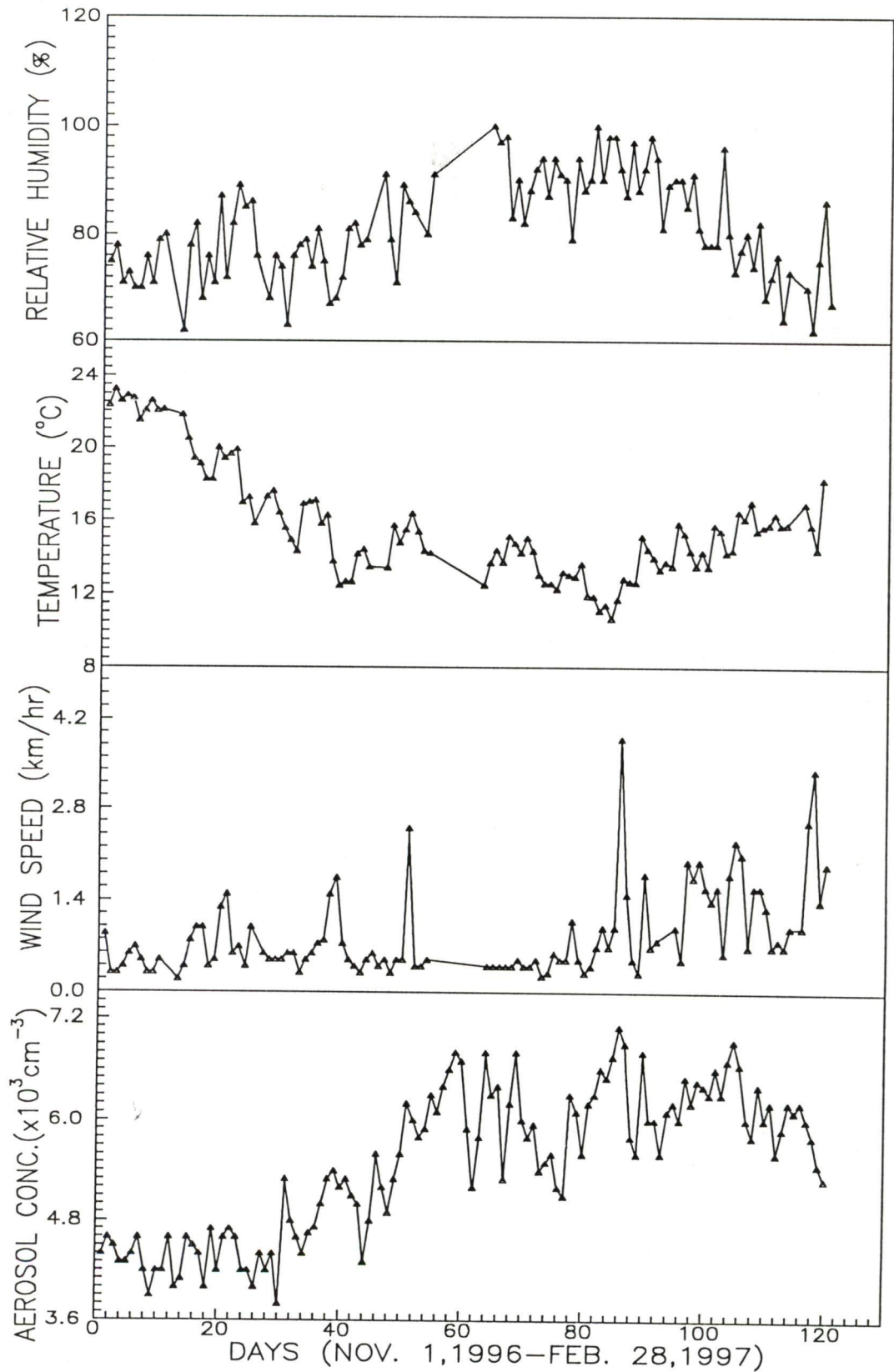


Figure 4.4 - Variation of aerosol concentration, wind speed, temperature and relative humidity during November, 1996-February, 1997

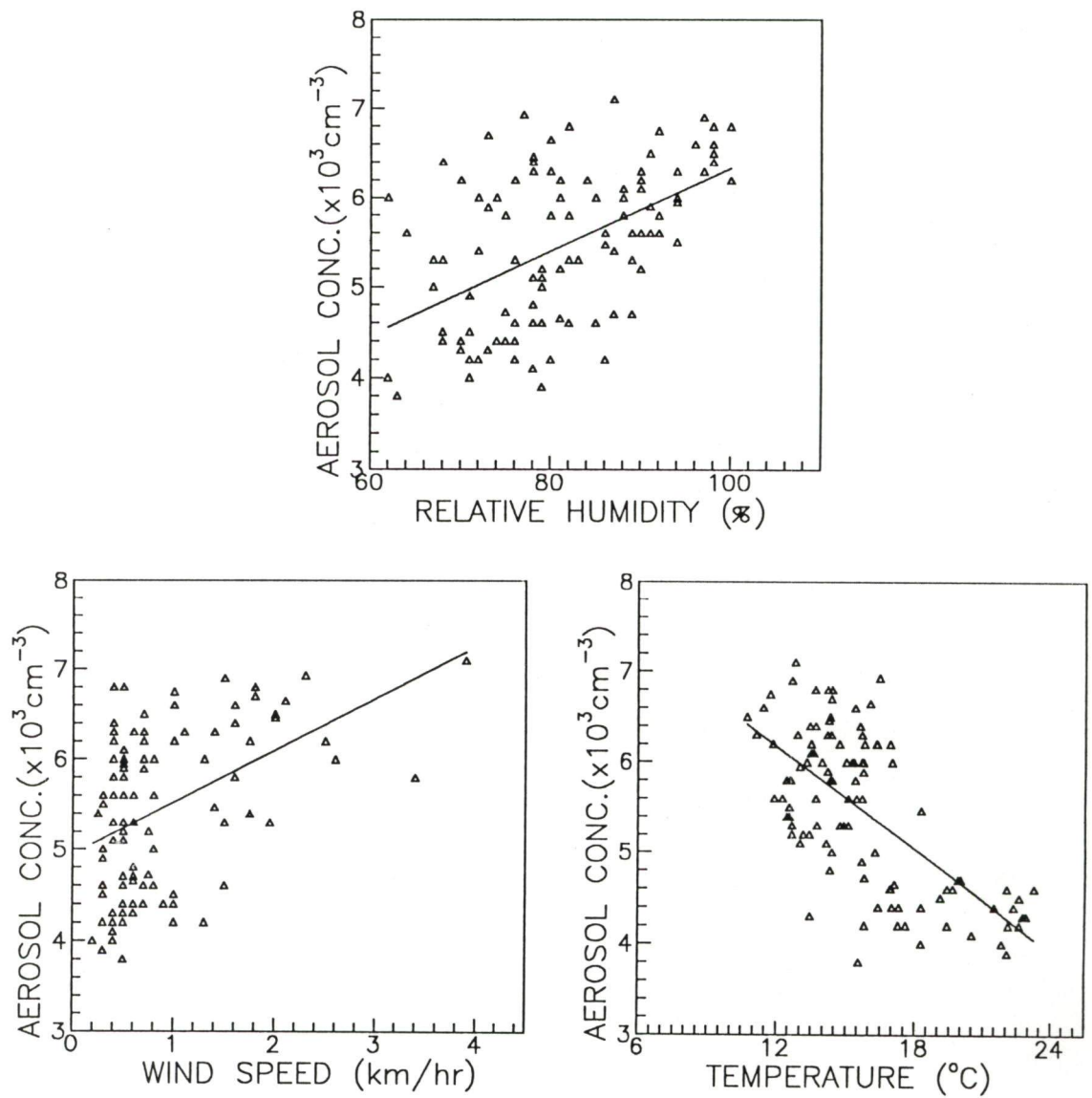


Figure 4.5 - Variation of aerosol concentration in relation to wind speed, temperature and relative humidity during November, 1996-February, 1997.

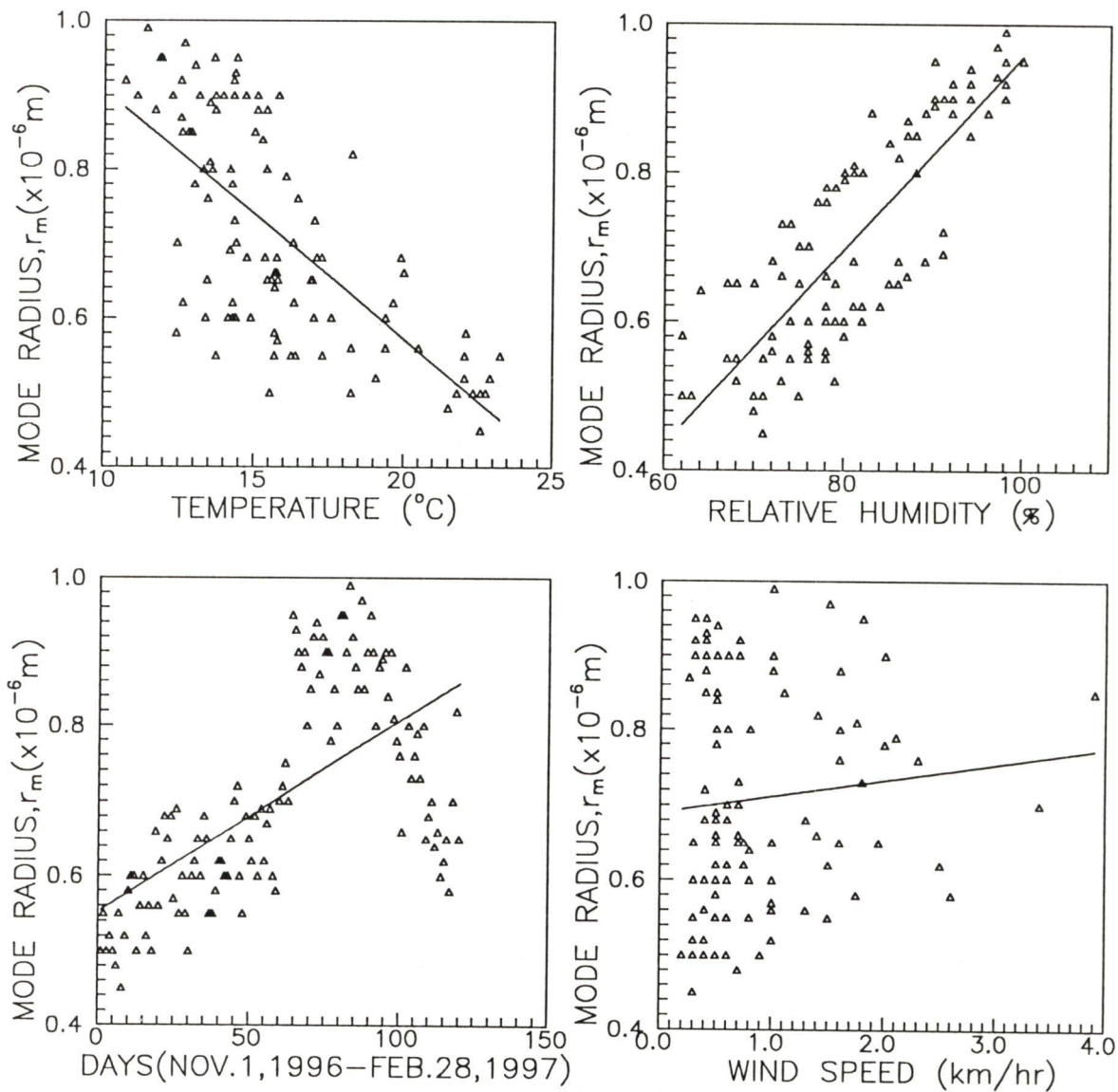


Figure 4.6 - Variation of mode radius in relation to wind speed, temperature, relative humidity and rainfall during November, 1996-February, 1997.

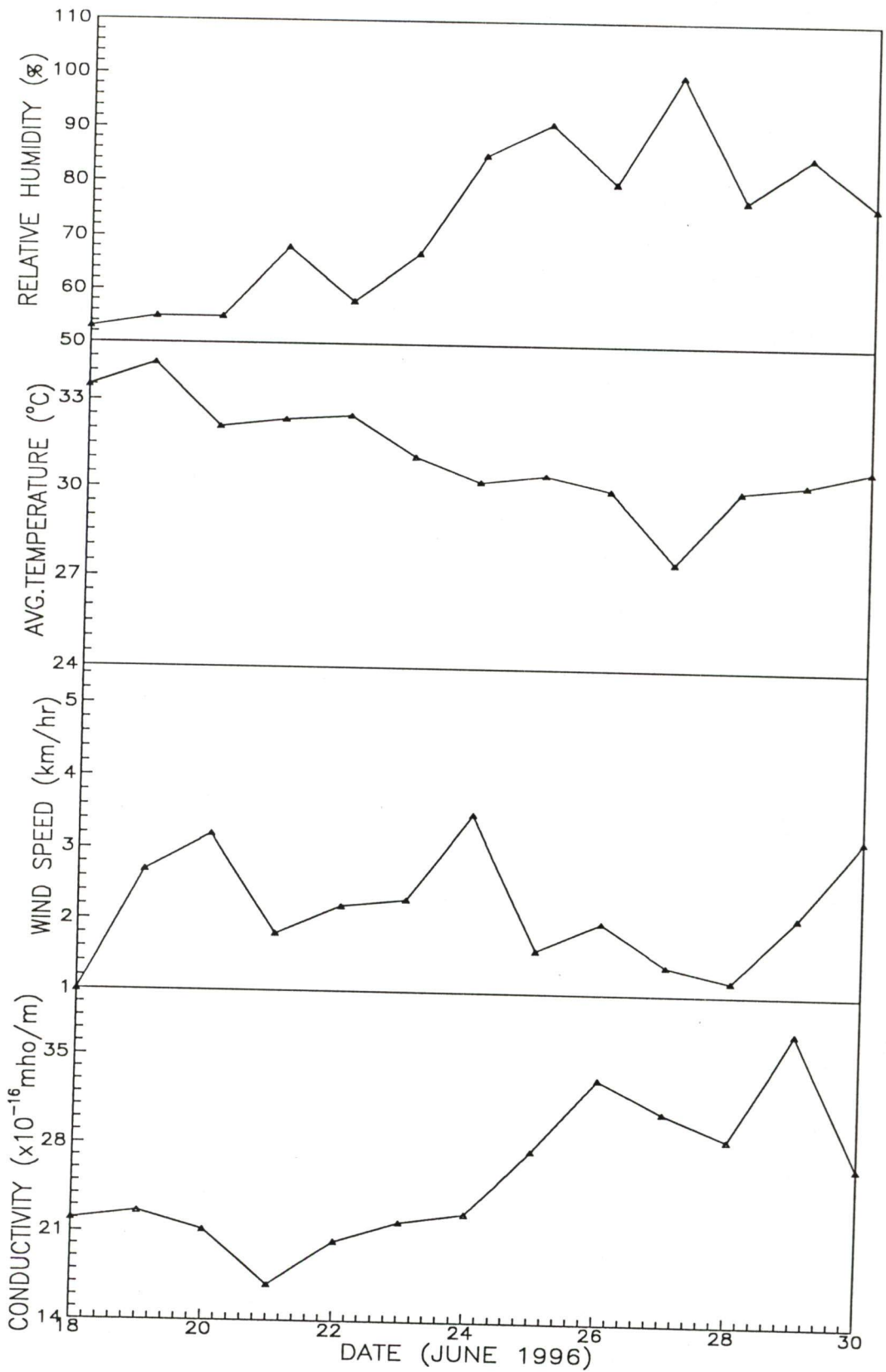


Figure 4.7 - Variation of positive conductivity, wind speed, temperature and relative humidity for June 1996 (18-30 June 1996)

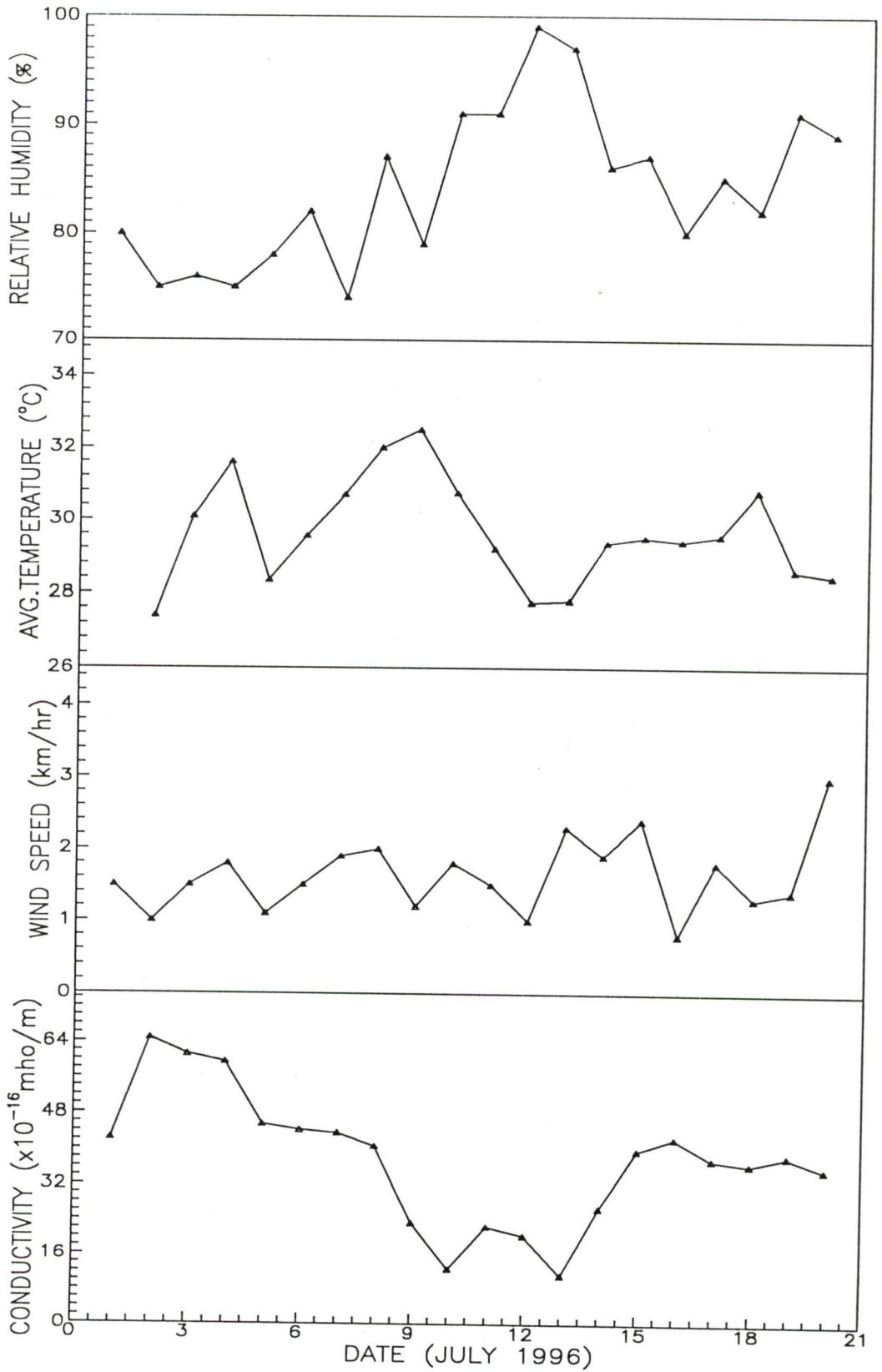


Figure 4.8 - Variation of positive conductivity, wind speed, temperature and relative humidity for July 1996 (1-20 July 1996)

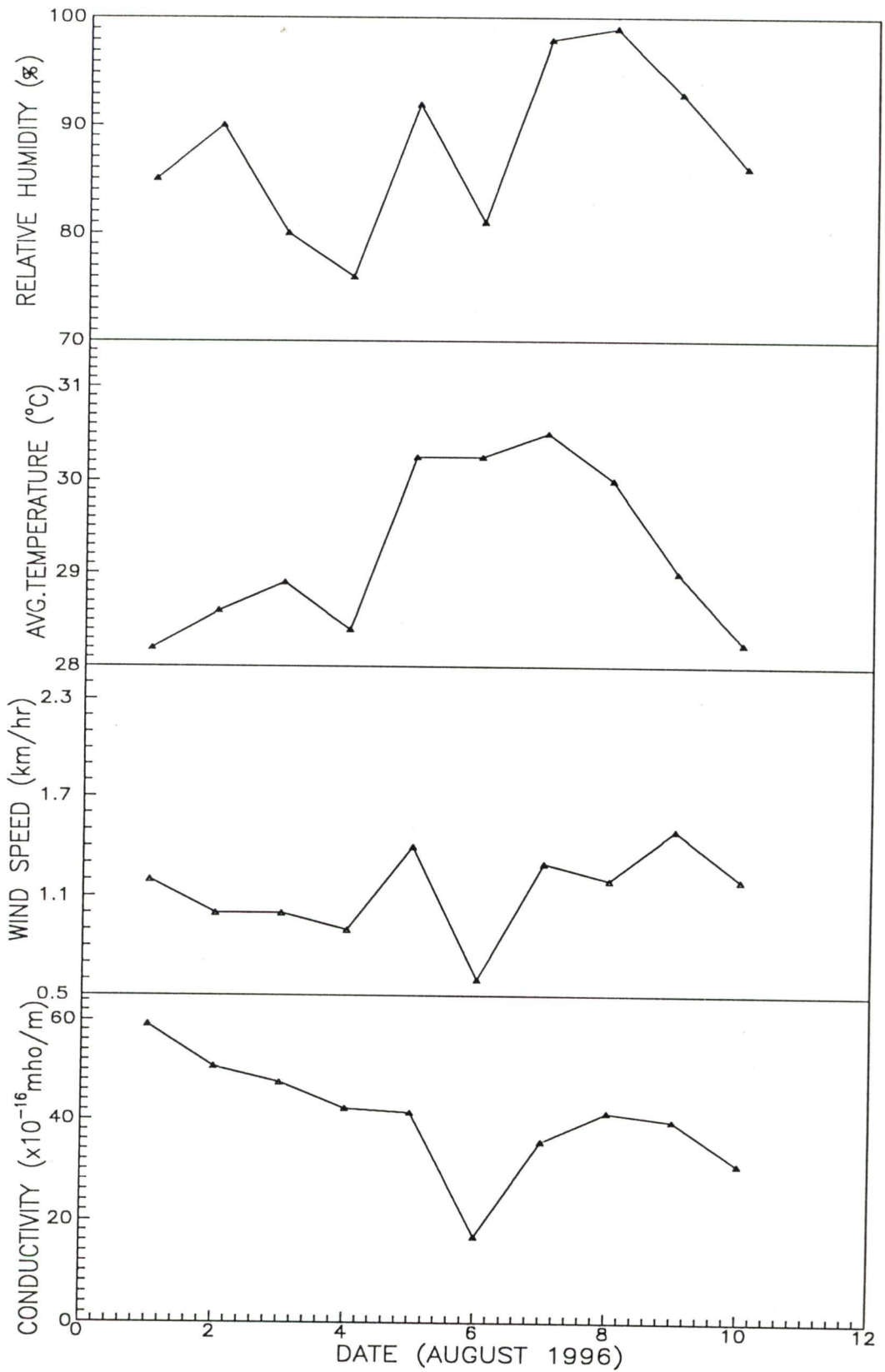


Figure 4.9 - Variation of positive conductivity, wind speed, temperature and relative humidity for August 1996 (1-10 August 1996)

Chapter 5

*Study Of
Ionospheric Particles
At Low Latitude
F₂-Region Using
SROSS-C2 Data*

During last four decades the system of ionosphere has been studied extensively by many researchers. These studies include experimental as well as theoretical methods. On experimental side, balloons, rockets, satellites, coherent and incoherent scatter radar, magnetometers and number of ground-based instruments have been used to study the ionosphere. On the other hand, studies have been conducted with 1-, 2- and 3-dimensional numerical models. Initially these models were restricted for specific regions (high-, mid- and low-latitude). But during last one decade many globalize models were developed to study the ionosphere. It is a well known fact that ionospheric system changes its behavior with altitude, latitude, longitude, universal time, season, solar cycle and geomagnetic activity. These changes occur due to solar, magnetospheric, mesospheric and tropospheric processes as well as coupling among these. The basic mechanism which, affects more than any other process is solar extreme ultraviolet (EUV) and ultraviolet (UV) radiation, but magnetospheric electric field, particles precipitation and heat flows have a significant role in altering the atmosphere. Also, gravity waves and tides propagating up from the lower atmosphere can appreciably affect the ionosphere. These processes affect the density, composition, and temperature of ionized and neutral constituents in the ionosphere. At mid-latitudes, the average electron density distribution tends to be uniform, with a gradual

transition from dayside high densities to nightside low densities. The equatorial electron densities also tend to be uniform on the dayside [193].

The ionosphere varies in composition and in temperature appreciably from hour to hour or from day to day or season to season. The ionospheric weather disturbances can affect over-the-horizon radars, HF communication surveying and navigation systems that use global positioning satellite (GPS), satellite tracking, satellite life time and power grids [27, 102, 197].

After more than 40 years of extensive research we have reached to a point where specific forecasting are possible regarding ionospheric behavior. There are several agencies with infrastructure have been created to study the ionospheric system and their effects on other natural atmospheric processes and many man-made activities. Some of the agencies are National Aeronautics and Space Administration (NASA), National Oceanic and Atmospheric Administration (NOAA), Indian Space Research Organization (ISRO), European Space Agency (ESA) etc.

In this chapter the author has described the Retarding Potential Analyzer (RPA) payload of Stretched Rohini Series Satellite (SROSS-C2) launched by ISRO which is used to study the ionospheric composition and temperature anomalies. The results of about one year of study over the Indian region have been presented in this chapter.

5.1 STUDIES ON D, E AND F REGIONS

There are several experimental and theoretical approaches to study the different regions of ionosphere i.e. D, E and F region. Experimental studies make use of artificial satellites, established in the ionosphere by rockets. Also

the radio waves emitted either by natural processes or by man-made transmitters are used to study the ionosphere. For the purpose of D and E region investigation, Indian Middle Atmospheric Programme (IMAP) has been carried out with involvement of many institutions and funded by several agencies. The implementation of the observational phase of IMAP was conducted during 1982-89 in which a total of 9 rockets were launched. This campaign was carried out in two phases, i.e. for (a) intercomparison of different techniques used to measure ion/electron densities and related parameters in D region and (b) investigation of D region and associated phenomena. The main measuring instruments (payloads) are Gerdian Condenser, Langmuir Probe, Spherical Probe, Optical Ozonsonde, Optical Nitric Oxide and Lyman-alpha photometers.

In the Indian context for the investigation of F region the satellites have been developed by ISRO under the SROSS programme. These satellites were proposed to have a near circular orbit of about 425 km. The Space Science Division of National Physical Laboratory (NPL), India proposed RPA experiment for the SROSS satellite.

5.2 THE SROSS MISSION AND RPA PAYLOAD

On May 4, 1994 the SROSS-C2 satellite was launched by the ASLV-D4 rocket in an orbit of 930 km x 429 km. After two months of operation in this high altitude orbit, the satellite apogee was brought down to 620 km. The life of this satellite is predicted to be more than five years. SROSS-C2 is the fourth satellite of the Stretched Rohini Series Satellite programme of ISRO and it was designed, developed, fabricated and tested in ISRO Satellite Centre (ISAC),

Bangalore. It is 114 kg satellite carrying 6 kg hydrazine fuel and is designed to generate 50 watt onboard power. Figure 5.1 shows the configuration of satellite with its main parts.

The SROSS-C2 satellite had an orbit having 46° inclination with the equatorial plane and having 917 km apogee and 429 km perigee. This is a spin-stabilized satellite with spin rate of 5 revolutions per minute. Figure 5.2 shows the motion of the satellite in its orbit. The satellite moves in the orbit keeping the spin axis perpendicular to the orbital plane. In this kind of orbital motion RPA sensors face the velocity vector once in each spin cycle of satellite. The angle θ between the sensor normal and satellite velocity vector keeps on changing from 0 to 360° at the rate of $30^{\circ}/\text{sec}$. The RPA measurements are taken when the sensor normal faces the satellite velocity vector. But in a spin stabilized satellite this situation remains for a fraction of a second. Hence measurement are taken within some limits of θ . The RPA sensors collect data within $\pm 30^{\circ}$ (for ions) and within $\pm 90^{\circ}$ (for electrons) of the satellite velocity vector once in each spin period. The velocity of satellite is 7.8 km/sec and orbital period around 100 minutes. The orbits of satellite during different time has been given below

First placed orbit	-	429 km x 917 km
After one year	-	429 km x 628 km
After two years	-	428 km x 617 km
Present orbit	-	428 km x 615 km

The retarding potential analyzer aeronomy payload was designed and developed at NPL, New Delhi for SROSS series of satellites. The RPA payload was switched on in orbit first time on May 21, 1992 using SROSS-C satellite

through ground commands issued from ISRO Satellite Tracking Centre (ISTRAC), Bangalore. Again on May 4, 1994 the RPA payload placed in orbit by SROSS-C2 mission. The design and development of RPA for SROSS series of satellite was taken up by NPL under SROSS aeronomy satellite project (SASP), in the year 1985-86. The instrument was designed for minimum power consumption, size and weight to have maximum possible reliability and flexibility of its operation in space through ground commands.

The RPA experiment onboard the SROSS-C2 consists of an ion RPA, electron RPA and a potential probe for making simultaneous measurements of the ion and the electron plasma parameters. The electron and the ion RPA sensors are identical in structure but differ in terms of voltages applied on the various grids of the respective sensors. These sensors are pentode vacuum tube like structure. Different electrodes are known as the entrance grid, the retarding grid, the suppressor grid, the collector shield grid and the collector electrode. These grids are very fine and made from gold plated tungsten wire.

The entrance grid is a double grid, which is kept at the spacecraft potential in ion sensor. In electron sensor voltage on it is varied from 0 to +5 V in eight discrete steps through ground telecommands. Retarding grid is also a double grid and acts as a energy filter for ions or electrons entering the sensor. It allows only those ions/electrons whose energies are greater than the applied voltage bias. Suppressor grid is a single grid and held at appropriate potential to prevent electrons/ions from reaching the collectors of ions/electrons sensors respectively. Potential on this grid is kept positive in electron sensor and negative in ion sensor. Collector shield grid protects the sensitive electrometer

connected to the collector from electrical disturbances generated by changing potentials on other grids. It is held at spacecraft potential in both the sensors. The collector electrode is a gold plated solid metal plate, which is insulated from grids and the body of the sensor. It is electrically connected to the input of electrometer amplifier. Electrometer amplifier measures the positive and negative currents collected by the RPA sensors.

5.2.1 Objective

The scientific objectives of SROSS mission are:

- a. To study the behavior of electron and ion density and temperature anomaly in low latitude region.
- b. To study the special features of energetics of the equatorial and low latitude ionosphere.
- c. To establish the response of the thermal structure to the dynamical effects.

In order to achieve these scientific objectives the following parameters is measured using RPA payload.

- i. Total ion density N_i
- ii. Ion temperature T_i
- iii. Ion composition O^+ , O_2^+ , NO^+ , H^+ , He^+
- iv. Electron temperature T_e
- v. Suprathermal electron flux (STEF) (up to 30 eV)
- vi. Irregularities in the electron and ion densities
- vii. Satellite potential with respect to plasma

Measuring parameters accuracy

Parameter	Limit of measurement	Accuracy
N _i and N _e	5×10 ² to 5×10 ⁶ cm ⁻³	± 5%
T _i and T _e	500 to 5000 K	± 5%
STEF	1×10 ⁷ to 1×10 ⁹ cm ⁻² sec ⁻¹	±10%

5.2.2 Principal of Operation

The RPA sensor is analogous to pentode vacuum tube where ionospheric plasma serves as the cathode. The ion and electron enter the sensor through its open aperture and pass through the region which is electrically segmented by a series of very fine gold plated tungsten wire electrode and then reach the collector electrode. The current thus collected over the collector plate varies from tens of microamperes down to fraction of pico-amperes. Electrometer amplifier measures this current. By changing the bias voltage on the retarding grid, different energy electrons/ions reach the collector plate to cause the collector current. This gives the measurement of flux in different energy ranges. Characteristic curves (Figure 5.3) of the collector current (I) versus retarding grid bias (V) are generated separately for electrons and ions. These characteristic curves are used for deriving different ionospheric parameters of interest.

5.2.3 Data Collection and Dissemination

The RPA payload does not possess any onboard memory for storing data therefore the data is recorded at the ground stations. The longitude and latitude coverage of data is restricted to certain limited regions. The data is collected at

ISRO, Bangalore (12.5° N, 77.3° E) and Lucknow (26.8° N, 80.8° E) ground stations, and also from foreign ground stations located in Mauritius (20° S, 56° E). In our study we have taken only the Bangalore station data. In general two day-time and two night-time passes are visible over Bangalore during a 24 hours duration. Since the telemetry down link is common to both RPA and GRB payloads, therefore data of only one payload can be transmitted from the satellite at a time. Hence out of four visible passes data for two orbits is recorded for RPA payload everyday. After recording the data it is processed at ISTRAC, Bangalore, to generate altitude and orbital parameters of the satellite.

The data are recorded into a VAX computer at ground station. Then data is passed through some prescribed quality check criteria. Now for every pass of the satellite, a set of four files is generated in a Computer Compatible Floppy (CCF) format. These files are *.RPA, *.OPT, *.LBT and *.SUM. The *.RPA file contains raw data transmitted from the payload in digital form, which is grouped set wise in 22 ms interval. For every pass there is one RPA file. OPT file contains the orbital parameter such as longitude, latitude, altitude, sun angle, mag. angle, orbit no. of the satellite at one second interval during a pass. For each pass there is one OPT file. The third file in CCF is the *.LBT file which contains raw data from a pass. One LBT file is generated for one pass. The health monitoring parameters of the satellite and payload like supply voltage, current, temperature etc. are recorded in this file. The fourth file in CCF is the *.SUM file which have the summary records of quality check of the data received from satellite.

The OPT file contains the orbital parameters at 1 sec interval during a pass. But for processing of the payload data the orbital parameters are required for each set i.e. every 22 ms in analog form. Therefore next step in data processing is to interpolate and convert the data in readable form from OPT file. Thus a new file known as *.TMT is created which contains the processed values of RPA data. This one file contains all the information of RPA and OPT files. Thus a single *.TMT file is created for each pass.

5.2.4 Data Reduction and Analysis

The data in the form of *.TMT file is reduced to form *.SET files. The structure and format of the *.SET file is same as that of *.TMT file except that the TMT file contains the entire data of a pass i.e. electron RPA data, ion RPA data and potential probe data. The SET file contains the different data sets for these elements. Further from one SET file 30 to 50 another SET files are created which are called sub-sweeps. Hence for each TMT file around 100 SET files are created which include both the ion and electron RPA data. In present analysis we have studied the behavior of ion composition and ion and electron temperature anomaly with respect to the altitude, longitude and latitude. The method of analysis has been explained below. Analyzed data is used for graphical representation of results and scientific analysis. Figure 5.4 gives the brief description of various processes involved in the data collection, dissemination, reduction and analysis.

The selection of data for our scientific interest has been done in two ways. (1) The study of lower region (according to availability of SROSS-C2 data at that height i.e. 425-475 km) of ionosphere. The selection of data has

been done by plotting the altitude with respect to orbit numbers of satellite for different months. As an example, Figure 5.5 shows the altitude coverage of SROSS-C2 during the month of October 1995. The data is selected for altitude range 425-475 km for all longitude and latitude. (2) For the study of vertical profile of electron and ion temperature and density over a fixed longitude and latitude, the maximum possible passes has been selected by plotting the longitude with respect to latitude. For example, Figure 5.6 shows the longitude and latitude coverage of satellite during October 1995. According to this plot the longitude $79^{\circ} \pm 1$ and latitude $20^{\circ} \pm 1$ has been selected for present study.

5.2.4.1 Determination of total ion density from Ion RPA data

For determining the total ion density during a pass, a SET file is created in which the data sets following conditions are selected

- i. The angle θ should be less than 20° or more than 340°
- ii. The ion RPA retarding grid bias is zero volt

The total ion density is calculated by the following formula

$$N = \eta A e U_s I \quad (5.1)$$

where, N = Total ion density, η = efficiency of the sensor = 0.5

A = collector area = 20 cm^2 , e = electron charge = $1.6 \times 10^{-19} \text{ C}$

U_s = satellite velocity = 8 km/sec , I = ion current

5.2.4.2 Determination of ion density, composition and temperature

Ionosphere is a multiconstituent plasma which comprises of different ion species. The most common ion species of our interest in the altitude regions

between 430 km to 650 km are O⁺, O₂⁺, NO⁺, H⁺, He⁺. These ions, get retarded at different voltages due to their masses, results in decrease of ion current at different voltage corresponding to the ion masses giving rise to a composite I-V curve as shown in Figure 5.3. The ion current reaching the sensor in response to the retarding voltages is governed by the equation

$$I = AeU_s \eta \cos \theta \sum_{i=0}^n N_i \left\{ \frac{1}{2} + \frac{1}{2} \operatorname{erf}(x) + C_i \frac{\exp(-x^2)}{2\sqrt{\pi}U_s \cos \theta} \right\} \quad (5.2)$$

where, θ = angle between the velocity vector and probe normal

N_i = density of i^{th} ion (m^{-3})

$x = U_s \cos \theta - \{[e(V+V_s)]^{1/2} / kT_i\}$,

V_s = the satellite potential w.r.t. plasma,

V = probe potential w.r.t. satellite,

k = Boltzmann constant = $1.38 \times 10^{-23} \text{ JK}^{-1}$

$C_i = (2kT_i / m_i)^{1/2}$, most probable velocity of the ion constituent

T_i = ion temperature (K), m_i = mass of ion (kg)

Once the I-V curve is obtained, the main task is to recover the ion parameters of density and temperature using the above equation. Ion density gives the total ion concentration as well as information on the composition of the major ion constituents. U_s and θ , are available from the measurements. Equation (5.2) is a non-linear equation and therefore unknown parameters are obtained by computerized curve fitting. The approach is that the computer programme first constructs a model I-V curve with the help of the above equation by using typical values of the unknown variables N_i , T_i , V_s , which are selected as reasonable approximations for the anticipated ambient ionospheric

conditions. Estimation procedure involves adjusting these parameters in the computer generated curve applying least square method of minimizing standard errors. By iteration we update the model curve step by step using the variables. Every time the standard error is calculated and iterations are continued until the best least square fit to the measured curve is obtained. When the two curves match, the fitted variables will yield the needed plasma parameters corresponding to the experimental curve.

The saturation current around zero volt retarding voltage gives the total ion density as all the ions reach the sensor and collected by probe without any retardation. Equation (5.2) reduces to

$$I_{i,0} = N_i e \eta A U_s \cos \theta \quad (5.3)$$

where, $I_{i,0}$ = Saturation current for the i th ion at zero retarding voltage

Therefore total ion density can be calculated first by knowing U_s and θ without having any information of T_i and V_s .

To find the temperature from I-V curve for RPA data, first step is to make separate files of individual sweeps (*.SET file) from the corresponding *.TMT file. *.TMT file contains the data of entire orbit. The data within $\pm 40^\circ$ of theta limits has been considered for ion temperature analysis. For generating I-V curve 64 sets of data are taken in one complete sweep. Each set of data is collected after every 22 ms, duration of each sweep becomes 1.408 sec. During this period retarding grid voltage is swept from 0 to 22 V in up and down sweeps and theta changes by 45° at 5 rpm spin rate. For each sweep of ion RPA one set file is created. Each SET file contains all the RPA data and orbital parameters for each sweep. The T_i values and different ion compositions so

derived are put in a file in a specified format (Table 5.1). The file is finally processed in grapher.

5.2.4.3 Determination of electron temperature

The I-V curve obtained from the electron RPA curve is shown in Figure 5.3. Here the log of electron current measured by the probe is plotted against the retarding grid voltage. Three distinct regions are identified in this curve. When the probe voltage is positive relative to plasma, electrons are accelerated towards the probe and we have a fairly flat saturation portion of the probe characteristics. When the probe voltage is made negative with respect to plasma, the incoming electrons experience a retarding field and the probe current decreases exponentially resulting in retarding region of characteristic. The region is linear on a semi log scale. As the probe is made more negative, the low energy thermal electrons repelled away. But probe still collects a small current, which is due to higher energy suprathermal electrons. The lower flat portion of the curve denotes the suprathermal region. In the day time this flux is more and also get contaminated by the plate electrons if its probe is sunlit. The retarding region of I-V curve is related to the distribution of electron energies and hence can be used to obtain electron temperature (T_e).

The relationship between the collector current (I) and retarding grid voltage (V) can be given as

$$I_e = I_0 \exp\left[\frac{-e(V + V_s)}{kT_e}\right] \quad (5.4)$$

where, $I_0 = \frac{1}{4} \eta e A N_e U_e$ = the random current when probe is at plasma

potential i.e. for $V+V_s = 0$

η = efficiency of the probe, A = area of the probe = 20 cm^2

N_e = electron density (m^{-3}), e = electron charge = $1.6 \times 10^{-19} \text{ C}$

U_e = mean thermal velocity of the electron = $\sqrt{\frac{8kT_e}{\pi m_e}}$

m_e = mass of electron = $9.1 \times 10^{-31} \text{ kg}$

T_e = electron temperature (K), V = retarding grid voltage w.r.t satellite

V_s = satellite potential w.r.t. plasma

Equation (5.4) may be written as

$$\ln I_e = \ln I_0 - \frac{e(V + V_s)}{kT_e} \quad (5.5)$$

During a single I-V curve the satellite potential can be assumed to remain constant. Therefore I_0 and V_s may be taken as constant. The above equation represents a linear relationship in $\ln I_e$ and V with slope (e/kT_e) , the temperature can be determined from the slope of the semi logarithmic plot of the I-V curve. Therefore above equation now becomes

$$\frac{d}{dV}(\ln I_e) = \frac{e}{kT_e} \quad (5.6)$$

On using the values of e and k the electron temperature can be obtained easily from equation (5.6). The slope of the linear region of the I-V curve gives the electron temperature. The approach that has been adopted for evaluating the slope is the linear curve fitting in which least square technique is employed to fit a straight line to the measured data in the retarding region.

To find the electron temperature from I-V curve of electron-RPA data, first step is to make separate files of individual sweeps (*.SET) from the corresponding orbit *.TMT file. TMT file contains the data of the entire orbit. The data within $\pm 60^\circ$ of the angle θ limits has been considered for electron temperature analysis.

For generating one I-V curve 64 data points are taken in one complete sweep. As each data set is collected after 22 ms, duration of each sweep becomes 1.408 sec. During this period retarding grid voltage is swept from +2V to -32V. For each sweep of electron RPA, one SET file is created. Each SET file contains the RPA data and orbital parameters for that sweep. To obtain the slope of straight line of linear region of I-V curve, the least square fit method has been used. Finally the T_e values are derived and put in a separate file in a specified format (Table 5.2). The file is finally processed in GRAPHER.

5.3 RESULTS AND DISCUSSION

The data from the electron and ion RPA of SROSS-C2 have been analyzed for total ion density, ion composition (H^+ , He^+ , O^+ , O_2^+) and the temperature of ions and electrons for different orbits expanding over ten months (October 1995 to July 1996). The lower height covered by SROSS-C2 satellite was the major point of attention of this study. The total altitude coverage by the satellite is from 425 km to 615 km, but we have chosen the data for lower region i.e. 425-475 km in the present study.

The results of this study for the period from October 1995 to July 1996 have been plotted in Figures 5.7, 5.8, 5.9.....5.16. The plots are only representatives of the kind of variation and only few specific months have been

selected for Figures. Results of all other months have been discussed in the text. The selection of these months were based on some special behavior and trends of density and temperature of ions and electrons, described in detail in the next few paragraphs. The ion density behavior of representative months have been given in Figures 5.7, 5.9, 5.11, 5.13 and 5.15, while the temperature variations have been plotted in Figures 5.8, 5.10, 5.12, 5.14 and 5.16. A combined outcome of density and temperature variation with months for a fixed height range (425-475 km) and longitude 79° and latitude 20° , has been plotted in Figures 5.17 and 5.18 respectively. A detailed study of these results suggests different behavior of ion density and ion-electron temperature during different time and weather conditions. The variation of these parameters during the time of study with longitude, latitude and height has been summarized in Tables 5.3 and 5.4.

An inference can be drawn from a close look on these results that the total ion density always lies between 10^{10} to 10^{13} m^{-3} for all the months. The O^+ ions have the same variation and their density is also approximately the same as for total ion density showing that the maximum contribution to the ionospheric ion density is by these ions. Other ions like O_2^+ , He^+ , H^+ vary considerably but remaining well below this level. The O_2^+ ions vary from 10^8 to $5 \times 10^8 \text{ m}^{-3}$. The He^+ ions vary from 10^9 to $3 \times 10^{10} \text{ ions m}^{-3}$ while H^+ ions vary from 10^9 to $10^{11} \text{ ions m}^{-3}$. Thus one may conclude that the contribution to the total ion density next to O^+ ions is by H^+ ions and then by He^+ ions while the contribution of O_2^+ ions is the least. The variation of ion densities and ion-

electron temperatures with respect to longitude, latitude and height during different months has been given below.

5.3.1 Variation of Ion Densities

In the month of October 1995 the total ion density varies from 10^{10} to $7 \times 10^{11} \text{ m}^{-3}$ (Figure 5.7a) with respect to longitude. The Figure shows that the O^+ ions have almost the same values of density as total ions while O_2^+ ion vary in between 10^6 to 10^9 m^{-3} in relation to longitude. The H^+ and He^+ ions have concentrations from 10^6 to 10^{10} m^{-3} in this month. The best fit line to the density of these ions shows a constant behavior with longitude for total, O^+ and O_2^+ ions while an increasing trend for H^+ and He^+ ions have been found. The total, O^+ and O_2^+ ion densities show decreasing trend with latitude (Figure 5.7b) having same density values as mentioned with longitude. The H^+ and He^+ ions have the tendency to increase with latitude. Figure 5.9(a) shows that the total ion density varies from 3×10^{10} to $8 \times 10^{11} \text{ m}^{-3}$ with longitude in the month of November 1995. The O^+ ions vary from 3×10^{10} to $7 \times 10^{11} \text{ m}^{-3}$ and increase with longitude. The O_2^+ ions also increase with longitude but vary in between 10^6 to $2 \times 10^{10} \text{ m}^{-3}$. The H^+ and He^+ ions have also the same values as O_2^+ ions but H^+ increases with longitude. However the ion densities of above species have been found to decrease with latitude (Figure 5.9b), having the same range of values.

The ion density in the month of December 1995 has almost the same behavior except that the He^+ ions decrease while the H^+ ions increase with latitude. Figures 5.11(a) and 5.11(b) show that in the month of January 1996

the ion density variation with longitude and latitude has opposite trends. In general in the months of February and March 1996 the behavior of above ions is the same as for October to December 1995.

Figures 5.13(a) and 5.13(b) show that for the month of April 1996 the ion densities have some specific features as O^+ and total ions have two density clusters, one varying from 3×10^{10} to $8 \times 10^{10} \text{ m}^{-3}$ and the other from 2×10^{11} to $9 \times 10^{11} \text{ m}^{-3}$. O_2^+ , H^+ and He^+ have the same behavior as in previous months. The total ion and O^+ ion density increases with longitude and decreases with latitude. H^+ and He^+ ions decrease with longitude on the other hand only He^+ decreases with latitude. For the month of May 1996 Figures 5.15(a) and 5.15(b) show that the total ion density varies from 2×10^9 to $8 \times 10^{12} \text{ ions m}^{-3}$, which was maximum compared to all other months. The density increases with longitude and decreases with latitude. The H^+ ion density was also maximum compared to all other months and varied from 10^6 to $7 \times 10^{12} \text{ m}^{-3}$ but having decreasing trend with longitude and was almost constant with latitude. The O^+ and O_2^+ ions increase with longitude and latitude varying between 2×10^{10} to $8 \times 10^{11} \text{ m}^{-3}$ and 10^6 to 10^{10} m^{-3} respectively. The density of He^+ ions increases with longitude and decreases with latitude and varies from 10^6 to 10^{10} m^{-3} .

The O^+ and total ion density in the month of June 1996 have concentrated around 10^{11} m^{-3} showing almost constant behavior with longitude and latitude. The O_2^+ and H^+ ions vary from 10^6 to 10^{10} m^{-3} . The He^+ ion decreases with longitude and increases with latitude. In the month of July 1996, the O_2^+ ion density was almost constant with longitude and latitude while O^+ and total ion density increases with both longitude and latitude. The O^+ ion

varies from 2×10^9 to $2 \times 10^{11} \text{ m}^{-3}$ while total ion density varies from 3×10^9 to $5 \times 10^{12} \text{ m}^{-3}$. The H^+ and He^+ ions have shown opposite behavior with longitude and latitude. They increase with longitude and decrease with latitude. The H^+ and He^+ ions vary from 10^6 to $7 \times 10^{12} \text{ m}^{-3}$ and 10^6 to 10^{10} m^{-3} respectively.

On certain occasions in the months May, June and July 1996 the H^+ ion density became close to the total ion density while for all other occasions the O^+ ion densities were almost the same as total ion density. This increase of H^+ ions superceding the values for O^+ ions can be attributed to the influence of tropospheric phenomena. The troposphere during above months in Indian subcontinent is quite disturbed with lot of thunderclouds and intense rain due to monsoon.

5.3.2 Variation of Ion and Electron Temperature

In the longitude and latitude range of our interest ($79^{\circ} \pm 1 \text{ E}$, $20^{\circ} \pm 1 \text{ N}$) the data points for height variation of electron and ion temperatures are very small and therefore the results of height variation of these parameters can not be taken highly reliable. Henceforth we will not discuss the height variation of temperature though it is included in Figures 5.8, 5.10, 5.12, 5.14 and 5.16. It has also been given in Table 5.4.

Figure 5.8(a) shows that the ion temperature increases with longitude and latitude but decreases with height. The ion temperature varies from 600 to 1200 K, while the electron temperature varies from 600 to 2000 K with longitude and latitude (October 1995). Figure 5.8(b) shows that the electron

temperature slightly increases with longitude while it decreases with latitude having values from 600 to 2000 K. In the month of November 1995, the ion and electron temperature decrease with longitude while increases with latitude. From Figure 5.10(a) it is clear that the ion temperature varies from 600 to 1200 K with longitude and latitude. The electron temperature varies from 600 to 2250 K with longitude and latitude.

The ion temperature shows an increasing trend with longitude and latitude having values from 600 to 1300 K in the month of December 1995. The electron temperature also increases with longitude and latitude and varies from 500 to 2500 K. Figure 5.12(b) shows that the electron temperature increases with latitude while decreases with longitude in the month of January 1996. It ranges from 1000 to 3500 K. Figure 5.12(a) shows that the ion temperature varies in between 600 to 1400 K and decreases with longitude while increases with latitude. The ion temperature was almost constant having an average value of 1500 K.

In the month of February 1996 the ion temperature decreases slightly with longitude and increases with latitude. The ion temperature varies from 500 to 2200-K for longitude. The electron temperature fluctuates in between 1000 to 3000 K for longitude and latitude. The ion temperature varies from 400 to 3200 K with longitude and latitude in the month of March 1996. The ion temperature decreases slightly with latitude and increases with longitude. The

electron temperature varies from 1000 to 3200 K with longitude and latitude having an increasing trend.

Figure 5.14(a) shows the ion temperature characteristics during April 1996. The temperature varies from 600 to 1600 K with longitude and latitude. The electron temperature (Figure 5.14b) shows some special features as two temperature zones have been observed. One region is concentrated around 1000 K and the other varies from 1500 to 4500 K when plotted against longitude and latitude. Figures 5.16(a) and 5.16(b) show that the ion and electron temperature increase with latitude while ion temperature decreases with longitude but electron temperature increases during May 1996. Ion temperature varies from 400 to 1500 K while electron temperature varies from 500 to 4500 K with longitude and latitude.

The ion temperature has shown an increasing behavior with longitude and latitude and varies from 800 to 1400 K during June 1996. The electron temperature varies from 500 to 3500 K both for longitude and latitude having an increasing trend with longitude and being constant with latitude. July 1996 also shows a splitting in electron temperature as in the month of May 1996. One range is around 800-900 K and other from 1300 to 4000 K with longitude and latitude. The ion temperature varies from 400 to 1700 K and increases with longitude and latitude.

The average monthly variation of ion density (Figure 5.17) for fixed longitude and latitude (79° , 20°) and height (425-475 km) shows that the total ion density was maximum in the month of May 1996 ($2 \times 10^{11} \text{ m}^{-3}$) and it was minimum during November 1995 ($1 \times 10^{10} \text{ m}^{-3}$). The O^+ ions also show the same

behavior as total density and this makes clear that O^+ ion is dominant in the ionosphere. The density of O_2^+ was minimum during February 1996 (10^8 m^{-3}) and maximum in April 1996 (10^9 m^{-3}), while H^+ was minimum in October 1995 ($8 \times 10^9 \text{ m}^{-3}$) and maximum in May 1996 ($8 \times 10^{10} \text{ m}^{-3}$). He^+ was maximum in ionosphere in the height range of our interest during March 1996 ($2 \times 10^{10} \text{ m}^{-3}$) and minimum during October 1995 (10^9 m^{-3}). Figure 5.18 shows that the average temperature of the months were found to be maximum in November 1995 (2000 K) for ion and Jan 1996 (1800 K) for electron, while minimum temperature was observed during October 1995 both for ions (750 K) and electrons (800 K). Figure 5.18 also shows that the average electron temperature exceeds the average ion temperature except in the month of November 1995. In this month the electron temperature remains at 1500 K while the ion temperature has increased to 2100 K, much above the values in other months.

5.3.3 Discussion

Garg and Das [49] have shown that the ion density varies from 10^9 to 10^{11} m^{-3} covering the same latitude as for the present study. It is very clear from their result that the O^+ ion density is quite close to the total ion density. The H^+ and He^+ ions show minimum contribution to the total ion density. They found that the ion temperature varies from 700 to 2000 K while electron temperature varies from 800 to 3000 K. Schunk and Raitt [190] have shown using their theoretical model that the maximum contribution in the total ion density was due to O^+ ion which varies from 10^{10} to 10^{11} m^{-3} during summer and winter seasons at 400 to 500 km height range. We have also found the

same density behavior of O⁺ in winter (December 1995-February 1996) and summer (April-July 1996) seasons. Schunk and Sojka [192] studied the vertical profile of O⁺ density for solar maxima and solar minima during summer and winter seasons. During summer they found that the O⁺ density varies from 5×10^{10} to 10^{11} m⁻³ and during winter season it varies from 2.5×10^{10} to 4×10^{10} m⁻³. They also observed that the density increases up to 300 km and after that it decreases significantly. Our experimental results (Figure 5.17) are in good agreement with those of Schunk and Sojka [192] as O⁺ ion density varies from 10^{10} to 10^{11} m⁻³ during winter and from 5×10^{10} to 2×10^{11} m⁻³ during summer seasons for the fixed height range 425-475 km. Schunk and Sojka [192] also calculated the vertical profile of ion temperature both for summer and winter season during solar maximum and minimum conditions. They observed increasing trend in temperature with height. Ion (O⁺) temperature varies from 1000 to 1200 K in summer and 900 to 1000 in winter season during solar minimum. In solar maximum condition the temperature varies from 1450 to 1550 K during summer and from 1200 to 1250 during winter season. Figure 5.18 shows that the ion temperature varies from 900 to 2000 K during winter (November 1995-February 1996) and from 1000 to 1300 K during summer (April-July 1996) season for a fixed height range of 425-475 km. This result is somewhat contrary to the results obtained by Schunk and Sojka [192]. The reason may be that they have done calculations for high latitudes while our experiments were performed at low latitudes. Schunk and Sojka [192] also calculated the vertical profile of electron temperature during solar maximum and solar minimum conditions. Their results show that the temperature varies

from 1750 to 2400 K during both solar maximum and minimum conditions for the height range 400 to 500 km. It is clear from Figure 5.18 that the electron temperature varies from 1000 to 1800 K during winter season (November 1995-February 1996) while from 1200 to 1300 K during summer (April-July 1996) for the height range of our interest. Thus our results are in good conformity with the experimental and theoretical studies by different workers.

Table 5.1(a) - Ion temperature (T_i) and ion densities at various longitudes and latitudes for height 425-475 km during October 1995

Orbit	Time (UT) Hr. Min. Sec.	Long. Lat.	Height	Theta	Sun Ang.	T_i	$N(O^+)$	$N(O_2^+)$	$N(H^+)$	$N(He^+)$
7784111	16 55 15.20	76.5 6.80	429.6	012	095	620	1.09E+11	4.24E+06	1.65E+06	1.93E+09
7784115	16 56 08.64	78.8 9.30	429.6	012	092	710	1.07E+11	1.82E+07	1.04E+06	1.01E+06
7784118	16 56 35.41	79.9 10.6	429.8	013	089	620	9.71E+10	1.02E+06	1.06E+06	5.05E+09
7784119	16 56 47.95	80.4 11.2	429.9	351	109	730	1.04E+11	1.23E+09	7.78E+06	2.88E+06
7784125	16 57 54.26	83.3 14.2	430.9	338	117	600	8.63E+10	1.09E+08	1.86E+09	1.16E+06
7784128	16 58 22.42	84.5 15.5	431.5	018	078	630	7.94E+10	1.70E+08	1.81E+09	3.24E+09
7784129	16 58 35.07	85.1 16.1	431.8	358	096	650	8.33E+10	3.93E+08	7.89E+08	1.01E+06
7784131	16 59 01.87	86.3 17.3	432.5	002	091	630	7.10E+10	1.37E+08	1.07E+07	1.01E+06
7784132	16 59 14.47	86.8 17.8	432.9	341	110	660	6.10E+10	1.01E+06	1.02E+06	4.03E+09
7784135	16 59 41.27	88.1 19.0	433.8	343	106	620	5.60E+10	4.24E+07	1.58E+09	1.01E+06
7784137	17 00 08.00	89.3 20.2	434.7	344	104	670	4.71E+10	1.06E+09	1.75E+09	1.70E+08
7829110	16 09 25.66	67.9 5.30	434.3	335	138	750	2.73E+11	1.02E+06	1.40E+10	1.67E+06
7829111	16 09 53.64	69.1 6.60	433.3	352	123	650	2.80E+11	1.02E+06	1.03E+06	1.01E+06
7829114	16 10 34.58	70.8 8.50	432.2	353	122	800	2.69E+11	3.01E+08	1.01E+06	1.01E+06
7829116	16 11 01.35	71.9 9.70	431.6	343	129	730	2.34E+11	1.00E+06	1.01E+06	1.01E+06
7845113	15 56 12.14	70.2 10.5	433.2	349	126	660	2.32E+11	6.39E+08	1.02E+06	1.01E+06
7845116	15 56 52.95	72.0 12.4	432.1	341	130	830	2.16E+11	1.27E+08	1.02E+06	1.00E+06
7845119	15 57 21.11	73.2 13.7	431.5	004	114	820	2.10E+11	9.13E+07	1.01E+06	1.01E+06
7845123	15 58 16.04	75.6 16.2	430.7	004	109	690	1.80E+11	1.00E+06	1.01E+06	1.00E+06
7845128	15 58 56.86	77.4 18.0	430.3	355	113	820	1.73E+11	1.02E+06	1.00E+06	1.01E+06
7845132	15 59 51.79	80.0 20.4	430.1	354	112	660	1.68E+11	1.48E+08	1.01E+06	1.01E+06
7860110	15 39 35.9	64.1 6.30	439.8	351	132	540	3.37E+11	1.02E+06	1.06E+06	1.00E+06
7860116	15 41 12.02	68.1 10.8	435.7	343	133	620	2.30E+11	3.93E+08	1.03E+06	1.01E+06
7860125	15 42 49.15	72.3 15.2	432.7	357	118	780	1.40E+11	5.35E+07	4.83E+08	1.01E+06
7860129	15 43 44.08	74.7 17.7	431.6	353	119	740	8.47E+10	7.18E+07	1.00E+06	1.01E+06
7860136	15 44 53.05	77.9 20.8	430.8	353	116	780	4.93E+10	1.02E+06	1.02E+06	1.01E+06
7860138	15 45 21.21	79.3 22.0	430.6	1	102	740	5.08E+10	1.02E+08	1.01E+06	1.00E+06
7875118	15 26 31.89	66.8 12.0	437.9	20	110	730	2.87E+11	2.34E+09	1.12E+06	6.71E+09
7875121	15 27 12.70	68.6 13.9	436.3	357	122	810	2.28E+11	3.00E+08	1.03E+06	1.02E+06
7875136	15 30 0	76.8 21.9	431.7	0	114	840	4.64E+10	1.02E+06	6.31E+07	1.00E+06
7875138	15 30 39.7	78.1 23	431.4	336	129	720	3.82E+10	1.02E+06	2.17E+07	2.77E+09

Table 5.1(b) - Ion temperature (T_i) and ion densities at various heights for longitude ($79^0 \pm 1$) and latitude ($20^0 \pm 1$) during October 1995

Orbit	Time (UT) Hr. Min. Sec.	Long.	Lat.	Height	Theta	Sun Ang.	T_i	$N(O^+)$	$N(O_2^+)$	$N(H^+)$	$N(He^+)$
7845132	15 59 51.79	80.0	20.4	430.1	354	112	660	1.68E+11	1.48E+08	1.01E+06	1.01E+06
7860136	15 44 53.05	77.9	20.8	430.8	353	116	780	4.93E+10	1.02E+06	1.02E+06	1.01E+06
7910124	23 25 45.48	78.8	21.2	531.2	6	46	620	3.43E+09	1.18E+08	2.28E+09	1.00E+06
7910125	23 25 59.56	79.5	20.6	532.5	8	45	630	3.06E+09	1.81E+08	1.68E+09	1.09E+09
7910126	23 26 12.32	80.0	20.1	533.8	337	58	500	2.85E+09	1.47E+08	6.48E+09	1.01E+06
7910127	23 26 26.34	80.7	19.5	535.1	338	57	650	2.67E+09	2.28E+08	1.00E+06	2.95E+09
7925119	23 11 17.35	78.3	19.5	526.6	356	51	600	5.77E+08	1.23E+06	1.36E+09	4.24E+08
7993132	11 53 19.36	79.2	19.5	469.6	351	143	1070	3.23E+11	4.57E+08	3.06E+07	1.03E+06
7993134	11 53 47.52	80.5	20.7	467.4	349	143	1120	2.53E+11	1.02E+06	2.50E+08	1.09E+06
8009126	11 38 42.95	78.3	20.9	474.0	352	146	1000	2.48E+11	1.73E+09	1.05E+06	1.01E+06
8059123	19 19 24.50	79.6	20.8	455.8	346	101	800	3.28E+10	1.75E+07	1.00E+06	1.71E+09
8074127	19 05 05.44	79.5	18.6	453.4	358	91	680	3.85E+10	7.74E+07	1.01E+06	1.01E+06
8208126	15 13 00.70	80.9	19.9	430.7	345	135	720	7.84E+10	1.00E+06	1.01E+06	4.47E+09
8223121	14 58 06.08	79.3	19.2	431.6	336	142	720	2.91E+11	1.02E+06	1.18E+06	4.33E+09
8223123	14 58 34.24	80.5	17.9	431.0	355	125	760	4.64E+11	1.02E+06	1.09E+06	1.01E+06

Table 5.2 (a) - Electron temperature (T_e) at various longitudes and latitudes for height 425-475 km during October 1995

Orbit	Time (UT)			Long.	Lat.	Height	Theta	Sun Ang.	T _e
	Hr.	Min.	Sec.						
7784010	16	54	49.772	75.5	5.70	429.7	46	65	741
7784011	16	55	1.3640	76.0	6.20	429.6	357	109	796
7784012	16	55	12.648	76.4	6.70	429.6	303	153	773
7784013	16	55	29.856	77.1	7.50	429.6	46	62	746
7784014	16	55	41.116	77.6	8.10	429.6	350	114	783
7784017	16	56	20.540	79.3	9.90	429.7	333	128	768
7784019	16	56	48.680	80.4	11.2	430.0	11	91	786
7784020	16	56	59.920	80.9	11.7	430.1	314	142	710
7784022	16	57	28.104	82.1	13.0	430.5	353	104	741
7784024	16	57	56.196	83.4	14.3	431.0	31	68	774
7784025	16	58	7.5280	83.9	14.8	431.2	336	118	725
7784028	16	58	35.688	85.1	16.1	431.9	15	80	810
7784030	16	59	3.8480	86.4	17.3	432.6	54	42	715
7784031	16	59	15.112	86.9	17.8	432.9	357	94	758
7784033	16	59	43.208	88.2	19.1	433.8	35	57	782
7829010	16	09	13.116	67.4	4.70	434.7	4	118	901
7829012	16	09	41.604	68.6	6.00	433.7	36	89	868
7829013	16	09	52.824	69.1	6.60	433.4	333	139	874
7829014	16	10	7.0560	69.6	7.20	432.9	348	128	878
7829018	16	10	46.480	71.3	9.10	431.9	307	148	837
7829019	16	11	3.3520	72.0	9.80	431.5	35	85	840
7829020	16	11	14.640	72.5	10.4	431.3	333	135	855
7829030	16	05	36.252	58.7	-5.8	444.9	14	156	884
7829032	16	06	9.9960	60.0	-4.1	443.2	55	116	873
7829035	16	06	38.204	61.1	-2.7	441.8	43	148	904
7829036	16	06	49.420	61.6	-2.2	441.2	11	372	777
7829038	16	07	11.996	62.5	-1.0	440.1	50	85	864
7829039	16	07	23.196	62.9	-0.5	439.5	344	138	994
7829045	16	08	30.780	65.7	2.70	436.4	325	146	794
7845013	15	55	46.008	69.1	9.30	434.0	25	10	818
7845014	15	55	57.272	69.6	9.80	433.6	319	143	816
7845015	15	56	14.120	70.3	10.6	433.1	43	83	775
7845016	15	56	25.428	70.8	11.1	432.8	339	132	795
7845018	15	56	53.588	72.0	12.4	432.1	357	117	880
7845020	15	57	21.728	73.2	13.7	431.5	18	100	935
7845022	15	57	49.888	74.4	15.0	431.0	37	82	836
7845024	15	58	17.936	75.7	16.3	430.7	53	67	872
7845025	15	58	29.312	76.2	16.8	430.5	351	118	830
7845028	15	59	8.7560	78.0	18.5	430.2	307	143	753
7845029	15	59	25.632	78.8	19.3	430.2	31	83	848
7845030	15	59	36.896	79.3	19.8	430.1	326	134	725
7845031	15	59	53.760	80.1	20.5	430.1	45	70	779

Table 5.2 (b) - Electron temperature (T_e) at various heights for longitude ($79^\circ \pm 1$) and latitude ($20^\circ \pm 1$) during October 1995

Orbit	Time (UT)			Long.	Lat.	Height	Theta	Sun Ang.	T_e
	Hr.	Min.	Sec.						
7845029	15	59	25.632	78.8	19.3	430.2	31	83	848
7845030	15	59	36.896	79.3	19.8	430.1	326	134	725
7845031	15	59	53.768	80.1	20.5	430.1	45	70	779
7845032	16	00	5.056	80.6	21.0	430.1	338	123	812
7860035	15	44	53.688	77.9	20.8	430.8	11	103	937
7910026	23	25	43.232	78.7	21.3	531.0	307	79	1033
7910028	23	26	11.328	80.0	20.1	533.7	312	74	1318
7910030	23	26	39.536	81.3	18.9	536.4	319	69	1120
7925023	23	11	17.968	78.3	19.5	526.7	13	44	784
7925024	23	11	29.280	78.8	19.0	527.8	304	85	705
8059022	19	19	9.6320	78.9	21.4	454.8	325	122	898
8059023	19	19	26.552	79.7	20.7	456.0	38	51	668
8059024	19	19	37.856	80.2	20.2	456.7	326	119	905
8059025	19	19	54.712	81.0	19.5	457.9	41	47	723
8074028	19	04	39.328	78.3	19.7	451.8	47	45	652
8074029	19	04	50.592	78.8	19.2	452.5	336	113	819
8208023	15	12	33.216	79.6	21.1	431.2	342	139	855
8208025	15	13	1.3760	80.9	19.9	430.7	6	121	898
8223021	14	57	39.928	78.0	20.3	432.2	8	121	811
8223022	14	57	51.212	78.6	19.8	431.9	305	147	868
8223023	14	58	08.020	79.4	19.1	431.5	28	103	850
8223024	14	58	19.372	79.9	18.6	431.3	327	145	849

Table 5.3 - Average variation of ion density with longitude, latitude and height (for fixed longitude and latitude)

Month	Variation	With Longitude (Height 425-475 km)	With Latitude (Height 425-475 km)	With Height (Long-79°, Lat-20°)
October 1995	Constant	Total, O ⁺ , O ₂ ⁺ , H ⁺ He ⁺	H ⁺ , He ⁺ Total, O ⁺ , O ₂ ⁺	H ⁺ , He ⁺ , O ₂ ⁺ Total
	Increase			
November 1995	Constant	Total, O ⁺ , O ₂ ⁺ , He ⁺ H ⁺	H ⁺ Total, O ⁺ , O ₂ ⁺ , He ⁺	O ⁺ , H ⁺ Total, O ₂ ⁺ , He ⁺
	Increase			
December 1995	Constant	O ₂ ⁺ Total, O ⁺ , H ⁺ He ⁺	H ⁺ , He ⁺ Total, O ⁺ , O ₂ ⁺	O ₂ ⁺ , He ⁺ Total, O ⁺ , H ⁺
	Increase			
January 1996	Constant	Total, O ⁺ , O ₂ ⁺ H ⁺ , He ⁺	H ⁺ , He ⁺ Total, O ⁺ , O ₂ ⁺	H ⁺ , O ₂ ⁺ , He ⁺ Total, O ⁺
	Increase			
February 1996	Constant	Total, O ⁺ , O ₂ ⁺ , H ⁺ He ⁺	He ⁺ , H ⁺ Total, O ⁺ , O ₂ ⁺	O ₂ ⁺ , He ⁺ , H ⁺ Total, O ⁺
	Increase			
March 1996	Constant	Total, O ⁺ , O ₂ ⁺ , He ⁺ , H ⁺	O ₂ ⁺ , He ⁺ , H ⁺ Total, O ⁺	O ₂ ⁺ , He ⁺ , H ⁺ Total, O ⁺
	Increase			
April 1996	Constant	Total, O ⁺ , O ₂ ⁺ He ⁺ , H ⁺	O ₂ ⁺ H ⁺ Total, O ⁺ , He ⁺	Total O ₂ ⁺ , He ⁺ , H ⁺ O ⁺
	Increase			
May 1996	Constant	Total, O ⁺ , O ₂ ⁺ , He ⁺ H ⁺	O ⁺ , H ⁺ O ₂ ⁺ Total, He ⁺	O ₂ ⁺ He ⁺ , H ⁺ Total, O ⁺
	Increase			
June 1996	Constant	O ⁺ H ⁺ Total, O ₂ ⁺ , He ⁺	Total, O ⁺ He ⁺ , H ⁺ O ₂ ⁺	Total, O ⁺ He ⁺ , H ⁺ O ₂ ⁺
	Increase			
July 1996	Constant	O ₂ ⁺ Total, O ⁺ , He ⁺ , H ⁺	O ₂ ⁺ Total, O ⁺ He ⁺ , H ⁺	He ⁺ Total, O ⁺ , O ₂ ⁺ , H ⁺
	Increase			
	Decrease			

Table 5.4 - Average variation of ion and electron temperature with longitude, latitude and height (for fixed longitude and latitude)

Months	Variation	With Longitude (Height 425-475 km)	With Latitude (Height 425-475 km)	With Height (Long-79 ^o , Lat-20 ^o)
October 1995	Constant Increase Decrease	T_e T_i	T_i T_e	T_e T_i
November 1995	Constant Increase Decrease	T_i, T_e	T_i, T_e	T_i, T_e
December 1995	Constant Increase Decrease	T_i, T_e	T_i, T_e	T_i, T_e
January 1996	Constant Increase Decrease	T_i, T_e	T_i, T_e	T_i, T_e T_i
February 1996	Constant Increase Decrease	T_i T_e	T_i, T_e	T_e T_i, T_e
March 1996	Constant Increase Decrease	T_i, T_e	T_i T_e	T_i, T_e
April 1996	Constant Increase Decrease	T_i, T_e	T_e T_i	T_i, T_e
May 1996	Constant Increase Decrease	T_e T_i	T_i, T_e	T_i, T_e
June 1996	Constant Increase Decrease	T_i, T_e	T_e T_i	T_i, T_e
July 1996	Constant Increase Decrease	T_i T_e	T_i, T_e	T_i, T_e

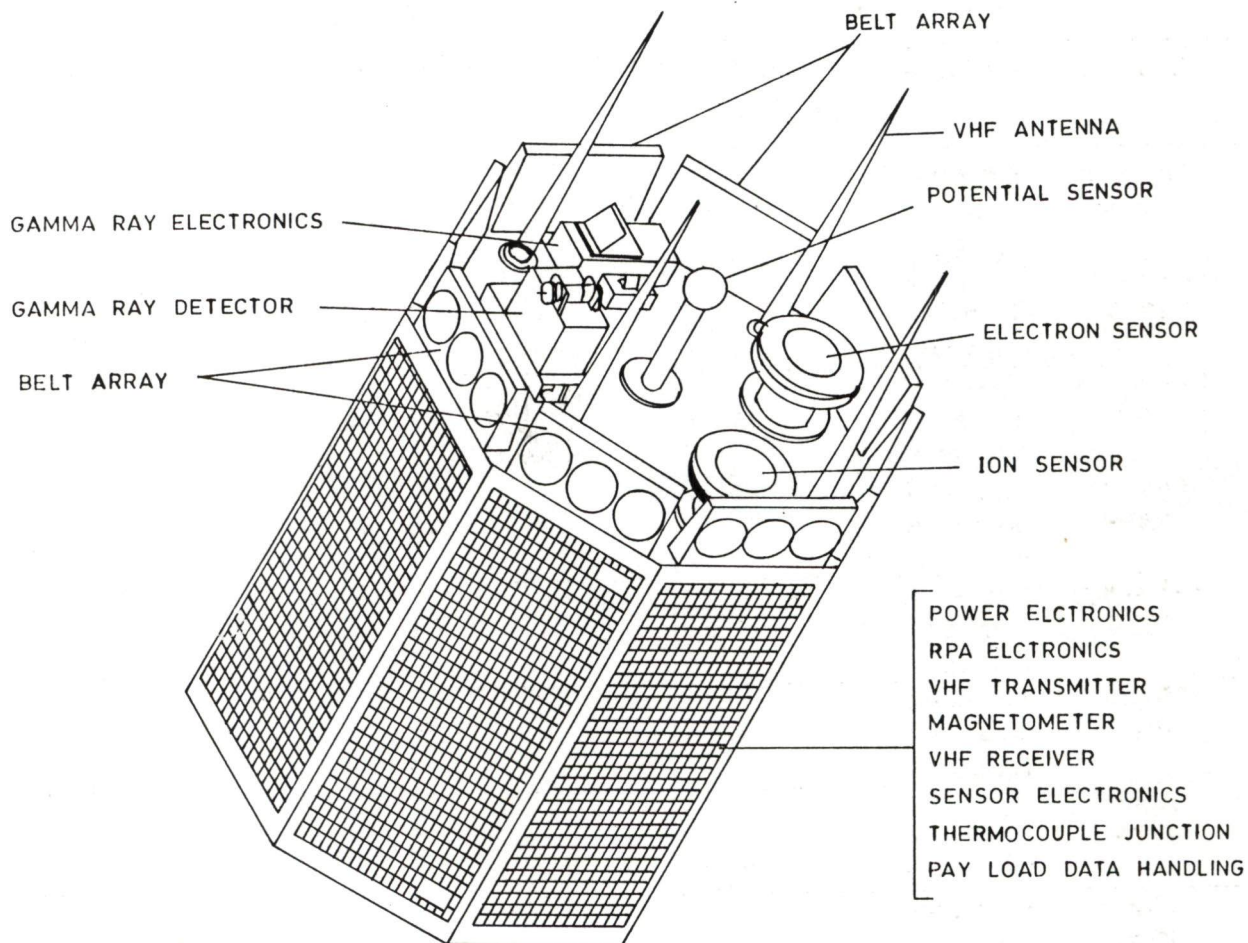


Figure 5.1 - Orbital configuration of SROSS-C2 satellite

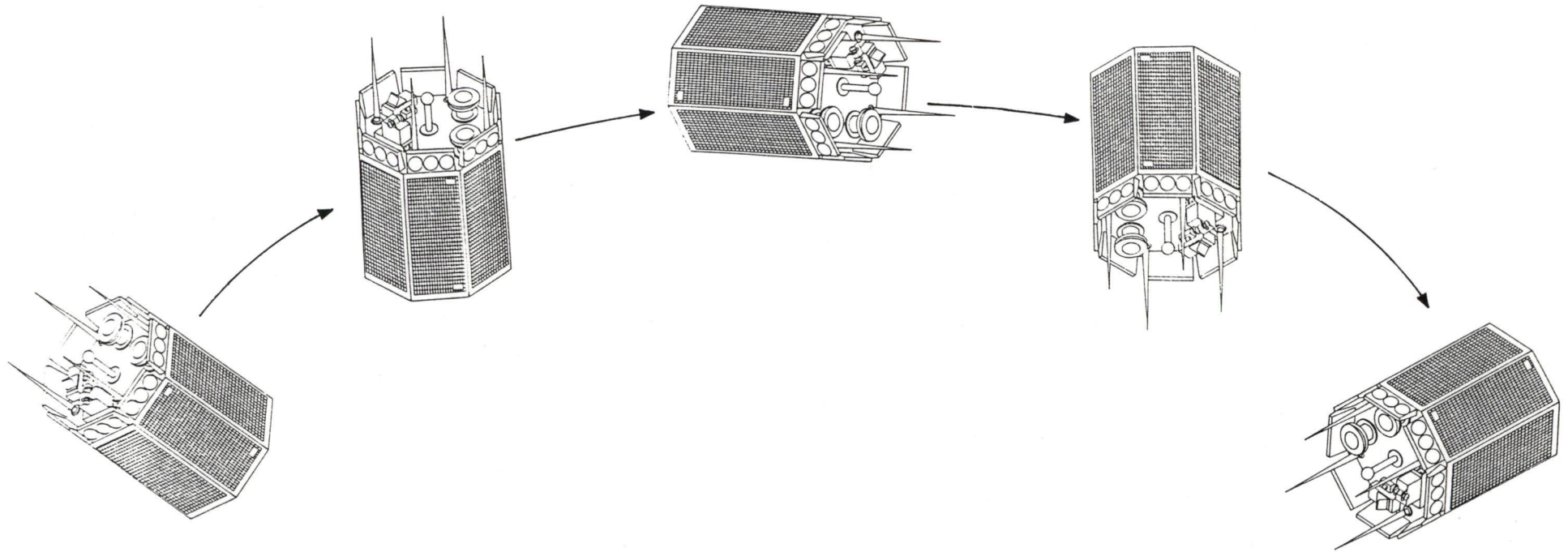


Figure 5.2 - Motion of SROSS-C2 satellite in orbit

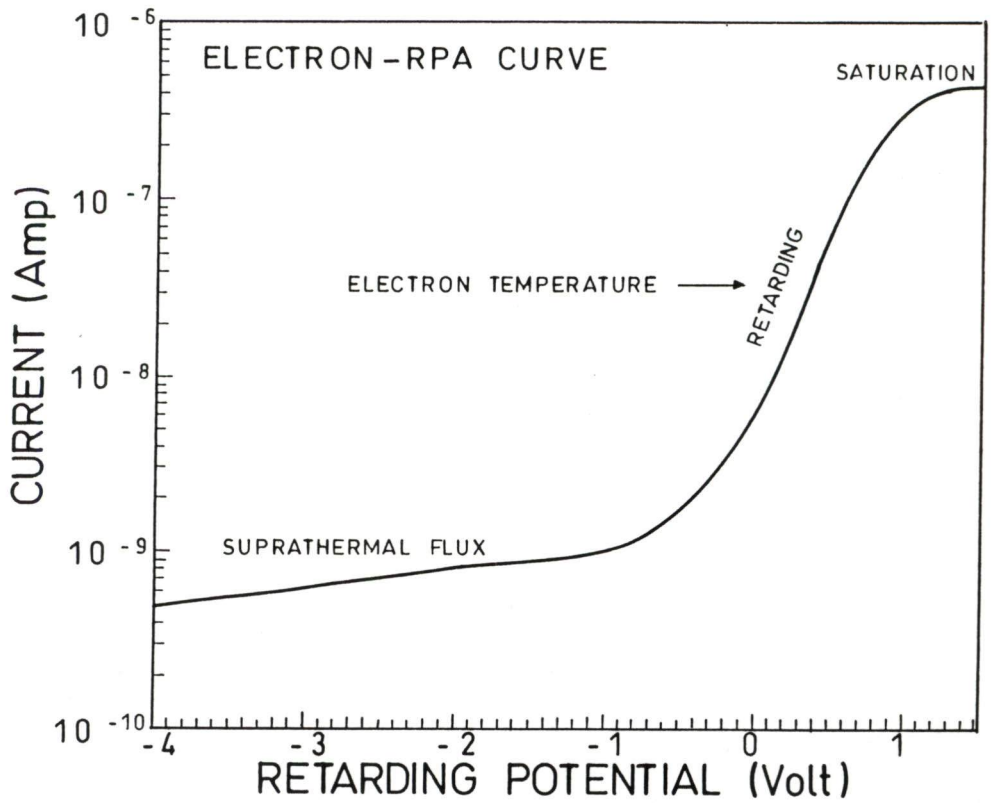
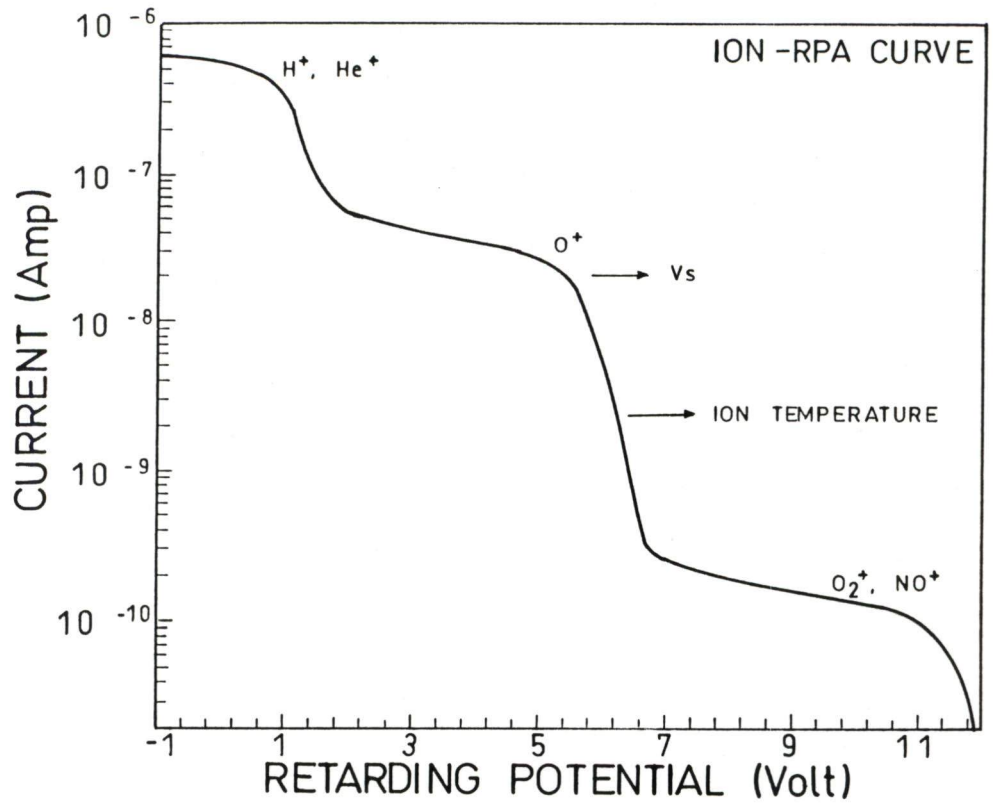


Figure 5.3 - Characteristics curves of ion and electron RPA

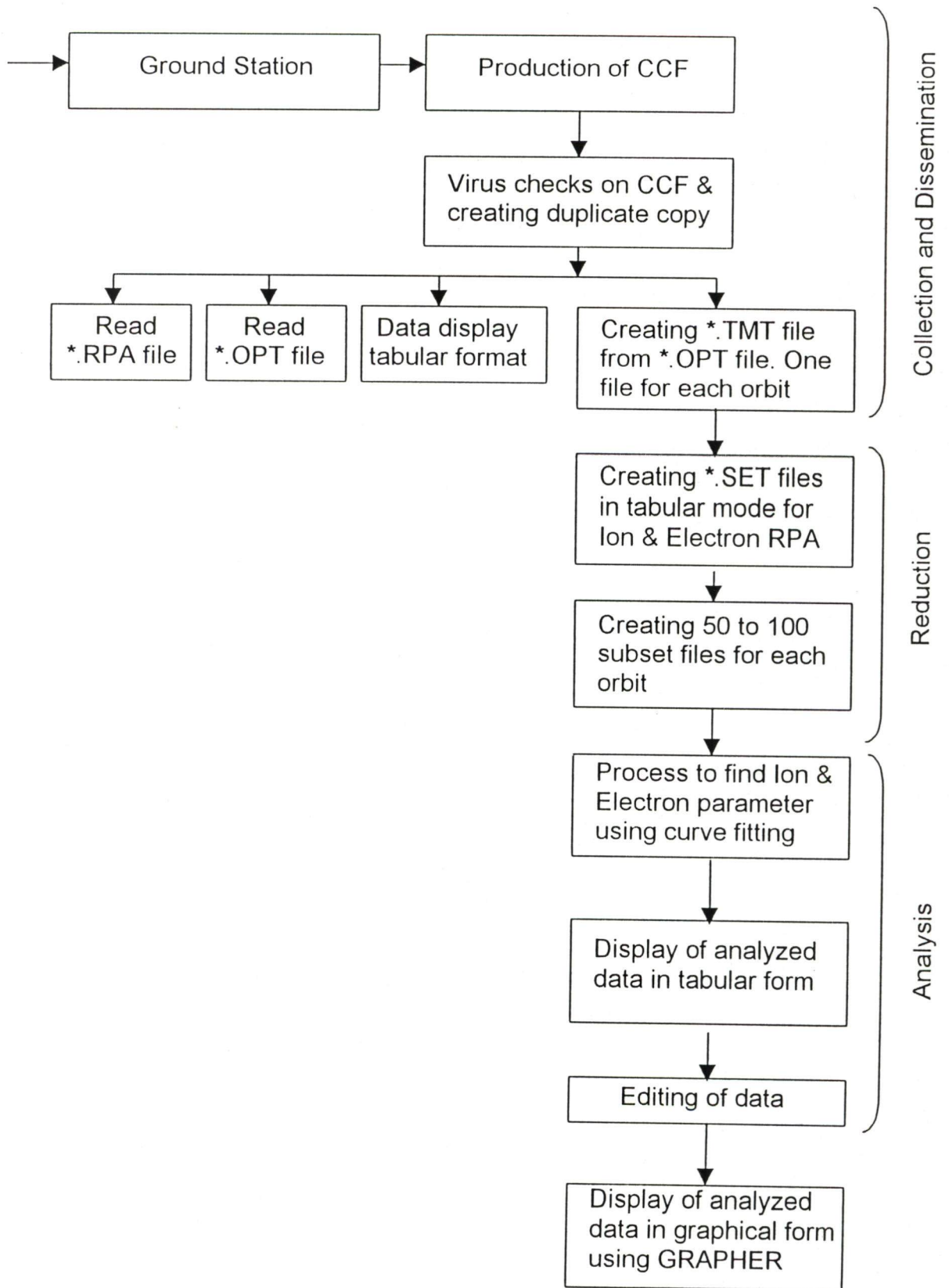


Figure 5.4 - Flow chart of collection, reduction and analysis of RPA data

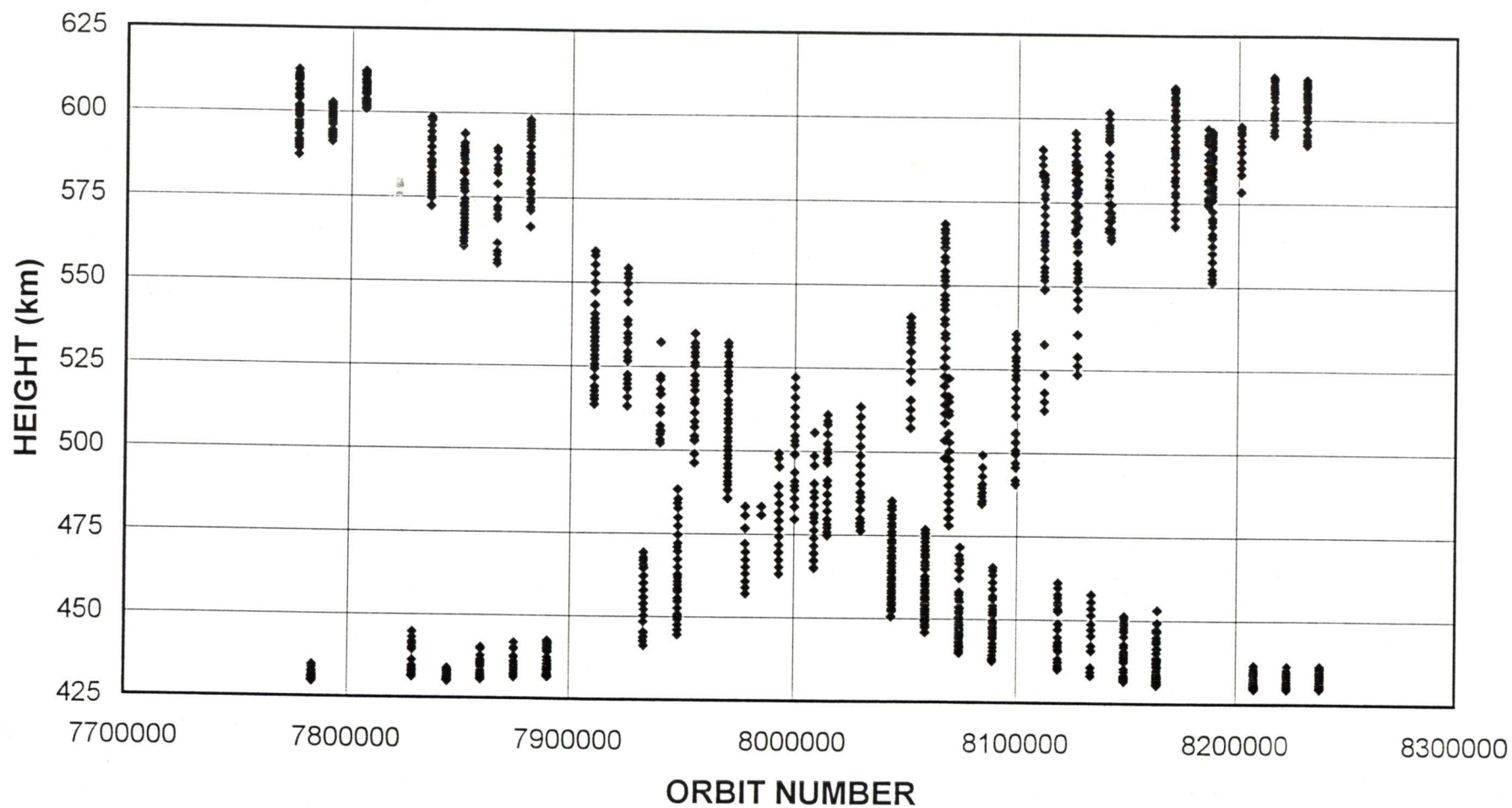


Figure 5.5 - Altitude coverage by SROSS-C2 satellite during October 1995

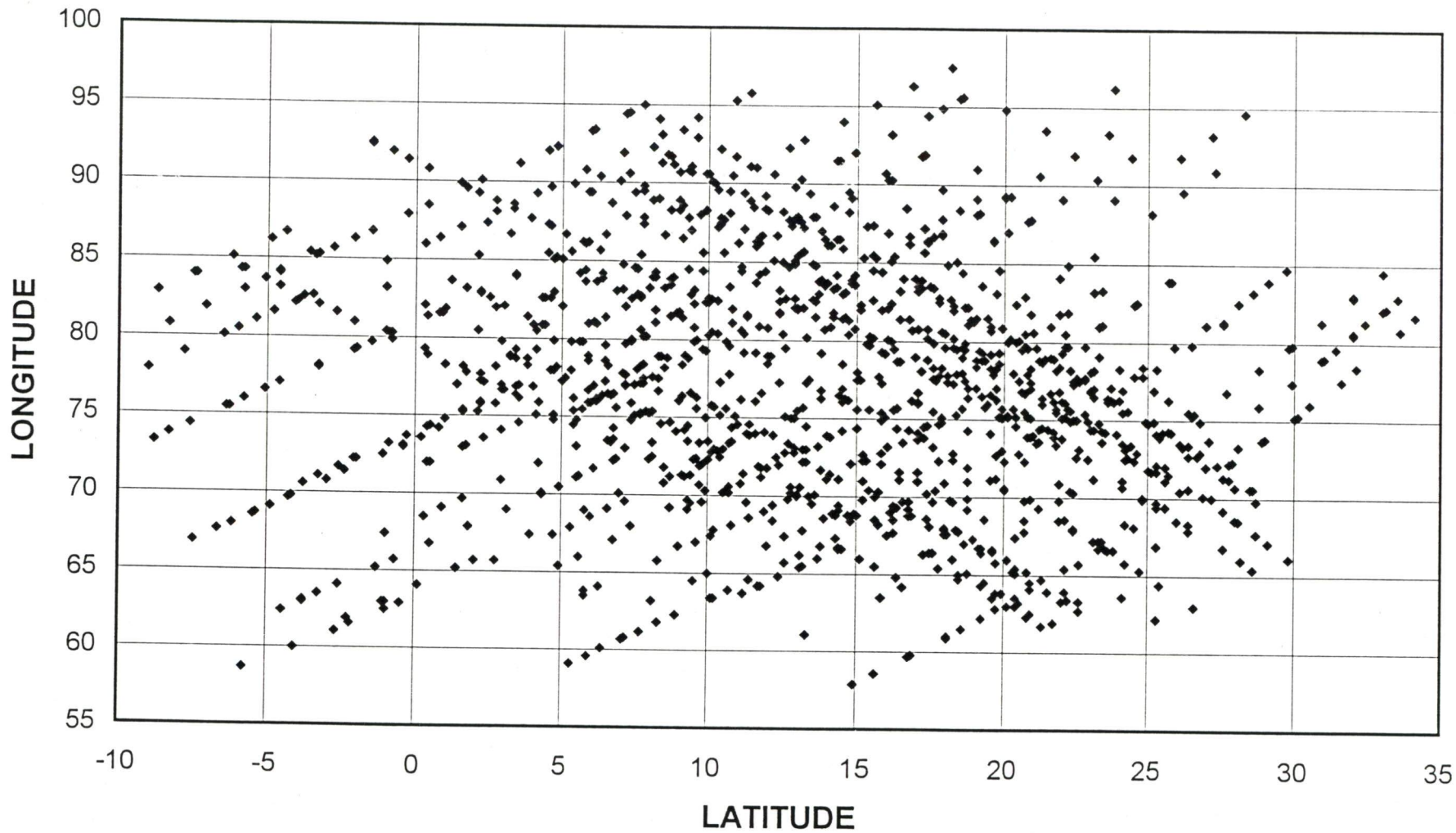


Figure 5.6 - Longitudes and latitudes covered by SROSS-C2 during October 1995

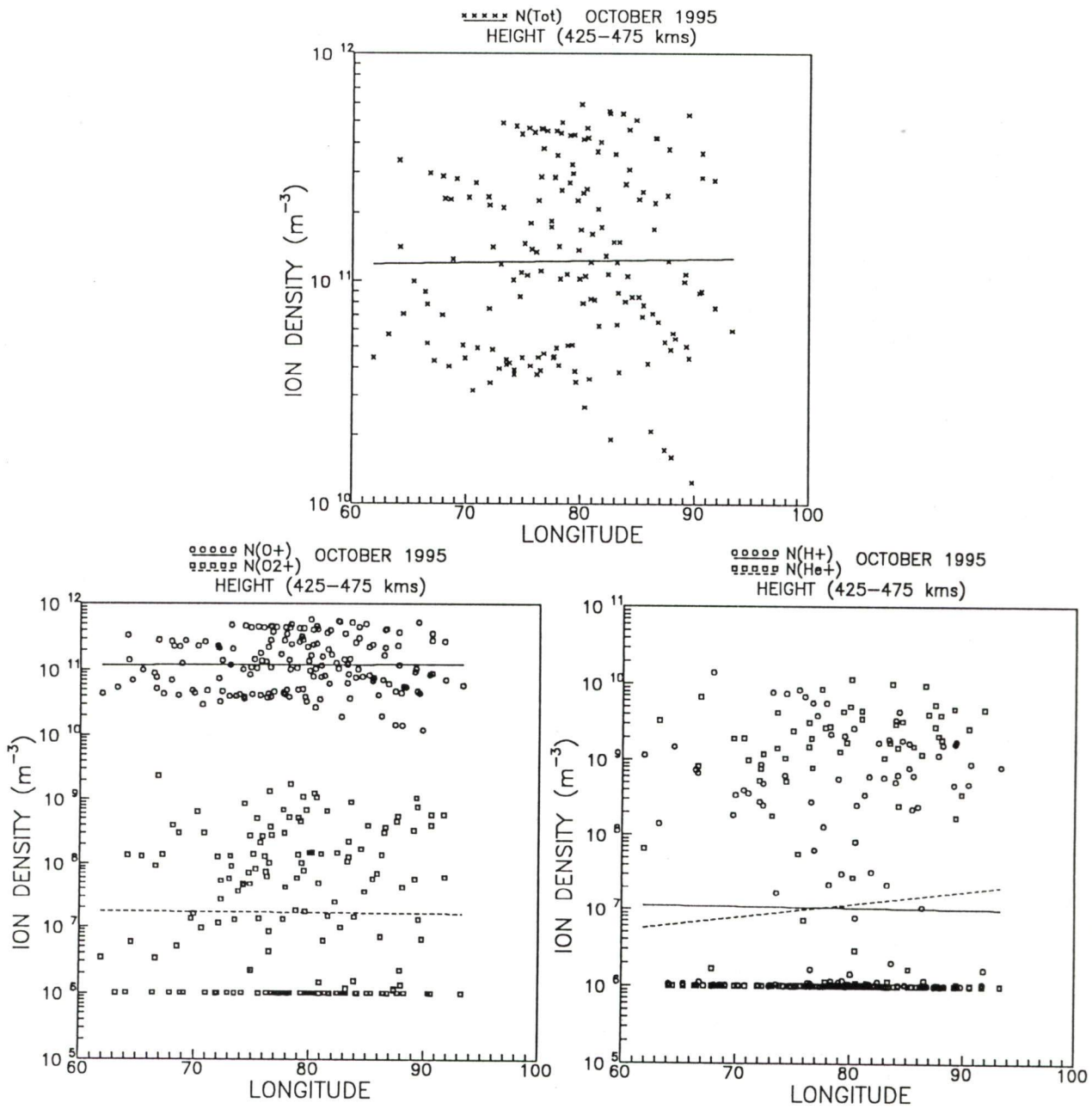


Figure 5.7(a) - Longitudinal variation of ion densities for altitude 425-475 km in the month of October 1995

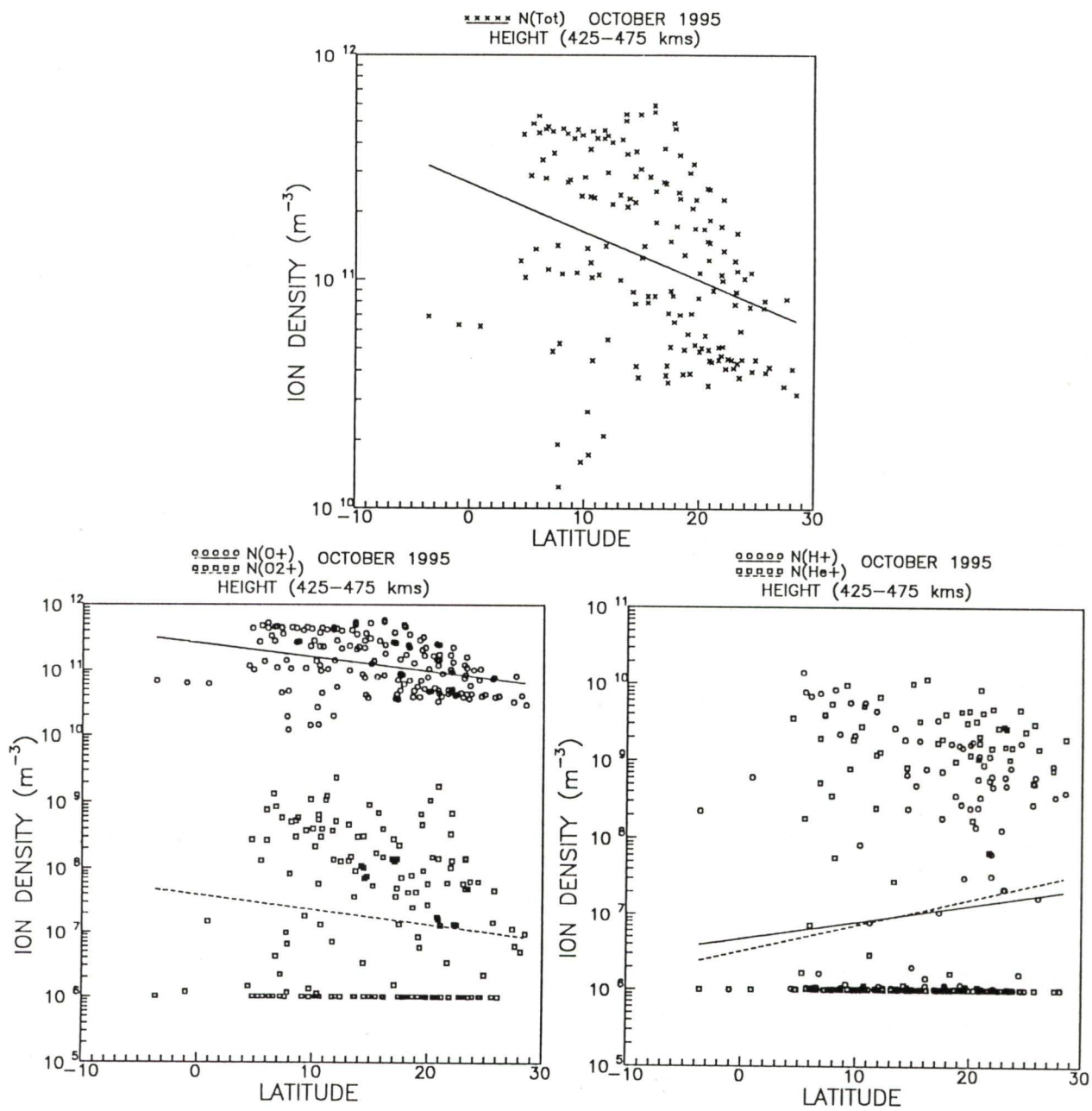


Figure 5.7(b) - Latitudinal variation of ion densities for altitude 425-475 km in the month of October 1995

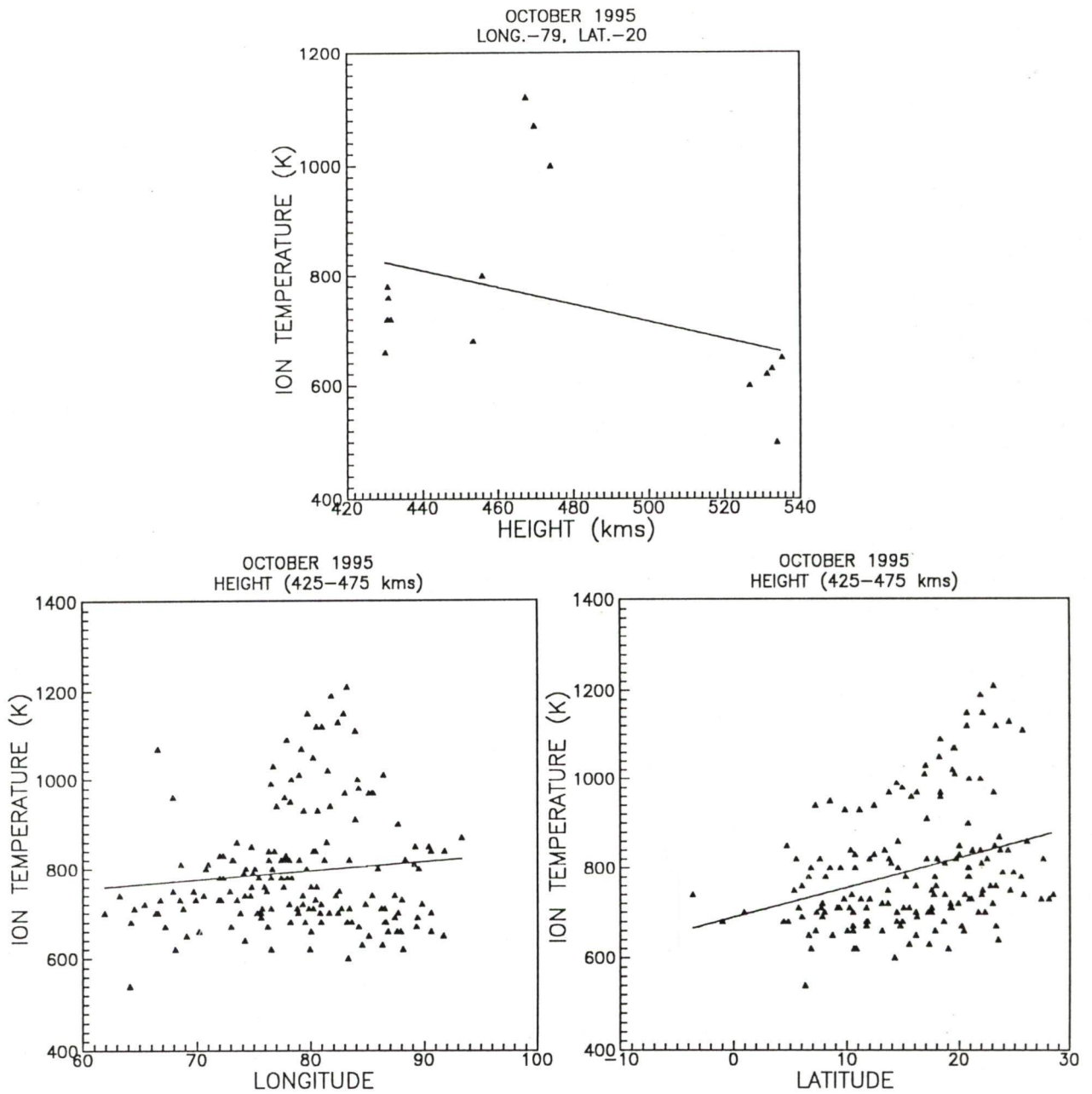


Figure 5.8(a) - Temperature of ions during October 1995 as function of longitude, latitude and height

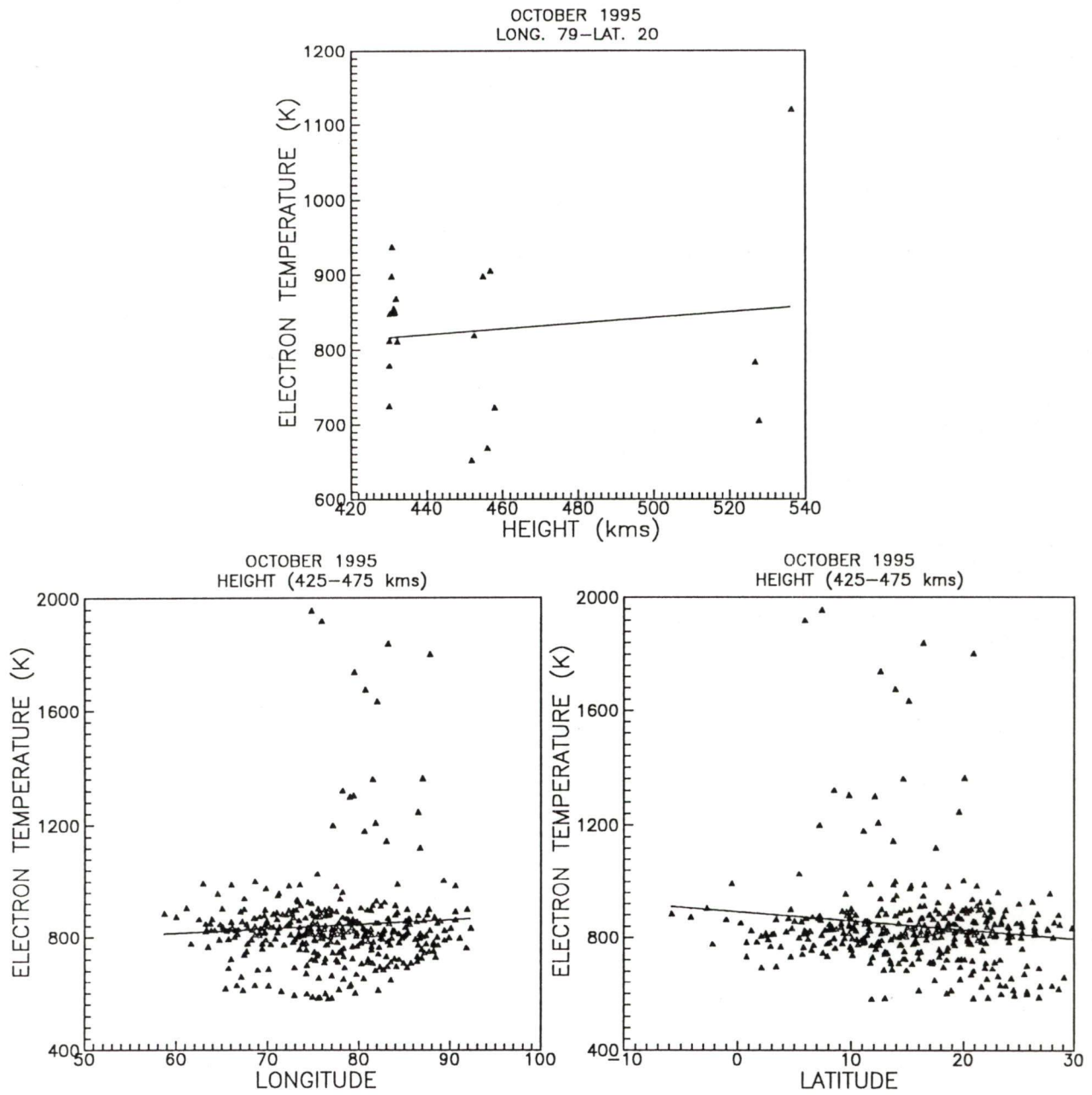


Figure 5.8(b) - Temperature of electrons during October 1995 as function of longitude, latitude and height

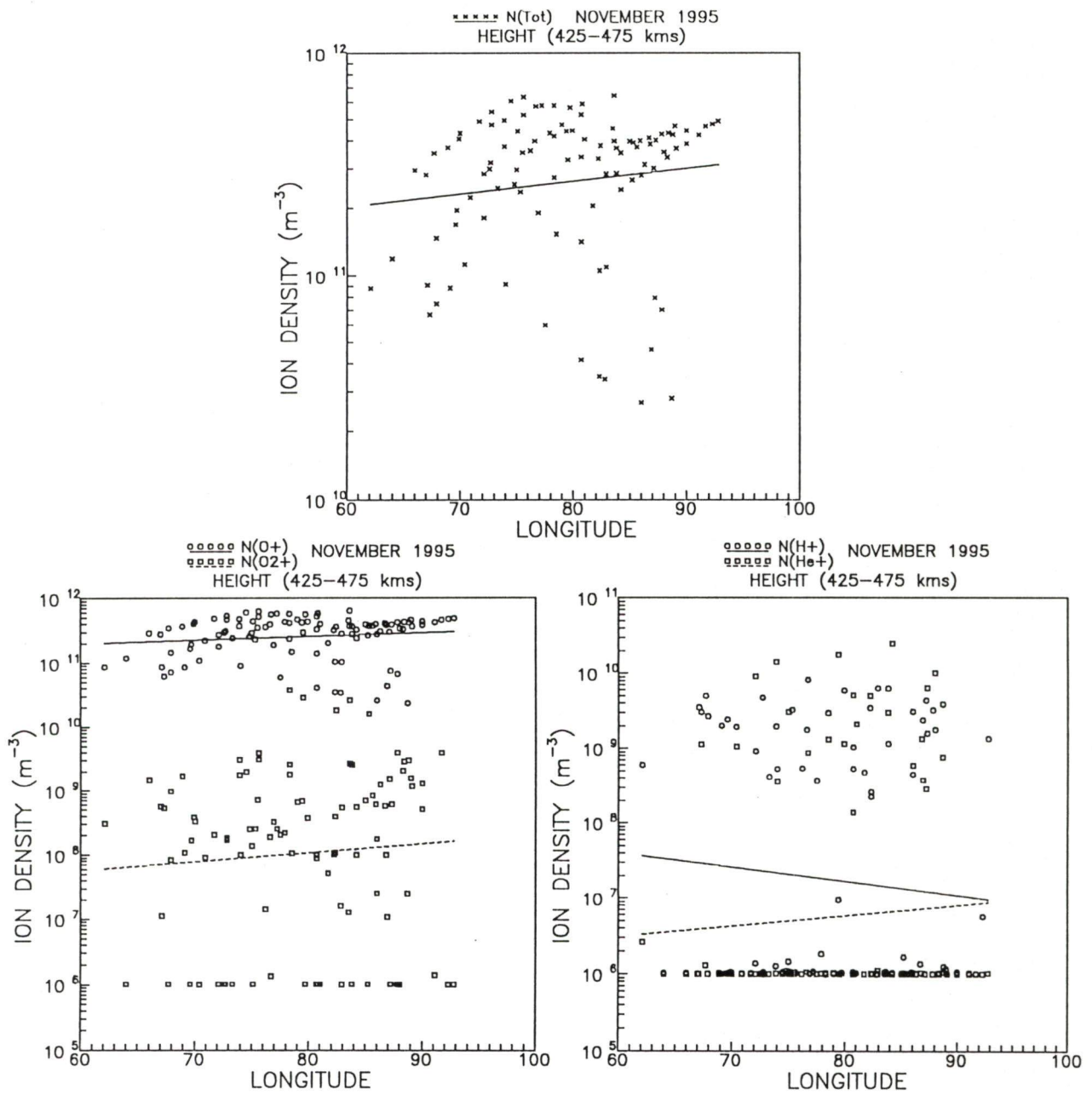


Figure 5.9(a) - Longitudinal variation of ion densities for altitude 425-475 km in the month of November 1995

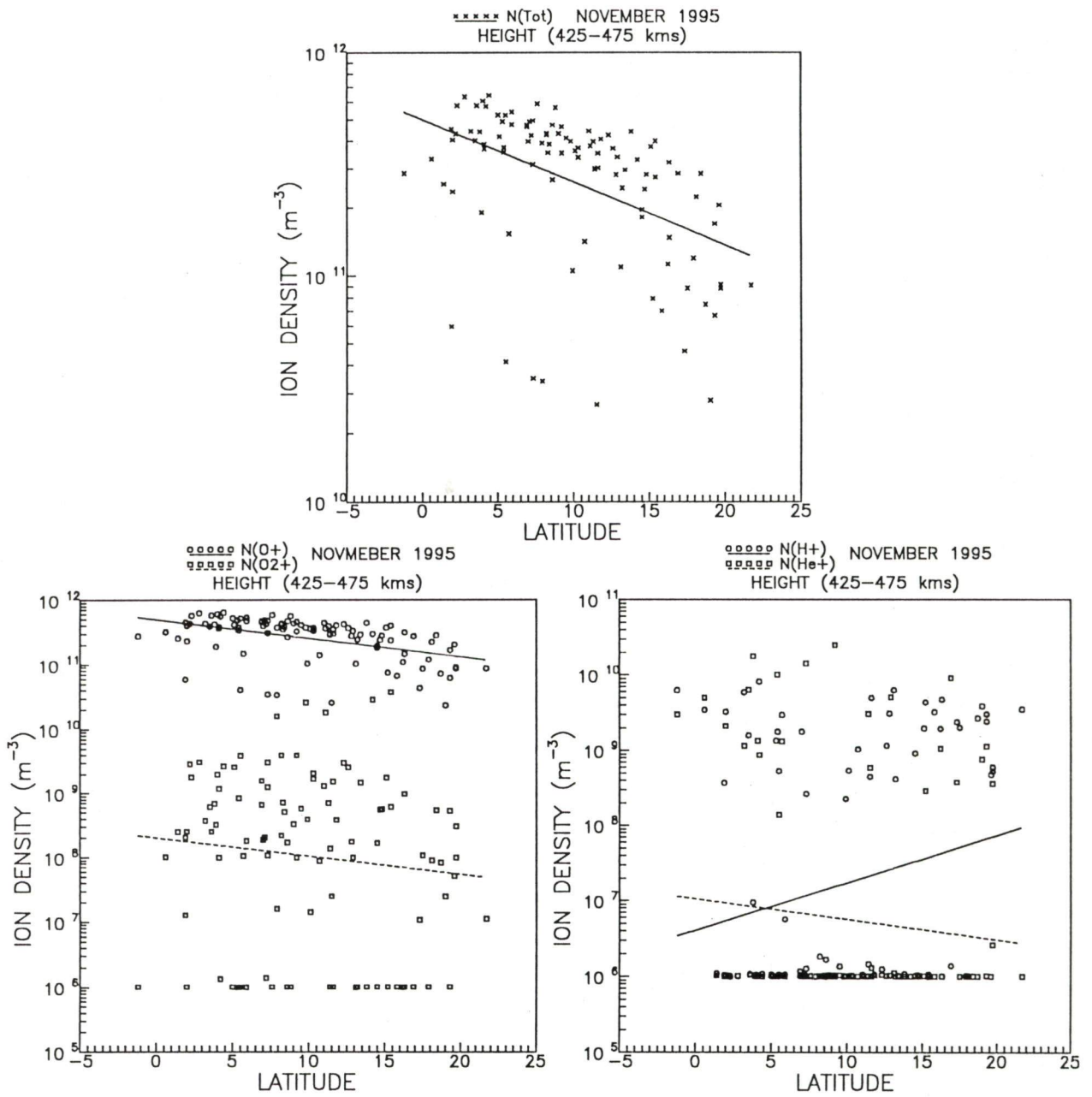


Figure 5.9(b) - Latitudinal variation of ion densities for altitude 425-475 km in the month of November 1995

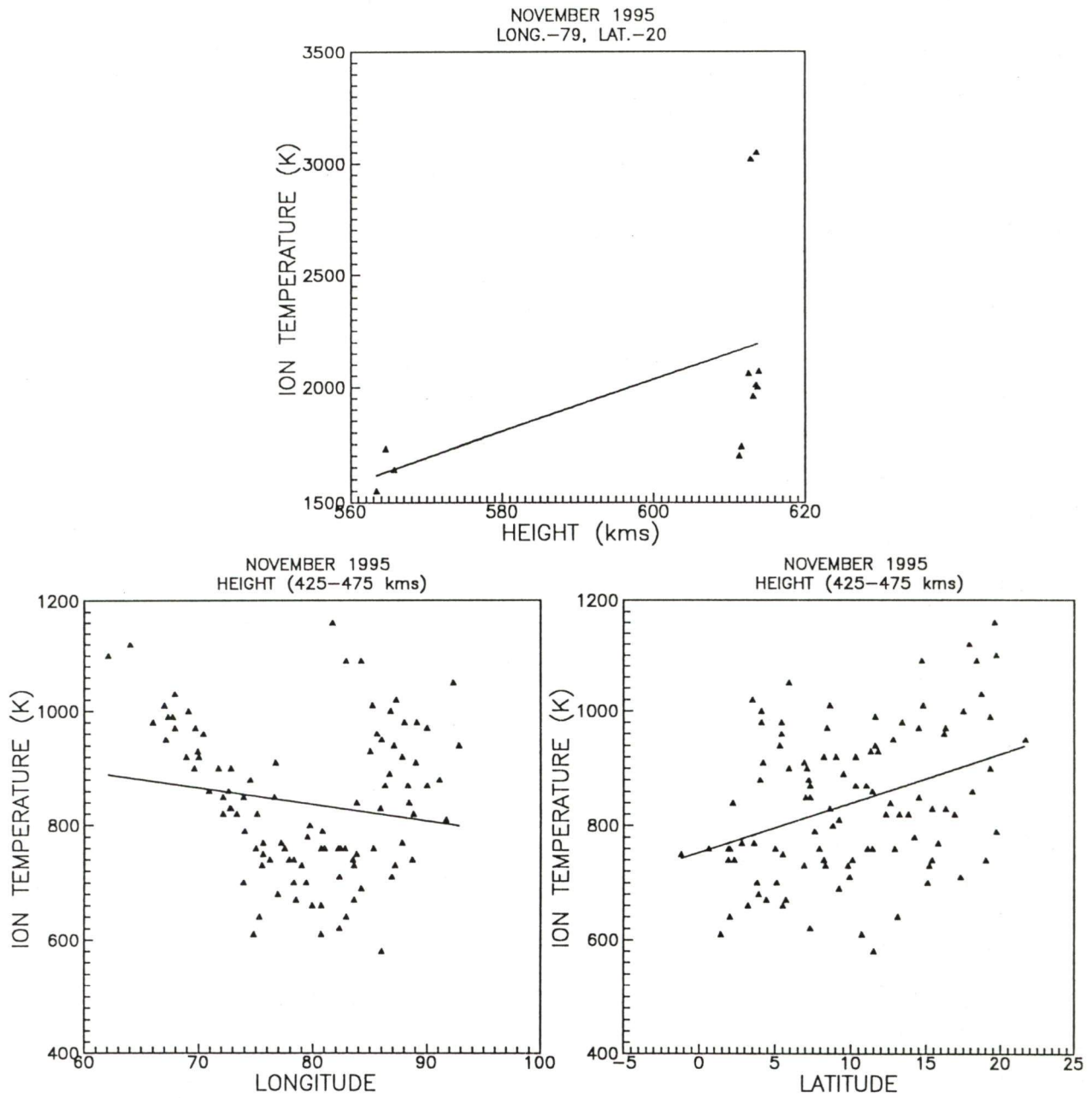


Figure 5.10(a) - Temperature of ions during November 1995 as function of longitude, latitude and height

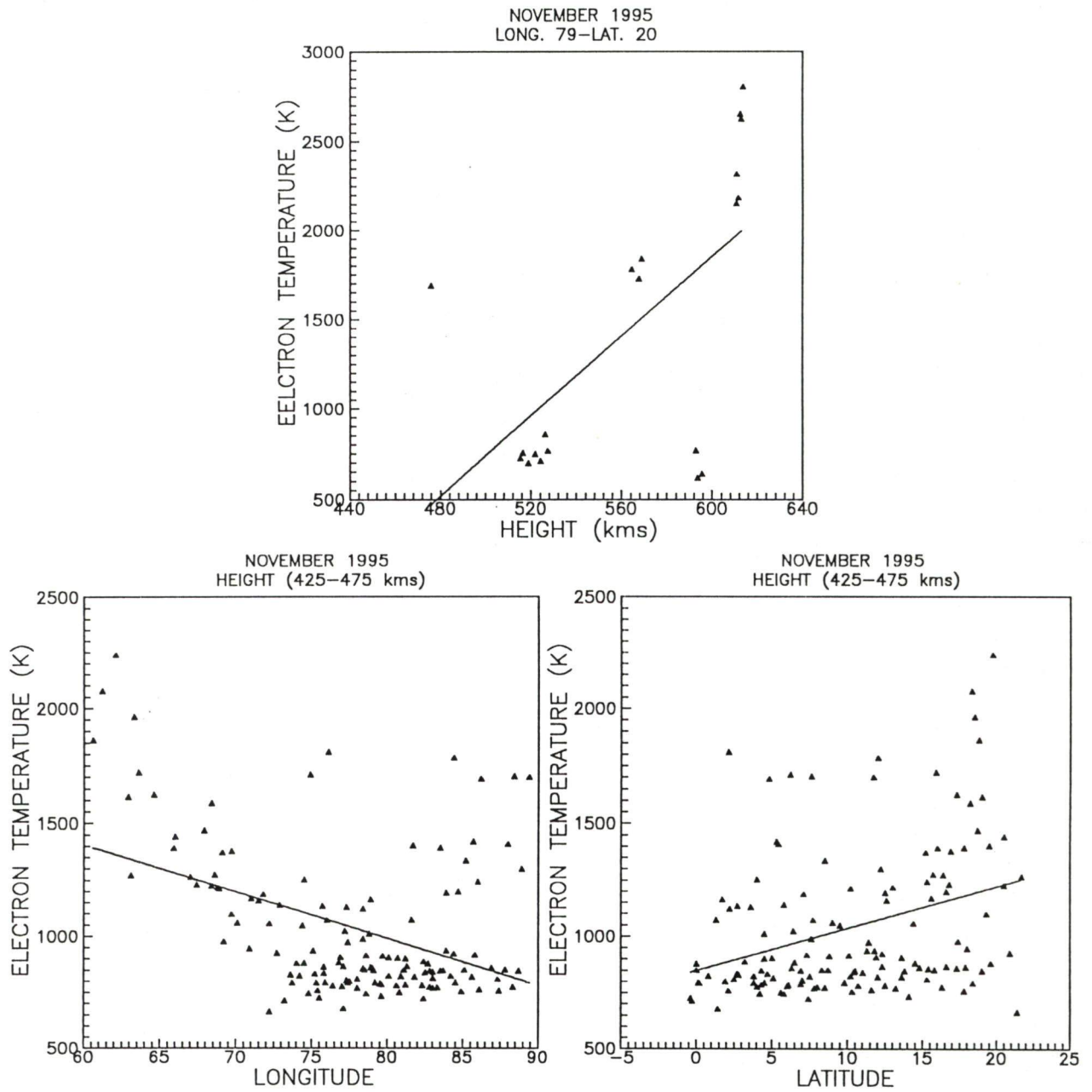


Figure 5.10(b) - Temperature of electrons during November 1995 as function of longitude, latitude and height

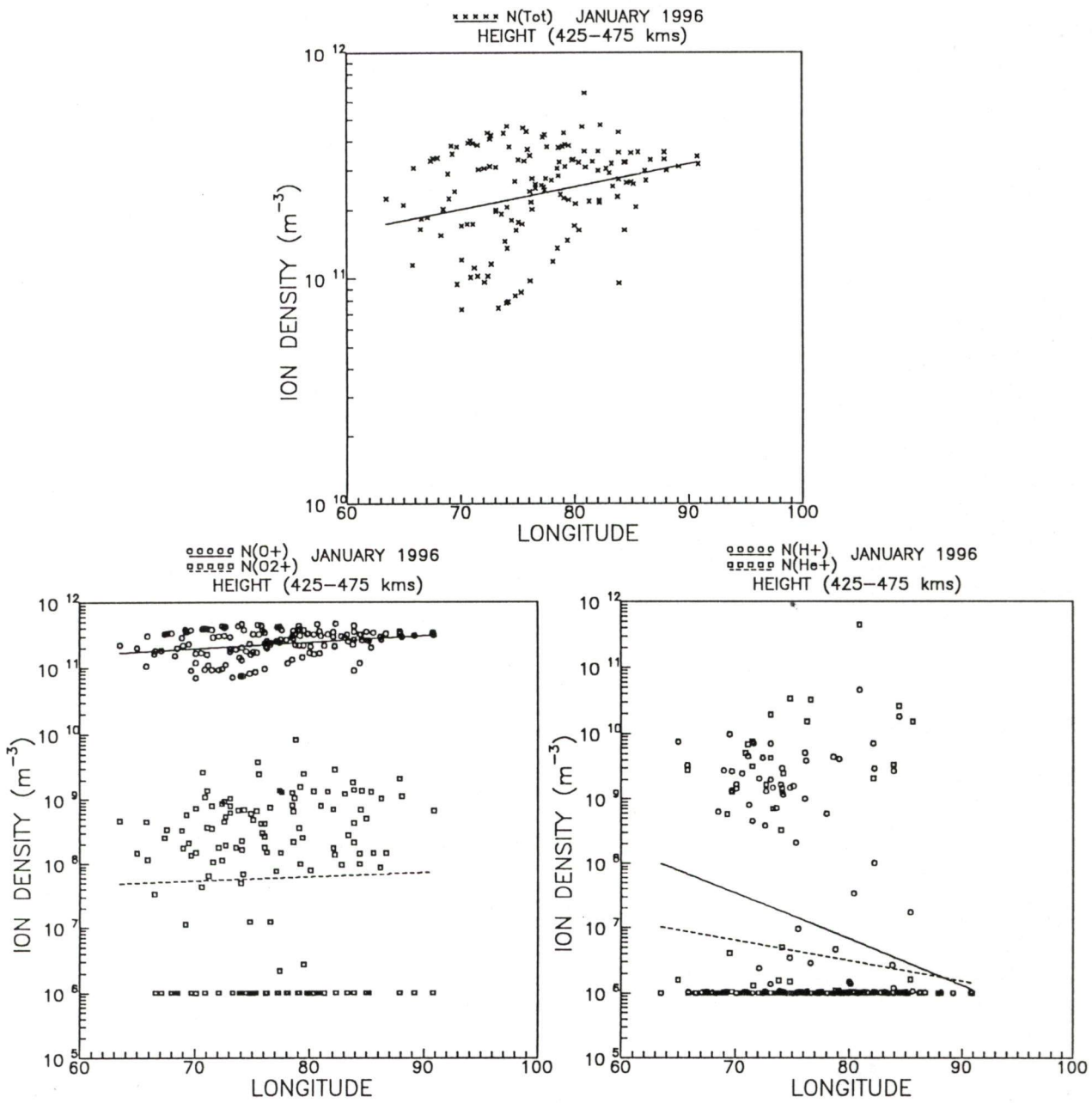


Figure 5.11(a) - Longitudinal variation of ion densities for altitude 425-475 km in the month of January 1996

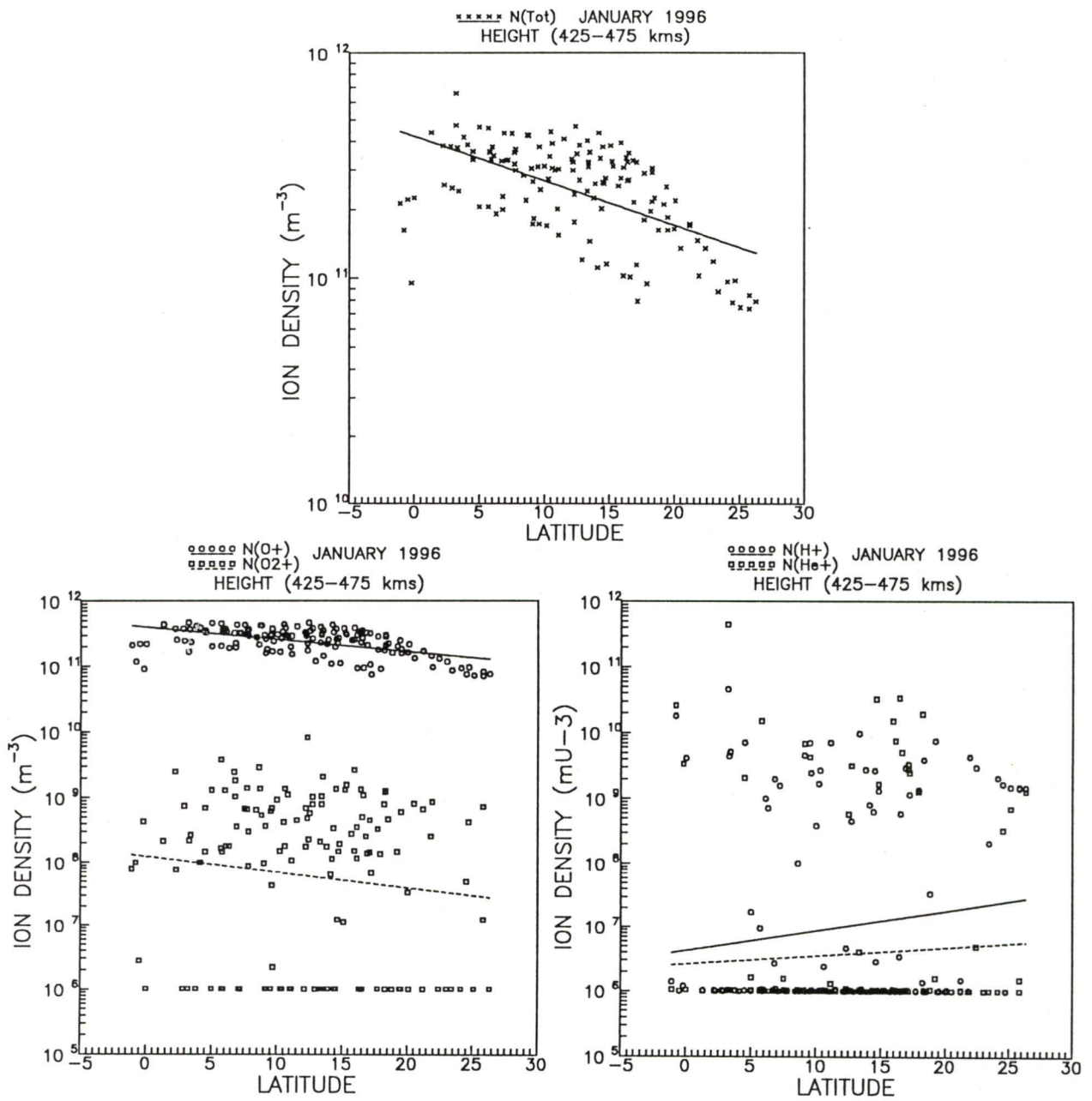


Figure 5.11(b) - Latitudinal variation of ion densities for altitude 425-475 km in the month of January 1996

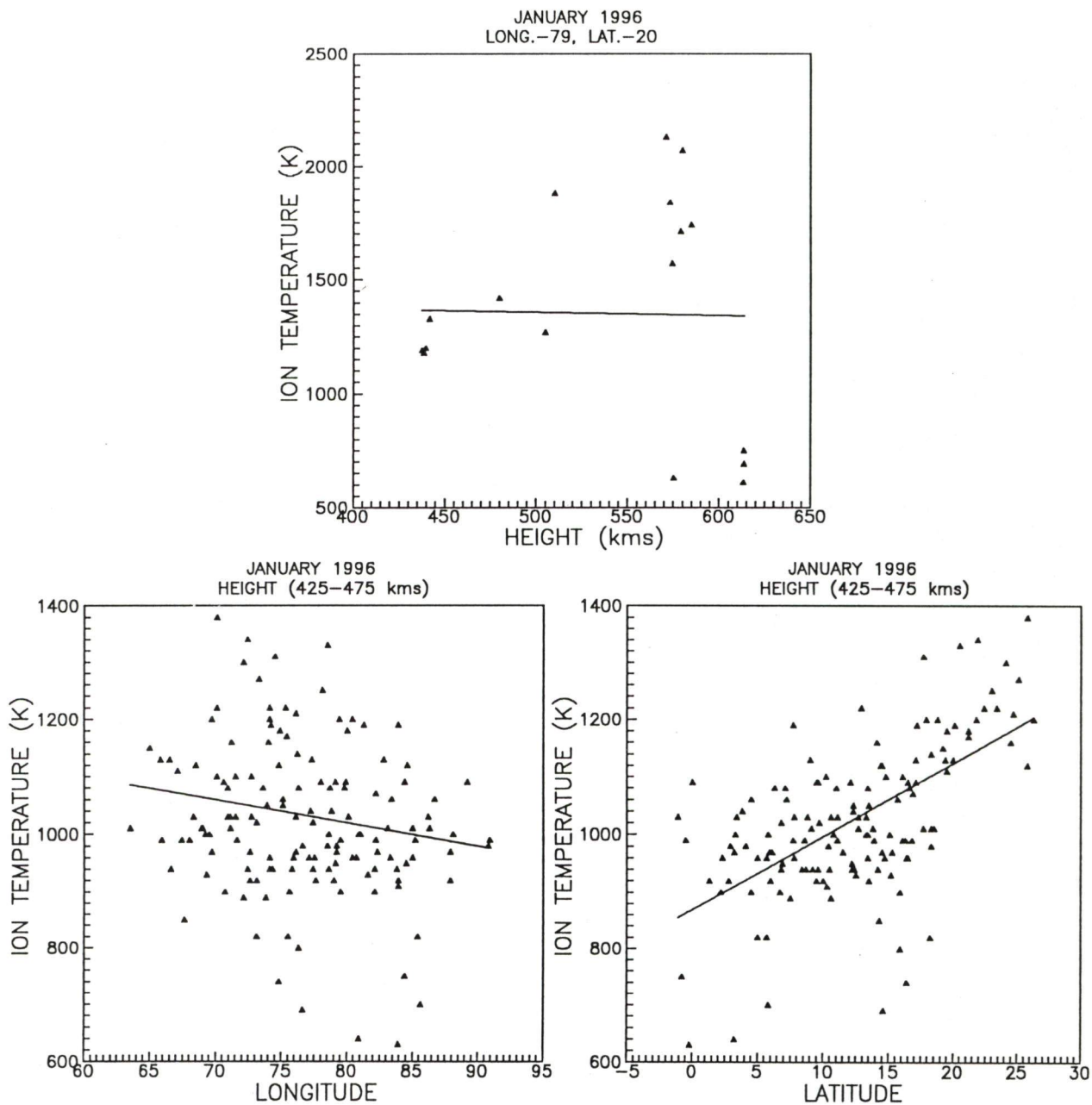


Figure 5.12(a) - Temperature of ions during January 1996 as function of longitude, latitude and height

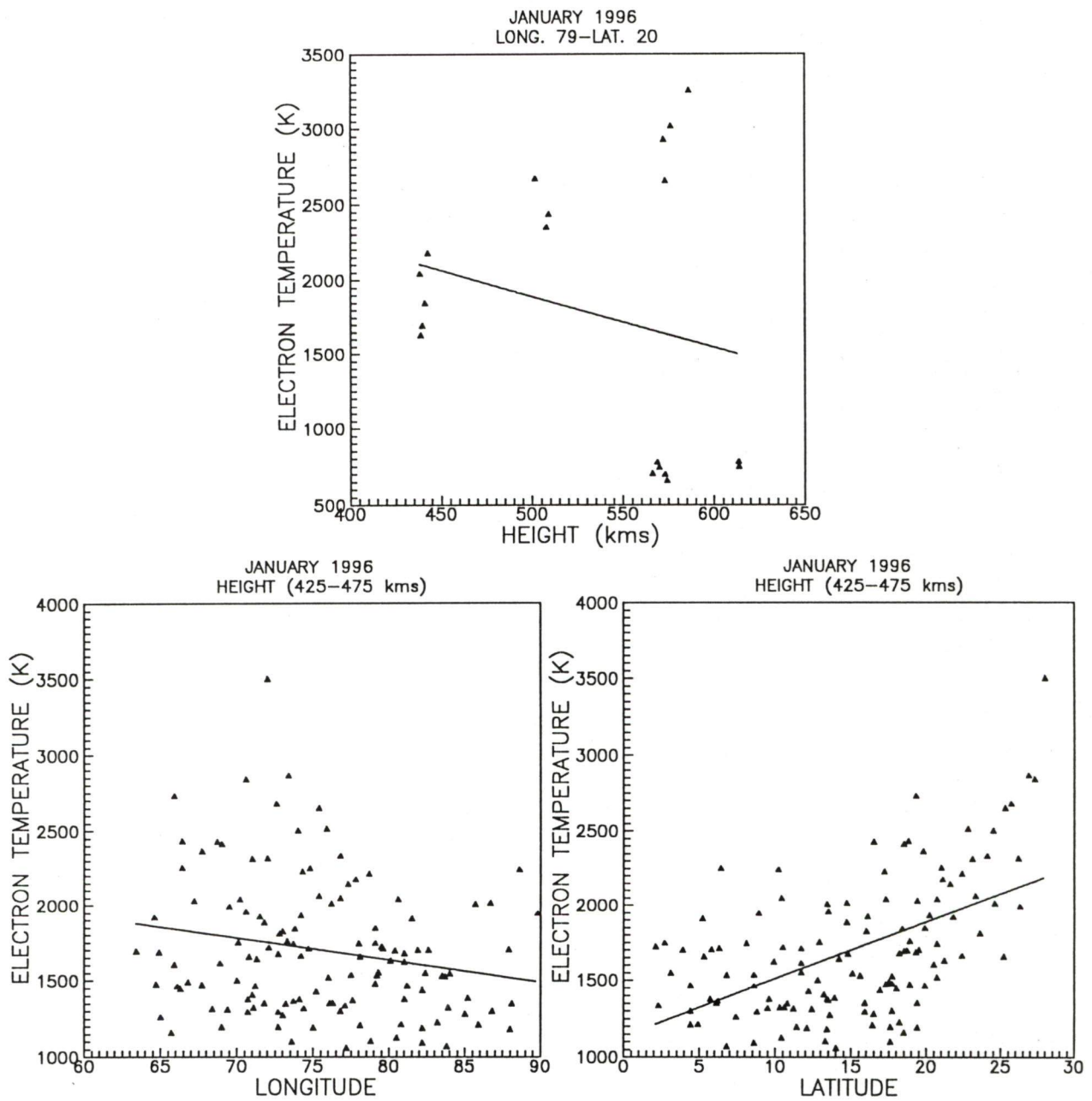


Figure 5.12(b) - Temperature of electrons during January 1996 as function of longitude, latitude and height

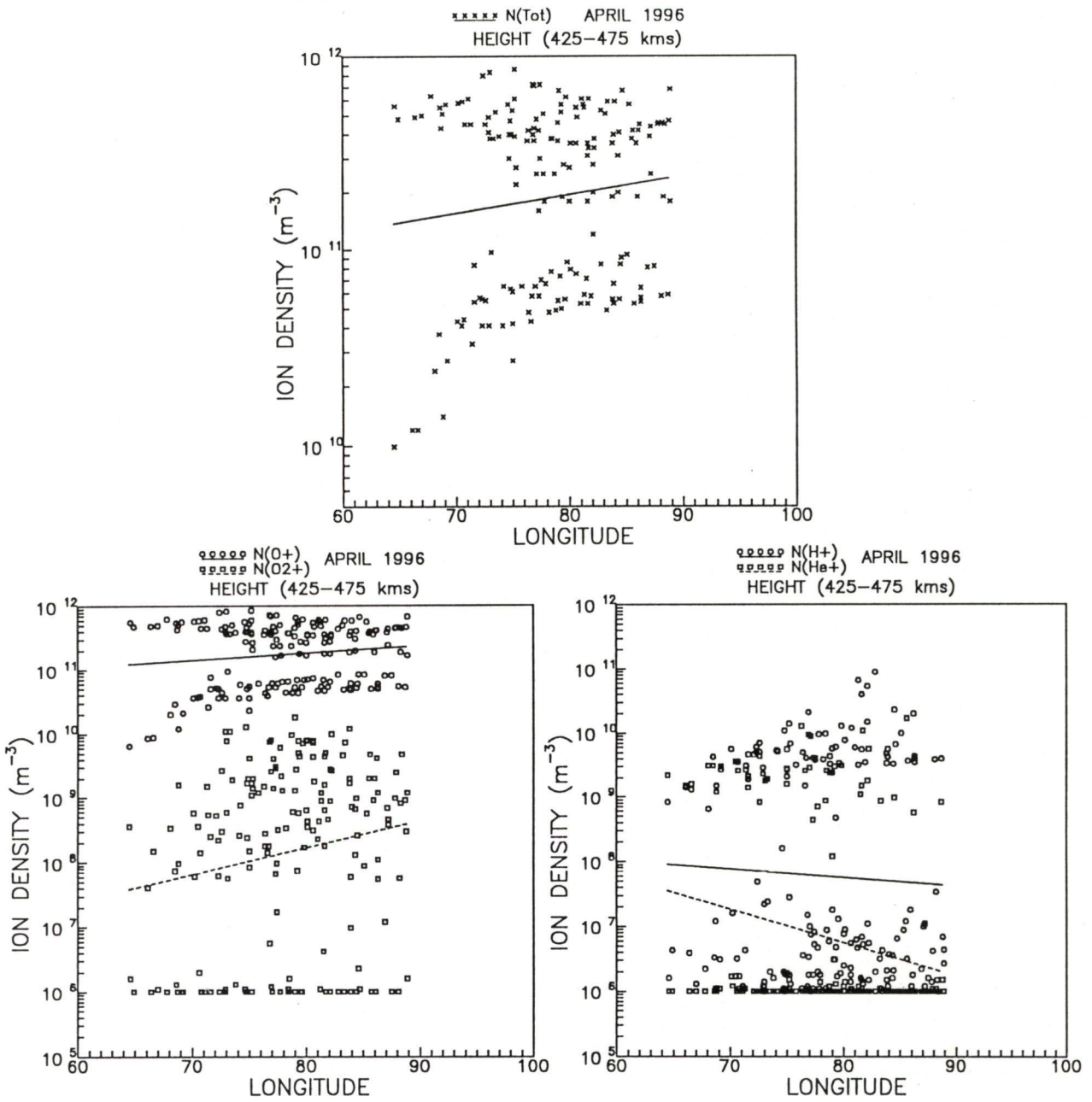


Figure 5.13(a) - Longitudinal variation of ion densities for altitude 425-475 km in the month of April 1996

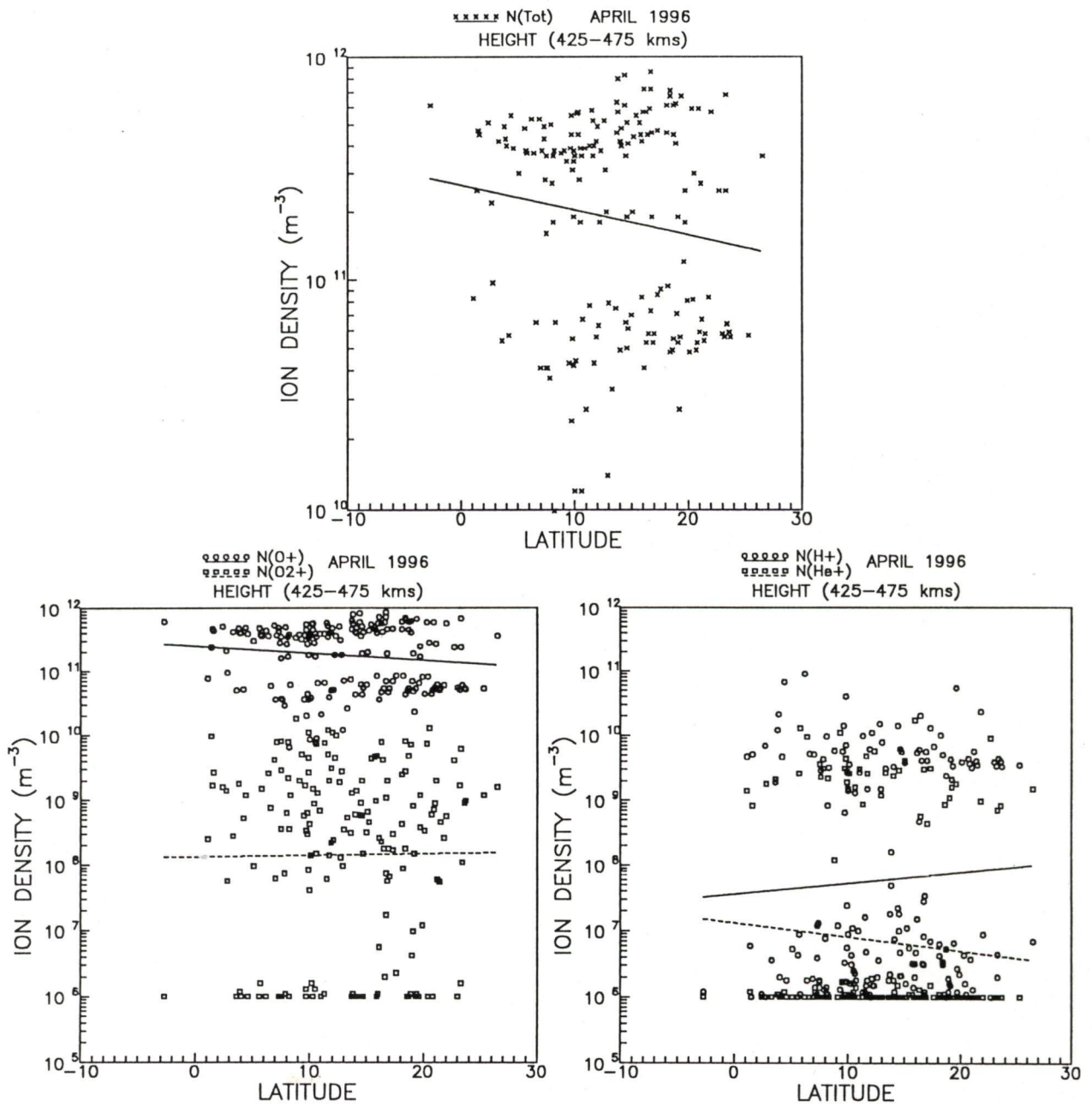


Figure 5.13(b) - Latitudinal variation of ion densities for altitude 425-475 km in the month of April 1996

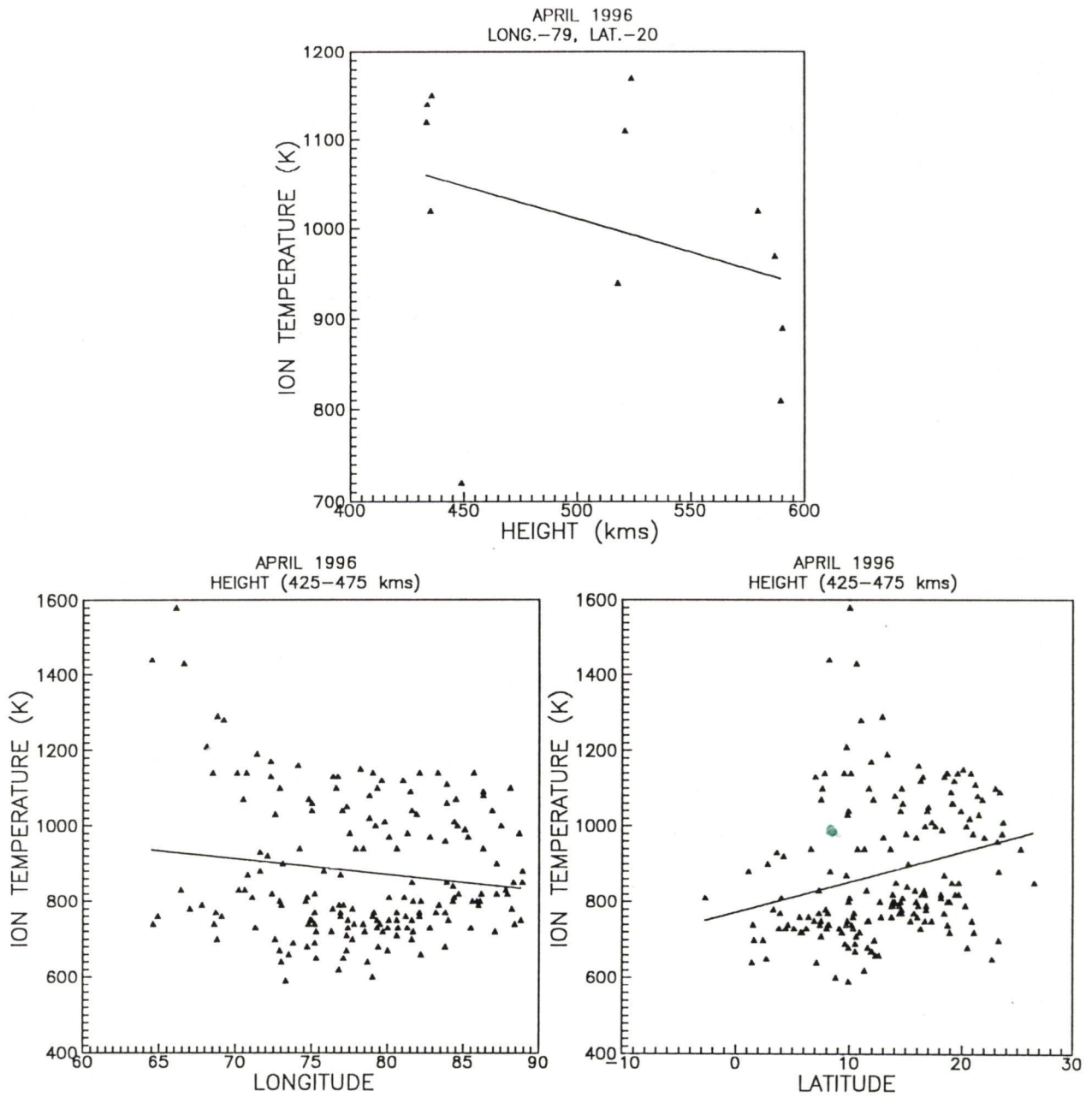


Figure 5.14(a) - Temperature of ions during April 1996 as function of longitude, latitude and height

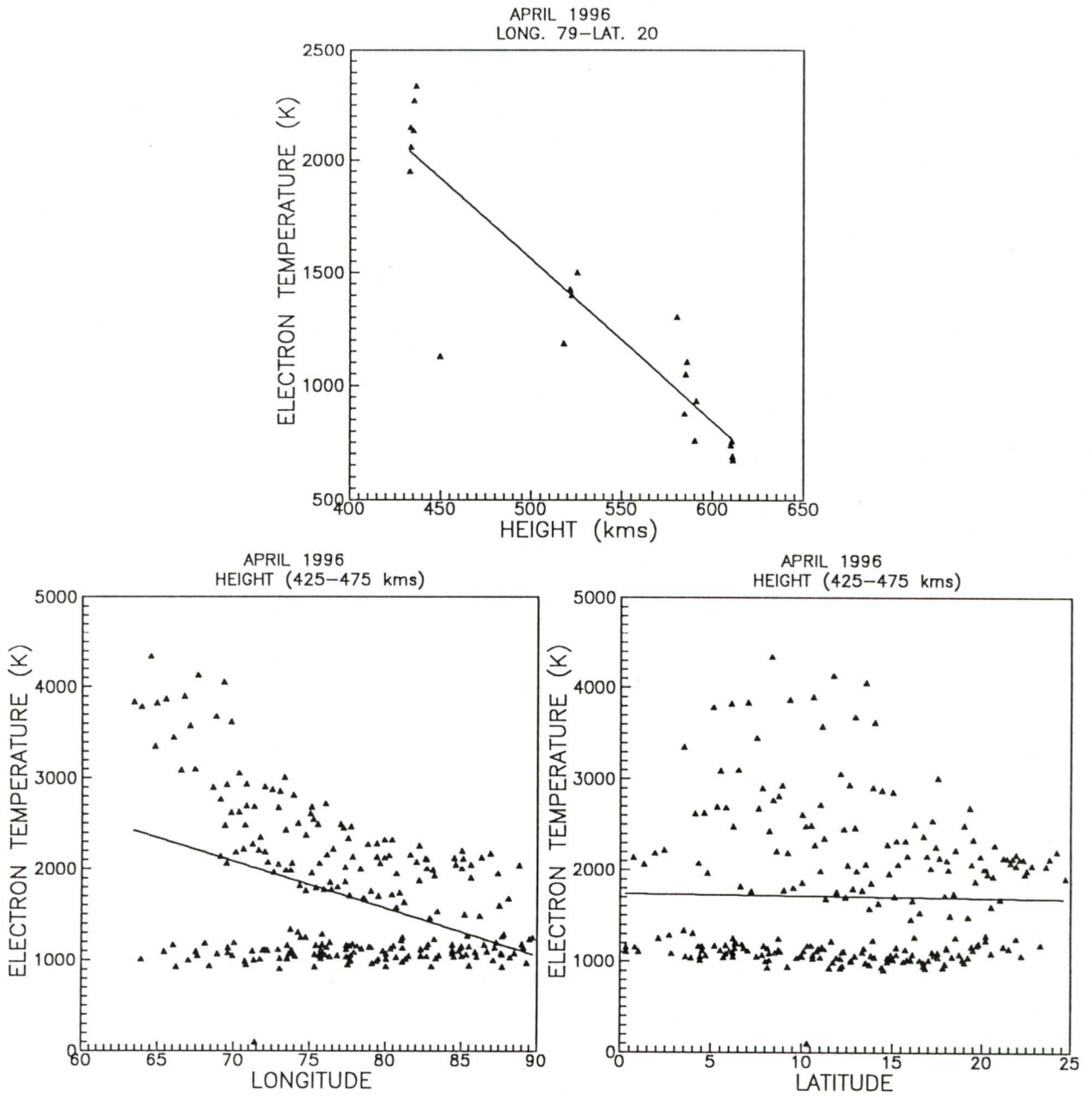


Figure 5.14(b) - Temperature of electrons during April 1996 as function of longitude, latitude and height

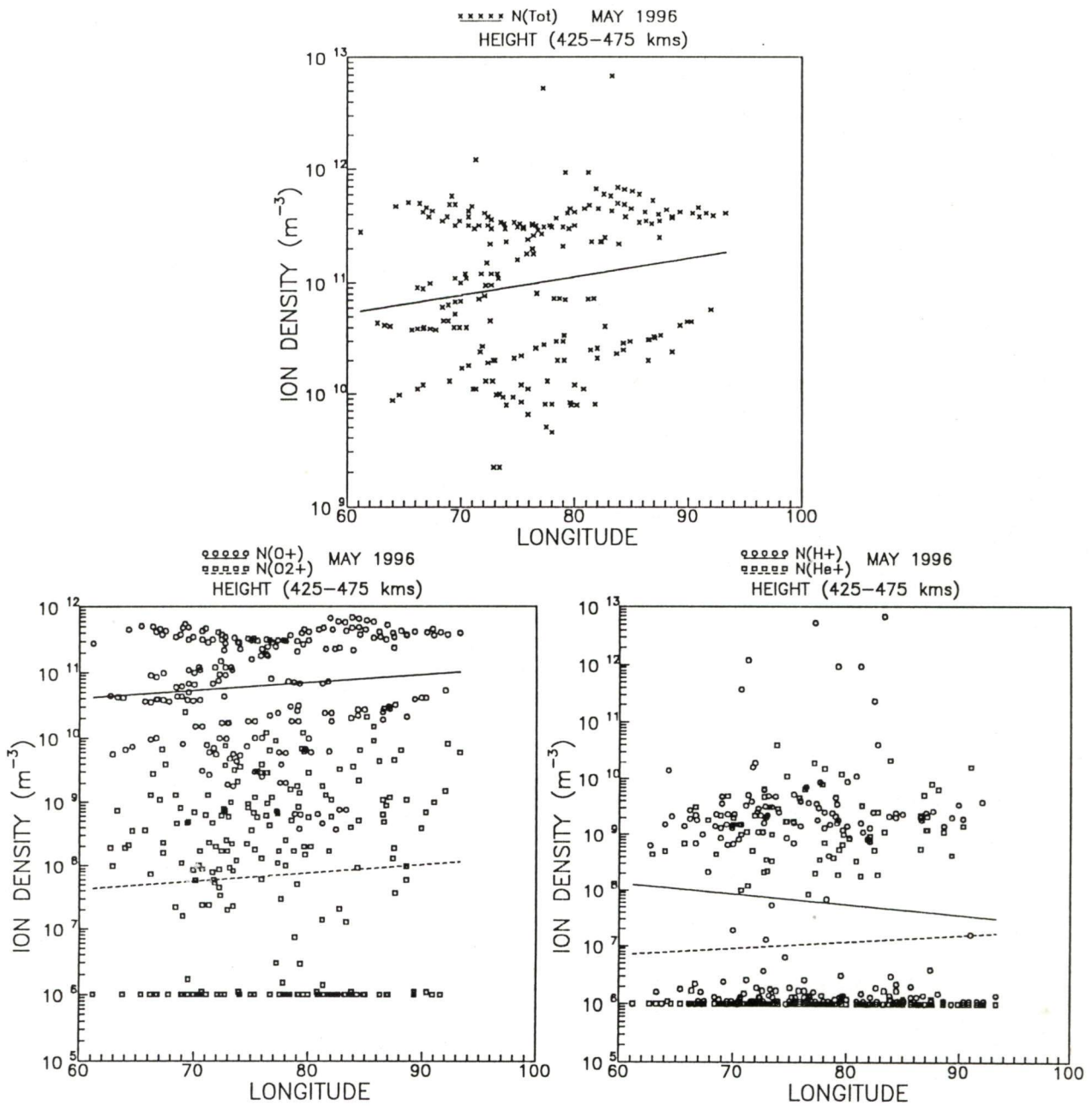


Figure 5.15(a) - Longitudinal variation of ion densities for altitude 425-475 km in the month of May 1996

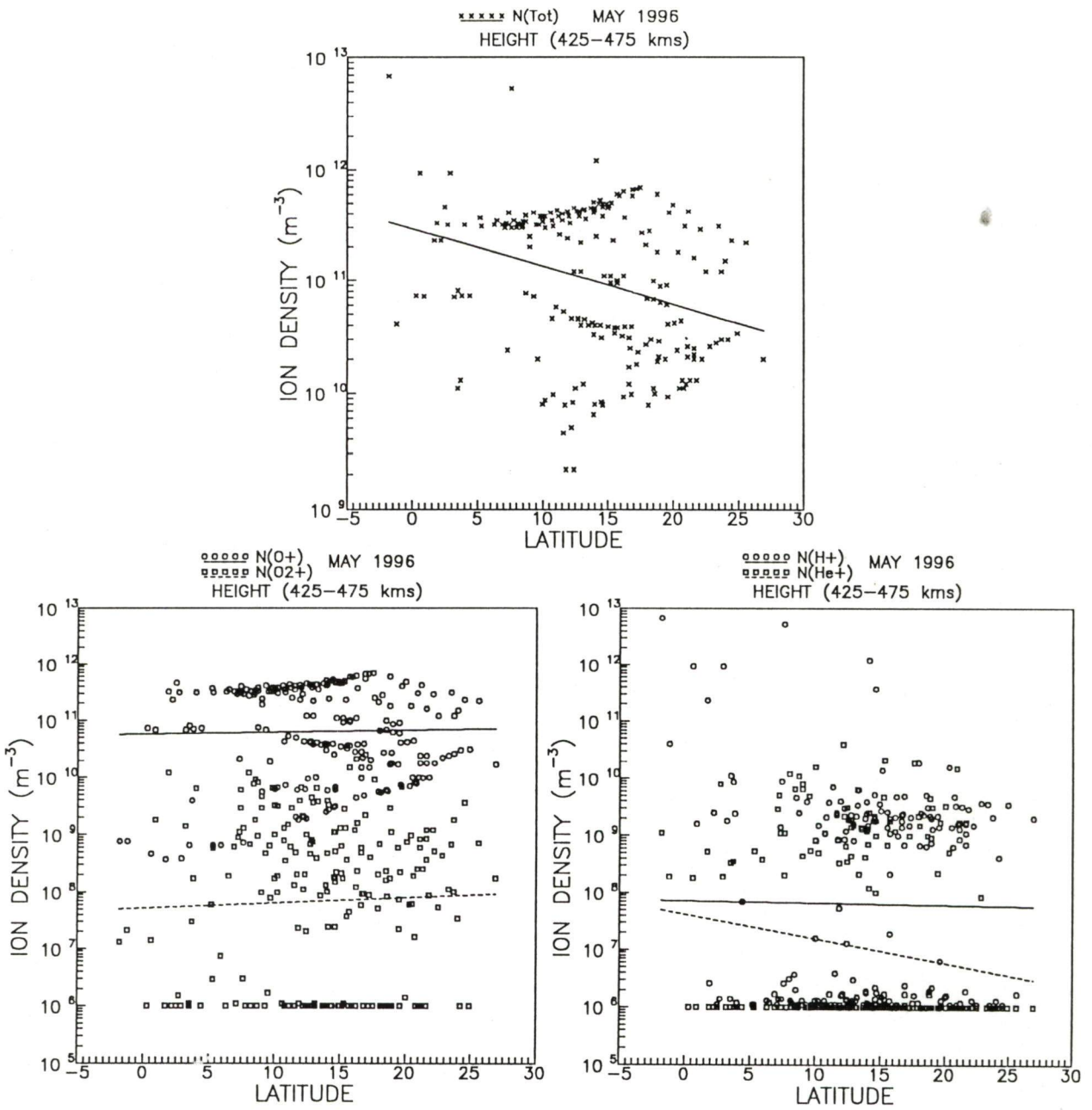


Figure 5.15(b) - Latitudinal variation of ion densities for altitude 425-475 km in the month of May 1996

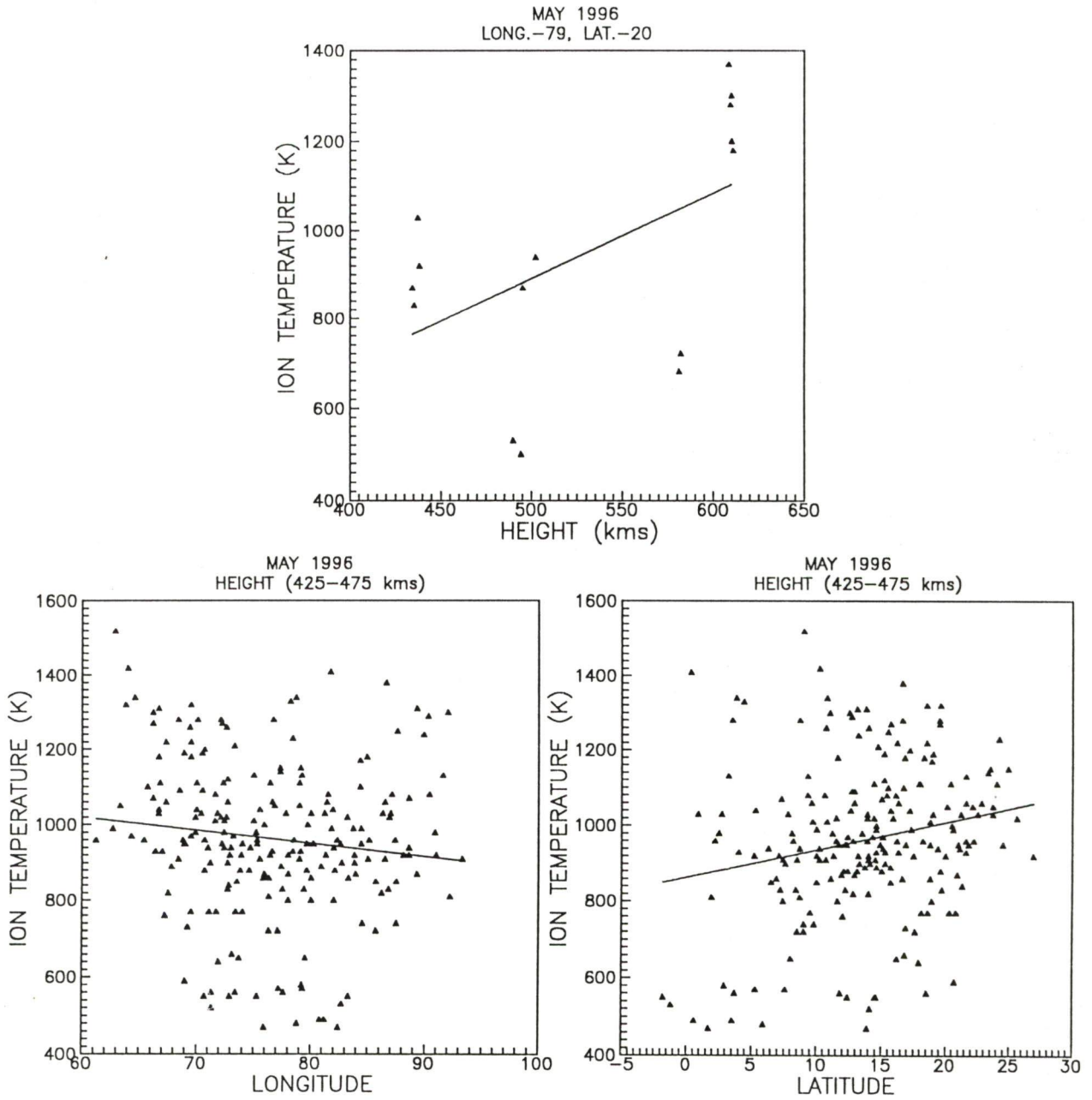


Figure 5.16(a) - Temperature of ions during May 1996 as function of longitude, latitude and height

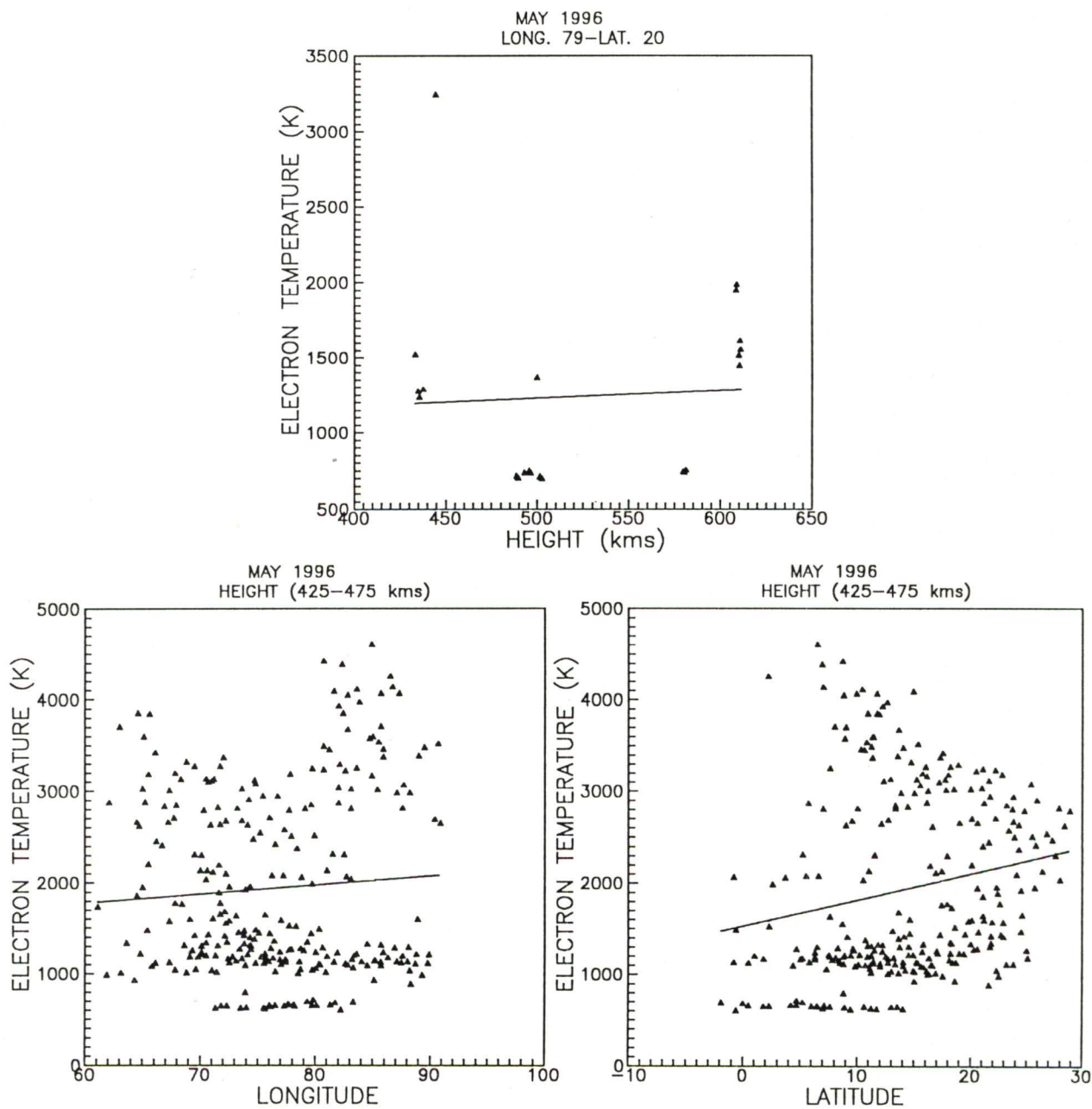


Figure 5.16(b) - Temperature of electrons during May 1996 as function of longitude, latitude and height

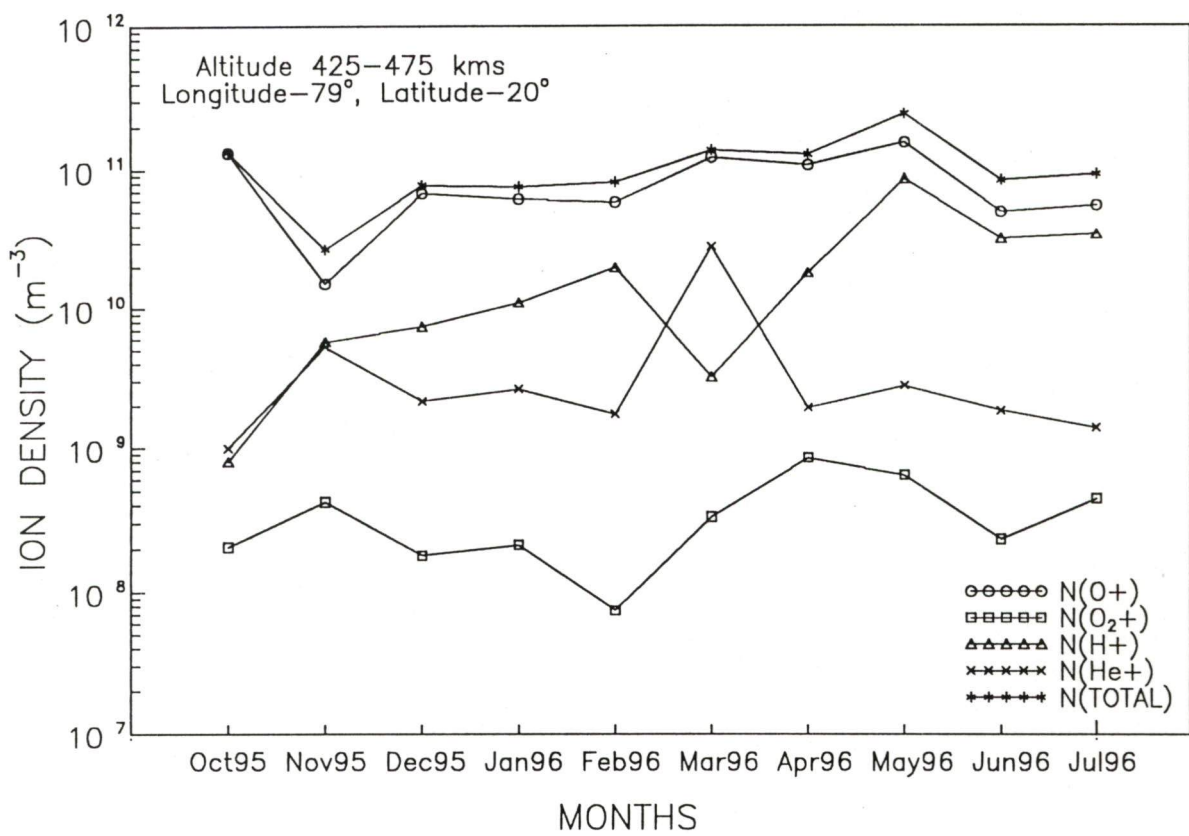


Figure 5.17 - Monthly variation of ion densities (O⁺, O₂⁺, H⁺, He⁺)

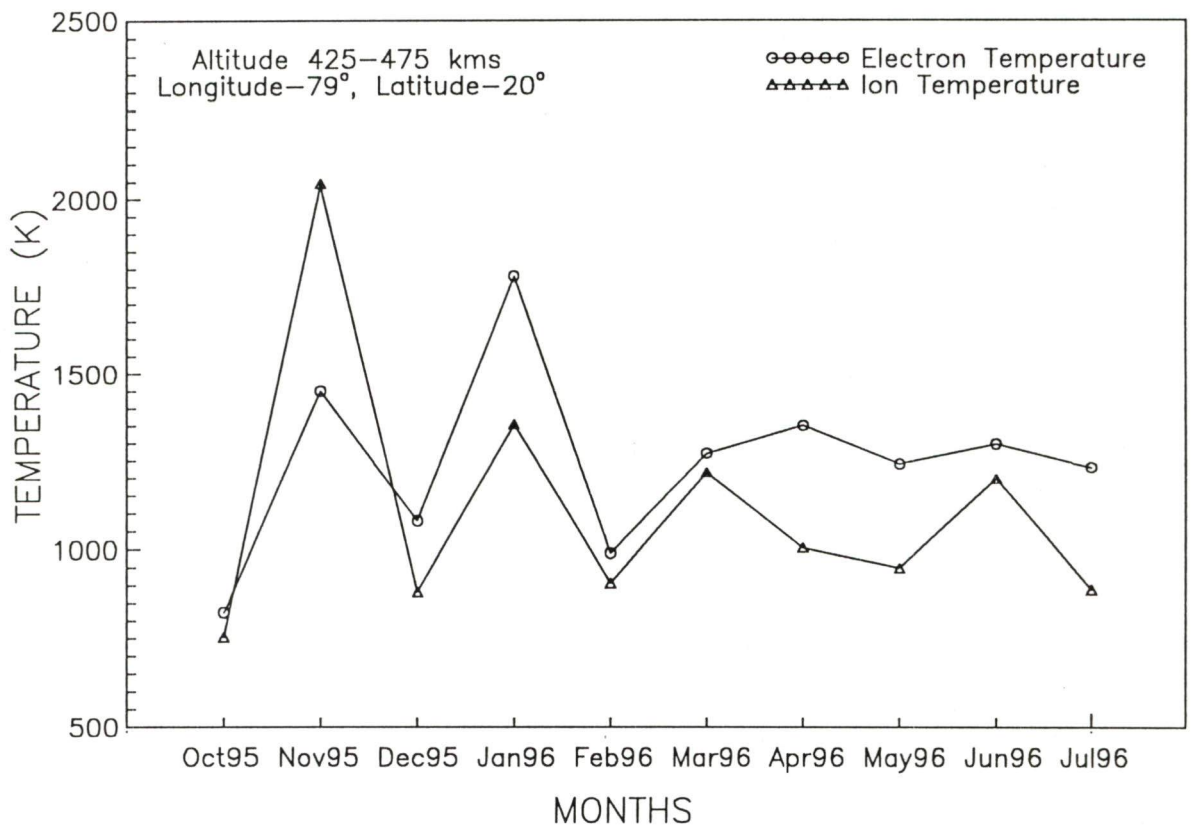


Figure 5.18 - Monthly variation of ion and electron temperature

Chapter 6

*Conclusions
And
Recommendations*

Study of atmospheric particles and electrical conductivity in different weather conditions can be used as a tool to investigate the various atmospheric phenomena produced by nature as well as by the modern civilization. The radiative properties of lower atmosphere, cloud formation, wind dynamics, lightning discharges, radio communication, satellite tracking, aviation etc. are the main fields of interest. The author has tried to correlate the density distribution of atmospheric aerosols/particles and electrical conductivity with the meteorological parameters, which are governing factors to seasons and weather. This thesis also includes the study of low latitude (over Indian subcontinent) ionospheric particles (ions and electrons). The ion density and ion-electron temperature behavior of ionosphere have been studied in detail during different seasons (winter, summer, monsoon).

6.1 CONCLUSIONS

The introductory survey by the author related to these aspects give an indication that after a lot of efforts of various researchers, some of the important features of atmosphere like the behavior of atmospheric aerosols and electrical conductivity in relation to meteorological parameters are still not fully understood. The lower atmospheric electrical phenomena which are highly

effective in troposphere-ionosphere interactions and which is significantly governed by atmospheric particles are still a major field of interest for scientific community.

Two instruments were used for the present study (1) Laser Scatterometer and (2) Gerdian Cylinder. The laser scatterometer is used for the aerosol measurements in five different size ranges, while the Gerdian cylinder was used to measure the atmospheric conductivity during different seasons. The description of these instruments and working principle have been given in Chapter II.

The solar eclipse is one of the spectacular events of nature, which provide vehicle to researchers to study the behavior and structure of the sun as well as associated phenomena in the lower atmosphere. The author used the solar eclipse of 24 October 1995 to study the aerosol density distribution and the conductivity of lower troposphere. A detailed programme has been made to use this opportunity and the measurements were done from 21-27 October 1995. The observations of three days (23-25 October 1995) have been discussed in chapter III. The author found that the aerosol size spectrum shifts towards higher end and it was attributed to lowered temperature and increased humidity during eclipse. The decrease of temperature and the increase of humidity enhance the condensation process that results in the higher density of large size particles. Also the electrical conductivity was increased on eclipse

day than the normal days. The ionization rate increases during the eclipse, which causes the increase of conductivity. The wind does not play any significant role in governing the aerosol concentrations and conductivity during the eclipse.

The disturbed and fair-weather conditions can also be used to study the aerosol and atmospheric electrical conductivity behavior because these parameters are known to be highly dependent on meteorological factors. The author tried to use a full year 1996-97 to study the aerosol concentration and conductivity in two phases (1) disturbed weather (monsoon, June-September 1996) and (2) fair weather (winter, November 1996-February 1997) and the results are presented in chapter IV. This study concludes that the aerosols and electrical conductivity are very much affected by the meteorological parameters. The two weather conditions have shown different behavior of aerosol concentration. Rain plays very important role in changing the characteristics of aerosols. Heavy rain shifts the size spectrum towards lower end of aerosol size with decreasing density in monsoon season. During winter the aerosol concentration increases with decreasing temperature and increasing humidity. Mode radius also shifts towards lower values in monsoon due to scavenging. The higher value of the mode radius during winter results from the increased condensation. The study of unipolar conductivity in relation to meteorological parameters such as relative humidity, temperature, wind

speed and rain fall has been made during the June, July and August 1996. The conductivity has been found to decrease with increasing relative humidity and temperature. Wind was an important factor, which modifies the behavior of conductivity in short-term range. Although the observations were taken at Roorkee, the findings are expected to be valid for all the subtropical regions.

In addition to the study of lower tropospheric region the ionosphere in the height range 425-475 km (F_2 region) has been investigated using the Stretched Rohini Series Satellite (SROSS-C2) of Indian Space Research Organization (ISRO), India. The SROSS-C2 is a low latitude orbiting satellite and is basically meant for the study of ionosphere over Indian region. The onboard payload Retarding Potential Analyzer (RPA) has been used for this purpose. Here also the studies have been made in three different seasons (winter, summer, and monsoon) of the period October 1995 to July 96. The ion density and ion-electron temperature profiles were obtained for latitudinal and longitudinal variations. Also vertical profile of temperature and density has been studied for fixed longitude (79°) and latitude (20°), as well as the monthly variation of ion density and ion-electron temperature. The all results of present study have been shown in chapter V. The total ion density ($H^+ + He^+ + O^+ + O_2^+$) is mostly dominated by O^+ ions in the specific height range of our interest. The H^+ ions also show equal contribution to the total density in the summer of 1996. On average the total density varies from 2×10^{10} to $5 \times 10^{11} \text{ m}^{-3}$. The ion

temperature varies on average from 900 to 2000 K during winter season and from 1000 to 1300 K during summer. The electron temperature was always more than the ion temperature during the period of our study except in November 1995. It varies on average from 1000-1800 K during winter season (November 1995-February 1996) and from 1200 to 1300 K during summer and monsoon (April-July 1996) seasons.

6.2 RECOMMENDATIONS FOR FUTURE STUDIES

The Galactic Cosmic Rays (GCR) and Solar Cosmic Rays (SCR) have greater contribution to the production of ionization in the atmosphere. Therefore to study the precise role of atmospheric aerosols and electrical conductivity during different weather conditions and particularly at the time of solar eclipse, it is necessary to measure the cosmic rays at the height of interest. Also along with the cosmic rays the ionization rate and Cloud Condensation Nuclei (CCN) should be measured. After measuring these parameters, one can look into the solar-terrestrial relationship effectively. For the present study, around one and half years data of aerosols and electrical conductivity have been used for different weather conditions like monsoon, winter and summer with the meteorological variables. To the author's thinking the large number of data samples over many years would be more helpful to establish a better relationship among the atmospheric particles, electrical parameters and meteorological variables.

In the study of ionosphere the author described the results of SROSS-C2 satellite regarding ion and electron temperature and ion density only. Using this data one can study the suprathermal flux also. To study the ionospheric characteristics in relation to troposphere, the lightning discharges and thunderstorm may become important as these parameters are expected to have some impact on the ionosphere.

References

-
- [1] Agarwal, R. R., Rai, J. and Varshneya, N. C., "Effect of ionization and particulate pollutants on GEC parameters over the Indian subcontinent", *Indian J. Radio Space Phys.*, **24**, 159-165, 1995.
- [2] Agarwal, R. R. and Varshneya, N. C., "Global electric circuit parameters over Indian sub-continent", *Indian J. Radio Space Phys.*, **22**, 320-324, 1993.
- [3] Agashe, V. V. and Mahajan, R. D., "Study of atmospheric aerosols at Poona", Second Workshop on IMAP Scientific Results at VSSC, Trivandrum, April 24-28, 1988.
- [4] d'Alibard, T. F., Letter to *Acad. De. Sci.*, 1752.
- [5] d'Almeida, G. A., "Atmospheric aerosols", A. Deepak Publication, USA, 1991.
- [6] Alofs, D. J. and Liu, Tung-Hsi, "Atmospheric measurements of CCN in the super-saturation range 0.013-0.681%", *J. Atmos. Sci.*, **38**, 2772-2778, 1981.
- [7] Anderson, R. V., "Atmospheric electricity, turbulence and a pseudo-sunrise effect resulting from a solar eclipse", *J. Atmos. Terr. Phys.*, **34**, 567-572, 1972.
- [8] Anderson, R. V. and Dolezalek, H., "Atmospheric electricity measurements at Waldorf, Maryland during 7 March 1970 solar eclipse", *J. Atmos. Terr. Phys.*, **34**, 561-566, 1972.

- [9] Appleton, E. V., Watson-Watt, R. A. and Herd, J. F., "On the nature of atmospherics II and III", *Proc. Roy. Soc.*, **AIII**, 615-676, 1926.
- [10] Banks, P. M., Schunk, R. W. and Raitt, W. J., "NO⁺ and O⁺ in the high latitude F region", *Geophys. Res. Lett.*, **1**, 239-242, 1974.
- [11] Bansal, M. K. and Verma, T. S., "Aerosol measurements at Roorkee relating to the total solar eclipse of 24 Oct. 1995", *Indian J. Radio Space Phys.*, **27**, 260-263, 1998.
- [12] Bhartendu, M., "Correlation of electric potential gradients at land station and their implication on the classical picture of atmospheric electricity", *Pure App. Geophys.*, **84**, 13, 1971.
- [13] Bhaskaran, B., Mitchell, J. F. B., Lavery, J. and Lal, M., "Climate response of Indian subcontinent to doubled CO₂", *J. Climatol.*, **15**, 873-892, 1995.
- [14] Blanchard, D. C., "From raindrops to volcanos", Doubleday, Garden City, New York, 1967.
- [15] Blifford Jr., I. H. and Ringer, L. D., "The size and number distribution of aerosols in the continental troposphere", *J. Atmos. Sci.*, **26**, 716-726, 1969.
- [16] Boys, C. V., "Progressive Lighting", *Nature*, **118**, 749-750, 1926.
- [17] Brinton, H. C., Grebowsky, J. M. and Brace, L. H., "The high-latitude winter F region at 300 km: Thermal plasma observations from AE-C", *J. Geophys. Res.*, **83**, 4767-4776, 1978.
- [18] Brown, J. G., "The local variations of the earth's electric field", *Terr. Mag. Atmos. Elect.*, **40**, 413-425, 1935.

- [19] Cadle, R. D., Kiang, C. S. and Louis, J. F., "The global dispersion of the eruption clouds from major volcanic eruptions", *J. Geophys. Res.*, **82**, 1783-1786, 1976.
- [20] Chakraborty, B. and Lal, M., "Monsoon climate and its change in a doubled CO₂ atmosphere as simulated CSIRO9 model", *Terr. Atmos. Ocean. Sci.*, **5(4)**, 515-536, 1994.
- [21] Chalmers, J. A., "The effects of condensation nuclei in atmospheric electricity", *Geofis. Pure Appl.*, **36**, 211-217, 1957.
- [22] Chalmers, J. A., "Atmospheric Electricity", Pergamon Press, Oxford, 1967.
- [23] Chamberlin, J. W. and Hunten, D. M., "Theory of planetary atmospheres", *Intl. Geophys. Series*, **36**, Academic Press., New York, 1987.
- [24] Chandrasekhar, S., "Radiative Transfer", Oxford University Press, Oxford, UK, 1950.
- [25] Changnon, S. A., "The La Porte weather anomaly", *Bull. Am. Meteorol. Soc.*, **49**, 4-11, 1968.
- [26] Charlson, R. J., Longner, J., Rodhe, H. and Warren, S. G., "Perturbations of northern hemispheric radiative balance by back-scattering from anthropogenic sulfate aerosols", *Tellus*, **43**, 152-163, 1991.
- [27] Cliffswallow, W. and Hirman, J. W., "US space weather real-time observing and forecasting capabilities", *Solar-Terrestrial Predictions IV*, 185-198, 1992.
- [28] Crutzen, P. J., "The possible importance of CSO for the sulphate layer of the stratosphere", *Geophys. Res. Lett.*, **3**, 73-76, 1976.

- [29] Cobb, W. E. and Wells, H. J., "The electrical conductivity of ocean air and its correlation to global atmospheric pollution". *J. Atmos. Sci.*, **27**, 814-819, 1970.
- [30] Cubasch, U., Hasselmann, K., Hock, H., Mauer-Reimer, E., Mikolajewicz, U., Santer, B. D. and Sausen, R., "Time-dependent green house warming computations with a coupled ocean atmosphere model", *Clim. Dyn.*, **8**, 55-69, 1992.
- [31] Cunnold, D. M., Gray, C. R. and Merritt, D. C., "Stratospheric aerosol layer detection", *J. Geophys. Res.*, **78**, 920-931, 1973.
- [32] Dams, R. and De Jonge, J., "Chemical composition of Swiss aerosols from the Jungfrauoch", *Atmos. Environ.*, **10**, 1079-1084, 1976.
- [33] Das, S. K., Kulshrestha, S. M., Chatterjee, K., Chandrasekharan, C. K., "Meteorological parameters near the earth's surface along the path of totality during the total solar eclipse of 16 February 1980", *Proc. Indian Nat. Sci. Acad.*, **48A**, 202-208, 1982.
- [34] Deirmendzian, D., "Electromagnetic scattering on spherical polydispersions", American Elsevier, New York, 1969.
- [35] Denmann, H. H., Heller, W. and Pangonis, W. J., "Angular scattering functions for spheres", Wayne State University Press, Detroit, USA, 1966.
- [36] Deshpande, C. G. and Kamra, A. K., "Short time variations in atmospheric electrical parameters", *J. Atmos. Terr. Phys.*, **54**, 1413-1420, 1992.
- [37] Devara, P. C. S. and Raj, P. E., "A bistatic lidar for aerosol studies", *Inst. Electron. Telecommun. Eng. Tech. Rev.*, **4**, 412-415, 1987.

- [38] Devara, P. C. S. and Raj, P. E., "Study of atmospheric aerosols terrain-induced nocturnal boundary layer using bistatic lidar", *Atmos. Environ.*, **25A**, 655-660, 1991.
- [39] Devara, P. C. S., Raj, P. E., Sharma, S. and Pandithurai, G., "Lidar-observed long-term variations in urban aerosol characteristics and their connection with meteorological parameters", *Int. J. Climatol.*, **14**, 581-591, 1994.
- [40] Devara, P. C. S. and Raj, P. E., "A lidar study of atmospheric aerosols during two contrasting monsoon season", *Atmosfera*, **11**, 199-204, 1998.
- [41] Devara, P. C. S., Raj, P. E., Sharma, S. and Pandithurai, G., "Real time monitoring of atmospheric aerosols using a computer-controlled lidar", *Atmos. Environ.*, **29**, 2205-2215, 1995.
- [42] Dhanorkar, S. S., Deshpande, C. G. and Kamra, A. K., "Atmospheric electricity measurements at Pune during the total solar eclipse of 18 March 1988", *J. Atmos. Terr. Phys.*, **51**, 1031-1034, 1989.
- [43] Dolezalek, H., "Discussion on the fundamental problems of atmospheric electricity", *Pure Appl. Geophys.*, **100**, 8-43, 1972.
- [44] Dolezalek, H., "Effect of 7 March 1970 solar eclipse on atmospheric electricity, a contribution to the boundary layer discussion", *Arch. Met. Geophys. Biokl.*, **21**, 221-245, 1972.
- [45] Elster, J. and Geitel, H., "On the existence of electric ions in the atmosphere", *Terr. Magn. Atmos. Elect.*, **4**, 213-234, 1899.
- [46] Endoh, T., Twabuchi, T. and Magona, C., "Observations of the electric potential gradient at the surface in winter fogs", *J. Meteorol. Soc. Japan*, **50**, 389-400, 1972.

- [47] Flochini, R. G., Cabill, T. A., Shadon, D. J., Lange, S., Eldred, R. A., Feeney, P. J., Walfe, G. W., Simmeroth, D. C. and Sundar, J. K., "Monitoring California's aerosols by size and elemental composition", *Envir. Sci. Technol.*, **10**, 76-82, 1976.
- [48] Friedlander, S. K., "Gas to particle conversion: Smoke, dust and Haze", John Wiley and Sons, New York, USA, 1977.
- [49] Garg, S. C. and Das, U. N., "Aeronomy experiment on SROSS-C2", *J. Spacecraft Tech.*, **5(3)**, 11-15, 1995.
- [50] Ghosh, A. B., Bose, S., Lal, M. and Maitra, A., "Ground-based measurements of some minor constituents during the solar eclipse-1995", *TAO*, **8(4)**, 371-384, 1997.
- [51] Gish, O. H., "Discussion of atmospheric electrical observations at Huacayo, Peru, during the solar eclipse, Jan. 25, 1944", *Terr. Magn. Atmos. Elect.*, **49**, 123-124, 1944.
- [52] Gish, O. H., "Evaluation and interpolation of the columnar resistance of the atmosphere", *Terr. Magn.*, **99**, 159-168, 1944.
- [53] Goyal, R. K., "A study of aerosols", *Ph. D. Thesis*, University of Roorkee, Roorkee, India, 1985.
- [54] Goyal, R. K., Varshneya, N. C. and Verma, T. S., "Size distribution of large aerosols using cascade impactor at Roorkee", National Space Science Symposium, Pune, India, Dec. 7-10, 1983.
- [55] Grass, J. L. and Ayers, G. P., "Marine aerosol at southern mid-latitudes", *J. Geophys. Res.*, **88**, 10661-10666, 1983.

- [56] Gross, G. W., "Role of relaxation and contact time in charge separation during collision precipitation particles with ice targets", *J. Geophys. Res.*, **87**, 7170-7178, 1982.
- [57] Gumprecht, R. O. and Slipevich, C. M., "Tables of scattering function for spherical particles", Engineering Research Institute, University of Michigan Press, Ann Arbor, 1951.
- [58] Guo, Y., Barthakur, N. N. and Bhartendu, S., "Using atmospheric electrical conductivity as an urban air pollution indicator", *J. Geophys. Res.*, **101(D4)**, 9197-9203, 1996.
- [59] Haaf, W. and Jaenicke, R., "Results of improved size distribution measurements in the Aitken range of atmospheric aerosols", *J. Aerosol Sci.*, **11**, 321-330, 1980.
- [60] Hanel, G., "The properties of atmospheric aerosol particles as function of relative humidity at thermodynamic equilibrium with the surrounding of moist air", *Advances in Geophysics*, edited by H.E. Landsberg and J. Van Meighen, Academic Press, New York, USA, **19**, 73-188, 1976.
- [61] Hanel, G. and Lehmann, N., "Equilibrium size of aerosol particles and relative humidity: New experimental data from various aerosol types and their treatment for cloud physics applications", *Contr. Atmos. Phys.*, **54**, 57-71, 1981.
- [62] Harrison, R. M., "Pollution - Causes, Effects and Control", The Royal Society of Chemistry, Cambridge, UK, 1990.
- [63] Harshvardhan, "Aerosol-climate interactions", edited by P. V. Hobbs, *International Geophysical Series*, **54**, 75-95, 1993.

- [64] Hawkins, G. S., "Interplanetary debris near the earth", *Ann. Rev. Astronomy Astrophysics*, **2**, 149-164, 1964.
- [65] Hays, P. B. and Roble, R. G., "A quasi-static model of global atmospheric electricity 1. The lower atmosphere", *J. Geophys. Res.*, **84**, 3291-3305, 1979.
- [66] Herman, J. R. and Goldberg, R. A., "Sun, Weather and Climate", NASA-SP 426, Washington D. C., 1978.
- [67] Hidy, G. W. and Brook, J. R., "Proceedings of the Second International Congress", Academic Press, New York, USA, 1971.
- [68] Hobbs, P. V., Radke, L. F. and Shumway, S. E., "Cloud condensation nuclei from industrial sources and their apparent influence on precipitation in Washington state", *J. Atmos. Sci.*, **27**, 81-89, 1970.
- [69] Hodkinson, J. R., "The optical measurements of aerosols", *Aerosol Science*, edited by C. N. Davies, Academic Press, London, 1966.
- [70] Hoppel, W. A., Fitzgerald, J. W., Frick, G. M., Larson, R. E. and Mack, E. J., "Aerosol size distributions and optical properties found in the marine boundary layer over the Atlantic Ocean", *J. Geophys. Res.*, **95**, 3659-3686, 1990.
- [71] Hori, T., "Studies on fogs in relation to fog-preventing forest", edited by T. Hori, Tanne Trading, Sappora, Japan, 1953.
- [72] Houghton, H. G. and Chalker, W. R., "Scattering cross-sections of water drops in air for visible light", *J. Opt. Soc. Am.*, **39**, 955-957, 1949.
- [73] Huff, F. A. and Changnon Jr., S. A., "Precipitation modification by major urban area", *Bull. Am. Meteorol. Soc.*, **54**, 1220-1232, 1973.

- [74] Hulst, Van De, "Light scattering of small particles", John Wiley and Sons, New York, USA, 1957.
- [75] Hunten, D. M., Turco, R. P. and Toon, O. B., "Smoke and dust particles of meteoric origin in the mesosphere and stratosphere", *J. Atmos. Sci.*, **37**, 1342-1357, 1980.
- [76] Illingworth, A. J., "Charge separation in thunderstorms: Small scale processes", *J. Geophys. Res.*, **90**, 6026-6032, 1985.
- [77] India Meteorological Department (IMD), "Report on the total solar eclipse", 1995.
- [78] Intergovernmental Panel on Climate Change (IPCC), "Climate change: The supplementary report to the IPCC assessment", WMO-UNEP Rep. (Eds. Houghton et al.) Cambridge Univ. Press, UK, pp200, 1992.
- [79] Intergovernmental Panel on Climate Change (IPCC), "Radiative forcing of climate change", WMO-UNEP Rep. (Eds. Houghton et al.) Cambridge Univ. Press, UK, pp 339, 1994.
- [80] Israël, H., "Synoptic researches on atmospheric electricity", *J. Geophys. Res.*, Proc. Conf. on Atmospheric Electricity, 19-21 May 1954, 11-20, 1955.
- [81] Israël, H., "Atmospheric Electricity (Vol. I and II)", Israel Programme for Scientific Translations, Jerusalem, 1972.
- [82] Jain, S. L., Arya, B. C., Singh, S. K., Tripathi, O. P. and Hamid, A., "Measurements of various atmospheric parameters during a total solar eclipse", *TAO*, **8(4)**, 371-384, 1997.

- [83] John, T. and Garg, S. C., "Balloon measurement of the vertical profile of atmospheric electrical conductivity over Hyderabad", *Indian J. Radio Space Phys.*, **22**, 220-224, 1993.
- [84] Jones, C. D. and Hutchinson, W. C. A., "Plumes of space charge in the lower atmosphere", *J. Atmos. Terr. Phys.*, **38**, 485-494, 1976.
- [85] Jonsson, H. H. and Vonnegut, B., "Apparatus for measurements of the electrical conductivity of rain water with high resolution in space and time", *J. Appl. Meteorol.*, **30(8)**, 1220-1227, 1991.
- [86] Junge, C. E., "Aerosols", Handbook of Geophysics, Edited by Campen et al., McMillan, New York, USA, 1960.
- [87] Junge, C. E., "Vertical profiles of condensation nuclei in the stratosphere", *J. Meteorol.*, **18**, 501-509, 1961.
- [88] Junge, C. E., "Air Chemistry and Radioactivity", Academic Press, New York, USA, 1963.
- [89] Junge, C. E., Chagnon, C. W. and Manson, J. E., "Stratospheric Aerosols", *J. Meteorol.*, **18**, 81-108, 1961.
- [90] Kamra, A. K., "Electrification in an Indian dust storm", *Weather*, **24**, 145-146, 1969.
- [91] Kamra, A. K., "Measurements of electrical parameters of dust storm", *J. Geophys. Res.*, **77**, 5183-5200, 1972.
- [92] Kamra, A. K., "Inadvertent modification of atmospheric electricity", *Current Sci.*, **60**, 639-646, 1991.
- [93] Kamra, A. K. and Deshpande, C. G., "Possible secular change and land-to-ocean extension of air pollution from measurements of atmospheric electrical conductivity over the Bay of Bengal", *J. Geophys. Res.*, **100 (D4)**, 7105-7110, 1995.

- [94] Kamra, A. K. and Varshneya, N. C., "The effect of solar eclipse on atmospheric electric potential gradient", *J. Atmos. Terr. Phys.*, **29**, 327-329, 1967.
- [95] Kandalgaonkar, S. S., "A case study of weekly variation in electrical parameters of Athens", *Indian J. Radio Space Phys.*, **21**, 153-157, 1992.
- [96] Kandalgaonkar, S. S. and Manohar, G. K., "Variation in atmospheric electric field at Athens during 1966-1980", Proc. 9th Int. Conf. Atmos. Elect., St. Petersburg, Russia, 520-522, 1992.
- [97] Kandalgaonkar, S. S. and Manohar, G. K., "A study of the association of surface potential gradient with the onset of monsoon at Pune", *Indian J. Radio Space Phys.*, **22**, 349, 1993.
- [98] Kawano, M., "The local anomaly of the diurnal variation of atmospheric electric field", Recent Advances in Atmospheric Electricity, Edited by L.G. Smith, Pergamon Press, Oxford, 161-174, 1958.
- [99] Kawano, M. and Nakatani, S., "The results of routine observations of the ionization and the natural radioactive dust concentration in the atmosphere in Tokyo", *J. Met. Soc. Japan*, **36**, 135-140, 1958.
- [100] Kerkar, M., "The scattering of light and other electromagnetic radiations", Academic Press, New York, USA, 1969.
- [101] Khemani, L. T., Momin, G. A., Naik, M. S., Kumar, R. and Ramana Murty, B. V., "Observation of aitken nuclei and trace gases in different environments in India", *Water, Air and Soil Pollution*, **24**, 131-141, 1985.
- [102] Kleusberg, A., "The global positioning system and ionospheric conditions", Solar Terrestrial Predictions IV, 142-146, 1992.

- [103] Knudsen, W. C., "Magnetospheric convection and the high-latitude F₂ ionosphere", *J. Geophys. Res.*, **79**, 1046-1065, 1974.
- [104] Knudsen, W. C., Banks, P. M., Winningham, J. D. and Klumpar, D. M., "Numerical model of the convecting F₂ ionosphere at high latitudes", *J. Geophys. Res.*, **82**, 4784, 1977.
- [105] Koengisfeld, L., "Investigation of the potential gradient at the earth's ground surface and within the free atmosphere", *Thunderstorm Electricity*, edited by H. Byers, Chicago University Press, Chicago, 24-45, 1953.
- [106] Kourganoff, V., "Basic methods in transfer problems", Oxford University Press, Oxford, U.K, 1952.
- [107] Krishna Moorthy, K., Prabha, R. N., Prasad, B. S. N., Muralikrishnan, N., Gayathri, H. B., Narsimha Murthy, B., Niranjana, K., Ramesh Babu, V., Satyanarayana, G. V., Agashe, V. V., Aher, G. R., Singh, R. and Srivastava, B. N., "Results from MWR network of IMAF", *Indian J. Radio Space Phys.*, **22**, 243-258, 1993.
- [108] Krishna Murthy, B. V., "Aerosol and radiation budget in the middle atmosphere", *Indian J. Radio Space Phys.*, **17**, 203-219, 1988.
- [109] Lal, M., Cubasch, U. and Santer, B. D., "Effect of global warming on Indian monsoon simulated with a coupled ocean-atmosphere general circulation model", *Current Sci.*, **66(6)**, 430-438, 1994.
- [110] Landsberg, H. E., "Man-made climate changes", *Science*, **170**, 1265-1274, 1970.

- [111] Lane-Smith, D. R. and Markson, R., "Atmospheric electric measurements during the 1972 eclipse over Nova Scotia", *Electrical Processes in Atmospheres*, edited by H. Dolezalek and R. Reiter, Steinkopff, Darmstadt, 143-156, 1977.
- [112] Larsen, A., "Photographing of lightning with a moving camera", *Annual Report, Smithsonian Inst.*, 119-127, 1905.
- [113] Latham, J., "The electrification of thunderstorms", *Q. J. R. Meteorol. Soc.*, **107**, 277-298, 1981.
- [114] Latham, J. and Dye, J. E., "Calculations on the electrical development of a small thunderstorm", *J. Geophys. Res.*, **93**, 13141-13144, 1989.
- [115] Leadrer, B. P., Tanner, R. L. and Holford, T. R., "Diurnal variations, chemical composition and relation to meteorological variables of the summer aerosol in the New York subregion", *Atmos. Environ.*, **16**, 2075-2087, 1982.
- [116] de Leeuw, "Vertical profiles of giant particles close above the sea surface", *Tellus*, **38B**, 51-61, 1986.
- [117] Lenchow, D. H., Stankov, B. B. and Mahrt, L., "The rapid morning boundary layer transition", *J. Atmos. Sci.*, **36**, 2108-2124, 1979.
- [118] Liou, K. N., "An introduction to atmospheric radiation", Academic Press, New York, USA, 1980.
- [119] Lodge Jr., J. R., Waggoner, A. P., Klodt, D. T. and Crain, C. N., "Non-health effects of airborne particulate matter", *Atmos. Environ.*, **15**, 431-482, 1981.
- [120] Logan, N. A., "Survey of some early studies of the scattering of plane waves by a sphere", *Proc. IEEE*, **53**, 773-785, 1965.

- [121] Mahajan, K. K. and Shastri, S., "Has the ionospheric F2 region changed permanently during the last thirty years", *Adv. Space Res.*, **20(11)**, 2157-2160, 1997.
- [122] Mainwaring, S. J. and Harsha, S., "Size distribution of aerosols in Melbourne city air", *Atmos. Environ.*, **10**, 57-60, 1976.
- [123] Makino, M. and Ogawa, T., "Responses of atmospheric electric field and air-earth current to variations of conductivity profiles", *J. Atmos. Terr. Phys.*, **46**, 431-445, 1984.
- [124] Makino, M. and Ogawa, T., "Quantitative estimation of global circuit", *J. Geophys. Res.*, **90**, 5961-5966, 1985.
- [125] Manabe, S., Spelman, M. J. and Stouffer, F. J., "Transient response of a coupled ocean-atmosphere model to gradual changes of atmospheric CO₂: Part-2 Seasonal Response", *J. Climate*, **5**, 105-126, 1992.
- [126] Manes, A., "Particulate air pollution trends deduced from atmospheric electrical conductivity measurements at Bet-Dagan (Israel)", *Electrical Processes in Atmospheres*, edited by H. Dolezalek and R. Reiter, Steinkopff, Darmstadt, 109-118, 1977.
- [127] Mani, A., Sreedharan, C. R., Huddar, B. B. and Ramanathan, V., "Atmospheric electricity measurements over the Indian ocean", *Pure Appl. Geophys.*, **100**, 101-107, 1972.
- [128] Manohar, G. K., Kandalgaonkar, S. S. and Kulkarni, M. K., "Impact of a total solar eclipse on surface atmospheric electricity", *J. Geophys. Res.*, **100(D10)**, 20805-20814, 1995.

- [129] Manson, J. E., "Aerosols, Hand-book of Geophysics and Space Environment", edited by S. L. Valley McGraw-Hill, New York, 1965.
- [130] Markson, R. and Kamra, A. K., "Airborne and ground measurements of the atmospheric potential gradient during a solar eclipse", *J. Atmos. Terr. Phys.*, **33**, 1107-1113, 1971.
- [131] Markson, R., "Solar modulation of atmospheric electrification and possible implications for the sun-weather relationship", *Nature*, **273**, 103-109, 1984.
- [132] Markson, R., "Comparison of ionospheric potential and air-earth current as indicators of the global circuit current", Proc. 8th Int. Conf. Atmos. Elect. Uppsala, Sweden, 814-819, 1988.
- [133] Mason, B. J., "Clouds, rain and rain making", Cambridge University Press, Cambridge, England, 1975.
- [134] Mathpal, K. C., Varshneya, N. C. and Dass, N., "Precipitation-powered of cloud electrification", *Rev. Geophys. (Space Phys.)*, **18**, 361-378, 1980.
- [135] McCartney, E. J., "Optics of the atmosphere", John Wiley & Sons, New York, USA, 1976.
- [136] McCormick, M. P., Swissler, T. J., Chu, W. P. and Fuller, W. H., "Post-volcanic stratospheric aerosol decay as measured by Lidar", *J. Atmos. Sci.*, **35**, 1296-1303, 1978.
- [137] Meehl, G. A. and Washington, W. M., "South Asian summer monsoon variability in a model with doubled atmospheric carbon dioxide concentration", *Science*, **260**, 1101-1104, 1993.

- [138] Meinel, M. P. and Meinel, A. B., "Late twilight flow of the ash stratum from the eruption of Agung volcano", *Science*, **12**, 582-583, 1963.
- [139] Meyerott, R. E., Reagan, J. B. and Evans, J. E., "Volcanism and global atmospheric electricity in the lower atmosphere", 7th Int. Conf. Atmos. Elect., Am. Meteorol. Soc., New York, 1984.
- [140] Meyerott, R. E., Reagan, J. B. and Evans, J. E., "Tropospheric aerosol perturbations due to volcanism as measured by electrical conductivity of ocean air", *J. Geophys. Res.*, **90 (D4)**, 5925-5932, 1985.
- [141] Mie, G., "A contribution to the optics of turbid media, especially colloidal metallic suspension", *Ann. Phys.*, **25 (4)**, 377-445, 1908.
- [142] Mikasa, H., "Latest technologies aid in measuring air pollution", *J. Electr. Engg.*, **29(310)**, 26-32, 1992.
- [143] Misaki, M, Ohtagaki, M. and Kanazawa, I., "Mobility spectrometry of the atmospheric ions in relation to atmospheric pollution", *Pure Appl. Geophys.*, **100**, 133-145, 1972.
- [144] Mitra, S. K., "The Upper Atmosphere", Monograph Series No. V, The Asiatic Society, Calcutta, 1992.
- [145] Mikasa, H., "Latest technologies aid in measuring air pollution", *J. Electr. Engg.*, **29(310)**, 26-32, 1992.
- [146] Mohankumar, K. and Devnarayanan, S., "Effect of the solar eclipse of Feb. 16, 1980 on the meteorological parameters", Proc. of International Symp. on Solar Eclipse, 27-31 January, 1981.
- [147] Morita, Y., "The diurnal and latitudinal variation of electric field and conductivity in the atmosphere over the Pacific Ocean", *J. Meteorol. Soc. Japan*, **49**, 56-58, 1971.

- [148] Morita, Y. and Ishikawa, H., "On recent measurements of electric parameters and aerosols in the oceanic atmosphere", *Electrical Processes in Atmospheres*, edited H. Dolezalek and R. Reiter, Steinkopff, Darmstadt, 126-130, 1977.
- [149] Mühleisen, R., "On the deviation of the course of elements of atmospheric electricity on continents from the world-wide course", *J. Atmos. Terr. Phys.*, **8**, 146-157, 1956.
- [150] Mühleisen, R., "The global circuits and its parameters", *Electrical Processes in Atmospheres*, edited H. Dolezalek and R. Reiter, Steinkopff, Darmstadt, 467-476, 1977.
- [151] Muir, M. S., "Atmospheric electric space charge generated by the surf", *J. Atmos. Terr. Phys.*, **39**, 1341-1346, 1977.
- [152] Mukhopadhyaya, B. and Krishna Nand, "Aerosol size distribution over Pune assessed from atmospheric turbidity measurements", *National Space Science Symposium (NSSS)*, Pune, Dec. 7-10, 1983, 52.
- [153] Mukku, V. N. R., "Study of electrical conductivity and ions in relation to global electrical and local meteorological parameters", *Ph.D. Thesis*, University of Kashmir, India, 1982.
- [154] Murphy, J. M. and Mitchell, J. F. B., "Transient response of Hadley centre coupled model to increasing carbon dioxide: Part 2-Temporal and Spatial Evolution of Patterns", *J. Climate*, **8**, 57-80, 1995.
- [155] Nair, P. R. Krishna Moorhty, K. and Krishna Murthy, B. V., "Results of Multiwavelength radiometer studies at Trivendrum", Paper presented at second workshop on IMAP Scientific Results, VSSC, Trivendrum, Apr. 24-28, 1988.

- [156] Narsimha, R., Prabhu, A., Rao, K. N. and Prasad, C. R., "Atmospheric boundary layer experiment, Indian National Science Academy", **48A**, 175-186, 1982.
- [157] Neher, H. V., "Cosmic rays at high latitudes and altitudes covering four solar maxima", *J. Geophys. Res.*, **76**, 1637-1651, 1971.
- [158] Nickolaenko, A. P., Hayakawa, M. and Hobara, Y., "Temporal variations of the global lightning activity deduced from the Schumann resonance data", *J. Atmos. Terr. Phys.*, **58**, 1699-1704, 1996.
- [159] Nizamuddin, S., Ramanathan, R., Rao, A. M., Khera, M. K., Makhdomi, B. A., Raina, B. N., Rafiqi, A. R., Mukku, V. N. R., Goel, R. K., Pathak, P. P., Rai, J. and Varshneya, N. C., "Proceedings of International Symposium on Solar Eclipse," Indian National Science Academy, **48A**, 263-270, 1982.
- [160] Norville, K., Baker, M. and Latham, J., "A numerical study of thunderstorm electrification: Model development and case study", *J. Geophys. Res.*, **96**, 7463-7481, 1991.
- [161] Pahwa, D. R., Singhal, S. P. and Khemani, L. T., "Studies of aerosols at Delhi", *Mausam*, **45(1)**, 49-56, 1994.
- [162] Pangonis, W. J. and Heller, W., "Angular scattering functions for spherical particles", University Press, Detroit, USA, 1960.
- [163] Paoletti, D. and Spagnolo, "Atmospheric electricity in a rural site and its possible correlation with pollution: a preliminary study", *Atmos. Environ.*, **23(7)**, 1607-1611, 1989.

- [164] Parameswaran, K. and Vijayakumar, G., "Effect of atmospheric relative humidity on aerosol size distribution", *Indian J. Radio Space Phys.*, **23**, 175-188, 1994.
- [165] Parameswaran, K., Vijayakumar, G., Krishna Murthy, B.V. and Krishna Moorthy, K., "Effect of wind speed on mixing region aerosol concentration at a tropical coastal station", *J. App. Meteor.*, **34**, 1392-1397, 1995.
- [166] Park, P. M., Smith, M. H. and Exton, H. J., "The effect of mixing height on maritime aerosol concentration over the North Atlantic Ocean", *Quart. J. Roy. Meteor. Soc.*, **116**, 461-476, 1980.
- [167] Parungo, F., Bodhaine, B. and Bortniak, J., "Seasonal variation in Antarctic aerosols", *J. Aerosol Sci.*, **12**, 491-504, 1981.
- [168] Pasko, V. P., Inan, U. S., Bell, T. F. and Taranenko, Y. N., "Sprites produced by quasi-electrostatic heating and ionization in the lower ionosphere", *J. Geophys. Res.*, **102(A3)**, 4529-4561, 1997.
- [169] Patel, B. D., "Effect of ionization on the process of condensation and its role in cloud physics", *Ph.D. Thesis*, University of Roorkee, Roorkee, India, 1986.
- [170] Pendorf, R., "New tables of total Mie Scattering coefficients for spherical particles of real refractive index ($1.33 \leq n \leq 1.50$)", *J. Opt. Soc. Am.*, **47**, 1010-1015, 1986.
- [171] Peterson, J. T. and Junge, C. E., "Man's impact on climate", MIT Press, Cambridge, USA, 1971.
- [172] Petterssen, H., "Cosmic spherules and meteoritic dust", *Sci. Am.*, 123-132, 1960.

- [173] Pierce, E. T. and Whitson, A. L., "Atmospheric electricity and the waterfalls of Yosemite Valley", *J. Atmos. Sci.*, **22**, 314-319, 1981.
- [174] Prospero, J. M., Charlson, R. J., Mohnen, V., Jaenicke, R., Delany, A. C., Mayer, J., Zoller, W. and Rahn, K., "Atmospheric aerosol system - an overview", *Rev. Geophys. (Space Phys.)*, **21**, 1607-1629, 1983.
- [175] Rai, J., Bhattacharya, P. K. and Sapru, M. L., "Ionospheric disturbances due to thunderstorms", *Int. J. Electronics*, 34(6), 757-760, 1973.
- [176] Rai, J., "Some studies of lightning discharge and radio atmospherics", *Ph.D. Thesis*, Banaras Hindu University, Varanasi, India, 1974.
- [177] Retalis, D., "Atmospheric electric potential gradient measurements during the annual solar eclipse of 29 April, 1976", *J. Atmos. Terr. Phys.*, **43**, 999-1002, 1981.
- [178] Retalis, D., Pitta, A. and Praltidas, P., "The conductivity of air and other electrical parameters in relation to meteorological elements and air pollution in Athens", *Meteorol. Atmos. Phys.*, **46**, 197-204, 1991.
- [179] Retalis, D. and Retalis, A., "The atmospheric electric climate in Athens", Greece, Proc. 9th Int. Conf. Atmos. Elect., St. Petersburg, Russia, 61-64, 1992.
- [180] Robinson, E. and Robbins, R. C., "Emissions, concentrations and fate of particulate atmospheric pollutants", Report PR 6755, Stanford Research Institute, 25-34, 1968.
- [181] Rosen, J. M., "The boiling point of atmospheric aerosols", *J. Appl. Meteorol.*, **10**, 1044-1046, 1971.

- [182] Rosenberg, T. J. and Lanzetta, L. J., "Direct energy inputs to the middle atmosphere, Middle Atmosphere Electrodynamics", edited by N. C. Maynard, NASA CP-2090, 43-70, 1979.
- [183] Ruhnke, L., "Electrical conductivity of air on the Greenland icecap", *J. Geophys. Res.*, **67**, 2767-2772, 1962.
- [184] Sapkota, B.K. and Varshneya, N.C., "On the global atmospheric circuit," *J. Atmos and Terr. Phys.*, **52**, 1-20, 1990.
- [185] Saunders, C. P. R., Keith, D. and Mitzewa, R., "The effect of liquid water on thunderstorm charging", *J. Geophys. Res.*, **96**, 1107-1117, 1991.
- [186] Schmidt, E. W., Gieske, J. A. and Allen, J. M., "Size distribution of fine particulate emissions from a coal fired power plant", *Atmos. Environ*, **10**, 1065-1069, 1976.
- [187] Schonland, B. F. J. and Craib, J., "The electric fields of South African thunderstorms", *Proc. Roy. Soc. (London)*, **114**, 229-243, 1927.
- [188] Schunk, R. W. and Banks, P. M., "Auroral N₂ excitation and the electron density trough", *Geophys. Res. Lett.*, **2**, 239-242, 1975.
- [189] Schunk, R. W., Banks, P. M. and Raitt, W. J., "Effect of electric fields and other processes upon the nighttime and high-latitude F layer", *J. Geophys. Res.*, **81**, 3271-3282, 1976.
- [190] Schunk, R. W. and Raitt, W. J., "Atomic nitrogen and oxygen ions in the daytime high-latitude F region", *J. Geophys. Res.*, **85(A3)**, 1255-1272, 1980.
- [191] Schunk, R. W., Raitt, W. J. and Banks, P. M., "Effect of electric fields on the daytime high-latitude E and F regions", *J. Geophys. Res.*, **80**, 3121-3130, 1975.

- [192] Schunk, R. W. and Sojka, J. J., "Ion-temperature variations in the daytime high-latitude F region", *J. Geophys. Res.*, **87(A7)**, 5169-5183, 1982.
- [193] Schunk, R. W. and Sojka, J. J., "Ionosphere-thermosphere space weather issue", *J. Atmos. Terr. Phys.*, **58(14)**, 1527-1574, 1996.
- [194] Selvam, A. M., Manohar, G. K., Kandalgaonkar, S. S., Ramchandra Murty, A. S. and Raman Murty, B. V., "Electrical phenomena in pre-monsoon thunderstorm", Int. Conf. on Atmospheric electricity, July 28 - Aug.1, 1980.
- [195] Selvam, A. M., Vijayakumar, R. and Murty A. S. R., "Variation in atmospheric electric field and meteorological parameters at a typical coastal urban station during 1936-40 and 1962-66," *Theor. Appl. Climatology*, **48**, 15-22, 1993.
- [196] Sethuraman, S., "Dynamics of atmospheric boundary layer during the 1980 total solar eclipse", *Proc. Indian Nat. Sci Acad.*, **48A**, 187-195, 1982.
- [197] Shapka, R., "Geomagnetic effects on modern pipeline system", *Solar-Terristrial Predictions IV*, 163-170, 1992.
- [198] Shaw, G. E., "Aerosol-size temperature relationship", *Geophys. Res. Lett.*, **15**, 133-135, 1988.
- [199] Shifrin, K. S. and Zelmanovich, I. L., "Tables of light scattering, Part II: Coefficients of angular scattering", Hydro Meteorological Publishing House, Leningrad, 1967.

- [200] Singh, A. K., Niwas, S., Kumar, A., Rai, J. and Nigam, M. J., "Variations in atmospheric aerosols and electrical conductivity at Roorkee during the total solar eclipse of October 1995", *Indian J. Radio Space Phys.*, **28**, 1-10, 1999.
- [201] Singh, N., "Role of atmospheric ions on condensation and cloud formation process", *Ph. D. Thesis*, University of Roorkee, Roorkee, India, 1985.
- [202] Singh, R. P., Singh, A. K., Singh, U. P. and Singh, R. N., "Wave ducting and scattering properties of ionospheric irregularities", *Adv. Space Res.*, **14(9)**, 225-228, 1994.
- [203] Singhal, S. P., Agarwal, S. K., Pahwa, D. R. and Gera, B. S., "Stability studies with the help of acoustic sounding", *Atmos. Environ.*, **19**, 221-228, 1985.
- [204] Sivaram Krishnan, M. V. and Selvam, A. M., "Measurement of the two components of air-earth conduction current in the tropics", *Indian J. Meteor. Geophys.*, **22**, 499-524, 1971.
- [205] Spiro, R. W., Heelis, R. A. and Hanson, W. B., "Ion convection and the formation of the mid-latitude F region ionization trough", *J. Geophys. Res.*, **83**, 4255-4264, 1978.
- [206] Srivastava, G. P., Srinivasan, V. and De, A. K., "Measurements of atmospheric electricity parameters during the total solar eclipse of 16 Feb. 1980", *Proc. Indian Nat. Sci. Acad. Part A*, **48**, 271-279, 1982.
- [207] Stansbery, E. K., Few, A. A. and Geis, P. B., "A global model of thunderstorm electricity", *J. Geophys. Res.*, **98**, 16591-16603, 1993.

- [208] Sze, N. D. and Ko, M. K. W., "Is CS₂ a precursor for atmospheric COS?", *Nature*, **278**, 731-732, 1979.
- [209] Takagi, M., "On the regional effect in the global atmospheric electric field", *Electrical Processes in Atmospheres*, edited by H. Dolezalek and R. Reiter, Steinkopff, Darmstadt, 477-481, 1977.
- [210] Takagi, M. and Iwata, A., "A seasonal effect in diurnal variation of the atmospheric electric field on the pacific coast of Japan", *Pure Appl. Geophys.*, **118**, 953-963, 1980.
- [211] Takagi, M. and Iwata, A., "Correlation between the atmospheric electric field at a seaside station and the world-wide universal field", *Res. Lett. Atmos. Elect.*, **3**, 1712, 1983.
- [212] Takagi, M. and Kanada, M., "Global variation in the atmospheric electric field", *Pure Appl. Geophys.*, **100**, 44-53, 1972.
- [213] Takamura, T., Tanaka, M and Nakajima, T., "Effects of atmospheric humidity on the refractive index and the size distribution of aerosols as estimated from the light scattering measurements", *J. Meteor. Soc. Japan*, **62**, 573-581, 1984.
- [214] Tiwari, G. N. and Goyal, R. K., "Thermal modeling of a greenhouse: A pollution free controlled environment for crop productions", *Proc. Int. Symp. of Asian Monsoon and Pollution over the Monsoon Environment*, IIT Delhi, Dec. 2-5, 1997, 179.
- [215] Turco, R. P., Toon, O. B., Hamill, P. and Whitten, R. C. "Effects of meteoric debris on stratospheric aerosols and gases", *J. Geophys. Res.*, **86**, 1113-1128, 1981.

- [216] Twomy, S., "Atmospheric aerosols", Elsevier Scientific Publishing Company, Amsterdam, 1977.
- [217] Uchikawa, K., "Annual variations of the ionospheric potential, the air-earth current density and the columnar resistance measured by radiosondes", Electrical processes in Atmospheres, edited by H. Dolezalk and R. Reiter, Steinkopff, Darmstadt, 460-463, 1977.
- [218] Uman, M. A., "Lightning," McGraw Hill, New York, 1969.
- [219] Uman, M. A., "The lightning Discharge," Academic Press, London, 1987.
- [220] Vyas, B. M., Pandey, R., and Rai, R. K., "Planetary scale predictions in ionospheric absorption", Int. Workshop on Long Term Changes and Trends in Atmosphere, IITM Pune, Feb. 16-19, 1999, 46.
- [221] Volland, H., "Quasi electrostatic fields within the atmospheres", Handbook of Atmospheric, Vol. I, CRC Press, Florida, 1982.
- [222] Vonnegut, B., "The atmospheric electricity paradigm", *Bull. Amer. Meteorol. Soc.*, **75**, 53-61, 1994.
- [223] Wahlin, L., "Atmospheric Electrostatics", John Wiley and Sons, New York, USA, 1986.
- [224] Wallace, J. M. and Hobbs, P. V., "Atmospheric Science and Introductory Survey", Academic Press, New York, USA, 1977.
- [225] Wark, K. and Warner, C. F., "Air Pollution: Its Origin and Control", Don-Donnelly Publication, New York, USA, 1976.
- [226] Watkins, B. J., "A numerical computer investigation of the polar F-region ionosphere", *Planet. Space Sci.*, **26**, 559-569, 1978.

- [227] Wilson, C. T. R., "On some determination of sign and magnitude of electric discharges in lightning flashes", *Proc. Roy. Soc. (London)*, **92**, 555-574, 1916.
- [228] Wilson, C. T. R., "Investigations on lightning discharges and on the electric fields in the thunderstorms", *Phil. Trans. Roy. Soc. (London)*, **221**, 73-115, 1920.
- [229] Wilson, C. T. R., "The electric field of a thundercloud and some of its effects", *Proc. Roy. Soc. (London)*, **37**, 32-37, 1925.
- [230] World Climate Programme, WCP-55, "Report of the Experts Meeting on Aerosols and Their Climatic Effects", edited by A. Deepak and H. E. Gerber, World Meteorological Organization, Geneva, **107**, 1983.
- [231] Zuev, V.E., "Laser beams in the atmosphere", Plenum Publishing, New York, USA, 1982.